Biocatalytic Oxidation of Arsenic (III) with Concomitant Chromium (VI) Reduction by an Autotrophic Culture of Bacteria

By

Tony Ebuka Igboamalu

A thesis submitted to the Faculty of Engineering, Built Environment and Information Technology in the fulfilment of the requirements for the degree

Doctor of Philosophy in Chemical Engineering

at the

University of Pretoria

Supervisor

Prof Evans M.N. Chirwa

2018

Dedication

This thesis is dedicated to my family: Chief F.C. Igboamalu, my sons Brian and Tony Igboamalu, and my wife, Dr Silvia Igboamalu. I would like to thank them for their patience during these years of dedicated effort to complete this task.

Abstract

Title: Biocatalytic oxidation of arsenic (III) with concomitant chromium (VI) reduction by an autotrophic culture of bacteria

Author: Tony Ebuka Igboamalu

Supervisor: Professor Evans M.N. Chirwa

Department: Chemical Engineering

University: University of Pretoria

Degree: Doctor of Philosophy (Chemical Engineering)

Environmental sustainability has become a leading discussion in the world, coupled with a quest to minimise severe environmental pollution. The chrome mining and ferrochrome processing industrial revolution has contributed significantly to the world's environmental pollution. It is of interest to note that there are about 14 ferrochrome smelter plants in South Africa, and each plant generates considerable amounts of wastewater, requiring efficient treatment before discharge. If not properly managed, it could find its way into the environment (e.g. underground water), rendering it unsuitable for human consumption.

These industries often generate a wide range of toxic waste containing Cr(VI), As(III), cyanide and other co-pollutants that are either difficult or expensive to treat. This study proposed the biochemical treatment of multiple pollutants by detoxification of Cr(VI) to less toxic Cr(III), and this is used to provide energy and oxidizing potential to achieve detoxification of As(III) through oxidation to the less mobile As(V) species. Theoretically, the process is shown to be thermodynamically feasible with a Cr(VI) to As(III) stoichiometric mole ratio of 3:2.

Simultaneous detoxification of Cr(VI) and As(III) was achieved by using a mixed culture of chemoautotrophic anaerobic bacteria isolated from a cow dip site previously contaminated with arsenic, and from a wastewater treatment plant that received high levels of Cr(VI) from a nearby abandoned chrome ore refinery. Earlier experiments indicated that Cr(VI) is non-

inhibitive to cultures from the Brits Wastewater Treatment Plant at levels below 99 mg Cr(VI)/L.

Results obtained in the current study showed for the first time: Cr(VI) reduction coupled to As(III) oxidation, with As(III) serving as the principal electron donor. Experiments conducted with As(III) concentration ranging from 60-500 mg/L at a constant Cr(VI) concentration of 70 mg/L showed that As(III) enhanced Cr(VI) reduction rate at non-inhibitive Cr(VI) concentration (<100 mg Cr(VI)/L). With increasing Cr(VI) concentration to values greater than 100 mg/L, the redox process was inhibited. No Cr(VI) reduction and As(III) oxidation was obtained in cell-free cultures (control 1) and killed cells (control 2), which conclusively showed that the observed As(III) oxidation/Cr(VI) reduction was metabolically mediated. The 16S rRNA genomic sequence analysis indicated the predominance of *Exiquobacterium profundum, Bacillus licheniformis,* and *Staphylococcus epidermidis* as predominant species in the mixed culture.

A bench-scale study with immobilised glass and ceramic bead media bed reactors linked to anaerobic tank retrofit (CSTR) shows that both reactors were efficient in reducing Cr(VI) to a lower concentration, with Cr(VI) removal efficiency exceeding 90%. It was noted that the attached growth reactor was not only affected by system overload (>100 mg Cr(VI)/L and 170 mg As(III) /L), but also by low hydraulic detention time (<5 h), which was characterized by the increase in effluent Cr(VI) concentration. Biokinetic parameters of these strains in the batch and continuous-flow system were estimated using a modified non-competitive inhibition model with a computer program for simulation of the aquatic system AQUASIM 2.0.

Keywords: Arsenite oxidation, electron transport, Cr(VI) reduction, autotrophic consortium, detoxification, oxidation/reduction kinetics.

Declaration

I, **Tony Ebuka Igboamalu** declare that the thesis entitled "**Biocatalytic Oxidation of Arsenic (III) with Concomitant Chromium (VI) Reduction by an Autotrophic Culture of Bacteria**" submitted by me for the degree of Doctor of Philosophy is the record of work carried out by me during the period from 30th July 2013 to 31st October 2018 under the guidance of Prof. E.M.N. Chirwa of the University of Pretoria and has not formed the basis for the award of any degree, diploma, associateship, fellowship, titles in this or any other university or other institution of higher learning.

I further declare that the material obtained from other sources has been duly acknowledged in the thesis.

Date: __3/15/2019__   Mr. T.E. Igboamalu_____

Acknowledgement

First and foremost, I would like to thank my supervisor, Prof Evans Chirwa, for his excellent guidance and technical expertise, which set high standards for my PhD work. Every research student in our team could attest to his exceptional mentorship, exciting individuality, a resilient work ethic and a fun-loving charisma even in pressing situations. He is passionate about his students and goes the extra mile to advise and guide them throughout to obtain their degrees. He hand-picks his students and moulds them towards an exceptional professional career. His relationships to them, based on faith, could be compared to parent-child relationship. I would not have been able to go this far without him, most especially, he brings out the best technical skills in me. I would also like to thank him for funding my PhD research work and several conference and training exposures granted to me during this study.

I would like to express my heartfelt gratitude to colleagues in the research group at the Water Utilization and Environmental Division of the Department of Chemical Engineering, University of Pretoria, for their assistance and interest in my progress, and to Mrs Alette Devega and Mrs Elmarie Otto for their prompt assistance.

I would like to specially thank my father, Mr Igboamalu Francis Chukwudi, for his constant moral and spiritual support, and words of encouragement that helped me to reach the goals I set forward before starting this journey. My mother, Mrs Igboamalu Christiana Chinenye, has been a source of comfort and strength during the most difficult times. I would also like to take this opportunity to thank my siblings, Dr Igboamalu Chukwudi Christian, Mr Igboamalu Frank Nonso, Mr Igboamalu Henry Emeka, Mrs Obira Rita Ebele, Mrs Ubakwelu Stella Ogochukwu, Mrs Ndiwe Tina Chinyere, Mrs Edith Ifeoma, and my special twin sister Mrs Tonia Ujunwa.

Special thanks to God, my lovely, caring, kind and beautiful wife, Dr Igboamalu Silvia Chidimma, and my son, Igboamalu Brain Chukwudi jnr, for their support, words of encouragement and prayers.

Contents

List of Figures

List of Tables

List of Symbols

A	Cross-sectional area of a reactor column (L^2)
A_f	biofilm surface area (L^2)
C	Cr(VI) concentration at time, t (ML^{-3})
C_1	state variable (ML^{-3})
C_b	Cr(VI) concentration in the bulk flow (ML^{-3})
C_o	initial Cr(VI) concentration (ML^{-3})
C_r	Cr(VI) toxicity concentration (ML^{-3})
D_{wi}	dispersion coefficient (L^2T^{-1})
G	Gibbs free energy (KJ/mol)
j_c	Cr(VI) flux rate ($ML^{-2}T^{-1}$)
j_{flux}	mass transport rate (LT^{-1})
k	limiting constant (ML^{-3})
k_{ad}	adsorption rate coefficient (T^{-1})
K_c	Cr(VI) half velocity constant (ML^{-3})
k_d	cell death rate (T^{-1})
K_{mc}	maximum specific Cr(VI) reduction rate(T^{-1})
K_{ms}	maximum specific As(III) reduction rate(T^{-1})
K_s	As(III) half velocity constant (ML^{-3})
L	length of the reactor (L)
L_w	stagnant film thickness (L)
n	empirical dimensionless variable
Q	inflow rate ($L^{-3}T^{-1}$)
q_c	adsorption rate ($ML^{-3}T^{-1}$)
r_c	Cr(VI) reduction rate ($ML^{-3}T^{-1}$)
R_c	Cr(VI) reduction capacity coefficient (MM^{-1})
R_s	As(III) reduction capacity coefficient (MM^{-1})
S	As(III) concentration at time (ML^{-3})
S_r	initial As(III) concentration (ML^{-3})
t	time (T)

u	flow velocity (LT^{-1})
U	volume (L^3)
V	volume of the reactor (L^3)
V	velocity of flow (MT^{-1})
W	catalyst weight
X	biomass concentration at time, t (ML^{-3})
X^2	sum of deviation
X_o	initial biomass conc. (ML^{-3})
y	arbitrary variable
ρ_c	medium density (ML^{-3})
δ_{λ_i}	standard deviation
λ	model parameter by a constant

List of Abbreviations

AAS	Atomic adsorption spectrophotometer
AOX	Arsenic oxidase
APHA	American public health agency
ARR	Arsenic reductase
AS	Arsenic
ASBR	Anaerobic sequencing batch reactor
AWWA	American Water Works Association
BLAST	Basic logical alignment search tool
BMM	Basal mineral medium
CFU	Colony forming unit
CHRR	Cr(VI) reductase
CR	Chromium
CRB	Cr(VI) reducing bacteria
CSTR	Continuous stirred tank reactor
DASSLA	Differential algebra system solver
DLS	Damped least-square
DMA	Dimethyl arsenic acid
DMSO	Dimethyl sulfoxide
DNA	Deoxyribonucleic acid
DPC	Diphenyl carbohydrazide
EPS	Exopolly saccharides
ETP	Electron transfer process
FAD	Flavin adenine dinucleotide
FECR	Ferrochrome
GAC	Granular activated carbon
HPLC	High performance liquid chromatography
HRT	Hydraulic retention time
IC	Ion chromatography

LB	Luria-Bettani
LBB	Luria-Bettani broth
LMA	Levenberg-Marquardt algorithm
MG/KG	Milligram per kilogram
MG/L	Milligram per litre
MM	Millimetre
MO	Molybdenum
MSM	Mineral solution medium
MV	Millivolt
NAD	Nicotinamide adenine dinucleotide
NADP	Nicotinamide adenine dinucleotide phosphate
NCBI	National Centre for Biotechnology Information
NF	Nanofiltration
NM	Nanometre
OD	Optical density
ORP	Oxidation reduction potential
PAH	Poly aromatic hydrocarbon
PC	Plate count
BP	Base pair
PFR	Plug flow reactor
RBC	Rotary bed contactor
RO	Reverse osmosis
RRNA	Ribosomal ribonucleic acid
SB	Soy broth
SEM	Scanning electron microscopy
TEMP.	Temperature
TMA	Trimethyl arsenic acid
UF	Ultrafiltration
UG/L	Microgram per litre
UV	Ultraviolet
VSS	Volatile suspended solid
WHO	World Health Organization
WWTW	Wastewater treatment works

Research Outputs

Journal publications

1) Igboamalu T.E. & Chirwa E.M.N.,2018 "Autotrophic Oxidation of As(III) with Concurrent Cr(VI) Detoxification by a Mixed Culture of *Exiquobacterium profundum* and *Bacillus licheniformis*", *Journey of Hydrometallurgy.*, Revised paper submitted.

2) Igboamalu T.E. & Chirwa E.M.N., 2018. "Cr(VI) Remediation with Inorganic As(III) as an Electron Sink Immobilized in a Ceramic Bead Packed bed Biofilm Reactor". Chemical Engineering Transactions.

3) Mpumelelo T.M., Igboamalu T.E., & Chirwa E.M.N., 2018. "Phenol Degradation and Chromium(VI) Reducing Biofilm System: Effect of Shock-loading". Chemical Engineering Transactions.

4) Igboamalu T.E. & Chirwa E.M.N., 2018. "As (III) Oxidation and Electron Mass Transfer Kinetic in a Mixed Culture of *Bacillus sp*., and *Exiguobacterium sp*, from Cow Dip South African". Chemical Engineering Transactions: 10.3303/CET1864085.

5) Igboamalu T.E. & Chirwa E.M.N., 2017. "Kinetic Study of Cr(VI) Reduction in an Indigenous Mixed Culture of Bacteria in the Presence of As(III)". Chemical Engineering Transactions, 49, DOI:10.3303/CET1439207ISBN 978-88-95608-40-2; ISSN.

6) Igboamalu T.E. & Chirwa E.M.N., 2016. "Kinetic Study of Cr(VI) Reduction in an Indigenous Mixed Culture of Bacteria in the Presence of As(III)". Chemical Engineering Transactions, 49, DOI:10.3303/CET1439207ISBN 978-88-95608-40-2; ISSN.

7) Igboamalu T.E. & Chirwa E.M.N., 2014. "Cr^{6+} Reduction in an Indigenous Mixed Culture of Bacteria in the Presence of As^{3+}". Chemical Engineering Transactions, Volume 39, p. 1237-1242, Italian Association of Chemical Engineering/Associazione Italiana Di Ingegneria Chimica (AIDIC).

Conference proceedings

1) Igboamalu T.E. & Chirwa E.M.N., "Cr(VI) Reduction with As(III) as Inorganic Electron Source in a Continuous Flow Ceramic Bead Packed bed Bio-film Reactor with an Anaerobic Tank Retrofit: Pilot Study". Annual Water Environment Federation Technical Exhibition and Conference proceeding (WEFTEC) 2018, New Orleans Louisiana, USA.

2) Igboamalu T.E. & Chirwa E.M.N., "An Ideal Bioremediation Strategy for Arsenic (III) and Chromium (VI) Contaminated Site with Indigenous Mixed Culture of Facultative Bactria". WM Symposia conference proceeding 2018, Arizona, USA.

3) Igboamalu T.E. & Chirwa E.M.N., 2018. "Cr(VI) Remediation with Inorganic As(III) as an Electron Sink Immobilized in a Ceramic Bead Packed bed Biofilm Reactor". 21st Conference on Process Integration, Modelling and Optimisation for Energy Saving and Pollution Reduction Press conference proceeding 2018, Prague, Czech Republic.

4) Mpumelelo, T.M., Igboamalu, T.E., & Chirwa, E.M.N., "Phenol Degradation and Chromium(VI) Reducing Biofilm System: Effect of Shock-loading". 21st Conference on Process Integration, Modelling and Optimisation for Energy Saving and Pollution Reduction Press conference proceeding 2018, Prague, Czech Republic

5) Igboamalu T.E. & Chirwa E.M.N., "As (III) Oxidation and Electron Mass Transfer Kinetic in a Mixed Culture of Bacillus sp., and *Exiguobacterium sp*, from Cow Dip South African". International Conference on Industrial Biotechnology, IBIC conference proceeding 2018 Venice. Italy.

6) Igboamalu T.E. & Chirwa E.M.N., "Kinetic Study of Cr(VI) Reduction in an Indigenous Mixed Culture of Bacteria in the Presence of As(III)". 20th Conference on Process Integration, Modelling and Optimisation for Energy Saving and Pollution Reduction Press conference proceeding 2017, Tianjin China.

7) Igboamalu T.E. & Chirwa E.M.N., "Kinetic Study of Cr(VI) Reduction in an Indigenous Mixed Culture of Bacteria in the Presence of As(III)". 5th International Conference on Biotechnology proceeding 2016, Bologna.

8) Igboamalu T.E. & Chirwa E.M.N., 2014. "Cr^{6+} Reduction in an Indigenous Mixed Culture of Bacteria in the Presence of As^{3+}". 21st International Congress of Chemical and Process Engineering CHISA Conference proceeding 2014, Prague, Czech Republic.

9) Igboamalu T.E. & Chirwa E.M.N., "Kinetic Studies of Cr(VI) Reduction in an Indigenous Mixed Culture of Bacteria in the Presence of As(III)". Conference paper: 86th Annual Water Environment Federation Technical Exhibition and Conference (WEFTEC) 2014, New Orleans Louisiana, USA.

Book chapters

1) Evans M. Nkhalambayausi Chirwa*, Pulane E. Molokwane, Tshilidzi B. Lutsinge, Tony E. Igboamalu, Zainab S. Birungi. "Bioremediation of Industrial Wastes for Environmental Safety Volume 2: Biological Agents and Methods for Industrial Waste Management" *Springer Nature" Singapore,* 2018 (ISBN 978-981-13-3426-9).

CHAPTER 1

Introduction

1.1   Background

Arsenic (which originated from the Syrian word, and later from the Persian word, meaning yellow) is a chemical element represented by the symbol As and it was discovered in the 12th century by Albertus Magnus (Harper, 2001; Thomas Jefferson, 2018). It was formally used for human consumption (mixed with vinegar and chalk or rubbed on the face and arms) until its toxicity became widely known in the 18th century after numerous deaths, and was later used to commit murder (Alan, 1999; John, 2001; Vahidnia, 2007). Chromium (a Greek word meaning colour) is also a chemical element, represented by the symbol Cr, that was discovered in the 17th century as a red crystalline mineral crocoite and it was formally used as pigment (Wikipdia.org; Jefferson, 2018). These metalloids are known for their high toxicity and carcinogenicity to living organisms (Woutersen et al., 1986; OSHA Federal Register, 2006; Pechova & Pavlata, 2007). Toxic metals and metalloids pose a serious threat to the environment, mainly due to the increasing demand for products, of which the process of manufacturing results in the release of large volumes of waste containing metal and metalloid species (Mabrouk et al., 2014; Tsuji et al., 2014). Arsenic mostly exists in the environment as arsenite [As(III)] and arsenate [As(V)], the former being more toxic and mobile, whereas the latter easily precipitates as a hydroxide, which renders it less mobile and less toxic than As(III) (Singh et al., 2008; Cullen & Relmer, 2017). The highly oxidative metals and metalloids such as chromium, selenium, arsenic and others mainly originate from anthropogenic sources.

Chromium (Cr) exists in nature mainly as hexavalent chromium [C(VI)] and trivalent chromium [Cr(III)] (Lu et al., 2006; Oliveira, 2012). Other oxidation states of chromium are unstable such that they only occur transitionally under natural conditions. Of the two stable oxidation states of chromium, Cr(VI) is more toxic to living organisms and more mobile in the aquatic environment than the lower oxidation state [Cr(III)]. Cr(VI) toxicity is attributed to its high solubility and high

oxidizing potential (Shanker et al., 2005). Additionally, Cr(VI), which exists mainly as the oxyanions CrO_4^{2-} and $Cr_2O_7^{2-}$, does not partition easily in soil and other organic substrates because of its anionic valence state. In the environment, Cr(VI) may be reduced by living cells of certain organisms, either as necessity to detoxify the cell's immediate environment (Cervantes, 1991), or as a source of energy for cell growth and maintenance (Horitsu et al., 1987).

The energy for Cr(VI) reduction is derived from the oxidation of $NADH^+$ to release electrons to the cytochrome c,c_3 systems, which function as a conduit for electron flow to Cr(VI) reductase (Lovley & Philips, 1993; Chirwa & Wang, 1997a). The end products of the As(III) oxidation and Cr(VI) reduction readily form insoluble $Cr(OH)_3(s)$ and $As(OH)_5$, which precipitate easily at pH $\geq$ 5 (Meli, 2009; Kaimbi & Chirwa, 2015; Igboamalu & Chirwa, 2017). Cr(VI) pollution globally originates from both conventional sources, such as: chromate manufacture, electroplating, leather tanning, wood preservation, and the manufacture of dyes, paint pigment, pharmaceuticals and agricultural pesticides (Zakaria et al., 2007; Molokwane et al., 2008; Kumar et al., 2017). As(III) and Cr(VI) may co-exist in effluents from industrial processes such as wood treatment and gold enrichment. In many cases, the polluted waste streams are discharged directly into the environment without proper treatment (Smith & Steinmaus, 2009; Igboamalu & Chirwa, 2017).

Currently the removal of Cr and As at contaminated sites relies heavily on either pure chemical or physical/chemical methods (Park et al., 2005; Igboamalu & Chirwa, 2014). Chemical precipitation methods generate large volumes of toxic sludge, which is difficult to dispose of (Molokwane, 2010). The method of dilution to achieve a low-strength effluent is considered environmentally unsafe. The most recent proposals on bioremediation of toxic metals and metalloid species offer a possible environmentally friendly and cost-effective method for treatment and removal of metals and co-pollutant complexes such as Cr(VI), As(III), Se(VI)/Se(IV), and As(III)/Cr(VI) (Wessels, 2017; Bansal et al., 2017; Molokwane & Chirwa, 2013; Mtimunye & Chirwa, 2014).

Several bioremediations of toxic metals have utilized diverse microbial flora of *Bacillus sp*, *Exiquobacterium profundum sp* and *Staphylococcus sp*., which is resistant to this metal (Crapart et al., 2007, such as: *Exiguobacterium profundum sp* (a moderately thermophilic), *Bacillus sp*. JDM-2-1 *Staphylococcus capitis* (Zahoor & Rehman, 2009), *Bacillus safensis MS11*[101 Staphylococcus sciuri (Chellaiah Edward Raja, 2012), *Staphylococcus saprophyticus*, SIS22; *Staphylococcus sciuri*, SIS51 and *Staphylococcus xylosus* (Rizvi et al., 2016), *Staphylococcus haemolyticus*, *Staphylococcus saprophyticus*, *Staphylococcus epidermidis*, *Bacillus cereus* and *Bacillus*

thuringiensis (Igboamalu & Chirwa 2014). Microorganisms inhabit toxic metalloids by developing metal resistance mechanisms to protect themselves from toxic substances (Ahemed, 2014). Studies have demonstrated that vast facultative microbes could be used for detoxification of metalloids containing waste. Near complete As(III) oxidation was reported in a facultative microbe utilizing nitrate (NO_3^-) (Sun et al., 2010a) or chlorate (ClO_3^-) as terminal electron acceptors while conserving energy for cell growth and metabolism (Sun et al., 2010b). As(III) oxidation was independently achieved in a facultative microbe utilizing bicarbonate as sole carbon source (Dastidar & Wang, 2009). Independent Cr(VI) reduction and As(III) oxidation by Bacillus firmus TE7 were achieved (Bachate et al., 2013). Also, simultaneous redox conversion of Cr(VI)and Ar(III) under acidic conditions was achieved (Wang et al., 2013).

A preliminary study by Igboamalu and Chirwa (2014) showed a potential link between the oxidation of As(III) and the reduction of Cr(VI) under aerobic autotrophic conditions. In the 2014 study by Igboamalu and Chirwa, a two-step process in terms of Cr(VI) reduction was hypothesized whereby, in stage 1, Cr(VI) could be reduced to Cr(V) utilizing the microbial cell's NADH-dihydrogenase ($NADH^+$-dh). $NADH^+$ is readily oxidized to NAD, thereby donating two electrons to the membrane electron transporting proteins such as $NADH^+$-dh, ubiquinone and cytrochrome c-c_3, which in turn reduces the Cr(VI) reducing mediator — Cr(VI) reductase (Cervantes et al., 2001; Barak et al., 2006). According to Singh et al. (2008), the thermodynamics of the system dictates that the pentavalent intermediate [Cr(V)] should quickly decay to Cr(III) in the presence of any oxidizing agent in solution. When Cr(V) serves as the intermediate, As(III) will release two electrons ($2e^-$) coupled to two protons ($2H^+$) to reduce Cr(V) to Cr(III) (Igboamalu & Chirwa, 2017).

1.2   Aim and objectives

The aim and objectives of the thesis were to evaluate the use of biological catalysis to achieve detoxification of multiple pollutants such as As(III) and C(VI) in a contaminated site through electron transfer anaerobic condition. To achieve this objective, the experiment is sub-divided into four parts as follows:

– An evaluation of the performance of individual species in the current mixed culture to develop a co-culture system

- An evaluation of the fate of As(III) during Cr(VI) reduction at higher concentrations of both As(III) and Cr(VI) in a batch system

- An evaluation of the biofilm reactor systems in order to re-run it with media with better attachment properties (i.e. glass and ceramic bead packed bed media), in order to evaluate the fate or response of As(III) and Cr(VI) in the system at shock load effect

- Development of the kinetic model that would capture the co-dependence between As(III)→As(V) oxidation and Cr(VI)→Cr(III) reduction, and bio-kinetic parameters estimation of the strains using AQUASIM 2.0.

1.3 Methodology

The methodology of this present work was based on previous studies on Cr(VI) and its co-pollutant (As(III)). Previously, it was established that microorganisms exposed to toxic metals/metalloid ions developed diverse resistance mechanisms to tolerate the toxicity of toxic metal ions (Bachate et al., 2013). These resistance mechanisms involve specific biochemical pathways that can alter chemical properties of toxic metal ions, resulting in their detoxification (Silver & Phung, 2005). Several studies have been reported on biological reduction of Cr(VI) and oxidation of As(III) (Molokwane et al., 2008; Zakaria et al., 2007). Information from these studies was used to establish the theory of the present study.

1.4 Outline of dissertation

The outline of this dissertation is listed as follows:

Chapter 1 describes the background information, and the objective of this thesis.

Chapter 2 reviews current and previous studies on chromium and arsenic.

Chapter 3 describes materials and methods used in this study.

Chapter 4 presents experimental results and interpretation.

Chapter 5 describes Cr(VI) reduction and As(III) oxidation in a biofilm reactor.

Chapter 6 describes Cr(VI) reduction and the As(III) oxidation co-dependent model

Chapter 7 presents the conclusion of the thesis and future work required.

1.5   Research significance

South Africa is a huge industrial producer of ore and other metalloids. This can be correlated to high environmental pollutants in aqueous environments. During steel and chromate production, considerable quantities of waste are formed, which can be toxic, hence making the treatment of ferrochrome waste materials necessary. However, remediation strategies of this are of paramount importance, which requires that the neutralisation of multiple pollutants should be effective. According to Beukes et al. (2012), the remediation strategy in South African ferrochrome industries with regard to waste treatment involves Cr(VI) reduction with ferrous iron. This treatment strategy is inefficient as it is not cost effective and may produce harmful sludge. Exploring the ideal treatment strategy proposed, it could be perceived as an alternative to South African ferrochrome producers' treatment strategy, as it is cost effective and generates less harmful sludge at neutral conditions.

CHAPTER 2

Literature review

2.1 Chemistry of arsenic (As) and chromium (Cr)

2.1.1 Arsenic (As)

Arsenic (As) (atomic number: 33 and atomic weight: 74.9216), is a group (V) member of the periodic table and classified as a transition metal (Wackett et al., 2004). It is the 20th most profuse metalloid in the earth's crust, with a level of 1-2 mg/kg (Bhumbla & Keefer, 1994; Lievremont et al., 2009). It is known to be both acute and chronic to humans, and odourless, colourless and tasteless (Robert & Schwartz,1996). As a transition metal (metalloid), it mostly exists in different oxidation states, having arsenite (As(III)) and arsenate (As(V)) as the most dominant inorganic species in the environment (Smedley & Kinniburgh, 2002). In addition, other organo-arsenical species include: monomethylarsonic acid (MMA) and dimethylarsinic acid (DMA) (Ramech & Kumar, 2010) (see Figure 2.1).

Factors controlling the speciation of arsenic in the environment are mainly pH and redox-potential (Smedley & Kinniburgh, 2002) (see Figure 2.2). However, based on the physico-chemical features of the site and the structure of the microbial population, discrete arsenic species may predominate (David et al., 2009). Aqueous speciation of arsenic species shows that arsenate species H_3AsO_4 predominantly dominate at pH $\leq$ 2.2, whereas arsenite species predominate at pH as follows: ($H_3AsO_3^o$ at pH $\leq$ 9.2, $H_2AsO_3^-$ $\geq$ 9.2 and $HAsO_3^{2-}$ $\geq$ 12.3) (Wagman et al., 1968; Ferguson & Gavis, 1972). Equilibrium equation (2.6-2.7) shows that $H_2AsO_3^-$ anion is dominant in basic or slightly acidic solutions, while $HAsO_3^{2-}$ dominates in basic solutions (Wagman et al., 1968). The
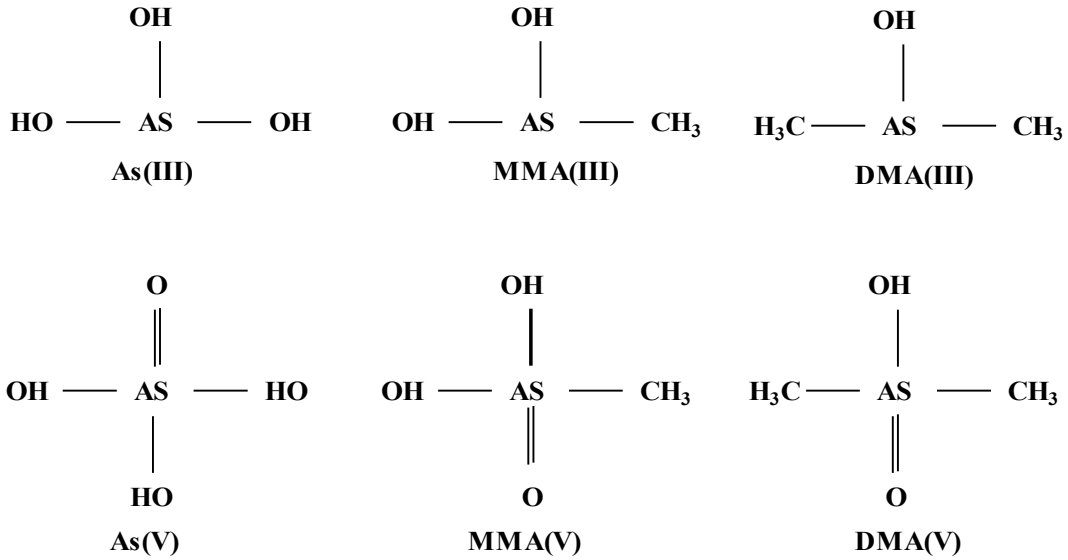
Figure 2.1: Arsenic species generally found in natural waters (Ramesh & Kumar, 2010)
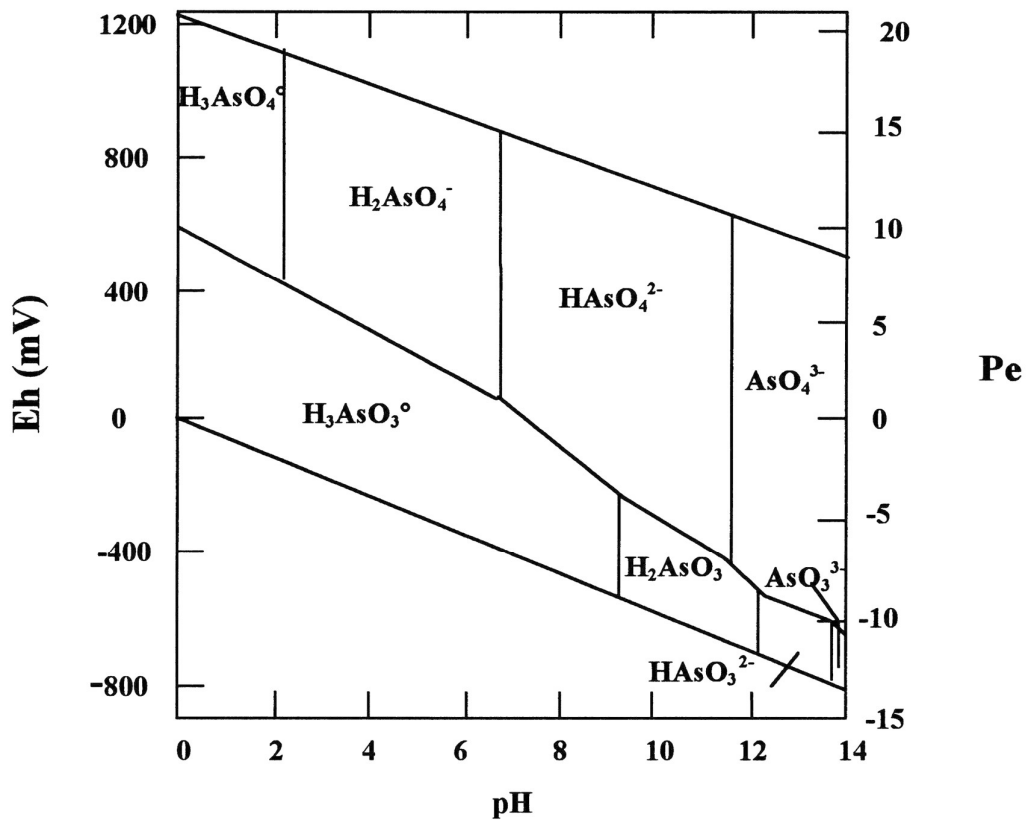
Figure 2.2: Redox potential (Eh)–pH diagram for aqueous arsenic species in the system AsO_2-H_2O at 25°C and 1 bar total pressure (Smedley & Kinniburgh, 2002)

As(V)/As(III) couple has a potential of + 130 mV, making it a much stronger oxidant than sulfate (sulfate/sulfide = −220 mV) (Oremland et al., 2009).

$$H_3AsO_3^o \Leftrightarrow H_2AsO_3^- + H^+ \qquad\qquad K_{a4} \quad = 10^{-9.2} \qquad\qquad\qquad (2.1)$$

$$H_2AsO_3^- \Leftrightarrow HAsO_3^{2-} + H^+ \qquad\qquad K_{a5} \quad = 10^{-12.3} \qquad\qquad\qquad (2.2)$$
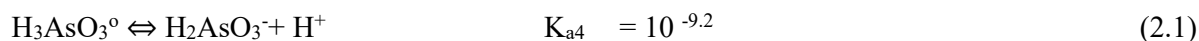
The biochemistry of arsenic species has also been demonstrated by researchers (Wang et al., 2013; Sun et al., 2010; Aniruddha & Wang, 2010; Sun et al., 2008). Aniruddha and Wang, (2010) reported that As(III) can be oxidised to As(V) in the presence of oxidizing agent by donating two electrons, while generating a considerable amount of energy for cell growth and metabolism (Equation 2.3).

$$As(III) \quad \rightarrow As(V) + 2e^- + energy \qquad\qquad\qquad\qquad\qquad (2.3)$$

2.1.2 Chromium (Cr)

Chromium (Cr) (atomic number: 24 and atomic weight: 51.9961) is a group VI member of the periodic table and is classified as a transition metal (Wackett et al., 2004). Chromium is the seventh most abundant element in the earth's crust, with an average concentration of 100 mg/kg (Oliveira, 2012). It exists in different oxidation states ranging from (-2) to (+6) (Zayed & Terry, 2003). Among chromium oxidation states, only chromium (+3) and (+6) are the most stable under natural pH and temperature conditions (Shupak, 1991). However, the existence and transformation of this metal/metalloid is controlled by physiochemical processes such as: oxidization and reduction reaction, electrochemical potentials and pH, precipitation or adsorption process, and solubility (Kimbrough, et al., 1999). The redox potential (Eh) and soil pH determine the possible oxidation of Cr from the trivalent to hexavalent form, as shown in Figure 2.3.

In aqueous state, the existence of chromium species is dependent on the pH of the aqueous solution and total Cr(VI) concentration (Dhal et al., 2013). Cr(III) predominates at pH less than 3.5, trivalent chromium hydroxyl species ($Cr(OH)^{2+}$, $Cr(OH)_2^+$, $Cr(OH)_3$, and $Cr(OH)_4^-$) predominates at pH greater than 3.5, while Cr(VI) (CrO_4^{2-}) on the other hand, predominates at or above pH of 6 (Barnhart, 1997). However, equilibrium equation (2.4–2.6) illustrates the existence of Cr(VI) species in aqueous solutions, where ($HCrO_4^-$) exists at pH values of 1 to 6 (Park et al., 2005). The

dichromate ion ($Cr_2O_7^{2-}$) is formed by dimerization of $2HCrO_4^-$ in Cr(VI) concentration above 10^{-2} (Sharma, 2002).

$$H_2CrO_4 \Leftrightarrow HCrO_4^- + H^+ \qquad K_{a1}=10^{0.6} \qquad\qquad (2.4)$$

$$HCrO_4^- \Leftrightarrow CrO_4^{2-} + H^+ \qquad K_{a2}=10^{-5.6} \qquad\qquad (2.5)$$

$$Cr_2O_7^{2-} + H_2O \Leftrightarrow 2HCrO_4^- \qquad K_{a3}=10^{-2.2} \qquad\qquad (2.6)$$
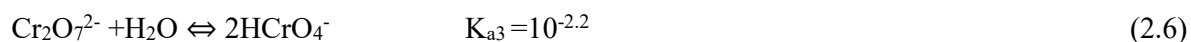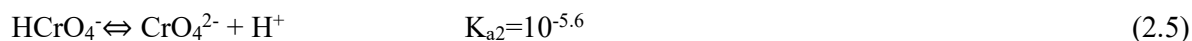
The biochemistry of Cr species has been demonstrated by many researchers (Molokwane et al., 2008; Suzuki et al., 1992). Suzuki et al. (1992), reported that NADH in the cell protoplasm can serve as an electron donor in stepwise reduction of Cr(VI) to intermediate Cr(V), which accepts two electrons from the same co-enzyme to yield Cr(III), as shown in equations 2.7 and 2.8. It has been suggested that the energy generated from Equation 2.8 can facilitate the microbial cell growth and metabolism (Wang & Shen, 1995; Suzuki et al., 1992).

$$Cr(VI) + \{NADH\}\ e^- \quad \rightarrow \quad Cr^{5+} \qquad\qquad (2.7)$$

$$Cr^{5+} + 2e^- \quad \rightarrow \quad Cr(III) + Energy \qquad\qquad (2.8)$$
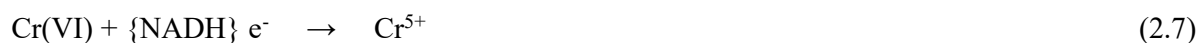
2.2 Occurrence and source of arsenic and chromium

2.2.1 Arsenic

Arsenic (a Syrian word that originated from the Persian word meaning yellow) is a chemical element represented as As and was first discovered in the 12th century by Albertus Magnus. It was formally used for human consumption (mixed with vinegar and chalk or rubbed on the face and arms) until its toxicity became widely known in the 18th century after numerous deaths, and it was later often used to commit murder (Alan, 1999; John, 2001; Vahidnia, 2007). Arsenic mostly occurs because of rock weathering and volcanic activities (Rhine et al., 2006). Examples of naturally occurring arsenic-bearing minerals (rocks) include: arsenian pyrite ($Fe(AsS)_2$), realgar (AsS), arsenopyrite (FeAsS), and orpiment (AsS_3) (Nordstrom, 2002). Arsenic concentration in igneous, metamorphic

and sedimentary rock has been reported ranging from 1.5-18 mg/kg (Smedley & Kinniburgh, 2002; Webster, 1999).
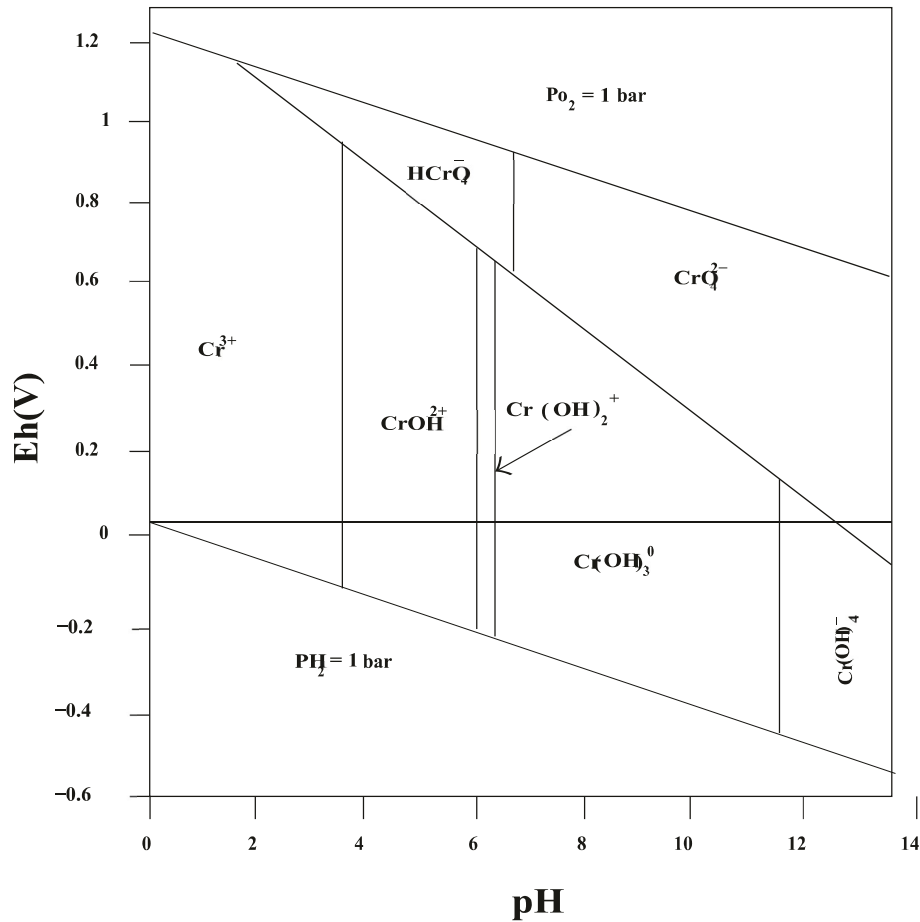
Figure 2.3: Redox potential (Eh)-pH diagram for Cr–O–H system **(**Palmer & Wittbrodt, 1991**)**

Geochemically, it is linked with sulphurous minerals of sulphur, iron and several other metals (such as Au, Ag, Cu, Sb, Cr, Ni and Co) (Lie`vremont et al., 2009). Anthropogenic activities such as smelter slag, coal combustion, run-off from mine tailing, hide tanning waste, pigment production, paint and dye, pharmaceutical manufacturing, wood processing, the glassmaking industry, electronics industry, chemical weapons and pesticides, etc. are the major source of arsenic contamination in ground water and soil sediments (Bhumbla, 1994, Kohler et al., 2001; Han et al., 2003; Cheng et al., 2009). In addition, mine wastewater and effluent from acid mine drainage have elevated arsenic contents (Williams, 2001; Johnson, 2003).

Arsenic concentration in soils generally ranges between 5-10 mg/kg (Boyle & Jonasson, 1973) and is governed by principal factors such as climate, organic and inorganic component of the soil, and redox potential respectively (Aniruddha & Wang, 2010). In natural waters, arsenic is generally present at very low concentration. However, Smedley et al., (1996) reported arsenic concentration in the range of 100-5,000 μg /L in unpolluted fresh waters located in areas of sulfide mineralization and mining. The concentration of arsenic in seawater generally varies between 0.09-24 μg/L, whereas, in fresh water, the concentration can vary between 0.15-0.45 μg/L respectively (Leonard, 1991). However, the presence of arsenic in the air is associated with wind, volcanic emissions, sea spray, forest fires and volatilization, which occur because of biomethylation (Lie`vremont, 2009).

2.2.2 Chromium

Chromium (a Greek word meaning colour) is also a chemical element (represented as Cr) and was discovered in the 17th century as a red crystalline mineral crocoite and formally used as pigment (Wikipdia.org; Jefferson, 2018). Chromium compounds are found in the environment from natural sources in the form of ore, in the hexavalent state. Free chromium in the form of chromate mainly originated from industrial activities (WHO, 1988; Merian, 1984). Naturally, chromite is the most prevalent form in the environment. It consists of two main refined products, which are: ferrochromium and metallic chromium (Westbrook, 1983; Hartford, 1983). Second, lead chromate (as crocoite) and potassium dichromate (as lopezite) are known to occur naturally in the environment (IARC, 1990). Industrial activities such as mining and smelting, industrial wastewater and leaching of soluble Cr(VI) compounds from wastes such as mine tailings, waste rock, dust and slag piles are the major source of chromium in the environment (Barceloux, 1999). Figure 2.4 indicates the total input of chromium in the environment; where metal use is the highest chromium input, followed by rock weathering and coal combustion (Merian, 1984).

Chromium is found in all matters, such as: rock, air, water and soil (Kimbrough, et al., 1999). In rocks, the most important mineral deposit of chromium is chromite (Mg, Fe^{2+}) (Cr, Al, Fe^{3+})$_2$O$_4$, which, however, is rarely pure (Kimbrough et al., 1999). The concentration of chromium in rocks varies from an average of 5 mg/kg (range of 2-60 mg/kg) in granitic rocks, to an average of 1800 mg/kg (range, 1100-3400 mg/kg) in ultrabasic and serpentine rocks (US NAS, 1974b). Chromium is present in most soils in its trivalent form, although Cr(VI) can occur under oxidizing conditions (ATSDR, 2008a). In the USA, the geometric mean concentration of total chromium was 37.0 mg/kg (range, 1.0-2000 mg/kg) based on 1319 samples collected in contaminated soils (ATSDR, 2000),

whereas at 173 Canadian sites, chromium soil concentration ranged from 10-100 mg/kg (d.w.) (CEPA, 1994c).

The concentration of chromium in uncontaminated waters is extremely low (< 1 μg/L or < 0.02 μmol/L) (CEPA, 1994c). Anthropogenic activities (e.g. electroplating, leather tanning) and leaching of wastewater (e.g. from sites such as landfills) may cause contamination of the drinking water (EVM, 2002). In the air, chromium is usually introduced through forest fires, volcanic eruptions, combustion and industrial emissions. Cr(VI) is reported to account for approximately one third of the 2700-2900 tons of chromium emitted into the atmosphere annually in the USA (ATSDR, 2008a). Based on USA data collected from 2106 monitoring stations from 1977 to 1984, the arithmetic mean concentrations of total chromium in the ambient air (urban, suburban, and rural) were in the range of 0.005-0.525 μg/m^3 (ATSDR, 2000).
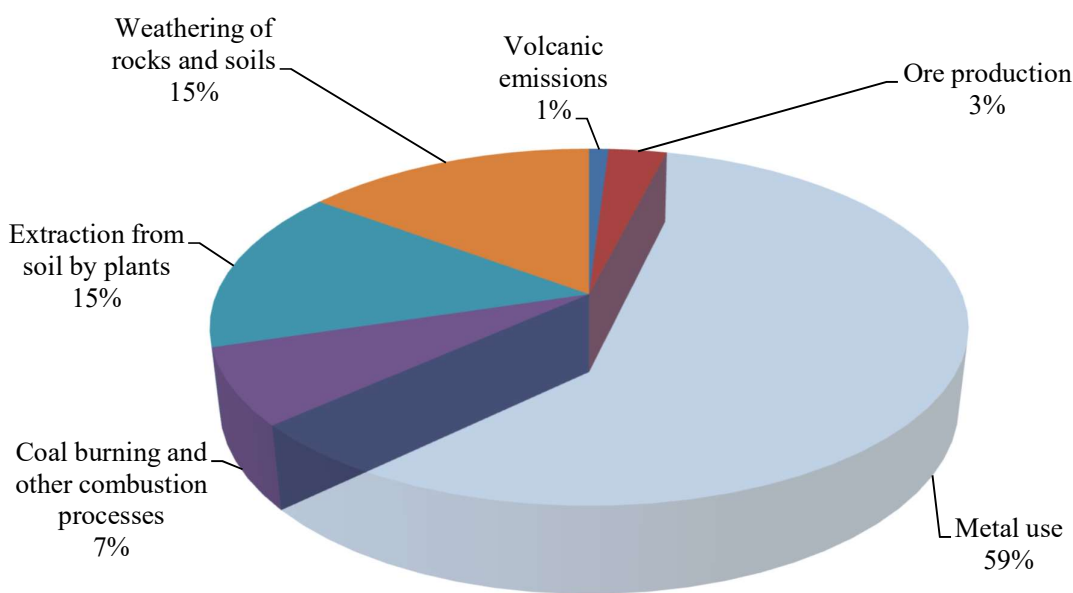
Figure 2.4: Total input of chromium in the environment (Mirian, 1984)

2.3 Environmental interaction of arsenic and chromium

As mentioned earlier, anthropogenic sources such as coal burning, mining operation and smelting, etc., are the major sources of these metalloids in the environment. The ultimate source of arsenic on the Earth's surface is igneous activity (Nriagu, 1994). Microbes carry out redox and covalent bond chemistry and play an important path in the metallic geo-cycle. Plants and animal bio-

accumulate these metallic compounds to levels above the environments limit (Rita Mukhopadhyay et al., 2002).

The major sources of human contamination and occupational exposure to arsenic are the burning of coal and industrial metal smelting, and more recently the semiconductor industry, as well as release from arsenic-rich ores during mining (Mukhopadhyay et al., 2002). Biomining releases soluble arsenic from rock and produces local environments of high and toxic arsenic levels. As(III) can also be released from arsenate-laden sediments by arsenate-respiring bacteria leading to arsenic contamination of the ground water (Oremland & Stolz, 2003).

The arsenate-respiring bacteria generally use As(V) as a terminal electron acceptor in the anaerobic respiration process (Oremland & Stolz, 2003). The released As(III) can be further oxidized to As(V) by certain bacteria via a detoxification mechanism or utilize the energy released during the oxidation process for cellular growth (Stolz et al., 2006). Because of the oxidation process, As(V) may be converted to water or lipid soluble organic compounds such as methylarsonic acid or dimethylarsinic acid (DMA), trimethylated arsenic derivatives (TMA), arsenocholine, arsenobetaine, arsenosugars, and arsenolipids by marine organisms such as phytoplankton, algae, crustaceans, molluscs, and fish (Knowles & Benson, 1983).

The possible processes in biogeochemical cycling of arsenic in the environment is described as follows: The arsenic geocycle is completed with the conversion of arsenobetaine back into inorganic arsenic species because of microbial metabolism (Dembitsky & Levitsky, 2004). Then, the arsenate (the main arsenic compound in seawater) is taken up by marine organisms, ranging from phytoplankton, algae, crustaceans, molluscs and fish (Knowles et al., 1983; Frankenberger, 2001). However, some arsenic is reserved by phytoplankton and metabolized into complex organic compounds. The transformation of inorganic arsenic into lipid-soluble compounds might be an adaptive mechanism for marine phytoplankton (Mukhopadhyay et al., 2002). These organisms are themselves consumed and metabolized by marine animals. Fish and marine invertebrates retain 99% of accumulated arsenic in organic form; and crustacean and mollusc tissues contain higher concentrations of arsenic than fish.

The chromium cycle in the environment is described as follows: As stated earlier, microbes play an important role in the cycle of chromium. The cycle consists of chromium from rocks and soil carried by water, animal and human to water. Another cycle consists of airborne chromium from natural

sources, such as fires, and from the chromate industry. This cycle also contains some hexavalent chromium, with by-products going into the water and air, but a very significant portion goes into the repository, the ocean, where it ends up as sediment on the ocean floor (Who, 1988; Kim et al., 2010).

2.4 Health impacts of arsenic and chromium

2.4.1 Arsenic (As)

The toxicity effect of hexavalent arsenic is a public health concern, considering its acute and chronic carcinogenic effect on humans (Mukhopadhyaya et al., 2002). This is because of wide utilization of arsenic in industrial and agrochemical applications (Lim & Shukor, 2014). The oxidation state of this metalloid determines its toxicity. Arsenic, like chromium, is also known to cause environmental and health problems to human and living organisms (Singh et al., 2008). Like Cr(VI), health impacts such as skin, liver, lung, bladder, kidney, urinary tract cancer, cardiovascular stress and hematopoietic system disorder have been reported on ingestion or inhalation of water or air contaminated by elevated concentrations of hazardous arsenic (Smith et al., 1992; Robert, 1996; Lim & Shukor, 2014). Factually, this affects lots of people around the world, but is particularly distinct in the deltaic regions of South Asia (e.g. Bangladesh, West Bengal), and also in Taiwan, and Cambodia (Oremland et al., 2009). Studies in Argentina have found increased bladder cancer risks associated with high levels of arsenic in drinking water, but little data exists about risks at lower concentrations (Michael et al., 2003). In Taiwan, India and Bangladesh, arsenic poisoning was called "black foot disease" because of the necrotic destruction of tissue (Mukhopadhyaya et al., 2002).

Due to the high toxicity of arsenic, the maximum contamination level of arsenic in drinking water was set at a much lower level of 10 µg/L (USEPA, 2001). This limit was later adopted by the European Union in 1998 (Lim et al., 2014). In 2006, the United States also adopted the WHO standard for lowering the federal drinking water standard or maximum limit of arsenic from 50 μg/L to 10 μg/L (Root et al., 2009). However, different countries on the globe have set the maximum permissible limits or standard of arsenic concentration in drinking water to regulate or minimize its health impacts (see Figure 2.5).

2.4.2 Chromium (Cr)

A reduced form of chromium (Cr(III)) has been reported as an essential micronutrient in the human diet at health acceptable concentration, as it is requisite for the normal sugar, lipid and protein metabolism of mammals (Mordenti & Piva, 1997), although there are uncertainties if chromium in reduced form (Cr(III)) is really an essential nutrient for microorganisms since no essential metabolic role has been reported to date (Ahemad, 2014). Regardless, an elevated level of chromium concentration has been reported to be very chronic and acutely toxic (Mak, 2012). Chromium toxicity depends intensely on its speciation, since different species exert different effects on animals, microbes and humans. Chromium is known for environmental health problems after exposure of organisms to moderate to high concentrations (Sharma et al., 1995). The toxicity is attributed to high solubility, mobility and bioavailability of the hexavalent state (James, 2002; Chirwa & Molokwane, 2011).

Argentina	AR	India	IN
Bangladesh	BD	Mexico	MX
Cambodia	KH	Nepal	NP
China	CN	New Zealand	NZ
Chile	CL	Australia	AU
Taiwan	TW	Jordan	JO
United State of America	USA	Japan	JP
Vietnam	VN	Canada	CA
SouthAfrica	SA		

	AR	BD	KH	CN	CL	IN	MX	NP	NZ	TW	USA	VN	AU	JO	JP	CA	SA
Country	50	50	50	50	50	10	50	50	10	10	10	10	7	10	10	25	10
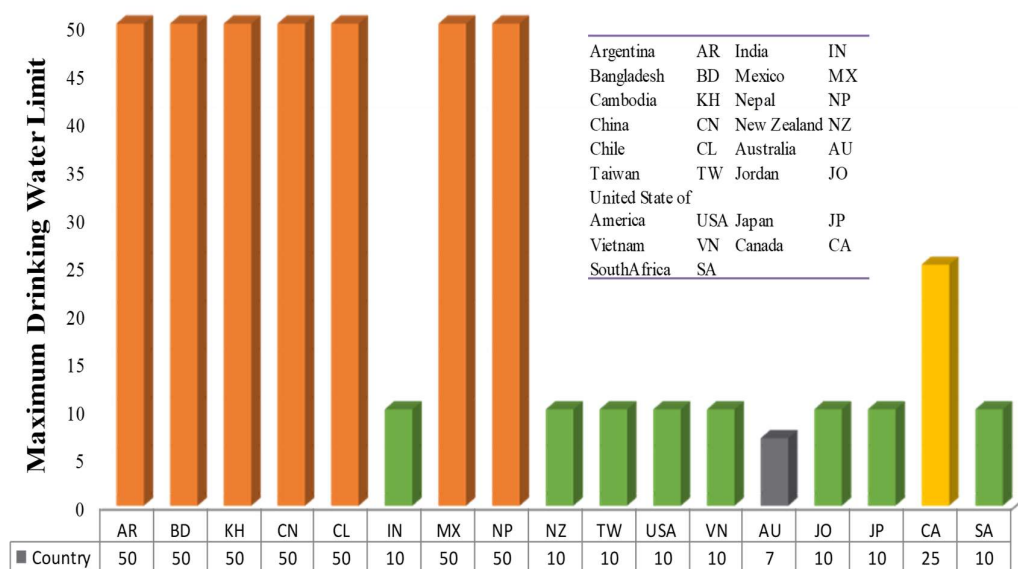
Figure 2.5: World arsenic maximum drinking water limit (Mohana & Pittman, 2007)

Among different oxidation states, Cr(VI) species, being strong oxidants, are more toxic (comparatively, 1 000 times more toxic than Cr(III) forms) and cause oxidative damage because of their mutagenic and carcinogenic nature (Chirwa & Molokwane, 2011). Cr(III), on the other hand, is relatively less toxic because it fails to cross through the membranes owing to its low solubility and tendency to be adsorbed in organic carbon and mineral surfaces (Cervantes et al., 2001; Codd et al., 2001; Daulton et al., 2007; Ahemad, 2014). It has an affinity with inorganic compounds and

consequently forms insoluble complexes that precipitate generally in the form of hydroxides, oxides, and sulphates (Nickens et al., 2010; Chirwa & Molokwane, 2011; Ahemad, 2014).

On ingestion or inhalation of Cr(VI) contaminated water or air, nose, throat, and lung irritation, kidney and liver cancer or even death have been reported (Barceloux, 1999). Additionally, Cr(VI) undergoes a redox cycle in the cell by reacting with several reducing compounds: NAD(P)H, FADH2, pentoses, cysteines, and antioxidants (ascorbate and glutathione), as well as one-electron reducers (glutathione reductase), to regenerate unstable intermediate Cr(V) (Ahemad, 2014). The regenerate intermediates produce a reactive oxygen species that easily combines with DNA-protein complex, modifying the cell DNA structure of the cell (Cervantes et al., 2001; Cervantes & Campos-García 2007; Cheung & Gu 2007; Nickens et al., 2010).

Finally, it changes the structure of soil microbial communities, thereby reducing microbial activities (Turpeinen et al., 2004). However, due to the toxic effect of chromium, the maximum regulatory standard of Cr(VI) and total chromium for drinking water, surface water and soil was set at 0 and 50 µg/L, 50 and 100 µg/L, and 250 µg/L respectively (Environmental Quebec, 1999). The first step in remediation of chromium often involves reduction of all hexavalent species to trivalent state, followed by extraction through precipitation. This conversion is beneficial since Cr(III) is about 1000 times less toxic than Cr(VI) (Sharma et al., 1995; Petrilli & Flora, 1997).

2.5 Arsenic, chromium production and industrial uses

Chromium ore is mined in many countries, but more than 90% of chromite comes from South Africa, Kazakhstan, India, Brazil, Finland, Turkey and Zimbabwe (Hoffmann et al., 2002). South Africa is among the largest chrome ore producers in the world, accounting for about 44% chrome ore production, as shown in Figure 2.6 (Mintek, 2004; Barhart, 1997). Based on 2007 statistics, the South African ferrochrome smelting industry produces approximately 46% of the global production volume of ferrochrome (FeCr), such being in the form of charge chrome (typically containing 48-54% Cr) (ICDA, 2008). However, there are currently 14 separate FeCr smelter plants in South Africa, with a combined production capacity of 4.4 million tons/year (Beukes et al., 2012).

Industrial utilization of chromium started in chromite mining, typically ferrous chromite, and its demand for different forms of chromium has continued to increase through the last decades (Kimbrough, et al., 1999). Chromium minerals such as crocoite ($PbCrO_4$) are too rare to be of profitable value such as chromium ores (Klein & Hurlbut, 1999). Chromite, on the other hand, is

one of the first minerals separated from a cooling magma, and is usually associated with ultrabasic rocks such as peridotites and serpentines, etc. (Klein & Hurlbut, 1999). Most industrial use of chrome includes: stainless steel production, pigment production, electroplating, leather tanneries, fungicide production and wood preservation, and as a catalyst in the synthesis of organic chemicals, etc. (Sandvik, 2004; Lipscher, 2004; Katz & Salem 1994; Barnhart, 1997). Steel industries are the major users of chromium, where steel in the form of iron and alloy is mixed with about 12% chromium to produce a non-corrosive stainless steel (Sandvik, 2004; Brown, 1995). Among the metal used, the metallurgical industries contribute up to 90%, followed by chemical (5%) and refractory industries (5%) (see Figure 2.7) (Dhal et al., 2013).

Arsenic utilization started in the medical field over 2 500 years ago when it was mainly consumed for the improvement of breathing problems as well as to give freshness, beauty, and plumpness to women's figures (Mendal & Suziki, 2002). Arsenic in the form of arsenic trioxide (As_2O_3) is one of the most common forms of arsenic, which is often used in manufacturing, the agricultural industry, and for medical purposes such as in the treatment of acute promyelocytic leukaemia (Ratnaike, 2003). Higher utilization of arsenic trioxide in suicide cases in the 18th century was reported and was referred to as "inheritance powder" (Oremland & Stolz, 2005). Arsenic trioxide has also proven to be useful in criminal homicides due to its unique characteristics: tasteless, colourless, highly toxic, and soluble in water (Rosen, 1999; Oremland & Stolz, 2005). During the 1970s, arsenic was mainly used in the agricultural industry in the form of an insecticide component to get rid of insects (Mandal & Suzuki, 2002; Cervantes et al., 1994; Spiegelstein et al., 2005). Arsenic was also used as cotton desiccants and wood preservatives (Mandal & Suzuki, 2002), in the ceramic and glass industry, the pharmaceutical industry, as food additives and in pigment manufacturing (Cervantes et al., 1994; Ratnaike, 2003).

Due to its high industrial utilization and the mining process, environmental contamination by these metals is of great concern and has received a lot of attention, and consequently legislation for the protection of the environment has gradually become more rigid. Figure 2.8 shows world metal contamination, where chromium and arsenic compounds are the most environmental contaminated metalloids, accounting for about 48% and 52% concentration when compared to other metal contamination countries (Dhal et al., 2013).

2.6   Arsenic and chromium removal techniques, and limitations

In a developing country like South Africa, for example, rapid mining activities have increased the demand for wastewater treatment and drinking water security. Compliance with increasingly stringent standards for heavy toxic metal in drinking water has led to the extensive application of water treatment systems for removal of contaminants. Due to the chronic and acutely carcinogenic effect of these metalloids, the minimum drinking water limit of arsenic and chromium, for example, was set at 50 ug/L and < 1 µg/L respectively (CEPA, 1994c; Mondal et al., 2013; Janet et al., 2016). However, there is a need to improve existing practices and to adapt future implementation. Currently, there are several methods for removing these metalloids from a contaminated site.

	South Africa	Iran	Finland	Others	Russian	Brazil	Madagasca	Turky	Zimbabwe	India	Kazakhstan
Countries	44	1	4	6	1	4	1	4	4	13	18
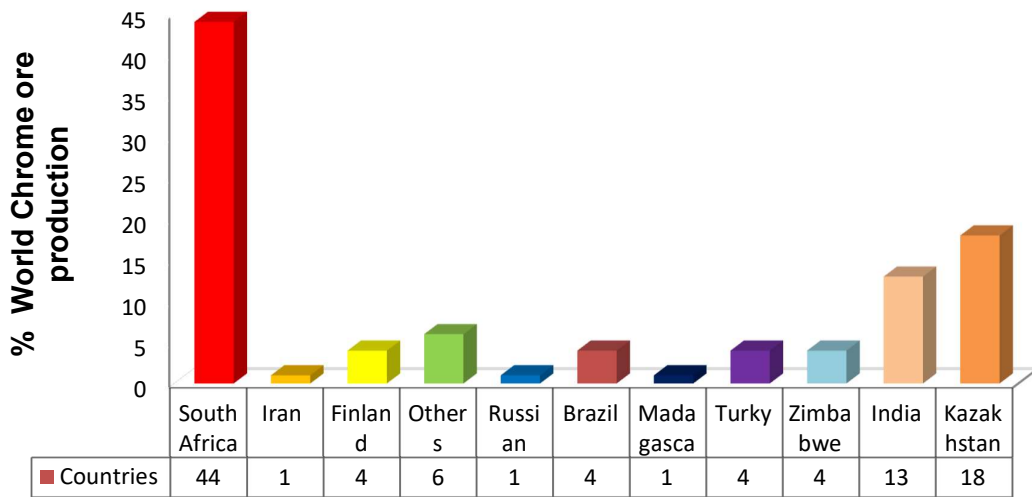
Figure 2.6: World chrome ore production (Armitage, 2002)

	Metallurgical	Chemical	Refractory
Chrome industries	90	5	5
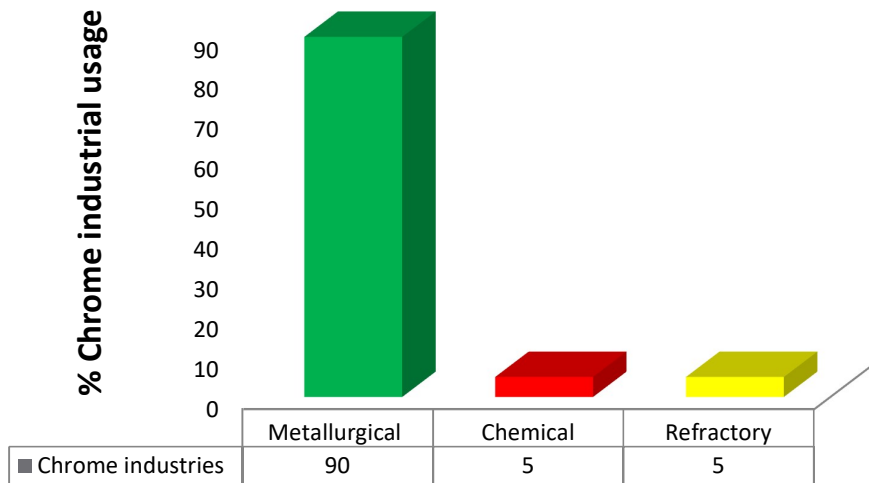
Figure 2.7: Industrial usage of chromium (Dhal et al., 2013)
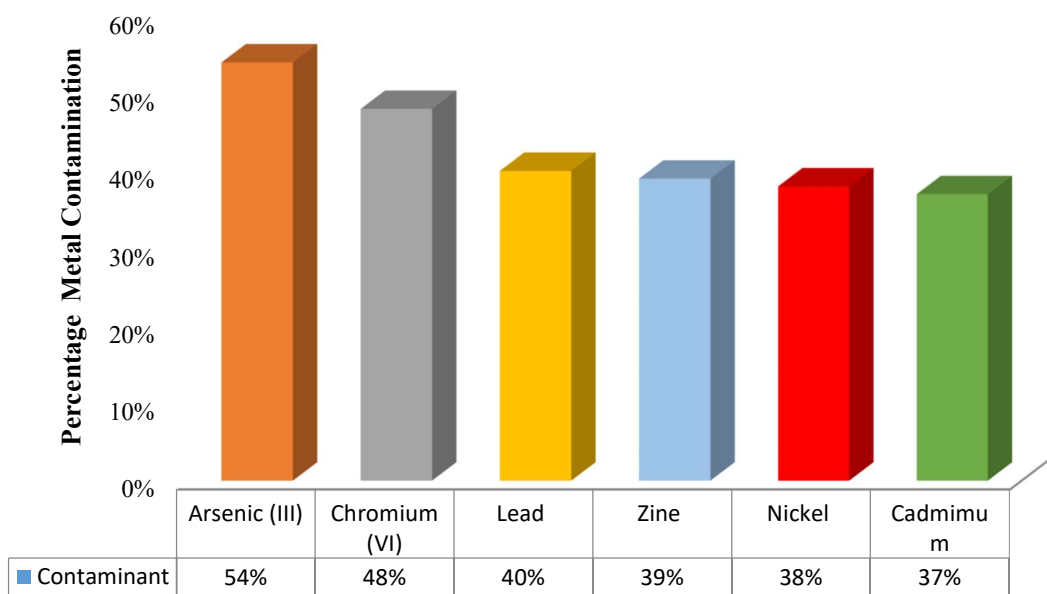
Figure 2.8: Wold metal contamination (Dhal et al., 2013)

There are two categories, namely physiochemical and biological treatment (Mahimairaja, 2005; Lim & Shukor, 2014). These technologies are based on remediation by reduction or oxidation. Remediation by reduction or oxidation can be applied as an ex-situ or in-situ process. An ex-situ remediation process is a strategy where a contaminated site is excavated and transported off-site for treatment, while an in-situ process is a strategy where the contaminated site is treated on-site. However, owing to the high costs of transport, landfill space and pumping attributed to the ex-situ process, the in-situ process seems to be more attractive (Hawley et al., 2004).

Some of the technologies that have been used or are currently in use for As(III) and Cr(VI) removal include: ion exchange, membrane, conventional, adsorption, and bioremediation processes. These treatment processes for As and Cr removal are currently installed worldwide. The most commonly-used treatment processes are coagulation (with ferric salts, also called chemical precipitation) combined with filtration and adsorption on (usually) Fe-based media (Mohan & Pittman, 2007). Current arsenic and chromium removal technologies are compared in Table 2.1. The major problems associated with some of these technologies when applied for arsenic and chromium remediation is the type of waste generated. The waste constitutes an amount of toxic arsenic and chromium, which may require further treatment before disposal. Such treatment may increase the operating and capital costs if on-site disposal or direct sewer discharge is not possible (Sullivan et al., 2010; Janet et al., 2016).

Most of these technologies are discussed below.

2.6.1 Ion exchange

Ion exchange is a physical treatment technology where an ion with a high affinity for the resin material of the ion exchange column replaces an ion with a lower affinity that was previously bound to the column resin. Ion exchange resins have been reportedly capable of removing Cr(VI) and As(III) to a concentration less than the detection limit (Hawley et al., 2004; Clifford et al., 2003). Ion exchange has been recommended for concurrent removal of As and other co-pollutants (Ghurye et al., 1999; Janet et al., 2016) although it can be subject to chromatographic peaking, which can release contaminants more than their influent concentration (Clifford et al., 2011). However, the problem associated with this technology is its high cost of resin regeneration and complexity in operation. Also, a pre-oxidation step for conversion of As(III) to As(V) is required for efficient As(III) removal (Johnston & Heijnen, 2001).

2.6.2 Membrane process

Membranes such as microfiltration, ultrafiltration (UF), nanofiltration (NF) and reverse osmosis (RO) are generally selective barriers allowing the passage of certain constituents with the rejection or exclusion of others in the water (USEPA 2000; Johnston & Heijnen, 2001). They have been reportedly used in water treatment to remove Cr(VI) and As(III) from wastewater. RO plants have been reportedly used for the remediation of arsenic in Argentinian (Cortina et al., 2016). Cr(VI) ions are too small to be removed by microfiltration or ultrafiltration membranes, unless a pre-treatment is performed to coagulate the Cr(VI) or As(III) into larger molecules (Hawley et al., 2004; USEPA, 2000; Johnston & Heijnen, 2001).

2.6.3 Conventional treatment process

Cr(VI) and As(III) removal has been reportedly achieved by conventional treatment process through pH adjustment or precipitation or coagulation, adsorption, sedimentation, oxidation etc. (Rhine et al., 2006; Clifford, 1993). Precipitation or pH adjustment involves the use of acid and base to remove Cr(VI) or As(III) as precipitate. Arsenic concentration removal of 350 µg/L was achieved by sorption or coprecipitation with ferric hydroxides (Berg et al., 2001). Unfortunately, the cost of setting up the required equipment and operation processes is expensively high for a large-scale treatment.

Adsorption is a physical/chemical process whereby the target metal ions present in the contaminated water are adsorbed onto the surface of the adsorbents (Hawley et al., 2004). Granular activated carbon (GAC) has been reportedly used to remove Cr(VI) and As(III) from wastewater. Second, activated alumina (AA) has also reportedly been used for the removal of As(III) from wastewater (Clifford, 1999). In addition, arsenic removal has been accomplished by filtration in an adsorbent bed using Bayoxide 33 without coagulant dosage (Janet et al., 2016). However, during regeneration, adsorbed chromium or arsenic would be released as Cr(VI) or As(III), creating a second waste stream that would require further treatment (Hawley et al., 2004). One major cost associated with adsorptive media is replacement of the adsorbent after exhaustion. Also, it can be labour intensive when corrosive chemical is used (Westerling, 2014).

Coagulation is a conventional treatment process whereby the target metal ion in the source water is removed by addition of coagulants like ferric chloride or aluminium chloride, etc. Arsenic removal has been achieved by the addition of poly-aluminium chloride, following a two-step filtration process (Garrido Hoyos et al., 2013, Katsoyiannis et al., 2015; Cortina et al., 2016). However, this process still needs an improvement, which will mainly involve optimum pH adjustment and coagulant dose (Sancha, 2006). The improvement will drastically increase the capital and operating cost of the technology, making it less cost efficient and highly labour intensive. Second, disposing waste from such treatment processes may not be feasible as it may require additional treatment and thus increase the costs of waste disposal (Sullivan et al., 2010).

2.6.4 Bioremediation process

The bioremediation process involves the application of microorganisms to reduce or oxidise metals or metalloids. Over the years, microorganisms have developed mechanisms to remediate both metal and metalloid contaminants from water and wastewater. The special ability of microorganisms is usually demonstrated by changes in the redox states of the corresponding metals or metalloids or by adsorption onto their surface. The net result of both the processes leads to the reduction in the mobility of these contaminants in the environment (Mtimuye, 2011).

Table 2.2 lists the several isolated heterotrophic and autotrophic As(III) oxidizing strains with their substrates and redo-x conditions for growth. To explore previous Cr(VI) reduction in batch studies, Table 2.3 bellow summarizes some the previous batch of investigation on biological Cr(VI) reduction. Chromium-reducing bacteria may utilize a variety of organic compounds as electron

donors for chromium reduction. However, most reported organic electron donors are natural aliphatic compounds, mainly low-molecular-weight carbohydrates, amino acids and fatty acids. Hydrogen may serve as the electron donor in *Desulfovibrio vulgaris* (Loveley & Phillips, 1994; Wang & Shen, 1994).

Table 2.1: Comparison of main arsenic and chromium removal technologies (Mohan & Pittman, 2007)

Technologies	Advantage	Disadvantage
Membrane technologies;		
Nanofiltration Reverse osmosis Electro-dialysis, etc.	Well-defined and high-removal efficiency; capable of removing another contaminant	Very high capital and running cost, pre-conditioning; high water rejection. Toxic waste produced
Ion-exchange	Relatively well known and commercially available Cheap: no regeneration required. Well-defined medium and capacity; pH independent; exclusive ion-specific resin to remove arsenic	Needs replacement after four to five regenerations. Not standardized; produces toxic solid waste. High-cost medium; high-tech operation and maintenance; regeneration creates a sludge disposal problem; As(III) is difficult to remove; life of resins

Coagulation/coprecipitation technologies;	Relatively well known and commercially available. Cheap; no regeneration is required; well-defined medium and capacity; pH independent; exclusive ion-specific resin to remove arsenic	Needs replacement after four to five regenerations. Not standardized; produces toxic solid waste. High-cost medium; high-tech operation and maintenance regeneration creates a sludge disposal problem; As(III) is difficult to remove; life of resins
alum coagulation iron coagulation lime softening		
Sorption technology;	Relatively well known and commercially available Cheap: no regeneration required. Well-defined medium and capacity; pH independent; exclusive ion-specific resin to remove arsenic	Needs replacement after four to five regenerations. Not standardized; produces toxic solid waste. High-cost medium; high-tech operation and maintenance; regeneration creates a sludge disposal problem; As(III) is difficult to remove; life of
Activated alumina Iron-coated sand Ion-exchange resin		
Precipitation/oxidation	Relatively simple, low-cost but slow process; in-situ arsenic removal; also oxidizes other inorganic and organic constituents in water. Oxidizes other impurities and kills microbes; relatively simple and rapid process; minimum residual mass	Mainly removes arsenic(V) and accelerates the oxidation process. Efficient control of the pH and oxidation step is needed

Table 2.2: Summary of batch studies on bacterial As(III) tolerance and oxidation (Kruger et al., 2013)

Micro-organism	As(III) concentration	Reference
Escherichia coli AW3110	0.1 mM/L	Carlin et al., 1995
E. coli W3110	1 mM/L	Carlin et al., 1995
E. coli W3110 pBC101	4 mM/L	Carlin et al., 1995
Bacillus subtilis	1 mM/L	Sato & Kobayashi, 1998
Thiomonas sp. 3As	6 mM/L	Arsène-Ploetze et al., 2010
Herminiimonas arsenicoxydans	5 mM/L	Muller et al., 2007
Corynebacterium glutamicum	12 mM/L	Ordonez et al., 2005
Microbacterium sp. A33	28 mM/L	Achour-Rokbani et al., 2010
Ochrobactrum tritici SCII24	50 mM/L	Branco et al., 2008, 2009
Bacillus sp. ORAs2	17 mM/L	Pepi et al., 2007
Pseudomonas sp. ORAs5	17 mM/L	Pepi et al., 2007
Micrococcus luteus	10 mM/L	Shakya et al., 2012
Vibrio parahaemolyticus	20 mM/L	Shakya et al., 2012
Thermus aquaticus	-	Gihring & Banfiled, 2001
T. thermophilus	-	Gihring et al., 2001
Alcaligenes faecalis	-	Ellis et al., 2001
Exiguobacterium profundum sp	20 mM/L	Crapart et al., 2007
Bacillus Firmus	50 mg/L	Bachate et al., 2012
Dechloromonas sp	0.9 mM/L	Sun e tal., 2010
Azospira sp. strain ECC1-pb2	0.9 mM/L	Sun e tal., 2010

Table 2.3: Summary of batch studies on bacterial Cr(VI) reduction conditions (Wang & Shen, 1994)

Microorganism	Substrate	Oxygen	Reference
Agrobacterium radiobacter	Glucose/fructose	Aerobic	Llovera et al., 1993
Achrombacter eurydice	Glucose/acetate	Anaerobic	Gvozdyak et al., 1986
Arthrobacter aurescens	Resting cells	Anaerobic	Llovera et al., 1993
Aeromonas dechromatica	Galactose/mannose	Anaerobic	Kvasnikov et al., 1985

Arthrobacter aurescens	VB broth	Aerobic	Horton et al., 2006
Arthrobacter sp	Glucose	Aerobic	Córdoba et al., 2008
Bacillus sp.	Glucose	Aerobic	Wang & Xiao. 1995
Bacillus sphaericus	VB broth	Aerobic	Pal & Paul. 2004
Bacillus subtilis	Glucose/acetate	Aerobic	Garbisu et al., 1998
Bacillus cereus	Glucose/acetate	Anaerobic	Gvozdyak et al., 1986
Bacillus megaterium	Nutrient broth	Aerobic	Cheung & Gu, 2007
Bacillus sp. ES 29	Luria-Bertani (LB)	Aerobic	Camargo et al., 2003
Bacillus thuringiensis	Luria-Bertani broth	Aerobic	Molokwane & Chirwa, 2009
Desulfovibrio vulgaris	Hydrogen	Anaerobic	Lovley & Phillips, 1994
Deinococcus radiodurans	Basal medium	Anaerobic	Frederickson et al., 2000
Escherichia coli	Glucose	Aerobic	Shen & Wang, 1993
Esche richia coli	Glucose	Aerobic	Shen & Wang, 1993
Escherichia coli ATCC 33456	Glucose/acetate	Anaerobic	Shen & Wang. 1994
Enterobacter cloacae	Glucose/acetate	Anaerobic	Ohtake, et al., 1990
Micrococcus roseus	Glucose/acetate	Anaerobic	Gvozdyak et al., 1986
Leucobacter sp.	LB broth	Aerobic	Zhu et al., 2008
Lysinibacilus sphaericus	LB broth	Aerobic	Molokwane & Chirwa, 2009
Ochrobactrum sp	Glucose	Aerobic	Zhiguo et al., 2009
Pantoea agglomerans	Acetate	Anaerobic	Francis et al., 2000
Pseudomonas	Glucose and LB broth	Aerobic	McLean et al., 2001
Pseudomonas aeruginosa	Glucose/acetate	Anaerobic	Gvozdyak et al., 1986
Pseudomonas dechromaticans	Glucose/peptone	Anaerobic	Romanenko & Korenkov, 1977
Pseudomonas chromotophila	Ribose/fructose	Anaerobic	LebedewL & Lyalikova, 1979
Pseudomonas putida	-		Ishibashi et al., 1989
Providencia sp.	Luria broth	Facultative	Thacker et al., 2006
Pseudomonas ambigua	Nutrient broth	Aerobic	Horitsu et al., 1987

Pseudomonas fluorescens	Glucose	Aerobic	Shen & Wang 1995
Sphaerotilus natans	Glucose-MSM	Aerobic	Caravelli, et al., 2008
Streptomyces griseus	Broth II medium	Aerobic	Laxman & More, 2002
Consortium (18 species)	LB-broth	Anaerobic	Molokwane et al., 2008

2.7 Microbial metabolism and metal resistance

The principal application of the bioremediation processes is subdivided into three major categories, which are: biosorption, biological reduction and biological oxidation. Several studies of microbial growth and toxic metal resistance have been demonstrated at different ranges of Cr(VI) and As(III) concentrations. Microbial tolerance to toxic metal could possibly involve some vital functions of the cell (Lim & Shukor, 2014). It has been said earlier that microorganisms play a vital role in the geochemical cycle of metalloids (Mukhopadhyay et al., 2002) and that they assist microbes to resist metallic disruptive effects for their ordinary physiology (Rosen, 2002). In addition, metallic resistance enzymes are located on the cell plasmids of the microbial cell (Silver & Phung, 1996). However, some microbes vigorously use these metalloids for metabolism activities, either as an electron donor (Bryan et al., 2009; Santini et al., 2000; Silver & Phung 2005; Kruger et al., 2013) or as a terminal electron acceptor for anaerobic respiration (Ahmann et al., 1994; Macy et al., 1996; Stolz & Oremland, 1999). Therefore, an understanding of microbial interaction with toxic metals or metalloid is of major importance to develop measures for an improved bioremediation process (Kruger & Bertin, 2013).

2.8 Microbial oxidation of As(III) to As(V)

A wide range of bacteria isolated from various contaminated environments were defined for their ability to oxidize As(III) to As(V). Chemoautotrophs are referred to as microbes that gain energy for growth by utilizing either As(III) as an autotrophic electron donor or As(V) as a respiratory electron acceptor as "arsenotrophs" (Oremland et al., 2009). The most famous microbial oxidation of As(III) to As(V) was observed in isolates from cattle-dipping tanks in South Africa (Green, 1918). Heterotrophic As(III) oxidation may represent a detoxification reaction on the cell's cytoplasmic (inner) membrane, whereas in chemoautotrophic As(III) oxidation energy released and uses CO_2 fixation as carbon source, in which As(III) serves as electron donor for oxygen, nitrate or

chlorate reduction (Anderson et al., 1992; Oremland et al., 2002; Santini et al., 2000; Sun et al., 2008; Aniruddha & Wang, 2010; Sun et al., 2010). From 2010 to 2017, a huge improvement has been made in this area, and a number of microorganisms capable of oxidizing As(III) to As(V) under both aerobic and anaerobic conditions have been reported (Aniruddha & Wang, 2010; Sun et al., 2010; Sun et al., 2008, Igboamalu & Chirwa, 2014-2017). In 2017, a distinct anaerobic As(III) oxidizing chemoautotrophic bacteria, commonly referred to *Exiquobacterium profundum*, was isolated from a cow dip in South Africa (Igboamalu & Chirwa, 2017).

Studies have reported that the microbial interaction with As(III) could be categorised as arsenic resistance structural asars gene (Rosen, 2002), or respiratory/non-respiratory oxidation structural oxidase (Aox) and reductase (Arr) genes (Muller et al., 2003). The transport of Arsenic is like phosphate transport. Arsenic enters the cells through the phosphate transporters (arsenate) or the aqua-glyceroporins (arsenite). In the cells, arsenate is reduced to arsenite by (Arr), which is further extruded out of the cell by the specific pump (Arr) (David et al., 2009). Conversely, arsenite may also be detoxified by (Aox) or possibly serve as electron donor (David et al., 2009). The arsenic oxidase (Aox), which is of interest in this report, is also a member of the larger DMSO reductase family of molybdenum enzymes but differs greatly to reductase (Arr) (Stolz et al., 2006). It is located on the outer surface of the inner membrane and exhibits arsenite oxidation activity as an electron acceptor. The molybdenum proteins structure consists of two subunits: a larger 88-kDa polypeptide containing the Mo-pterin and a HiPIP $3Fe^4S$ centre, and a smaller 14-kDa subunit with the Rieske $2Fe^2S$ centre (Anderson, 2001; Ellis et al., 2001) (see Figure 2.9). The large subunit structure of arsenite oxidase has a $3Fe^4S$ centre, and Ser99 (arsenite oxidase) where a Cys residue is required to bind (Ellis et al., 2001). As(III) enters (possibly coordinated by residues His195, Glu203, Arg419 and His423) through a flat, funnel-shaped cleft on the large subunit structure and after oxidation it lets As(V) exit the protein in the opposite way (Mukhopadhyay et al., 2002).

In the structure (Figure 2.9), it was anticipated that As(III) will bond firmly to the Mo centre of the larger subunit, the oxidized cofactor. Due to nucleophilic attack or denaturation (i.e. a process in which proteins or nucleic acids lose the quaternary structure, tertiary structure and secondary structure that is present in their native state, by application of some external stress or compound such as a strong acid or base, a concentrated inorganic salt (Mosby Medical Dictionary, 2009), the Mo-pterin cofactor is released from other molybdenum proteins (Hille, 2000; Mc Ewan, 2002, Mukhopadhyay et al., 2002). As a result, Mo(VI) is reduced to Mo(VI) with an electron transfer

initially to the [3Fe-4S] centre of the larger subunit. The [3Fe-4S] centre is re-oxidized by the transfer of two electrons to the [2Fe-2S] centre of the small subunit, which is reoxidized by the transfer of electrons to the respiratory chain (Anderson et al., 1992; Ellis et al., 2001). The proposed redox reaction for the process is shown in Equation 2.9 – 2.11 (Igboamalu & Chirwa, 2018).

$$As(III) \rightarrow 2e- + As(V) \tag{2.9}$$

$$Mo^{6+} + 2e- \leftrightarrow Mo^{4+} \tag{2.10}$$

Overall red-ox reaction; from combining Equation 2.9 and 2.10, gives

$$As(III) + Mo^{6+} \rightarrow As(V) + Mo^{4+} (\Delta G = -256 \text{ kJ/mol}) \tag{2.11}$$
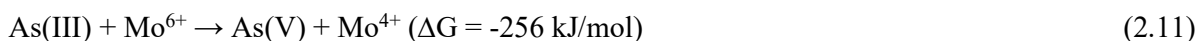
Arsenate produced through the oxidation process is released to the environment and was achieved when As(III) accept two-electron transferred from Mo(VI), thereby reducing Mo(VI) to Mo(IV) (Equation 2.11) (Mukhopadhyay et al., 2002). This thermodynamic process is feasible since two electrons are required for the redox process or cycle for the oxidation of As(III) to As(V). However, it is an exothermic redox process that generates a reasonable amount of energy for cell growth and metabolism.

2.9 Microbial reduction of Cr(VI) to Cr(III)

Most microorganisms in the presence or absence of oxygen can detoxify Cr(VI) to Cr(III). These microorganisms are known as chromium-reducing bacteria (CRB) (Kakonge, 2009). During the cells biotransformation of Cr(VI) to Cr(III), there is formation of intermediate oxygen radicals or intermediate oxidation states of chromium – Cr(V) and Cr(IV) – which might disrupt the metabolic activities of the microbial cells (Suziki et al., 1999; Dhala et al., 2013). Due to unique characters of chromium-reducing bacteria, they have developed an alternative mechanism such as chromate-resistant plasmid (Cervantes & Silver, 1992) and iron efflux system (Nies & Silver, 1995) to counter such problems in cellular mediated Cr(VI) to Cr(III) reduction. The mechanism of bacterial Cr(VI) reduction differs from strain to strain, and thus this depends on their bio-geochemical activities and nutrient utilization patterns (Megharaj et al., 2003; Lovley & Coates, 1997; Dhala et al., 2013). Considering chromium transport in the microbial cell (see Figure 2.10), Cr(III) compounds can easily bind firmly to different components of bacterial envelopes, thus making it almost impermeable owing to its insolubility (Nickens et al., 2010), while Cr(VI) cannot easily bind to the

bacterial membranes of the anionic components (Cervantes et al., 2001; Neal et al., 2002, Ahemad, 2014). Because of this, and some similarities with SO_4^- or PO_4^{3-} structure, Cr(VI) can easily be transported across the biological membranes via active sulphate transporters (Daulton et al., 2007; Collins et al., 2010).

A wide array of bacterial strains capable of reducing Cr(VI) to Cr(III) under both aerobic and anaerobic conditions has been reported (Molokwane et al., 2008; Zakaria et al., 2007; Cheung & Ji-Dong, 2006; Chirwa & Wang, 2000). Early observation showed that the Cr(VI)-reducing strains isolated are capable of reducing Cr(VI), deriving energy from phenol degradation (Chirwa & Wang, 2000). However, microbial reduction of Cr(VI) to Cr(III) can be direct enzymatic reduction or indirect reduction under anaerobic and aerobic conditions (Molokwane, 2010; Yang et al., 2009; Guha et al., 2000; Sedlak & Chan, 1997; Pettine et al., 1994).
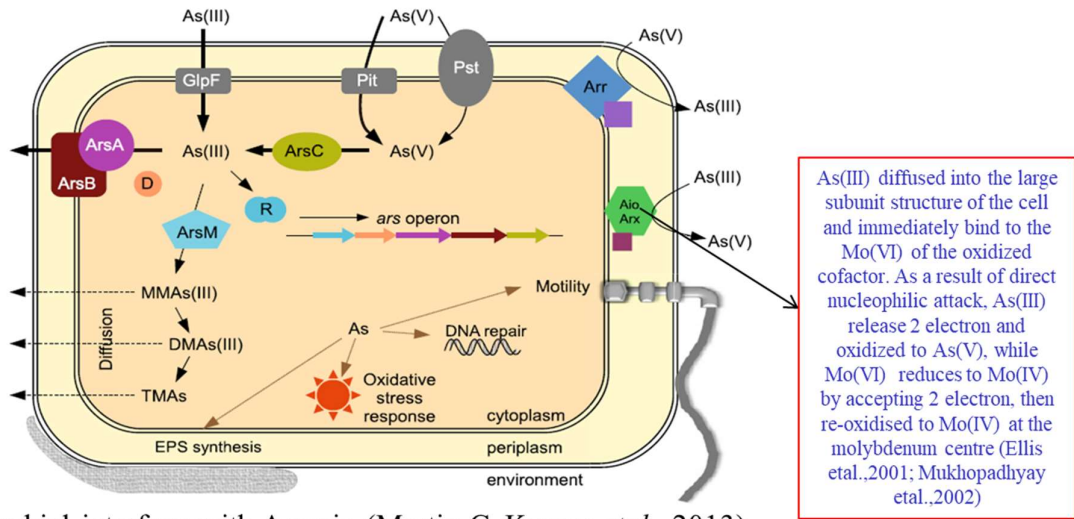
Microbial interface with Arsenic (Martin C. Kruger *etal.,* 2013)

As(III) diffused into the large subunit structure of the cell and immediately bind to the Mo(VI) of the oxidized cofactor. As a result of direct nucleophilic attack, As(III) release 2 electron and oxidized to As(V), while Mo(VI) reduces to Mo(IV) by accepting 2 electron, then re-oxidised to Mo(IV) at the molybdenum centre (Ellis etal.,2001; Mukhopadhyay etal.,2002)

$$As^{3+} + Mo^{6+} \xrightarrow{\text{Nucleophic attack}} As^{5+} + Mo^{4+}$$

Oxidation (+2e)

Reduction (-2e)

Cell re-oxidation (+2e)

Figure 2.9: Arsenic oxidase structure and cell interaction with arsenic (adapted from Martin C. Kruger et al., 2013)

Under anaerobic conditions, it was reported that Cr(VI) reduction is attributed to an energy-yielding dissimilatory respiratory process, in which Cr(VI) serves as a terminal electron acceptor (Dhal et al., 2013). In addition, it may also be attributed to soluble reductase; a membrane bound hydrogenase or cytochrome (Michel et al., 2001). Equation 2.12 described anaerobic reduction of Cr(VI) to Cr(III), using acetate as electron donor (Chirwa & Wang, 2000). As previously discussed, under anaerobic conditions, Cr(VI) accepts an electron from the cell NADH$^+$ for stepwise reduction of Cr(VI) to intermediate Cr(V), which accepts two electrons from the same co-enzyme to yield Cr(III) (see Figure 2.10) (Suzuki et al., 1992; Chirwa & Molokwane, 2011).

$$CH_3.COO^- + 1.5CrO_4^{2-} + 6.5H^+ \xrightarrow{CRB} 1.5Cr^{3+} + 2HCO_3^- + 2H_2O + 1.25H_{2(aq)} \qquad (2.12)$$
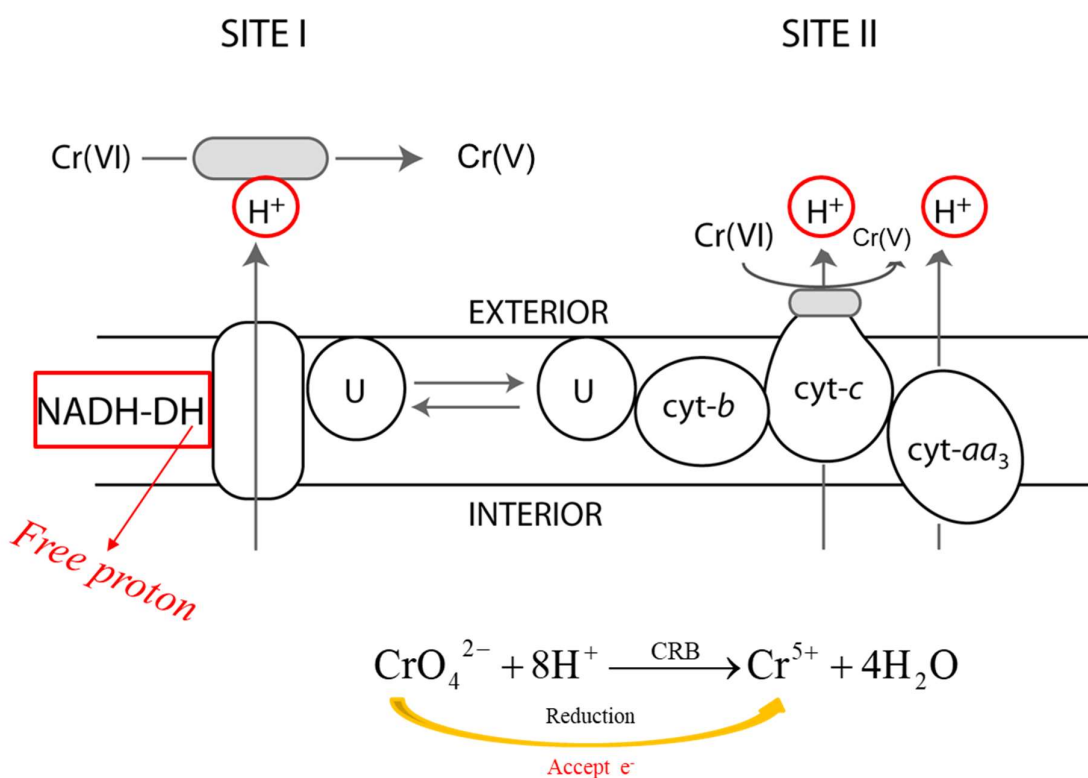
Figure 2.10: Mechanism of Cr(VI) reduction: an electron transport pathway (Chirwa & Molokwane, 2011)

2.10 Cr(VI) reduction linked to As(III) oxidation

Figure 2.11 describes the mechanism of Cr(VI) reduction linked to As(III) oxidation catalysed by facultative chemoautotrophic bacteria. Aniruddha and Wang (2010) reported that about 256 KJ/mol energy is generated during oxidation of As(III) to As(V). Further studies showed that about 467.95KJ of energy could be generated in the redox biochemical process (Wang, 2013). Recently, studies on Cr(VI) reductions linked to As(III) oxidation have been explored. According to Wang (2013), Cr(VI) reduction linked to As(III) oxidation was greatly accelerated by the addition of H_2O_2. This process was enhanced at acidic pH. As(III) oxidation using nitrate or chlorate as electron acceptor was also observed (Sun et al., 2008; Sun et al., 2010). Further studies under aerobic conditions show that the *Bacillus firmus* TE7 strain could completely reduce 15 mg/L Cr(VI) in the presence of 50 mg/L of As(III), although the study reported that Cr(VI) reduction was not linked to As(III) oxidation (Batchate et al., 2013). In addition, it was reported that selenium can serve as an electron acceptor during As(III) oxidation in the anaerobic respiration (Stolz et al., 2006), as much as generating a reasonable amount of energy for cell growth and metabolism. Recent studies also demonstrated that beside chlorate, nitrate, and selenium, Cr(VI) can be an alternate electron acceptor for As(III) oxidation (Igboamalu & Chirwa, 2014, 2016 & 2017). These follow the proposed redox cycle for oxidation of As(III) and reduction of Cr(VI) from a contaminated site or waste. The hydroxyl complex generated from the reduction of Cr(VI) to Cr(III) and oxidation of As(III) to As(V) could be enhanced by the addition of a dosage of Fe(III) forms Fe(III)/Cr(III) hydroxyl complex, which can adsorb As(V) to generate a fertilizer for agricultural use (Namasivayam & Senthilkumar, 1998). Indeed, the demonstration of As(III)-linked with these metalloids suggests it is a natural phenomenon, which with further investigation may yield new insight than those already described.

The processes leading to microbial Cr(VI) reduction with As(III) as an electron donor is shown in the two-step process Equation 2.13 – 2.16. Microbial oxidation of As(III) to As(V) has been demonstrated independently (i.e. without Cr(VI) or ClO_3^- or NO_3^-) as far back as 1918. Subsequently, various studies have reported the microbial interaction with As(III), of could either be by As resistance structure as ars genes (Rosen, 2002) or respiratory/non-respiratory oxidation structure (Muller et al., 2003). A previous study has shown that bacteria have developed various mechanisms for oxidizing As(III), resulting in energy generation while utilizing CO_2 as carbon source (Santinni et al., 2000). This is evident by demonstrating that some facultative bacteria may survive by utilising As(III) as an electron donor (Sun et al., 2010). As much as 256 KJ/mol of energy can be released during the oxidation of As(III) to As(V), which can be trapped for microbial growth.

$$As^{3+} \rightarrow 2e^- + As^{5+} \tag{2.13}$$

The intermediate product formed because of cell redox cycle gives Equation 2.14:

$$Cr^{6+} + e^- \rightarrow Cr^{5+} \tag{2.14}$$

$$Cr^{5+} + 2e^- \rightarrow Cr^{3+} \tag{2.15}$$

The overall red-ox reaction, from combining Equation 2.13 and 2.15, gives:

$$As^{3+} + Cr^{5+} \rightarrow As^{5+} Cr^{3+} \ (\Delta G = -256 - -468 \ kJ/mol) \tag{2.16}$$
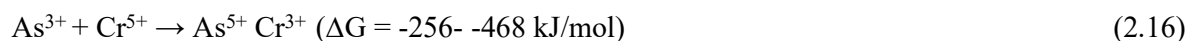
In contrast to previous studies, the current study deals with the isolation of As(III) and Cr(VI)-resistant mixed anaerobic bacteria, which can biocatalytically induce cell reduction of Cr(VI) to Cr(V) for simultaneous oxidation of As(III) to As(V) under neutral conditions (pH $\geq$7). The novelty of this work can be ascertained from the literature review, which suggested that Cr(VI) and As(III) predominate at pH range from 6-9, with the formation of a different type of species between pH >9 and <6 Equation 1 and 2 (Park et al., 2005; Dastidar & Wang 2009). In this study, it is demonstrated for the first time that As(III) can serve as an electron donor for Cr(VI) reduction when both As(III) oxidation and Cr(VI) reduction processes are present in a single or mixed culture as shown in Equation 2.13 – 2.16. Equation above shows the individual stages of As(III) oxidation Equation 2.13, and step wise reduction of Cr(VI) Equation 2.14 – 2.15. Equation 2.14 – 2.15. occurs as a result of the redox cycle in the microbial cell, which generates an intermediate product Cr(V) (Cervantes et al.,2001). From biocatalytic redox reactions Equation 2.16, As(III) donate 2e-, and oxidized to As(V), while Cr(V) an intermediate product formed, on the other hand accept 2e-, and reduced to Cr(III). However, the reaction is feasible since only two electrons are required for Cr(V) reduction. Secondly, based on bioenergetics consideration, the reaction is feasible as indicated a highly exothermic reaction equation, releasing reasonable amount of energy for cell growth (Igboamalu & Chirwa, 2014).

2.11 Bioremediation applications

Wide applications of Cr(VI) bioremediation have been studied, either in a batch process or continuous-flow process. In these applications, a variety of organic substrates in combination with

basal mineral medium has been utilized. However, microorganisms can be employed as suspended cell or attached cell. In most applications, complete reduction of Cr(VI) concentrations ranging typically from 5 to 150 mg/L was achieved at various time intervals. The application of Cr(VI) bioremediation can be categorised into batch process and continuous-flow process.

$$As^{3+} + Cr^{5+} \rightarrow As^{5+} + Cr^{3+} \, (\Delta G = -256 \text{ kJ/mol})$$
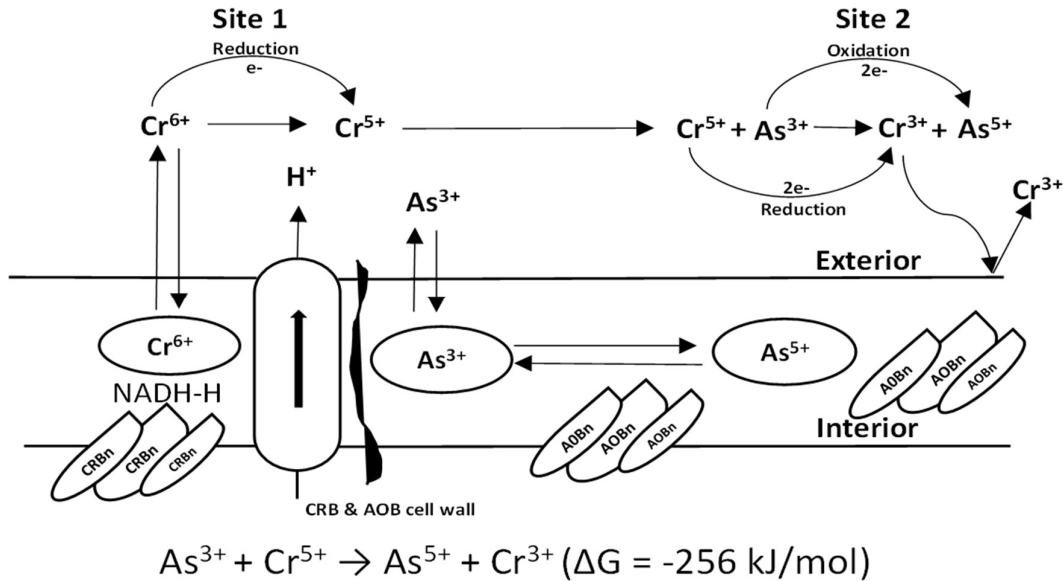
Figure 2.11a: Mechanism of Cr(VI) reduction linked to As(III) oxidation (Igboamalu & Chirwa, 2017)

Microbial process

Cr^{6+}/Cr^{3+} redox cycle was derived from Suzuki et al.,(1992)

$$Cr^{6+} + e\text{-} \rightarrow Cr^{5+} \quad \text{(intermediate product)}$$

$$Cr^{5+} + 2\,e \rightarrow Cr^{3+} \tag{1}$$
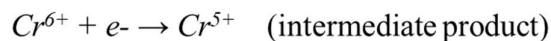
As^{3+}/As^{5+} redox cycle was derived from Aniruddha and Wang, (2010)

$$As^{3+} \rightarrow 2e^- + As^{5+} + 256KJ \tag{2}$$

Chemical process

$$As^{3+} + Cr^{5+} \rightarrow As^{5+} + Cr^{3+} + \Delta G = -256 \text{ kJ/mol} \tag{3}$$
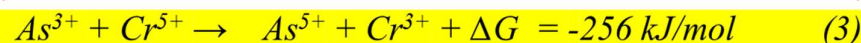
Figure 2.11b: Electron transfer model (Igboamalu & Chirwa, 2014)

2.11.1 As(III) bioremediation with batch system

Microbial oxidation of As(III) to As(V) was first observed in certain microorganisms in cattle-dipping tanks in 1918 (Green, 1918). A number of microorganisms capable of oxidizing As(III) to As(V) under both aerobic and anaerobic conditions have been isolated and identified since. Heterotrophic As(III) oxidation may represent a detoxification reaction on the cell's cytoplasmic (inner) membrane, whereas autotrophic As(III) oxidation releases energy that is used for CO_2 fixation and cell growth under both aerobic and anaerobic conditions (Anderson et al., 1992; Ilyaletdinov & Abdrashitova 1981; Santini et al., 2000). However, the autotrophic As(III) oxidation process may be preferred over the heterotrophic one because of its lower nutritional requirements and lower potential for production of any harmful organic metabolites. The first heterotrophic As(III)-oxidizing bacteria were described in 1918 (Green,1918), whereas an autotrophic As(III) oxidizing strain, *Pseudomonas arsenitoxidans*, was first reported in 1981 (Ilialetdinov & Abdrashitova, 1981).

2.11.2 Cr(VI) bioremediation with batch system

Cr(VI) reduction in a batch system is employed as a suspended or attached growth system. In a batch process, microorganisms are placed in liquid suspension by appropriate mixing techniques or grown on a media. Since 1977, when biological Cr(VI) reduction was first reported by Romanenko and Koren'kov, numerous authors have published on biological chromate reduction. A variety of microorganisms, including bacteria and fungus, have been identified that can reduce Cr(VI), hence this reduction is agreed to be enzymatic. Most batch studies have been aimed at optimizing physical conditions, establishing the biochemical mechanisms involved and analysing kinetic potential (Caravelli & Zaritzky, 2009).

Successful Cr(VI) reduction with microbes in a batch assay under several conditions has been reported by many researchers (Wang et al., 2000; Mazerski et al., 1994; Shen & Wang, 1994a). However, studies have shown that microbes acting as a consortium perform better than individual pure isolates (Molokwane et al., 2008). Most of this study was done under aerobic conditions, however, only few studies were done under anaerobic conditions. Shen and Wang (1993, 1994)

reported a high Cr(VI) reduction under anaerobic conditions. Molokwane et al., (2008) on the other hand, reported high Cr(VI) reduction, where anaerobic conditions were achieved by purging 99% of pure nitrogen gas. The optimal redox potential range for Cr(VI) reduction has not been clearly reported or understood. The rate of Cr(VI) reduction was reported to be superior in cell suspensions at -240mV than with -198 mV in *a radiobacter* grown at different carbon and energy sources (LIovera et al., 1982; Wang & Sheng, 1994). At redox potential > -140 mV, there was no Cr(VI) reduction observed within the first hour (Gvozdyak et al.,1986). At a high redox potential value of about > +250 mV in *B. subtilis* cultures, Cr(VI) reduction occurred after one hour of incubation as the redox potential decreased (Gvozdyak, 1986). In *Bacillus* sp., Cr(VI) reduction occurred at the start of the experiment with a redox potential of about +250 mV and sustained at a persistent rate during the course of the incubation, regardless of a rapid drop in redox potential to > -500 mV after 48 h of incubation (Wang & Xiao, 2005).

In a different observation, *E. coli* ATCC 33456 cell concentration of 104 cells ml incubated under anaerobically conditions utilizing glucose as the sole carbon source rapidly lowered the redox potential to -400 mV (Shen & Wang, 1994). However, no significant Cr(VI) reduction was noted at such redox potential. In a different cell concentration under aerobic conditions, Cr(VI) reduction was seen when the redox potential increased to > +150 mV from a low redox potential of -500 mV after 6 h incubation (Shen & Wang, 1994).

The optimal pH and temperature for Cr(VI) reduction has been widely reported with different chromium-reducing bacteria. For example, in an *Ent.cloacae*, pH and temperature ranging from 7.0-7.8 and 30-37°C were reported (Komori et al., 1989). In *E. coli*, a pH range of 3-8 and a temperature range of (10-45) °C were reported with optimum value at pH 7 and a temperature of about 36 °C (Shen and Wang, 1994). In *Bacillus* sp., optimum pH and temperature were recorded at 7 and 30 °C (Wang & Xiao; Shen & Wang, 1994).

2.11.3 Bioremediation with continuous-flow system

Most continuous flow reactors were designed as attached growth (biofilm system); were consortium or pure cultures responsible for bioremediation are grown on the media. Media typically used in attached growth system include: soil, rocks, gravel, plastic beads, and glass beads, etc. A continuous-flow reactor system can be operated in anaerobic or aerobic conditions, either by up flow or down flow feed. Advantages of continuous flow system to batch system includes; they biofilm attached system that immobilise metal compounds, and the microbes attached are less

vulnerable to metal toxicity than batch reactors in suspension which is more vulnerable to metal toxicity. Due to its advantage over batch systems, continuous-flow reactors have been used for treatment of high effluent Cr(VI) containing waste. However, many types of anaerobic reactors exist, such as up-flow anaerobic sludge blanket reactors, expanded granular sludge blanket reactors, multiplate reactors, anaerobic filter, fixed-film reactors, down-flow fixed-film reactors, fluidized bed reactors, anaerobic ponds, anaerobic sequencing batch reactors (ASBR), two-phase digestion and up-flow fixed-film reactors (Mulligan, 2002).

2.11.4 As(VI) oxidation with continuous-flow system

Arsenic remediation in a continuous-flow system involves two fundamental stage approaches. The first approach is the oxidation of As(III) by arsenite oxidizing bacterial strains. The second approach involves the removal of the As(V) produced. Studies have demonstrated the removal efficient of As(III) in a fixed-bed biological filtration unit. A biofilm reactor fed with high iron oxide and As(III), developed the required strains for As(III) oxidation to As(V) (Casiot et al., 2006). In a different pilot scale biofilm study, a 90% As(III) oxidation rate was obtained at influent As(III) concentration of 100 ug/l (Michon, 2006).

2.11.5 Cr(VI) bioremediation with continuous-flow system

Biofilm studies in continuous-flow systems have been demonstrated by many researches (Mtimuye, 2011; Slabbert, 2010; Molokwane et al., 2009; Nicolella et al., 2000; Stoodley et al., 1999; Chirwa & Wang 1997). According to Stoodley et al., (1999) and Nicolella et al., (2000), biomass limitation improves culture flexibility and allows high specific biomass retention, which increases volumetric yield in a continuous-flow system. An innovative two-stage bioreactor was reported for reduction of Cr(VI) by separating cell growth from the Cr(VI) contacting phase to avoid Cr(VI) toxicity, with near complete Cr(VI) removal (Wang & Sheng, 1994). Chirwa and Wang (1997) reported biofilm flexibility by observing remediation after Cr(VI) overloading. This illustrates that attached growth systems enable higher volumetric reduction rates than suspended growth systems. However, higher Cr(VI) removal was observed in the biofilm system than in the suspended system, and this is attributed to culture adaptation and mass transport resistance across the attached biofilm layer (Wang & Chirwa, 2001). This suggests that the exposure of Cr(VI) toxicity to bacterial cells decreases with an increase in biofilm depth. In addition, a continuous system is preferred over a batch system as it is commercially applicable and allows easier handling and operation (Ahmad et al., 2010).

2.12 Biofilm theory and structure

Environmental microbiologists have long recognized that complex bacteria communities are responsible for driving the biochemical processes that maintains the biosphere (Davey et al., 2000). Moreover, it becomes clear that these natural assemblages of bacteria function as a cooperative consortium, in a relatively complex and coordinate manner (Costerton et al., 1995). For this study, biofilms are defined as an assemblage of microorganisms or communities of bacteria attached to a solid substratum and embedded in a "glycocalyx" matrix consisting of self-excreted exopolysaccharides (EPS) (Aniruddha & Wang, 2010). EPS consists of polysaccharides, proteins, glycoproteins, glycolipids, and in some cases, certain amounts of extracellular DNA (e-DNA) (Flemming et al., 2007). It is one of the key components of the biofilm matrix, because it mediates the process of adhesion between the bacterium and the attachment surface (Donlan & Costerton, 2002).

According to Watnick and Kolter (1999), the biofilms of single species are formed in multiple steps. These steps resulting from the association between the bacterium and the attachment surface and other microorganisms already present on the surface finally lead to the formation of the three-dimensional biofilm matrix (Watnick & Kolter, 2000). Studies from Haack and Warren on microbial biofilms suggest stable accumulation of metals, however these microbes secrete polymers that can immobilize metal compounds by passive sequestration processes (Lie`vremont et al., 2009). In addition, they are less vulnerable to metal toxicity than planktonic cell population, which opens new perspectives for biofilm-mediated bioremediation processes (Harrison et al., 2005; Harrison et al., 2007).

Several studies have been conducted to investigate and understand the complex structure of the EPS and its components (Flemming et al., 2007). However, the most widely accepted theory is the creation of the microenvironment, which helps to counter severe pH changes in the bulk liquid, and also to resist toxic substances from entering the biofilm matrix. In addition, the close spacing of the cells in the matrix was important for effective transport of essential nutrients across the cells (Rittmann, 2001).

Other studies on biofilms show that biofilms are not simply organisms containing slime layers on the surface; instead biofilms represent the biological systems with a different level of organisms,

well structured, coordinated, and functional communities (O'Toole et al., 2001). Secondly, biofilms have been found positioned onto the surface in various mechanisms. The most common mechanism is the flagellar motility and different methods of surface translocation, including twitching, gliding, darting and sliding (Davey et al., 2000). Other mechanisms include the synthesis of cellulose, thereby forming a fibrous pellicle that places cells near the air-water interface. In addition, some species have magnetosomes (intracellular structure consisting of a crystal magnetic mineral) surrounded by a membrane that causes the cells to passively align with the earth's geomagnetic field, thereby restricting lateral excursion (Davey et al., 2000).

In the applications of biofilm, packed bed reactors are the most common type of biofilm reactors, the cells are usually attached to a stationary medium and are generally used for aerobic and anaerobic treatment of wastewater (Rittman, 2001). A fluidized bed and RBC reactor is another kind of biofilm reactor that is commonly employed for wastewater treatment. The cells in the fluidized bed reactors are immobilized and kept in suspension under a high effluent recycle flow rate (Aniruddha & Wang, 2010). The biggest advantage of the packed bed reactor over the other reactors is the capacity to withstand higher substrate loading rate due to the presence of strong attachment force between the cells and the surface (Aniruddha & Wang, 2010). Secondly, attached biomass system is anticipated to enhance biofilm growth, which provides protection of useful microorganisms against toxicity through mass transport resistance. However, bacteria grown in suspension is known to be highly susceptible to toxic compounds such as Cr(VI) (Nkhalambayausi-Chirwa & Wang 2001). For this reason, this study used a packed bed reactor for Cr(VI) reduction with As(III) as an electron source.

2.13 Summary

The co-existence of Cr(VI) and As(III) suggests a redox cycle, which provides the potential for simultaneous bioremediation of these metals/metalloids in a single close system. Generally, remediation of these metalloids involves reduction of Cr(VI) to Cr(III) and oxidation of As(III) to As(V), which are often treated separately. To date, bioremediation of Cr(VI) together with As(III) has not been achieved in a single system, and the mechanism of combined toxic metal detoxification is not well understood. However, this study explores combined bioremediation of Cr(VI) and As(III) in a single system. Consent and combined detoxification of these metalloids were based on thermodynamic principles and the redox process. The induced redox cycle was achieved by combining biocatalytic oxidation of Arsenic Equation 2.16, originally derived from Anirudha and

Wang (2010) and biocatalytic reduction of chromium Equation 2.12, from Suziki et al. (l999). Thus, free energy is generated through the overall redox cycle as it is an exothermic reaction.

Apart from research studies done from 2014 to 2017, very few studies have been done on simultaneous Cr(VI) reduction and As(III) oxidation (Wang, 2013; Batchate et al., 2013). Wang's (2013) study that was previously reviewed is different from the present study since As(III) oxidation is facilitated in the presence of hydrogen peroxide: a compound containing oxygen. There is little difference between Wang's (2013) study and the study by Batchate et al., (2013). According to Batchate et al., (2013) simultaneous Cr(VI) reduction and As(III) oxidation were achieved with the *Bacillus firmus* strain TE7 under aerobic conditions. However, the present study is different from the studies of Wang (2013) and Batchate et al. (2013) since Cr(VI) reduction and As(III) oxidation were achieved under anaerobic conditions. The present study was evaluated under anaerobic conditions since As(III) is mostly stable, and released from laden sediments (less or no oxygen zone) by arsenate-respiring bacteria (Oremland & Stolz, 2006).

CHAPTER 3

Materials and methods

3.3 Source of micro-organism

Water and soil samples from an old cow dip farm in Tzaneen (Limpopo Province, South Africa) and dried sludge samples from sand-drying beds at Brits Wastewater Treatment Works (North West Province, South Africa) were used as inoculum for the mixed culture of anaerobic bacteria. It was reported earlier that various cow dips in Limpopo (South Africa) routinely used arsenic-based compounds for cattle dipping for about half a century to combat East Coast fever in cattle (Perry, 2016). High As(III) concentration of up to 46.6 mg/kg was reported in one of the cow dips in this province (Ramudzuli & Horn, 2014). Cr(VI)-reducing cultures were collected from a wastewater treatment plant that received high levels of Cr(VI) from an abandoned chrome processing facility in Brits (North West Province, South Africa) (see Appendix A). The plant received periodic overflows from the Cr(VI) refining foundry during the period 1996 to 2006. Cr at the plant was detected at levels of approximately 2.45 mg/L, 2.63 mg/L and 25.44 mg/L in the influent water, mixed liquor of aeration tanks, and dried sludge, respectively (Molokwane et al., 2008). It was therefore anticipated that microorganisms in sludge should exhibit resistance to Cr(VI) toxicity.

The cultures from the cow dip and sludge were grown in basal mineral medium (BMM), which was prepared by dissolving (in 1 L of deionised water): 10 mM NH_4Cl, 30 mM Na_2HPO_4, 20 mM KH_2PO_4, 0.8 mM Na_2SO_4, 0.2 mM $MgSO_4$, 50 μM $CaCl_2$, 25 μM $FeSO_4$, 0.1 μM $ZnCl_2$, 0.2 μM $CuCl_2$, 0.1 μM NaBr, 0.05μM Na_2MoO_2, 0.1μM $MnCl_2$, 0.1μM KI, 0.2 μM H_3BO_3, 0.1 μM $CoCl_2$, and 0.1 μM $NiCl_2$ (Roslev et al., 1998). The medium was sterilized before use by autoclaving at 121°C and 1.20 atm pressure for 15 min. All chemicals were purchased from Merck (South Africa). Cultures were grown in cooled BMM by adding either 2 mL of liquid samples from the cow dip and/or 0.2 g sludge sample from the Wastewater Treatment Plant. Cultures were grown at 30°C under continuous shaking at 120 rpm for 24 hours or until visible growth occurred.
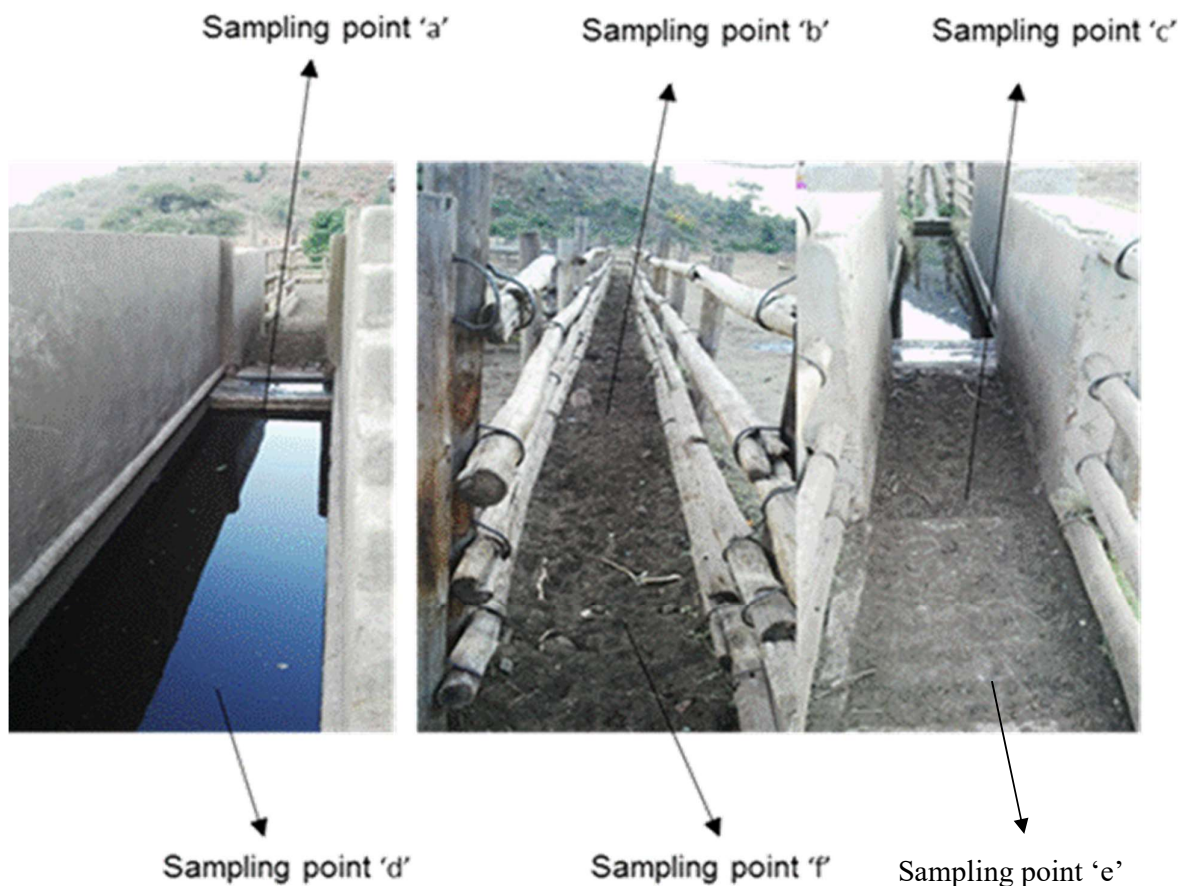
Figure 3.1: Cow dip sample collection location (a-f) for possible arsenic (III) resistant bacteria isolation (Igboamalu & Chirwa, 2017)

3.2 Culture enrichment

For culture enrichment, BMM was amended with 70 mg/L of Cr(VI) and 120 mg/L As(III), and 0.2 g sludge and 2 mL cow dip waster was added to 100 mL of the solution (Igboamalu & Chirwa, 2014). Anaerobic cultures were prepared in 100 mL serum bottles purged for 5-10 min with 99.9% N_2 gas and sealed with silicone rubber stoppers and aluminium seals. As(III)- and Cr(VI)-resistant bacteria were isolated by directly plating enriched cultures on nutrient agar containing 40 and 30 mg/L of As(III) and Cr(VI), respectively. Pure isolates were obtained by serial dilution method, and sub-culturing of morphological different colonies, as previously described by Molokwane et al. (2008). Batches were incubated under shaking at 120 rpm in a rotary environmental shaker (Labotech, Gauteng, South Africa) at 30 ± 0.2ºC. The inoculant was amended with Cr(VI) and As(III) to acclimatize the culture in the sludge samples. However, anaerobic cultures were grown

in a 100 mL serum bottle purged with 99.9% of nitrogen gas for about 5 to 10 minutes. The bottle was then closed with silicone rubber and aluminium stoppers.

3.3 Culture isolation

Using the spread method (Molokwane et al., 2008), cultures were isolated by depositing 1 mL of serially diluted sample from the 7th to the 10th test tubes using a pipette into Petri dishes containing sterilised nutrient agar. The nutrient agar was then incubated for about 24 h at 30 ± 0.2°C to develop separate identifiable colonies. After 24 h of incubation, individual colonies from the latter agar plates were then transferred into new sterilised agar plates with a sterile wire loop based on their colour and morphology. Subsequently, the plates were then incubated for 24 h at 30 ± 0.2°C. The isolated cultures were then stored as pure stock solution at -70°C.

3.4 Culture storage and sub-culturing

20 mL of sterile glycerol (20%, v/v) was added to 80 mL bacteria culture. The mixture was checked to evenly disperse the glycerol before transferring into 2 mL screw-cap tubes. Subsequently, the transferred samples in the 2 mL screw-cap tubes were stored at -70 °C for further use. For each experimental run, the frozen cultures were melted for about 10 to 20 min. The enriched cultures were plated on nutrient agar plates containing 40 and 30 mg/L of As(III) and Cr(VI) respectively using a sterile inoculating loop, incubated for about 24 h at 36 ± 0.2°C in an insulated incubator.

3.5 Culture characterization

Genomic DNA was extracted from the pure cultures using a DNeasy tissue kit (QIAGEN Ltd, West Sussex, UK). The 16S rRNA genes of isolates were amplified by reverse transcriptase-polymerase chain reaction (RT-PCR) using primers pA and pH1 (Primer pA corresponds to position 8-27; Primer pH to position 1541-1522 of the 16S gene). An internal primer pD was used for sequencing (corresponding to position 519-536 of the 16S gene). The resulting sequences were matched to known bacteria in the GenBank using a basic BLAST search of the National Centre for Biotechnology Information (NCBI, Bethesda, MD) using *Thermicanus aegyptius* as an outgroup for G(+ve) aerobes and *Enterobacter amniqenus* as the outgroup for G(–ve) anaerobes. The 16S rRNA gene sequences of the purified strains were aligned with reference sequences corresponding to phenol and PAH-degrading organisms. Sequence alignment was verified manually using the

program BIOEDIT (Ibis Therapeutics, Carlsbad, CA). Pairwise evolutionary distances based on an unambiguous stretch of 1541 bp were computed by using the Jukes and Cantor method (Jukes & Cantor, 1969). Phylogenetic tree diagrams were then constructed using the neighbour-joining method (Tamura et al., 2013).

3.6   Microbial analysis

Isolates labelled (C_{R1}, C_{R2}, C_{R3}, C_{R4}, C_{R5}, C_{R6}) from dried sludge samples, and (A_1, A_2, A_3, A_4, A_5, A_6), (Y_1, Y_2, Y_3, Y_4, Y_5, Y_6) and (A_{S1}, A_{S2}, A_{S3}, A_{S4}, A_{S5}, A_{S6}) from cow dip samples, were analysed for Cr(VI) resistance and reduction ability in the presence of As(III) and other pollutants such as lead, Cd, etc. This was achieved by growing the isolates into a 100 ml bottle covered with aluminium foil, containing nutrient broth amended with 70 mg/L Cr(IV), 120 mg/L As(III), and 1.5g NaHCO$_3$ at 36 ± 0.2ºC for 48 h. The cells were also tested with 50 mg/L Pb, 50 mg/L Cd, 50 mg/L Zn. The incubated nutrient broth was decanted at 6000 rpm centrifuge, and the remaining pellet was washed three times with a sterile saline solution (0.85% NaCl). Anaerobic conditions were maintained by purging 99.99% N$_2$ gas in the bottle containing harvested cells. 1 ml of the sample was initially withdrawn from the bottle for As(III) and As(V), and Cr(VI) quantification before reintroducing the cells in each bottles. The study was conducted on a 120-rpm orbital shaker (Labotech, Gauteng, South Africa). The samples withdrawn over time were centrifuged using a 2-5 ml Eppendorf tube at 6000 rpm for 10 min in a Minispin® Microcentrifuge (Eppendorf, Hamburg, Germany). In a 100 ml bottle containing 70 mg/L Cr(VI) and 120 mg/L As(III) concentration, an abiotic control batch was prepared using the same procedure as the other experimental batches, except that heat kill or no cells were added to the control batches.

3.7 Cr(VI)-reducing potential experimental plan

In 100 mL sterilised bottles containing BMM, the harvested cells previously tested, as described in the previous section, were re-suspended before adding Cr(VI) and As(III), to give a desired concentration. Cr(VI) and As(III) stock solution were added to give a final concentration of 50-500 mg/L and 80 mg/L respectively. Subsequently, the 100 mL bottles containing the harvested cells were purged with N$_2$ gas before sealing with silicon stoppers and aluminium seals. The experiments were conducted at 30 ± 0.2ºC over time at 120 rpm on the orbital shaker (Labotech, Gauteng, South Africa). Prior to inoculating the bottles with harvested cell, 1 mL of the sample was initially

withdrawn from the serum bottle to determine the absorbance of Cr(VI) before introducing the cells in each serum bottle. The samples withdrawn in serum bottles over time were centrifuged using a 2 mL Eppendorf tube at 6000 rpm for 10 min in a Minispin® Microcentrifuge (Eppendorf, Hamburg, Germany) and the supernatant was used for Cr(VI) reduction analysis.

3.8   As(III) oxidizing potential experimental plan

The capability of the cow dip isolates from soil and water to resist and oxidize As(III) was investigated. A 100 ml bottle containing harvested cells or strains amended with basal mineral medium (BMM) of As(III) concentrations ranging from 20-1000 mg/L, and 1.5g $NaHCO_3$ as sole carbon source, was checked. Anaerobic conditions were achieved by purging with 99.9% N_2 gas for 5 to 10 min before sealing with silicon stopper and aluminium seals, and then covered with aluminium foil. The bottles were incubated in a light-constrained control room at 36 ± 0.2°C on an orbital shaker at 120 rpm (Labotech, Gauteng, South Africa). At each sampling interval, samples were withdrawn, centrifuged using a 5ml Eppendorf tube at 6000 rpm for 10 min in a Minispin® Microcentrifuge (Eppendorf, Hamburg, Germany) for As(III) and As(V) analysis. Effect of carbon source, pH and oxidation reduction potential of the mixed strains were checked at 50 mg/L, 70 mg/L and 100 mg/L in a 100 ml bottle. An abiotic control batch was prepared using the same procedure as the other experimental batches, except that heat kill or no cells were added to the control batches.

3.9   Batch experimental plan

3.9.1   Effect of pH on Cr(VI) and As(III) microbial redox conversion

Optimum pH for Cr(VI) reduction linked to As(III) oxidation was checked by growing the mixed culture isolated from cow dip and dried sludge in a 100 ml basal mineral medium solution. The solution was amended with 70 mg/L, 120 mg/L concentrations of Cr(VI), As(III) and 1.5g $NaHCO_3$ at a different pH of 1,4,7 and 10. The pH concentration of the aqueous medium was adjusted by adding a certain concentration of H_2SO_4 and NaOH. All bottles were covered with aluminium foil, incubated at 36 ± 0.2°C on a 120 rpm orbital shaker (Labotec, Gauteng, South Africa). Anaerobic conditions were maintained by purging 99.99% N_2. Prior to inoculating the 100 mL bottles with harvested cell, 1-5 mL of the sample was initially withdrawn from the serum bottle to determine the absorbance of Cr(VI) and quantification of As(III) and As(V) before introducing the cells in each

serum bottle. The samples withdrawn in serum bottles over time were centrifuged using a 2 mL Eppendorf tube at 6000 rpm for 10 min in a Minispin® Microcentrifuge (Eppendorf, Hamburg, Germany) and the supernatant was used for Cr(VI) reduction analysis.

3.9.2   Effect of carbon source on Cr(VI) and As(III) microbial redox conversion

Effect of carbon source on induced Cr(VI) reduction linked As(III) oxidation, the isolates were grown in a 200 mL basal mineral medium containing 70 mg Cr(VI /L), and 120 mg As(III) /L with organic and inorganic carbon. $0.03MC_6H_{12}0_6$ and $0.01MNaHCO_3$ were used as organic and inorganic carbon source. Control bottles were prepared using the same procedure as the other experimental batches, except that no organic or inorganic carbon was added to the control batches. All bottles were covered with aluminium foil, incubated at 30 ± 2 ºC over time on a 120 rpm orbital shaker (Labotec, Gauteng, South Africa). Anaerobic growth was achieved by purging 99.99% N_2 gas. 1-5 mL of the samples were periodically withdrawn to determine the As(III) and As(V) concentration, and absorbance of Cr(VI). The samples withdrawn in serum bottles were centrifuged using a 2-5 ml Eppendorf tube at 6000 rpm for 10 min in a Minispin® Microcentrifuge (Eppendorf, Hamburg, Germany).

3.9.3 Effect of oxidation-reduction potential on Cr(VI) and As(III) redox conversion

The oxidation reduction potential of the basal mineral medium solution containing mixed culture isolates from cow dip and dried sludge was checked in a bottle. The solution was amended with 70 mg/L, 120 mg/L concentrations of Cr(VI), As(III) and 1.5g $NaHCO_3$. In a different experiment, the solution was amended with 50 mg/L, 120 mg/L concentrations of Cr(VI), As(III) and 1.5g $NaHCO_3$ for recheck. Anaerobic conditions were maintained by purging 99.99% N_2. Prior to inoculating the 100 mL bottles with harvested cells, 1-5 mL of the sample was initially withdrawn from the serum bottle to determine the solution's oxidation and reduction potential in millivolts as well as the pH. The samples withdrawn in serum bottles over time were centrifuged using a 2 mL Eppendorf tube at 6000 rpm for 10 min in a Minispin® Microcentrifuge (Eppendorf, Hamburg, Germany) and the supernatant was used for oxidation reduction potential analysis as well as the pH at the point of sampling.

3.9.4 Abiotic experiment

The abiotic control batches were prepared using the same procedure as the other experimental batches, except that heat kill or no cells were added to the control batches. Two different scenarios of abiotic experiments were conducted. First, in a 100 ml bottle containing mixed-culture isolates from cow dip and dried sludge. The solution was amended with 70 mg/L and 120 mg/L Cr(VI) and As(III) concentrations, and 1.5g of NaHCO$_3$. The control experiment was checked against a solution containing: (a) Cr(VI) and As(III), (b) As(III), Cr(VI) and isolates, (c) Cr(VI) and isolates. Second, in a different control experiment, a 100 ml bottle containing 50 mg/L and 120 mg/L Cr(VI) and As(III) concentration, 70 mg/L and 120 mg/L Cr(VI) and As(III) concentration and 100 mg/L and 120 mg/L Cr(VI) and As(III) concentration were checked. The solution was amended with 1.5g NaHCO$_3$ and heat-killed cells. Anaerobic conditions were achieved by purging 99.99% N$_2$ gas for 5-10 mins. Prior to inoculating the 100 mL bottles with harvested cells, 1-5 mL of the sample was initially withdrawn from the serum bottle to determine the absorbance of Cr(VI) before introducing the cells in each serum bottle. The samples withdrawn in serum bottles over time were centrifuged using a 2 mL Eppendorf tube at 6000 rpm for 10 min in a Minispin® Microcentrifuge (Eppendorf, Hamburg, Germany) and the supernatant was used for Cr(VI) reduction analysis.

3.9.5 Cr(VI) and As(III) threshold limit analysis

Cr(VI) and As(III) threshold limit analysis was checked with a mixed culture of isolates in a 100 ml bottle covered with foil. Cells harvested by centrifugation, as described above, were suspended in 100 mL BMM before adding Cr(VI) and As(III). Cr(VI) and As(III) were added from stock solutions to produce a set of batches with varying Cr(VI) concentration, i.e. 20-200 mg Cr(VI)/L, and a constant arsenic concentration of 120 mg As(III)/L in each batch. In a different batch study, bicarbonate was amended as carbon source. After adding Cr(VI) and As(III), the cultures were purged with N$_2$ gas (99.9% pure) for 15 minutes before sealing with silicon stoppers and aluminium seals. The experiments were conducted at 30 ± 0.2°C at 120 rpm on an orbital shaker (Labotech, Gauteng, South Africa). Prior to inoculating the 100 mL bottles with harvested cells, 1-5 mL of the sample was initially withdrawn from the serum bottle to determine the absorbance of Cr(VI) and quantification of As(III) and As(V) before introducing the cells in each serum bottle. The samples withdrawn in serum bottles over time were centrifuged using a 2 mL Eppendorf tube at 6000 rpm for 10 min in a Minispin® Microcentrifuge (Eppendorf, Hambury, Germany) and the supernatant was used for Cr(VI) reduction analysis.

3.9.6 Biocatalytic redox conversion of Cr(VI) with concurrent As(III) oxidation

Cr(VI) reduction linked to As(III) oxidation in a mixed culture of isolates were studied in a 100 ml bottle containing basal mineral medium. The solution was amended with 60-500 mg/L As(III) concentrations, 70 mg/L Cr(VI) concentration and 1.5g NaHCO$_3$. Heat-killed cells were checked in triplet for the abiotic transformation of As(III) and Cr(VI). All bottles were covered with aluminium foil, incubated at 36 $\pm$ 0.2^{o}C on a 120 rpm orbital shaker (Labotech, Gauteng, South Africa). Anaerobic conditions were achieved by purging 99.99% N$_2$ gas for 5 to 10 mins. Prior to inoculating the 100 mL bottles with harvested cells, 1-5 mL of the sample was initially withdrawn from the serum bottle to determine the absorbance of Cr(VI) and quantification of As(III) and As(V) before introducing the cells in each serum bottle. The samples withdrawn in serum bottles over time were centrifuged using a 2 mL Eppendorf tube at 6000 rpm for 10 min in a Minispin® Microcentrifuge (Eppendorf, Hambury, Germany) and the supernatant was used for Cr(VI) reduction analysis.

3.10 Analytical methods

3.10.1 Cr(VI) and total Cr

2 mL samples were collected from the effluent stream into Eppendorf-type centrifuge tubes at various intervals of the experiment. The samples were centrifuged at 6000 rpm, 2000 g (Hermle GmbH Z100 M mini-centrifuge) for 15 min to remove the cells as pellets at the bottom of the tubes. The cell-free supernatant used for analytical procedures was extracted from the centrifuge tubes with a pipette without re-suspending the separated cells. The concentration of Cr(VI) was quantified by measuring the absorbance of its visualised purple complex after adding 1,5-diphenylcarbohydrazide (1,5-DPC) at 540 nm using a UV Spectrophotometer (WPA Lightwave II, Labotech, South Africa). In a 10 ml flask, 200 mL of centrifuged sample was amended with 1 mL H$_2$SO$_4$ (1 N) for sample digestion, then topped up with distilled water. 0.2 mL of 15% 1,5-DPC was added. The concentration of Cr(VI) in the sample was proportional to the change in colour, which was recorded as absorbance at 540 nm wavelength (APHA/AWWA/WEF, 2012). Total Cr was measured at a wavelength of 359.9 nm using a Varian AA-1275 Atomic Adsorption Spectrophotometer (AAS) (Varian, Palo Alto, California, USA) equipped with a 3-mA chromium hollow cathode lamp. Cr was leached from soil samples using a diluted HCl solution (1 N HCl)

(Molokwane et al., 2008). Cr(III) was determined as the difference between total Cr and Cr(VI) concentration. The standard curve graph is shown in Appendix J.

3.10.2 Determination of As(III) and As(V)

As(III) and As(V) speciation were measured using a Metrohm Compact 930 Flex Ion Chromatograph (IC) (Metrohm, Herisau, Switzerland) equipped with a Metrosep A Supp 10 Guard/2.0 and Metrosep A Supp 5 100/4.0 column (Metrohm). Detection was done by a 944 Professional UV/Vis Detector and 856 Professional Conductivity Detector (Metrohm). As(III) was detected with UV/Vis, while As(V) was detected with a conductivity detector using the method reported earlier by Clement and Yang (1997). The mobile phase consisted (in 1 L deionized water) of: 5.6 g of NaOH, 3.364 g of $NaHCO_3$ and 12.8 g of Na_2CO_3 (3.0 mM Na_2CO_3 + 1.0 mM $NaHCO_3$ + 3.5 mM NaOH, respectively), operated at 35°C temperature, 8.42 MPa pressure and a flow rate of 0.80 mL/min. The chromatogram for the standard graph is shown in Appendix H.

3.10.3 Total viable biomass and growth

A quantitative analysis of biomass was conducted gravimetrically as a function of volatile suspended solids (VSS). The VSS was determined as the difference in dry weight of samples of known volume after igniting thoroughly dried samples at 550°C in a furnace. Results were calibrated against colony-forming units from a heterotrophic (pour) plate method on Luria-Bettani (LB) and Plate Count (PC) agar from soil samples dispersed in sterile saline (0.85% w/v NaCl) solution. The VSS values were used as model input values for the viable biomass concentration parameter (X_a, mg/L) during the kinetic studies. The accuracy within the allowable error range of ±5% was achieved by setting up the experiments in triplicates for biomass analysis.

Also, cell growth was spectrophotometrically determined at single wavelength $\lambda = 600$ nm using a UV Lightwave II spectrophotometer (Labotec, South Africa). The cuvette of 10 cm path length was used to carry the aliquot samples in the sample chamber of the spectrophotometer. The measurements were blanked to zero using sterile MSM as a reference. All the tests were conducted in triplicates and in comparison, to a control.

3.11 Reagents

3.11.1 Chemicals

Sodium arsenite ($NaAsO_4$, 99.9% purity), di-potassium chromate (K_2CrO_4, 99% purity), H_2SO_4 (99.9% purity), 1, 5 - diphenyl carbazide (99% purity), (0.85%) NaCl

All chemicals were purchased from Merck South Africa.

3.11.2 Standard solutions

Cr(VI) stock solution (1000 mg/L) was prepared by dissolving 3.74 g of 99% pure K_2CrO_4 (analytical grade) in 1 L deionized water. As(III) stock solution (1000 mg/L) was prepared by dissolving 1.75 g of $\geq$ 90% $NaAsO_2$ (Sigma-Aldrich) in 1L deionized water. As(V) stock solution (1000 mg/L) was prepared by dissolving 4.165 g of $\geq$ 98% $Na_2HAsO_4.7H_2O$ (Sigma-Aldrich) in 1L deionized water. 1000 mg/L Cr(VI) and As(III) stock solutions were used as sources of Cr(VI), As(III), and As(V). The standard solutions of Cr(VI) were prepared from the Cr(VI) stock solutions in a 10 ml volumetric flask by diluting a certain volume of Cr(VI) stock solution with distilled water to give desirable final concentrations of (0, 1, 2, 3, 4, 6 and 8) mg/L. From these data points (absorbance against concentration) a linear graph or calibration curve with the regression of 99.95% was obtained (see Appendix (D).

3.11.3 DPC solution

Diphenyl carbazide (Merck, South Africa) solution was prepared for Cr(VI) reduction analyses by dissolving 0.5 g of 1,5-diphenylcarbazide in 100 ml of HPLC grade acetone and was stored in a brown bottle covered with a foil. Eluent for As(III) and As(V) was prepared by dissolving 5.6 g of NaOH, 3.364 g of $NaHCO_3$ and 12.8 g of $NaCO_3$ in 1000 ml ultra-pure water.

3.12 Growth media

3.12.1 Basal mineral media

The cultures from the gold field, cow dip sludge were grown in basal mineral medium (BMM) which was prepared by dissolving (in 1 L of deionised water): 10 mM NH_4Cl, 30 mM Na_2HPO_4, 20 mM KH_2PO_4, 0.8 mM Na_2SO_4, 0.2 mM $MgSO_4$, 50 µM $CaCl_2$, 25 µM $FeSO_4$, 0.1 µM $ZnCl_2$, 0.2 µM $CuCl_2$, 0.1 µM $NaBr$, 0.05µM Na_2MoO_2, 0.1µM $MnCl_2$, 0.1µM KI, 0.2 µM H_3BO_3, 0.1 µM $CoCl_2$, and 0.1 µM $NiCl_2$ (Roslev et al., 1998). The medium was sterilized before use by autoclaving at 121°C and 1.20 atmos pressure for 15 min. All chemicals were purchased from Merck (South Africa). Cultures were grown in cooled BMM by adding either 2 mL of liquid samples from the cow dip and/or 0.2 g sludge sample from the Wastewater Treatment Plant. Cultures were grown at 30ºC under continuous shaking at 120 rpm for 24 hours or until visible growth occurred.

3.12.2 Commercial broth and agar

Luria-Bettani (LB) broth, Luria-Bettani (LB) agar, and Soy broth (Merck, South Africa) were prepared by respectively dissolving 25 g, 45 g, and 23 g in 1000 mL of distilled water. The LB and PC agar media were cooled at room temperature after sterilization at 121°C at 115 kg/cm^2 for 15 min and then dispensed into petri dishes to form agar plates for colony development.

3.13 Continuous-flow reactor experiment

3.13.1 Reactor set-up

The continuous-flow reactor experiment was investigated in a glass bead packed bed biofilm reactor (Reactor 1) and ceramic bead packed bed biofilm reactor (Reactor 3) with anaerobic tanks retrofit (Reactor 2 and 4) in series connection. The laboratory set-up is shown in Figure 3.2 and 3.3. Glass bead packed bed biofilm reactor (Reactor 1) was constructed from a Pyrex glass column (height: 70±0.01 cm, internal diameter: 10 ± 0.01 cm) packed with 7840 mm spherical Pyrex glass beads (Fisher Scientific Co, Pittsburgh, PA) (see Figure 3.4). The total external surface area of the glass beads available for cell attachment is 154,000 mm^2, in the packed bed reactor volume of 5500 cm^3 and area of 78.57 cm^2. Similarly, ceramic bead packed bed biofilm reactor (Reactor 3) was a Pyrex

glass column (height: 70 ± 0.01 cm, internal diameter: 10.0 ± 0.01 cm) packed with 2744, 15 mm spherical ceramic beads (Fisher Scientific Co, Pittsburgh, PA) (see Figure 3.5). The total external surface area of the ceramic beads available for cell attachment is 485,100 mm^2, in the packed bed reactor volume of 5500 cm^3 and area of 78.57 cm^2, while the anaerobic tank's retrofit is made of a sealed 1000 cm^3 reactor. Prior to assembling, the components of the pumps, control valves and the connecting tubing were autoclaved at 121°C for 15 min. Subsequently, the interior of the reactor was rinsed in 95% ethanol and dried. The 3 geometric of typical industrial scale set-up is shown in Figure 3.6 and 3.7. Other design parameters are shown in Table 3.1.

For a working reactor volume of 5500 cm^3, distilled water was used to pre-calibrate peristaltic pumps used to achieve the initial volumetric flow rate (Table 3.1). The actual volumetric flow was determined based on the calculated pore volume of the packed beds. Both reactors were operated in an up-flow mode to ensure near completely submerged condition. Reactors (R_1 and R_3) were designed to operate continuously at optimum hydraulic retention time approximately under volumetric flow rate of 0.0899 cm^3/s. The anaerobic retrofit tanks (R_2 and R_4) operated under the same volumetric flow at optimum hydraulic retention time approximately 3 h. Both reactors consist of sample ports of the same diameter, and 2 L influent and effluent tanks Table 3.1.
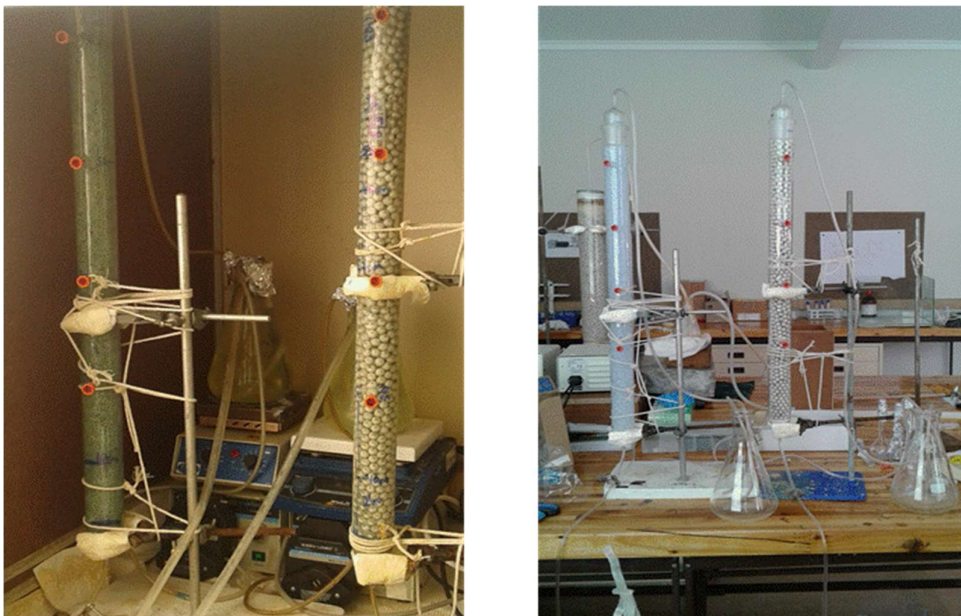
Figure 3.2: Reactors laboratory set-up prior to run

Figure 3.3: Reactors after 14 days' initial cell inoculation
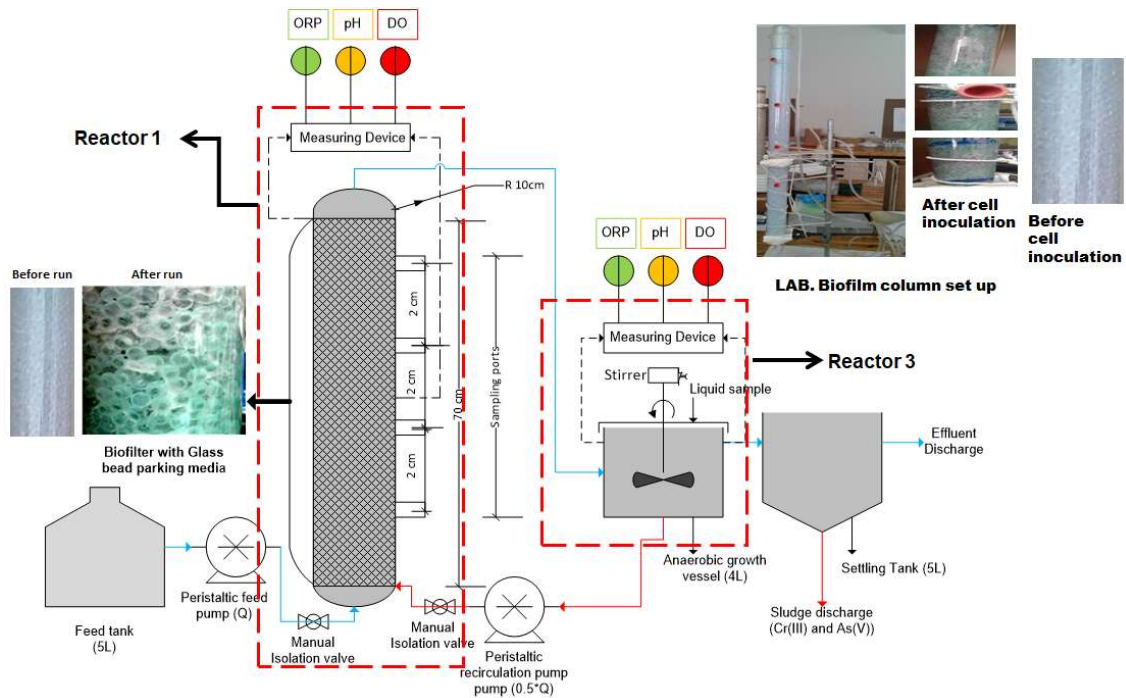
Figure 3.4: Continuous-flow glass bead packed bed with anaerobic CSTR retrofit and settling set
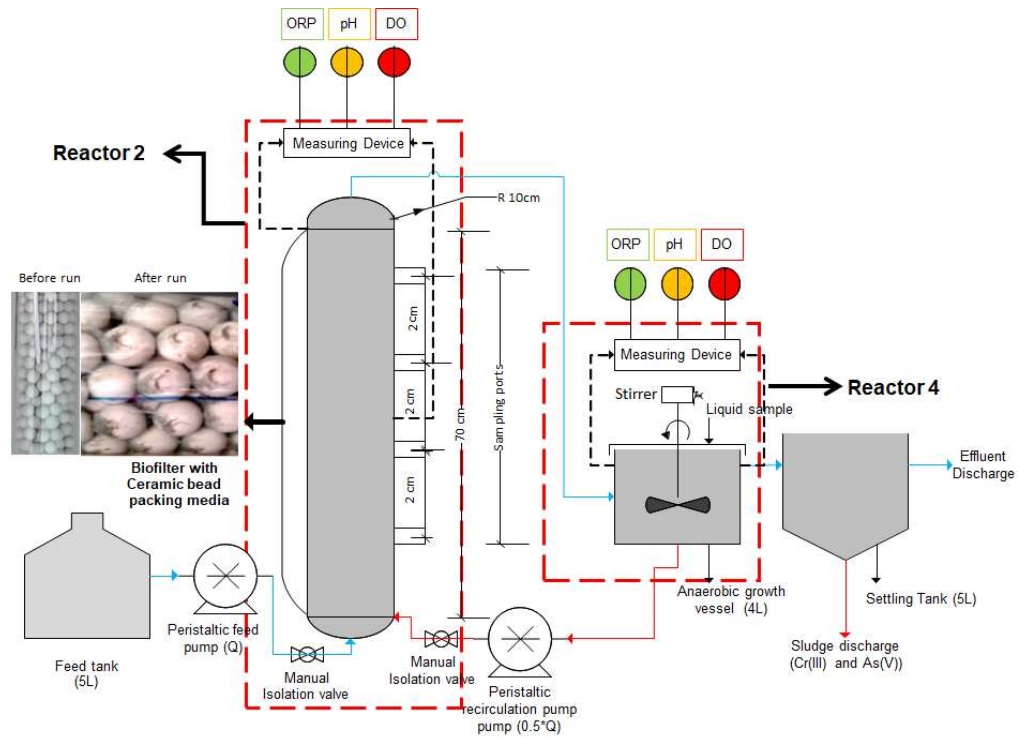
Figure 3.5: Continuous-flow ceramic bead packed bed with anaerobic CSTR retrofit and settling set-up
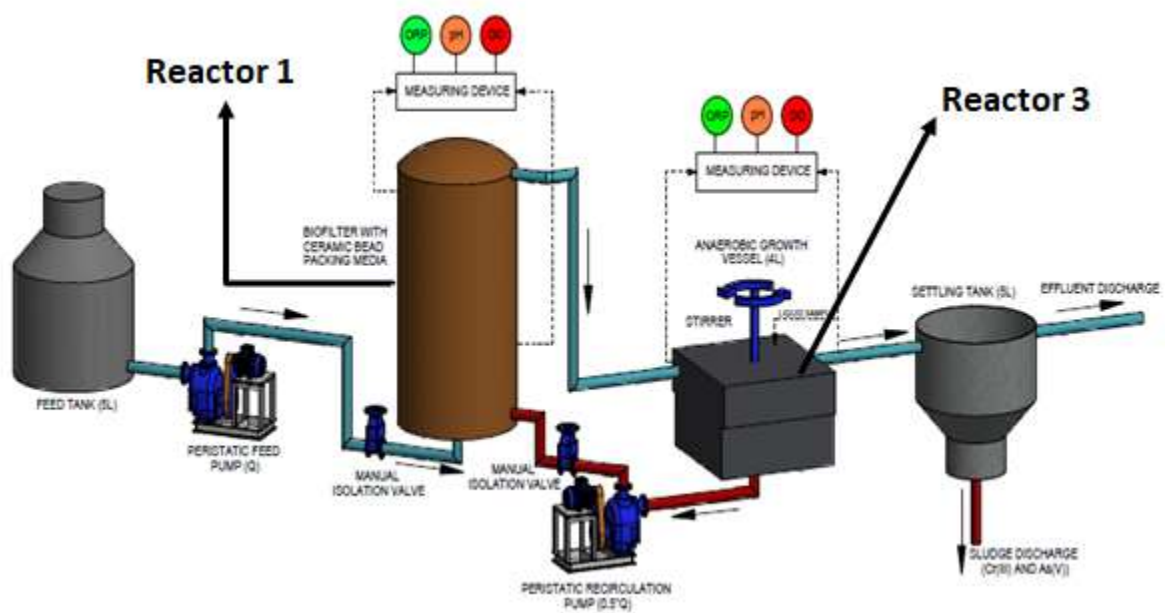
Figure 3.6: High rate anaerobic trickling filter reactor with glass bead media 3D model (pilot scale)
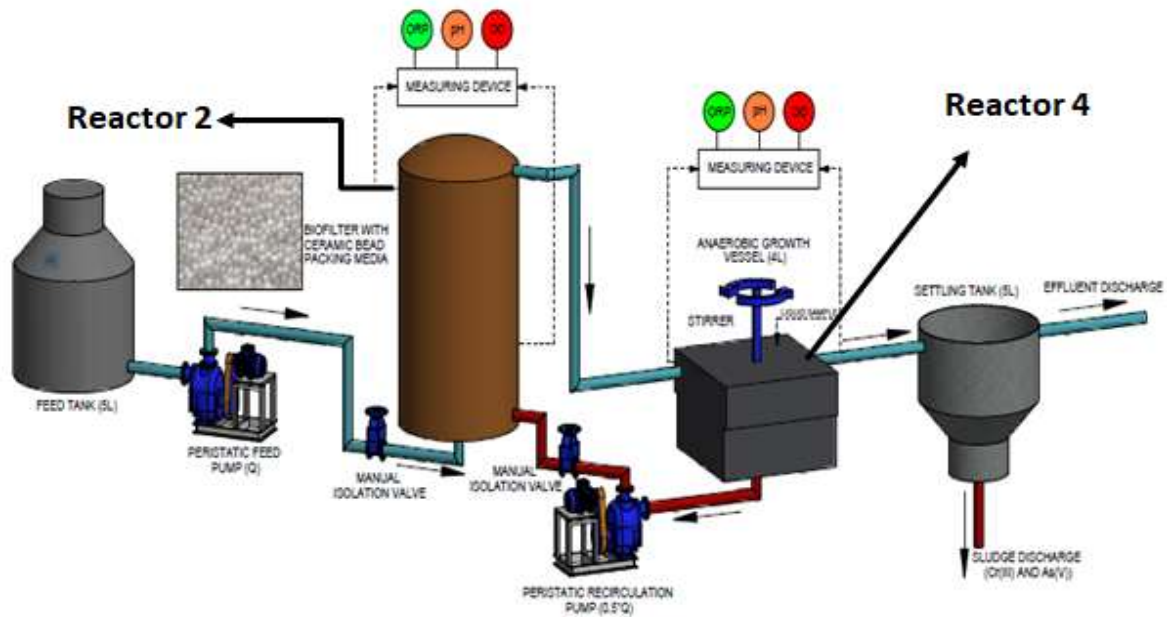
Figure 3.7: High rate anaerobic trickling filter biofilm reactor with ceramic bead media 3D model (pilot scale)

Table 3.1: Reactor design and steady-state operational param ***n/a: not applicable** eters

Reactor design parameters	Units	R1	R2	R3	R4
Height	cm	70	n/a	70	n/a
Packing height	cm	60	n/a	60	n/a
Diameter	mm	10	-	10	-
Diameter per bead (media)	mm	5	n/a	15	n/a
Reactor area	cm^2	79	n/a	79	n/a
Specific surface area	cm^2/cm^3	0.014		0.014	
Reactor volume	cm^3	5500	1000	5500	1000
Surface area per bead	mm^2	19.6	n/a	176.8	n/a
Total surface area of the (beads)	mm^2	154,000	n/a	485,100	n/a
Volumetric flow rate	cm^3/s	0.0899	0.0899	0.0899	0.0899
Porosity	%	69	n/a	72	n/a
Hydraulic retention time	h	11.73	3.08	12.24	3.08
Room temperature	ºC	31±0.2	31±0.2	31±0.2	31±0.2

3.13.2 Start-up culture

Stored harvested cells used in the batch experiment were incubated for 24 h. Subsequently, the cells were centrifuged at 6000 rpm (2820 g) for 10 min, and then thoroughly mixed with a basal mineral medium before being fed into the reactor. Before introducing the culture into the reactors, all the components of the reactors (column, feed tanks, tubes, valves, etc.) were autoclaved (HICLAVE HV-50 Hivayama South Africa) for 5 min at 121°C and ethanol cleaned.

3.13.3 Reactor start-up

Subsequent to reactor culture start-up, the reactors were inoculated with 100 mL overnight-grown anaerobic mixed culture, mixed with LB broth medium amended with 20 mg/L Cr(VI) and 30 mg/L As(III) for reactor acclimatization. This was incubated for 24 h in a temperature control room at 32 ± 0.2°C. After 24 h incubation, the reactor was operated under airtight conditions for more than 14 days until visible cell attachment was observed on the glass beads and column of the reactors (Figure 3.3). At this stage, glass and ceramic beads were collected from four different locations for scan electron microscopic analysis. However, after establishing biofilm growth or attachment on the glass and ceramic beads, the reactors were then operated under varying influent Cr(VI) and As(III) concentrations.

3.13.4 Cr(VI) reduction linked to As(III) oxidation

Both glass and ceramic bead reactors ('Reactor 1' and 'Reactor 3') were operated continuously for a period of 150 days over a range of influent Cr(VI) concentrations (30-200 mg/L) and As(III) concentrations in the ratio of 3:2 (51-340 mg/L) at liquid detention times (5-). Reactor double shocked load and response effect were evaluated at influent Cr(VI) concentration 100 mg/L and 200 mg/L and As(III) concentration of 170 mg/L and 340 mg/L. After double shock load effect, the reactors' recovery was evaluated at influent Cr(VI) concentration 40 mg/L and 30 mg/L and As(III) concentration of 68 mg/L and 51 mg/L. Both reactors were retrofitted with an anaerobic continuous-flow suspended growth tank, operated at liquid detention time of 3 h (approximately) to enhance optimum conversion of Cr(VI) to Cr(III) and As(III) to As(V). Flow from the anaerobic retrofit tanks were recirculated after 75 days (i.e. Phase IV) operational run to maintain the required microbial population or biofilm attached on the reactor media. Biological growth in the feed solution and tubes was minimized by close monitoring and periodical replacement. In addition, the

optimum operating conditions were maintained in the reactor by frequent monitoring of dissolved oxygen, pH, ORP, and temperature to achieve the desired optimum operating condition. From the sampling ports and final effluent from the anaerobic retrofit tank, samples were withdrawn over time and centrifuged using a 2-5 mL Eppendorf tube at 6000 rpm for 10 min in a Minispin® Microcentrifuge (Eppendorf, Hambury, Germany) and the supernatant was used for Cr(VI) reduction and As(III) oxidation analysis.

3.13.5 Steady-state determination

For each phase of experimental run, the reactor was continuously operated for at least more than 15 days to ensure steady-state conditions before changing the Cr(VI) and As(III) loading rate. The time taken by a completely mixed reactor to reach 95% of its steady-state concentration is at least three to four times the HRT. In the present study, the operation periods ranged from 14 to 28 times the HRTs, thus satisfying the steady-state assumptions for the entire operational phases. Second, steady state was also predicted when the effluent Cr(VI) concentration remained constant over a consecutive period.

3.14 Scanning electron microscopy

Scanning electron microscopy was done subsequently to reactor culture start-up, in order to examine biofilm growth, and establish the existence of biofilm on the glass beads. A sample of glass bead was removed from four locations in the biofilm reactor in order to have a randomly selected sample. The beads used were ground to create a rough surface area for microbial attachment. However, the procedure used the achieve scan electron microscopic study as listed below.

The procedure is as follows:

- Fixing the biomass with 2.5% glutaraldehyde dissolved in 0.075 M phosphate buffer (pH = 7.4-7.6) for 30 minutes

- Rinsing three times for five minutes each time with phosphate buffer

- Fixing with 0.25% aqueous osmium tetroxide three times for five minutes each time (in a fume hood)

- Rinsing three times with distilled water (in the fume hood)

- Dehydrating with 20, 50, 70, 90 and 99% ethanol for five minutes at a time

- Drying twice for 15 min at a time with hexamethyldisilazane

- Evaporating hexamethyldisilazane from the particles under atmospheric conditions for approximately 30 minutes

- Attaching particles to carbon tape, which in turn was fixed to an aluminium support

- Covering in gold under argon plasma

3.15 Routine monitoring

3.15.1 Dissolved oxygen (DO) concentration

Dissolved oxygen content of the reactor was measured using a DO meter (LD0101 Hatch South Africa). The DO meter was calibrated with standard buffers of 4 and 7 and disinfected with 95% ethanol before use.

3.15.2 pH and temperature

The pH and temperature of the effluents were measured using a pH meter (PHC101 Hatch South Africa) and the pH meter was calibrated with standard buffers of 4 and 7 and disinfected with 95% ethanol before use.

3.15.3 Oxidation Reduction Potential (ORP)

The ORP of the effluents was measured using an ORP meter (PHC101 Hatch South Africa). The ORP meter was calibrated with standard buffers of 4 and 7 and disinfected with 95% ethanol before use.

As(III)/Cr(VI) Autotrophic Redox Reaction in Batch Systems

4.1 Microbial analysis

4.1.1 Culture enrichment and isolation

Potential Cr reducing and As(III) oxidizing bacteria were isolated from different sources and the colonies were labelled (A1-A6), (As1-As6), (Cr1-Cr6) and (Y1-Y6) based on their tolerance to the toxicity of total arsenic (A), arsenite (As), chromium (Cr), or both chromium and arsenite (Y). The aim was to use As(III) as an electron donor and Cr(VI) as an electron sink in the system. The morphology of the cultures was determined by SEM, which showed a distribution of rod-shaped gram-negative and G-positive cells in the consortium (Figure 4.1). The image represented shows regions of mature biofilm development and the extracellular polymeric substances (EPS) that they formed. However, evidence of dense population of rod-shaped cells typically of *Bacillus* genera was identified with distinct small coccoid or filamentous cells (Figure 4.1a-b), whereas less dense population of gram-positive, motile rods cells, e.g. *Exiquobacterium* species with coccoid or filamentous cells, were seen (Figure 4.1 c-d). On the other hand, there was insignificant growth seen in the control studies (Figure 4.2 e-h). However, the observed evidence of biofilm growth and extracellular polymeric substances (EPS) suggests that Cr(VI) content in the presence of As(III) was indeed reduced by the biofilm formed.

The activity of Cr(VI)-reducing bacteria was indicated by the deposition of a bluish-grey precipitate within the mineral medium, signifying the formation of $Cr(OH)_3$ in solution. The mineral media was amended with bicarbonate to serve as the sole carbon source. Earlier studies showed that most bacteria utilise bicarbonate in the absence of CO_2 through the Calvin-Benson-Bassham cycle for growth and metabolism (Dastidar & Wang 2010). Preliminary observations showed that Cr(VI)

reduction all isolated reduced Cr(VI) to a certain degree in the presence of As(III) (Tables 4.1-4.2) (more data could be found in Appendix H).

The reduction of 70 mg/L Cr(VI) concentration in the presence of 120 mg/L of As(III) as inorganic sole electron supply became nearly completed after 144 h incubation (Table 4.1). Cr(VI) reduction in the anaerobic consortium with As(III) as an electron sink was further evaluated against killed culture controls, cell-free controls, and controls without arsenic (Figure 4.3 a-d). Higher Cr(VI) removal efficiency up to 98 % was seen in isolates (Cr_1-Cr_6) and (As_1-As_6) from cow dip (water sample) and dried sludge in comparison to (Y_1-Y_6) and (A_1-A_6) isolates from soil sample (Figure 4.4a-b). However, Cr(VI) reduction was not seen within heat kill cell (control 1) or Cr(VI) test in the absence of As(III) (control 2), indicating that Cr(VI) reduction was accomplished through metabolic activity.
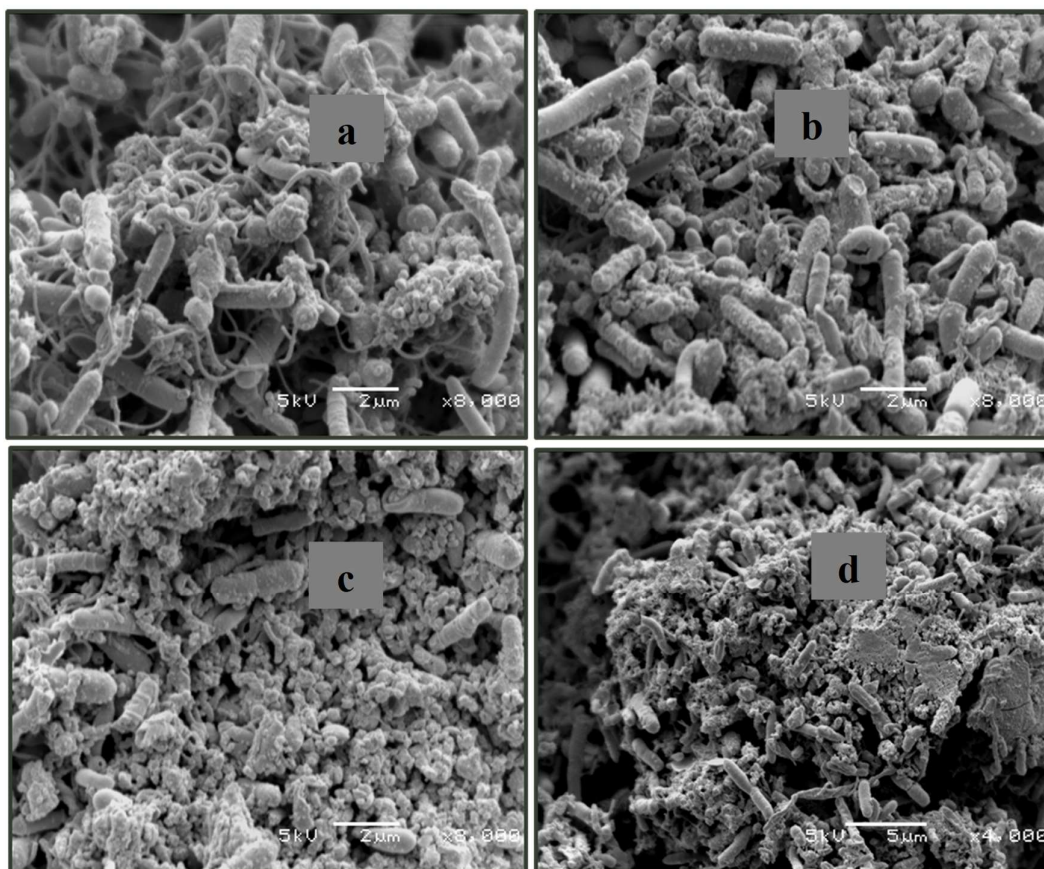
Figure 4.1: Morphological strains of the anaerobic consortium with Cr(VI) as electron sink and As(III) as electron donor (a) and (b) dense population of rod-shaped cells typically of *Bacillus* genera; (c) and (d) less dense population of gram-positive, motile rods cell

Furthermore, the survival of these microbes is attributed to an enzymatic membrane-bound structure such as reductase or energy yield dissimilatory process. As previously reported, under anaerobic conditions, Cr(VI) reduction is attributed to an energy-yielding dissimilatory respiratory process, in which Cr(VI) serves as a terminal electron acceptor (Dhal et al., 2013). In addition, it may also be attributed to soluble reductase, a membrane bound with the possibility of involving hydrogenase or cytochrome (Michel et al., 2001). The metal resistance shown by the isolates is aligned with earlier reports, where an organism isolated from a contaminated site also shows heavy metal resistance (Bachate et al., 2013; Dong et al., 2014). Second, the utilization of HCO_3^- or by fixing CO_2 via the Calvin-Benson-Bassham cycle suggests the evidence of chemoautotrophic bacteria.
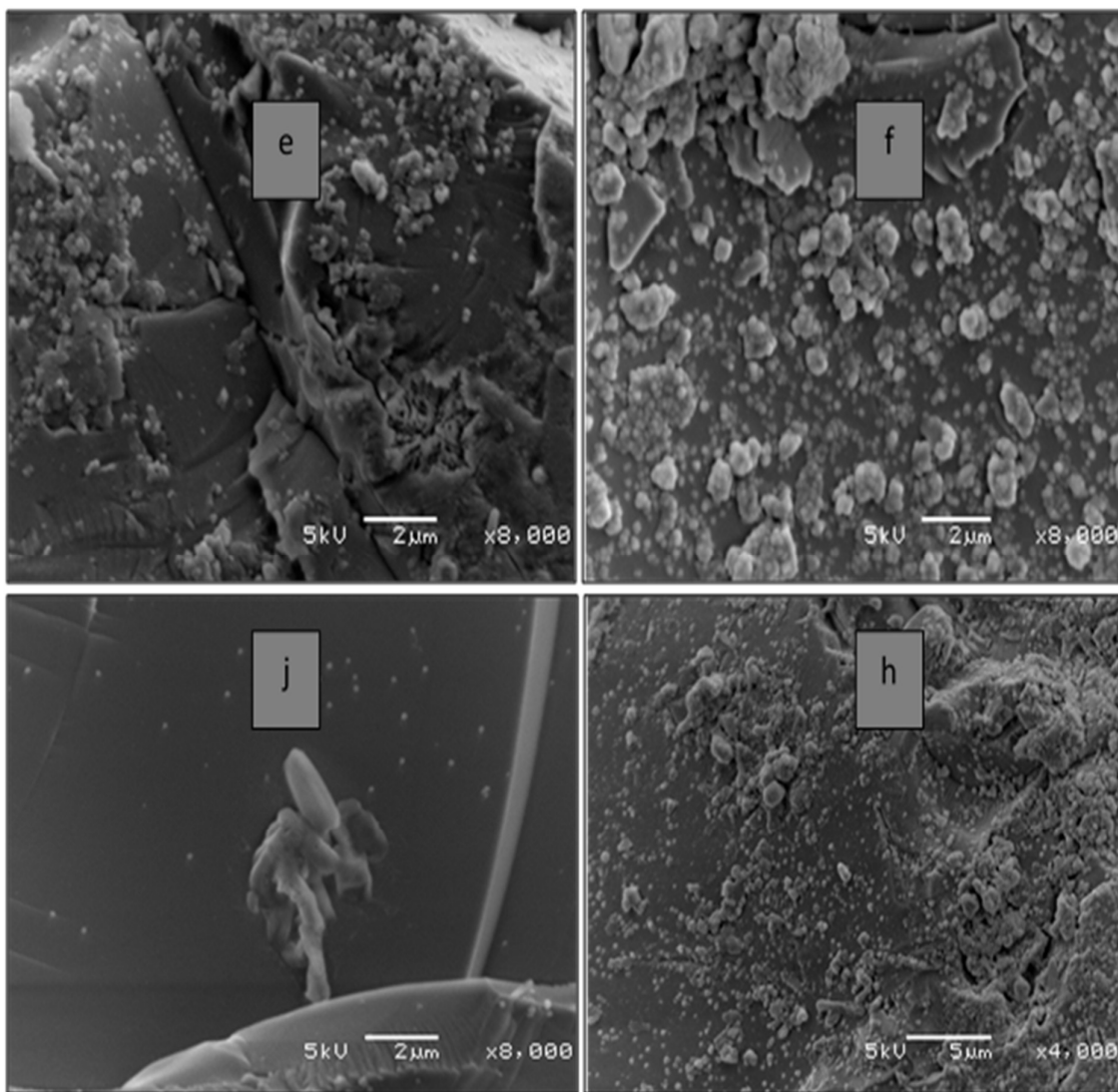
Figure 4.2: (e-h) Control studies showing less or insignifcant: morphological strains population
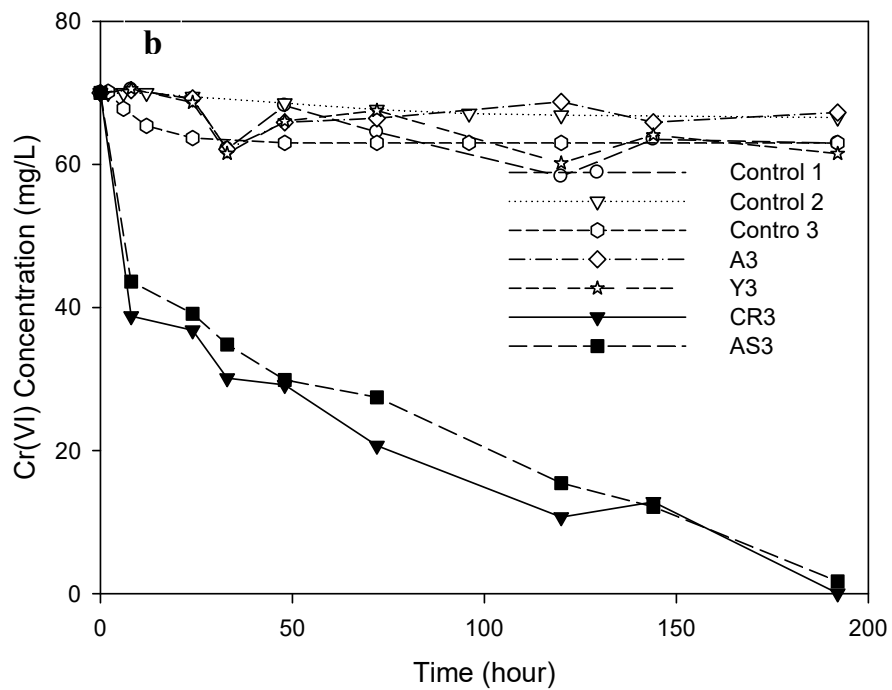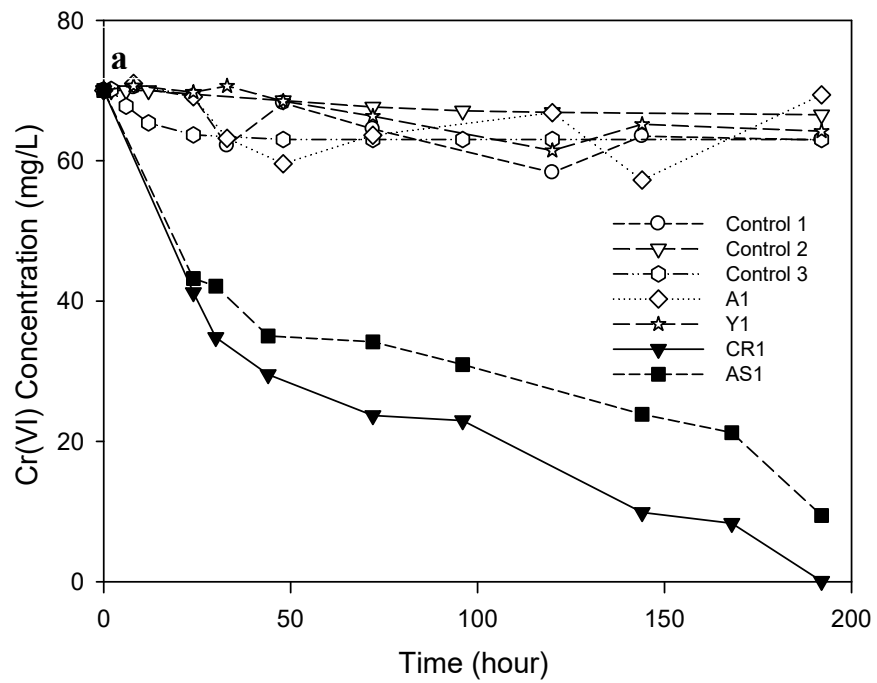
Figure 4.3a-b: Effect of Cr(VI) reduction with As(III) as an electron donor in different isolates (a) Isolate A_1, Y_1, CR_1, AS_1 (b) Isolate A_3, Y_3, CR_3, AS_3
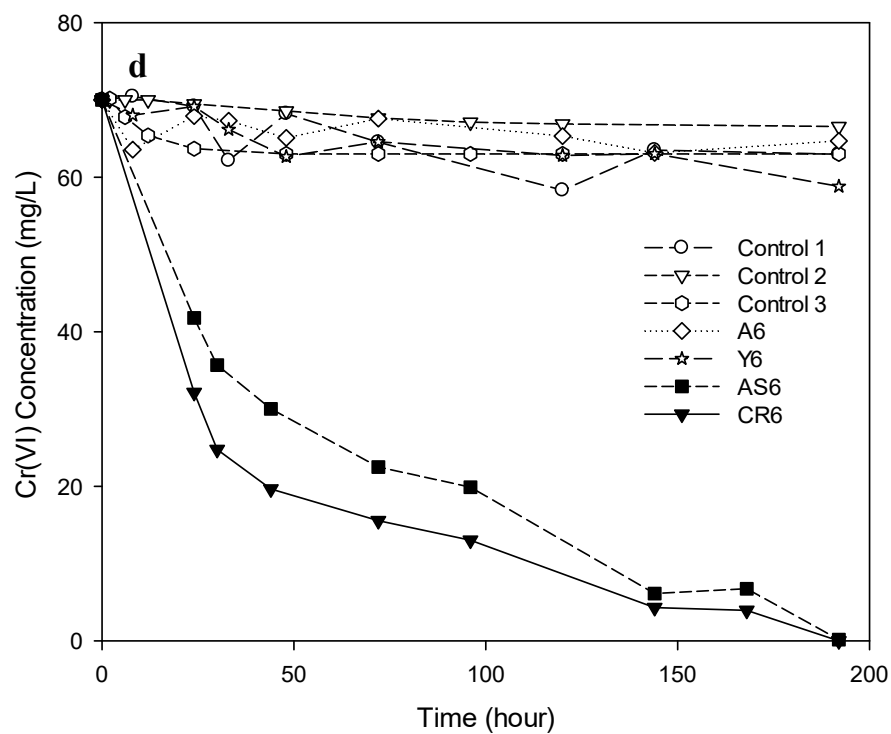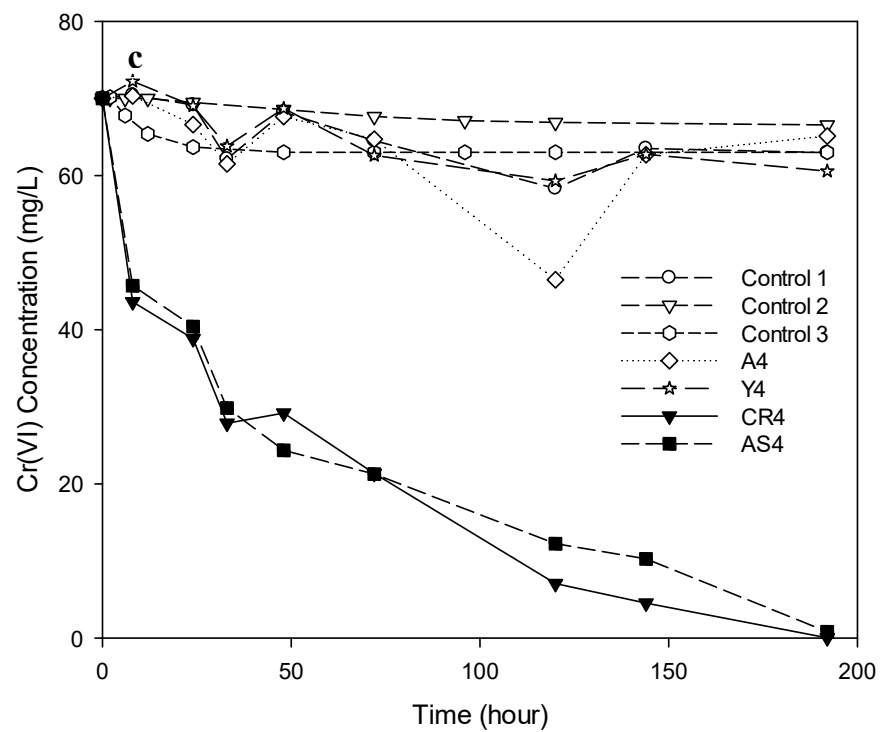
Figure 4.3c-d: Effect of Cr(VI) reduction with As(III) as an electron donor in different isolates (c) Isolate A_4, Y_4, CR_4, AS_4. (d) Isolate A_6, Y_6, CR_6, AS_6
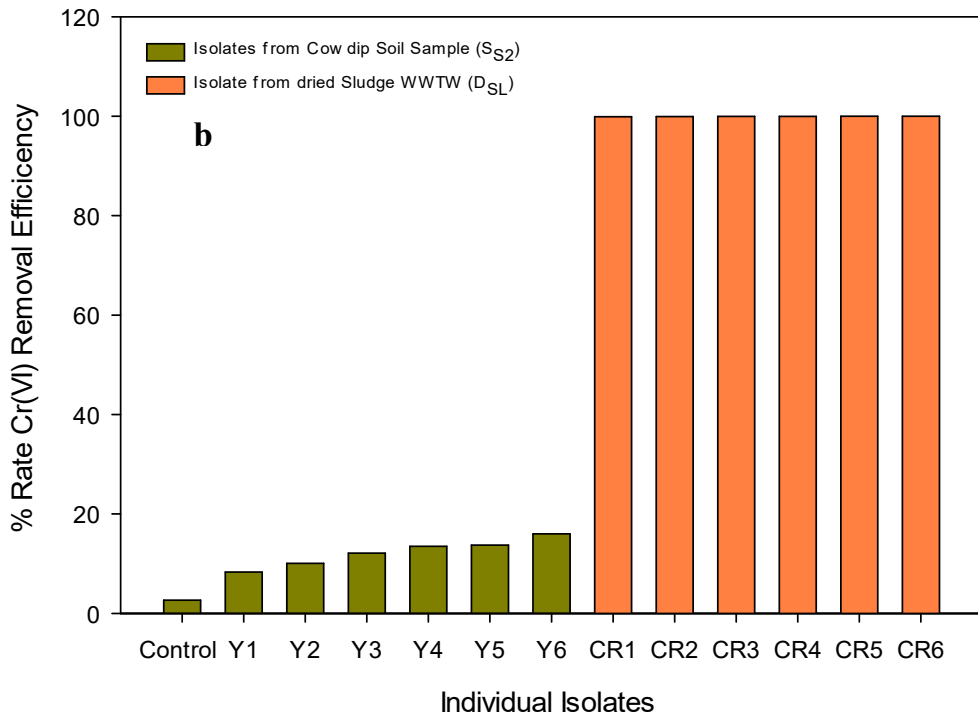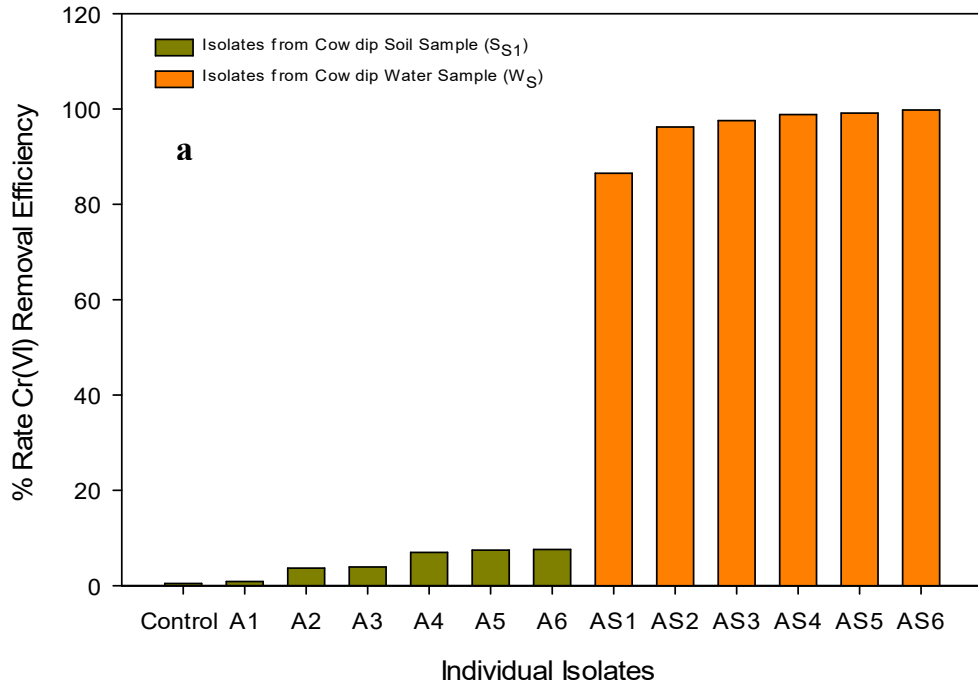
Figure 4.3e-f: Cr(VI) reduction efficiency of isolates sourced from (a) cow dip soil and water samples (b) dried sludge sample and cow dip soil

Table 4.1: Initial screening of Cr(VI)-reducing activity with 120 mg/L As(III) as electron donor with selected pure isolates A_3, Y_3, CR_3, and AS_3

Incubation time (hour)	Cr(VI) Concentration (mg/L)						
	Test 1				Control 1[II]	Control 2[III]	Control 3[IV]
	Isolate A_3[I]	Isolate Y_3[I]	Isolate As_3[I]	Isolate Cr_3[I]			
0	73±0.4	70±0.7	70±00	70±0.2	70±0.3	70±0.1	70±0.3
24	69±0.2	68±0.7	43±0.6	38±0.8	70±0.4	69±0.5	65±0.4
30	68±0.5	67±0.5	39±0.1	36±0.8	70±0.0	68±0.6	63±0.7
48	66±0.5	66±0.4	34±0.8	30±0.1	70±0.6	67±0.7	63±0.1
72	65±0.8	64±0.1	29±0.9	29±0.2	71±0.4	67±0.1	63±0.2
120	65±0.6	61±0.5	27±0.4	20±0.7	70±0.9	66±0.8	63±0.1
144	62±0.1	60±0.2	15±0.4	10±0.7	68±0.4	66±0.5	63±0.0
(%) Removed	5±0.9	10±0.4	77±0.9	84±0.7	2±0.3	4±0.5	9±0.9

Table 4.2: Initial screening of Cr(VI)-reducing activity with 120 mg/L As(III) as electron donor with selected pure isolates A_6, Y_6, CR_6, and AS_6

Incubation time (hour)	Cr(VI) Concentration (mg/L)						
	Test 3				Control 1[II]	Control 2[III]	Control 3[IV]
	Isolate A_6[I]	Isolate Y_6[I]	Isolate As_6[I]	Isolate Cr_6[I]			
0	69±0.9	70±0.0	70±0.5	70±0.8	70±0.3	70±0.1	70±0.3
24	68±0.9	69±0.2	41±0.8	32±0.1	70±0.4	69±0.5	65±0.4
30	67±0.6	66±0.2	35±0.7	24±0.8	70±0.0	68±0.6	63±0.7
48	67±0.3	64±0.6	30±0.1	19±0.6	70±0.6	67±0.7	63±0.1
72	65±0.3	63±0.0	22±0.5	15±0.6	71±0.4	67±0.1	63±0.2
120	65±0.1	62±0.8	19±0.9	13±0.0	70±0.9	66±0.8	63±0.1
144	63±0.2	62±0.7	6±0.1	4±0.3	68±0.4	66±0.5	63±0.0
(%) Removed	9±0.78	10±0.0	75±0.8	93±0.9	2±0.3	4±0.5	9±0.9

[I]Anaerobic consortium with Cr(VI) and As(III) amended
[II] Heat-killed cell with Cr(VI) and As(III) amended
[III]Cr(VI) and As(III) amended without anaerobic consortium
[IV]Anaerobic consortium with Cr(VI) amended without As(III)

4.1.2 Culture identification and phylogenetic characterisation

Earlier studies on Cr(VI) reduction using species from the source of this study were conducted by Molokwane et al. (2008), whereas studies on As(III) oxidation and associated species were studied by Dastidar and Wang (2010), Igboamalu and Chirwa (2014) and (2017), and Tapase et al. (2018). Among the distinctive bacteria strains isolated from the enriched culture, the most effective Cr(VI)-

reducing and As(III)-oxidizing bacteria were selected based on their best performance in the Cr(VI) reduction in the presence of high levels of As(III). The results based on the neighbour-joining method (Tamura et al., 2013) are shown in the phylogenetic tree (Table 4.3). From the consortium culture identified, the classifications were grouped into three significant categories, i.e. Cr(VI)-reducing *Bacilli* – *B. cereus*, *B. thuringiensis* – and associated *Bacilli*, candidate As-oxidising species – *Staphylococcus* sp. – from cow dip cultures, and enterobacteriaceae from human origins probably from the sludge sample. Cr(VI) reduction by *Bacillus cereusas* and *Bacillus thuringiensis* was earlier documented by Molokwane et al. (2008) and Molokwane and Chirwa (2009), whereas the As(III) oxidation by Staphylococcus sp. was suggested by Igboamalu and Chirwa (2014). *Exiguobacterium profundum* identified from the As-contaminated soil was earlier reported to oxidise As(III) to As(V) in deep sea samples exposed to long-term As(III) (Crapart et al., 2007).

4.1.3 Microbial growth analysis

Microbial growth and redox conversion of Cr(VI) and As(III) with the aid of anaerobic consortium was first studied by varying the initial Cr(VI) concentration from 50-70 mg/L at a fixed As(III) concentration of 120 mg/L (Figure 4.4 a). The growth of the anaerobic consortium was rapid in cultures with Cr(VI) and As(III) concentrations of 70 mg/L and 120 mg/L, respectively, whilst at the lower Cr(VI) concentration of 50 mg/L with As(III) concentration fixed at 120 mg/L, the consortium showed less growth (Figure 4.4b). The corresponding decrease in As(III) with microbial growth is indicated in Figure 4.4 c-d. It also shows the same pattern as Cr(VI) reduction with microbial growth at 70 mg/L where consortium shows rapid growth and less growth at 50 mg/L. This initial result showed that Cr(VI) as an electron sink was essential for the metabolic growth of the organisms as long as this occurred below a certain Cr(VI) toxicity threshold. The optimal optical density (OD at 600nm) recorded was 0.343 at 50 mg/L and 0.416 at 70 mg/L during the stationary growth phase. Cr(VI) reduction under these concentrations was related to microbial growth as cell density increases as well as the availability of Cr(V) for the complete redox process.

4.1.4 Cr(VI) reduction potential

The effect of Cr(VI) concentrations on the performance of the anaerobic consortium on Cr(VI) reduction with As(III) as a sole electron source was studied under initial Cr(VI) concentrations of 50, 70, 100, 200, 350, and 500 mg/L and with 80 mg/L As(III) concentration. 1.5 g of bicarbonate

was supplemented as carbon source in the anaerobic consortium. Data obtained indicates complete Cr(VI) reduction was achieved at lower Cr(VI) concentration, while incomplete reduction was when Cr(VI) concentration was increased above 100 mg/L (Figure 4.5a).

Table 4.3: Bacterial consortium analysis results indicating best matches

Isolate number	Blast result	Max ID
A_{S1}	*Exiquobacterium profundum*	100%
A_{S2}	*Bacillus licheniformis*	100%
A_{S3}	*Staphylococcus epidermidis*	100%
A_{S4}	*Bacillus cereus*	100%
A_{S5}	*Bacillus cytotoxicus*	100%
A_{S6}	*Bacillus cereus*	100%
Y_1	*Staphylococcus epidermidis*	99%
Y_2	*Staphylococcus capitis*	100%
Y_3	*Bacillus bacterium*	100%
Y_4	*Bacillus cytotoxicus*	99%
Y_5	*Bacillus cereus*	99%
Y_6	*Bacillus licheniformis*	99%
CR_1	*Bacillus thuringiensis*	100%
CR_2	*Bacillus methylotrophicus*	100%
CR_3	*Bacillus anthracis*	99%
CR_4	*Bacillus subtilis*	100%
CR_5	*Bacillus licheniformis*	99%
CR_6	*Bacillus sonorensis*	100%
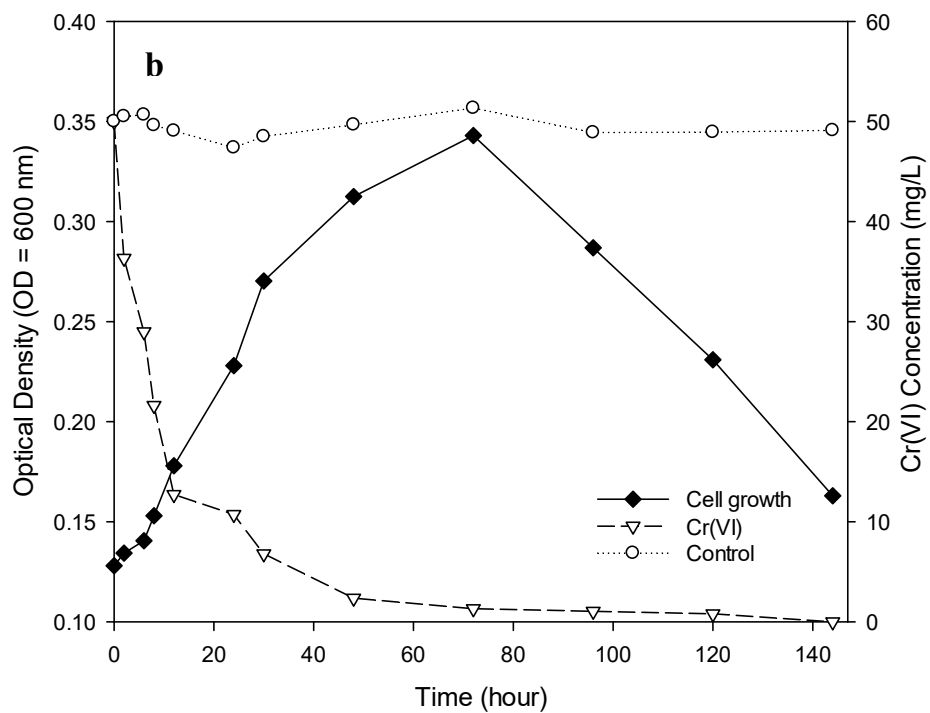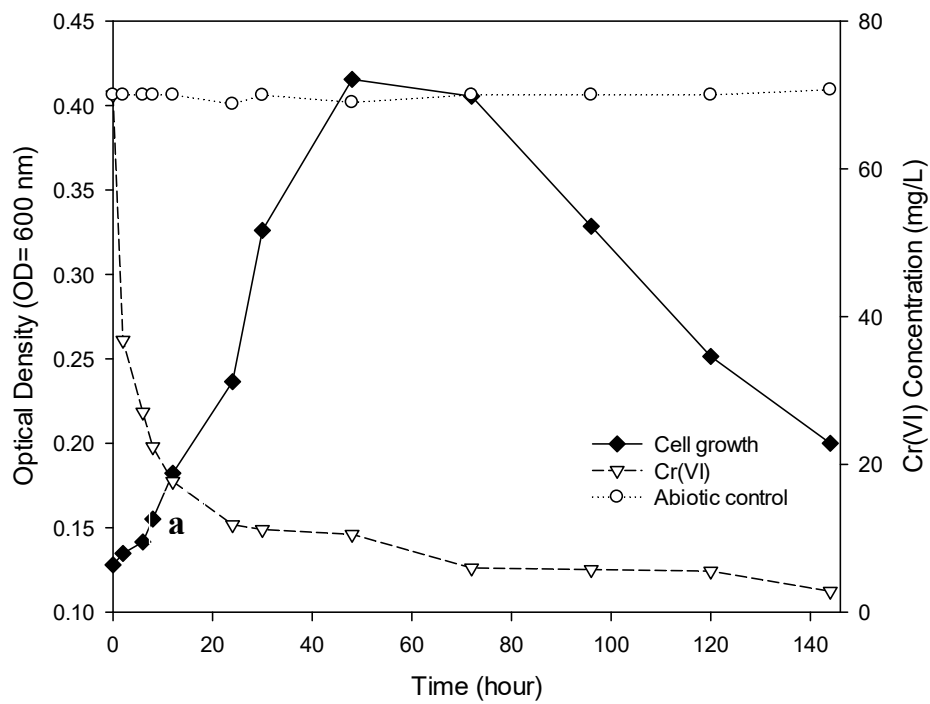
Figure 4.4: Growth and redox reaction in the presence of (a) 70 mg/L; (b) 50 mg/L Cr(VI) at 120 mg/L As(III) concentration
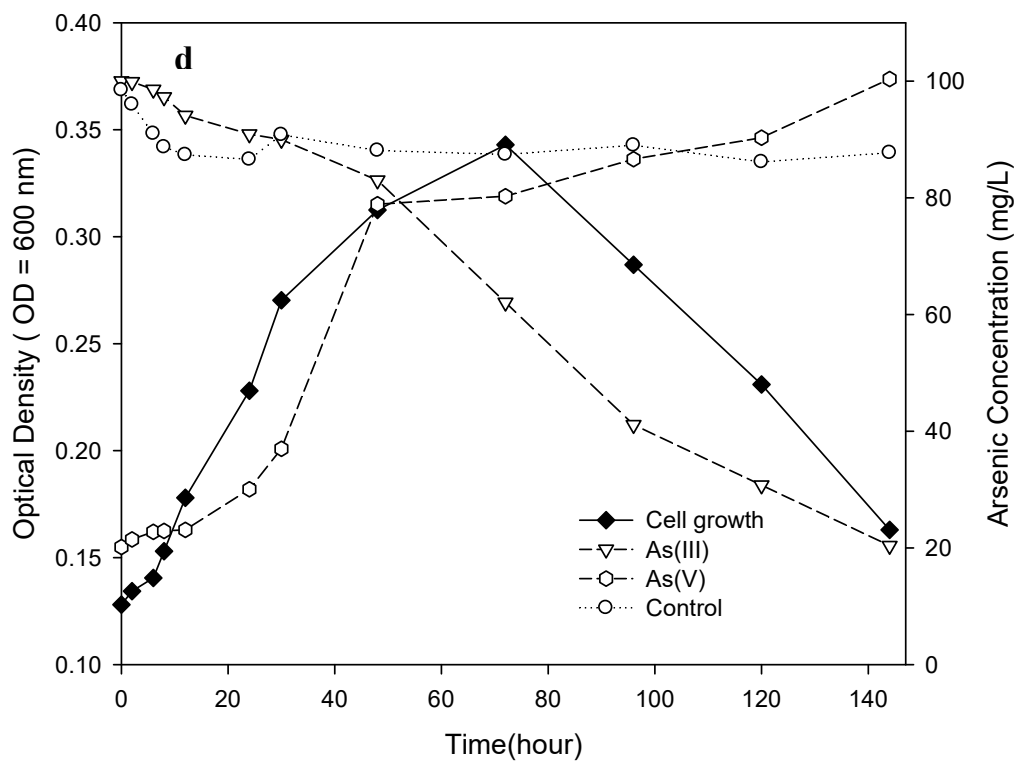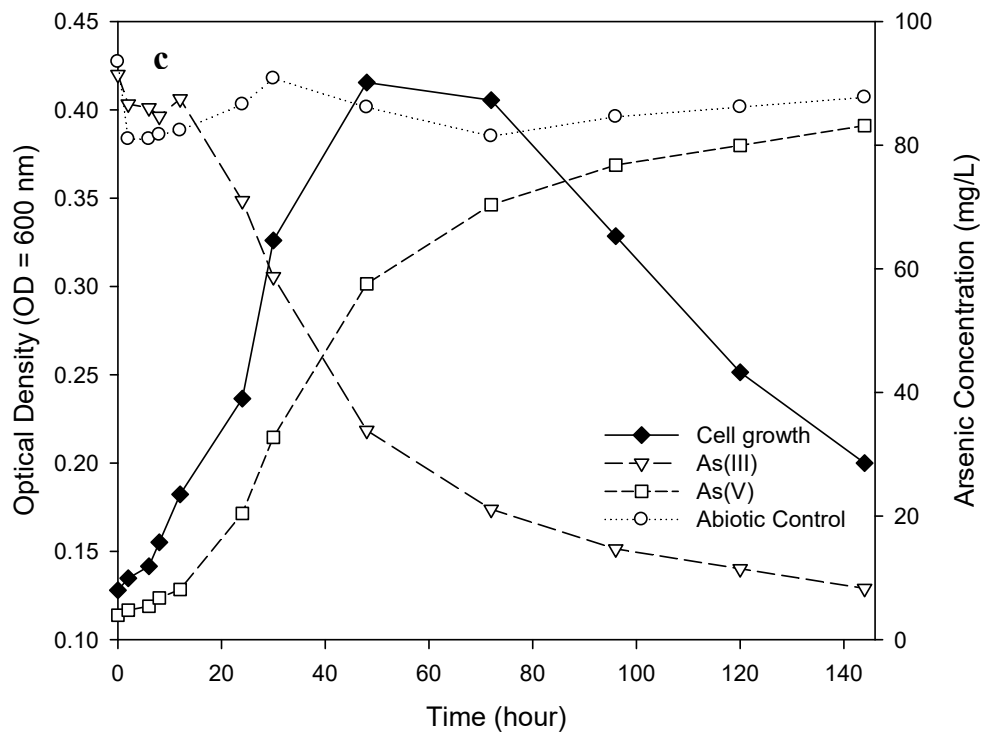
Figure 4.4: Growth and redox reaction in the presence of (c) 120 mg/L As(III) at 70 mg Cr(VI) / L; (d) 120 mg/L As(III) at 50 mg Cr(VI) /L

The average removal efficiency of Cr(VI) reduction observed at lower concentrations was 90, 80, and 50% at 50, 70, 100 mg/L, while 33, 3,1% at high concentration (Figure 4.5b). The optimum initial values of Cr(VI) reduction rate in this culture was 70 Cr(VI) mg/L. Under this concentration, complete removal of Cr(VI) was achieved within 48 h incubation. At values greater than 70 mg Cr(VI)/L, Cr(VI) reduction efficiency decreased due to the toxicity of Cr(VI) on the cells. The data obtained indicates that dual toxic effect of excessive Cr(VI) and As(III) concentration with high redox capability may additionally inhibit biological metabolic activities of the consortium. Earlier studies showed that Cr(VI) reduction predominantly occurs on the bacteria cells surface related to loss of transmembrane proton-motive potential (Shen & Wang, 1993; Chirwa & Wang, 1997).

$$Cr_2O_7^{2-} + 14H^+ + 6e^- \rightarrow 2Cr^{3+} + 7H_2O + 1.33v \ (E^0) \tag{4.1}$$
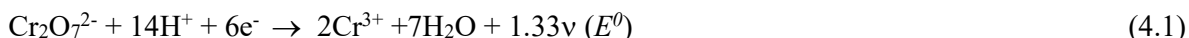
Cr(VI) redox potential is thermodynamically feasible following the reduction of Cr(VI) to Cr(III) at a relatively neutral pH through the following reduction-oxidation (redox) reaction in Equation 4.1., which can be precipitated as chromium hydroxide complex ($Cr(OH)_3(s)$) (Garrel & Christ, 1965). Even though Cr(VI) is very toxic to microbes, it was noted by Ahemed (2014) that microbial adapts to toxic Cr(VI) environment by developing a detoxification mechanism for the conversion of Cr(VI) to Cr(V) (Dastidar & Wang, 2010).

4.1.5 As(III) oxidation potential

As(III) oxidation capacity of the anaerobic consortium (As$_1$-As$_6$) was investigated in MSM amended by 1.5 g HCO_3^- over a range of initial As(III) concentration – 20, 30, 50, 100, 300, 500 mg/L – in the absence of Cr(VI) (Figure 4.6 a). No As(III) oxidation was observed within 24-48 h incubation. However, after 50 h, complete removal of As(III) was achieved in 240 h. In the latter cased, final As(III) removal efficiency ranged from 85-99% (Figure 4.6a). The As(III) reduction rate decreased at As(III) concentration vales above 500 mg/L (Figure 4.7). A detailed mass balance analysis using IC data for As(III) and As(V), and AAS data for total As in the system, showed that all the As (70 mg/L) added at the beginning of the experiment was accounted throughout the experiment. The sum of the As(III) and reduced species correlated with the total measured As in the AAS with less than ±5% error (Figure 4.6 b). There was no As(III) oxidation observed within 48 h of incubation, suggesting the need for induction time before As(III) oxidation occurs, as previously described (Suttigarn & Wang, 2005).
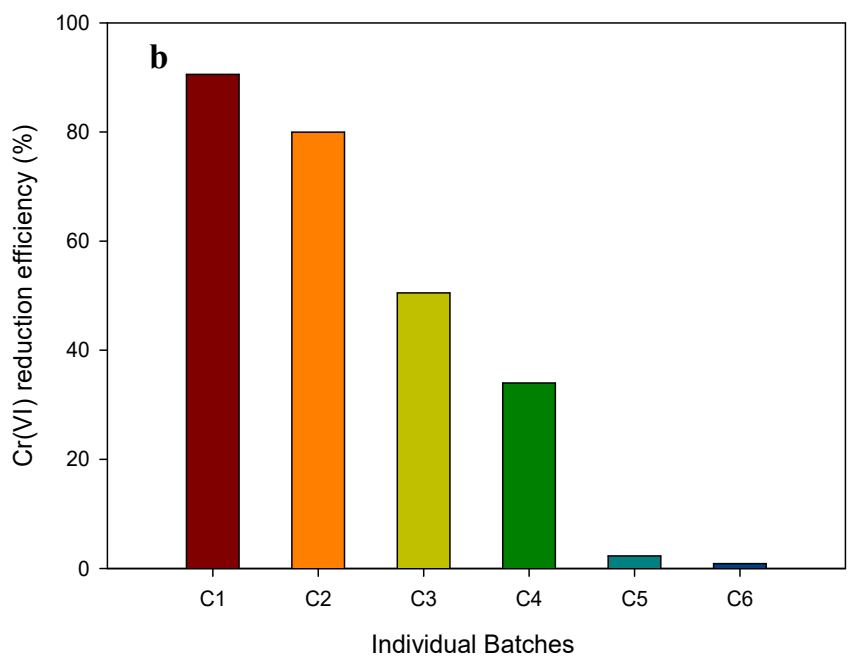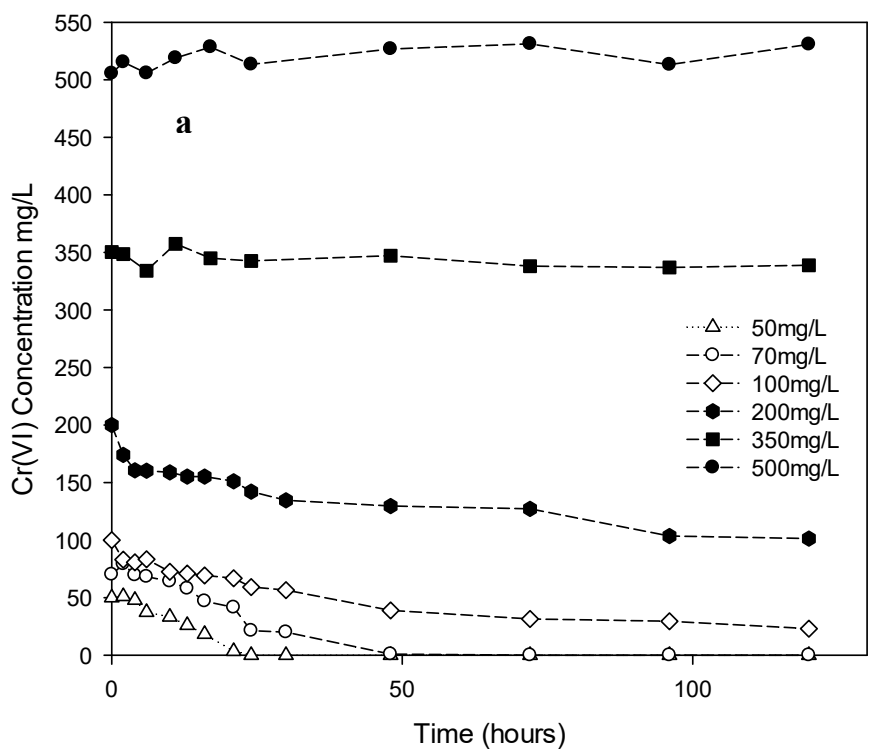
Figure 4.5: (a) Effect of initial concentration on Cr(VI) reduction ranging from 50-500 mg/L with 80 mg/L As(III) concentration; (b) Cumulative Cr(VI) reduction efficiency

A possible explanation is that microbial cells tend to produce the necessary enzyme or adapt to match the varying level of As(III) concentration in the solution (Suttigarn & Wang, 2005, Ahemed, 2014). After 50 h of incubation, As(III) oxidation was facilitated at concentration $\leq$ 500 mg/L with removal efficiency (84 - 99.8%) after 240 h of incubation. However, when the concentration was increased up to 1000 mg/L, there was insignificant or no As(III) oxidation (Figure 4.7).

The couple redox reaction of As(III) oxidation and Mo(IV) cell reduction was expressed as Equation 4.2. As previously reported, the mixed isolates within As(III) concentration threshold limit could detoxify As(III) due to some developed detoxification mechanisms (Suttigarn & Wang 2005, Ahemed 2014). These mechanisms consist of bound arsenite oxidase enzyme encoded by arsenite oxidase gene aioa (Heinrich-Salmeron et al., 2011). The viability is due to the presence of arsenite oxidase structure with two subunits, namely: a larger 88-kDa polypeptide containing the Mo-pterin with a HiPIP 3Fe^4S centre, and a smaller 14-kDa subunit with the Rieske 2Fe^2S centre (Anderson et al., 2001). Arsenite cell interaction was proposed to bond closely to the Mo(VI) of the oxidized cofactor, allowing a direct nucleophilic attack and transfer of two electrons (Mukhopadhyay et al.,2002). Under equilibrium condition, Mo(IV) is oxidized back to Mo(VI) with electron transfer from the 3Fe^4S HiPIP centre.

$$As^{3+} + Mo^{6+} \rightarrow As^{5+} + Mo^{4+} \; (\Delta G = \text{-256 kJ}) \tag{4.2}$$

Samples withdrawn were checked for the oxidation-reduction potential in millivolts (mV). This was done to ensure that the oxidation of As(III) involves an electron transport chain process. At 50 mg/L and 70 mg/L As(III) concentration with mixed culture was preliminarily investigated. In both experiments (50 mg/L and 70 mg/L), initial oxidation-reduction potential was recorded at -199 mV at pH 7.3 and -208 mV at pH 7.1 respectively (Figure 7 a and b). After 24 hr, oxidation-reduction potential increases to -174.4 mV at pH 7.19 and -120.6.3 mV at pH 7.16. Further increase was observed after 48 h recorded oxidation-reduction potential of -150 mV at pH 7.29 and -77.7 mV at pH 7.23. Similar patterns of oxidation reduction potential were found in both experiments. The oxidation strength of the solution increases from a less oxidizing condition to a more oxidizing condition with corresponding increase in pH. However, this is governed by the disappearance of As(III) and appearance of As(V), suggesting an electron transfer during redox conversion of As(III) to As(V), with beneficial use of energy released for cell growth metabolism. The slight decrease in oxidation reduction potential at 70 mg/L could be attributed to the reduction in the solution's metabolic activities.
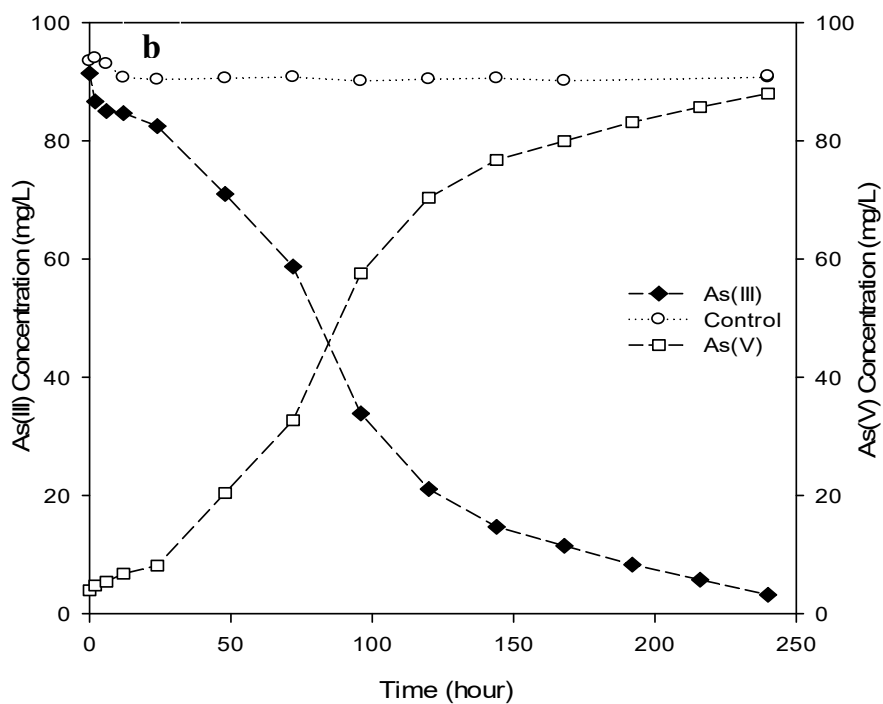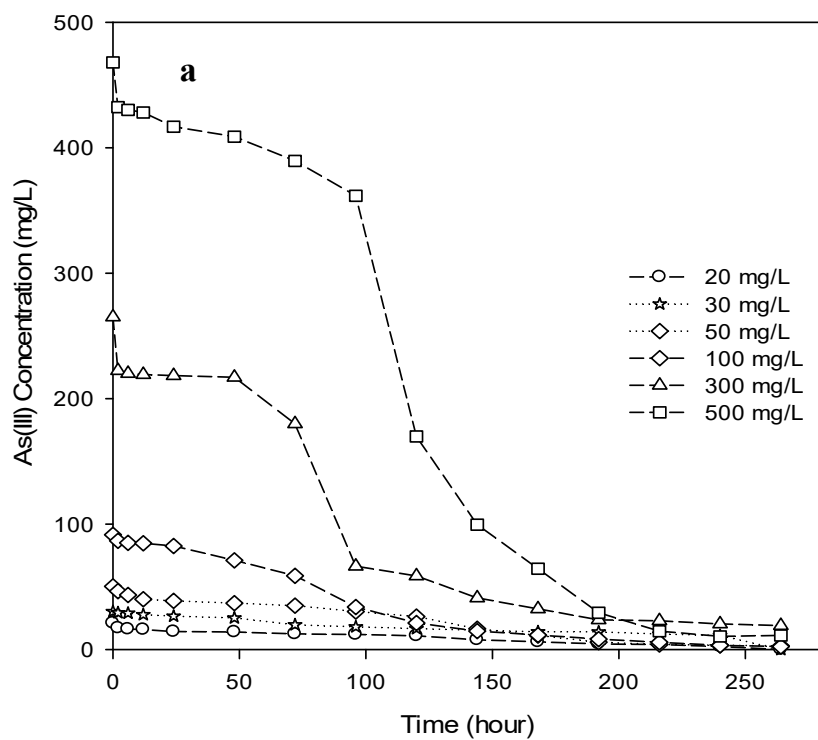
Figure 4.6: (a) Effect of initial concentration on As(III) oxidation at different concentration ranging from 20-500 mg/L: (b) As(V) formation and control at 100 mg/L As(III) concentration
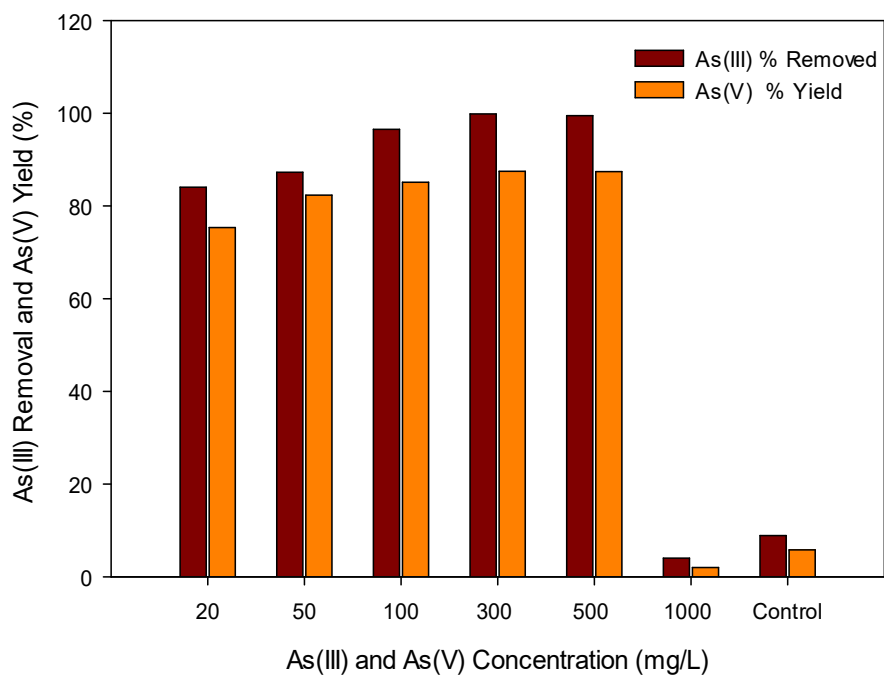
Figure 4.7: Percentage As(III) removed to As(V) formed
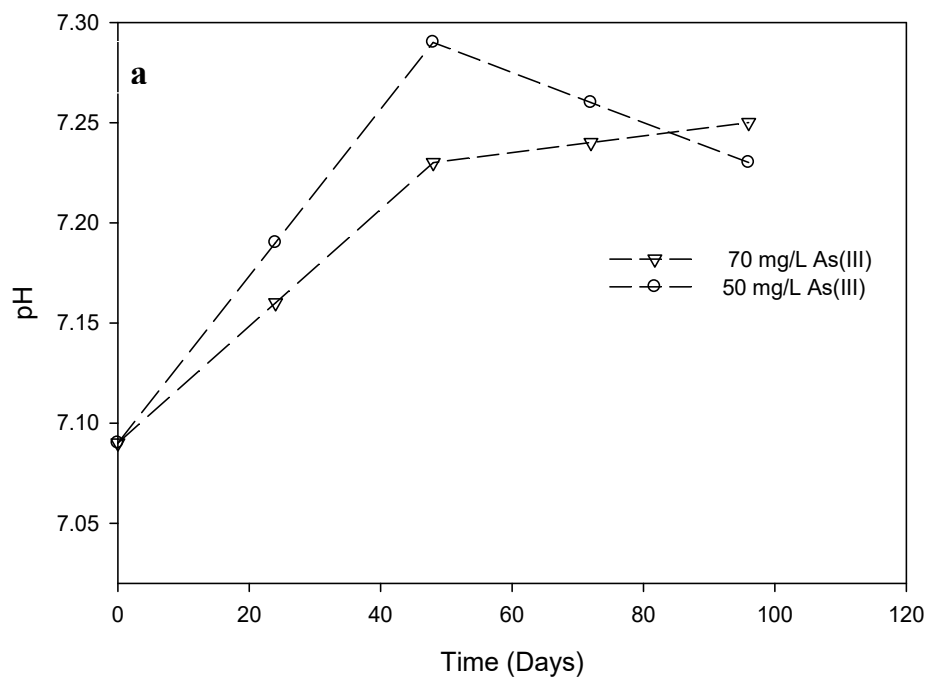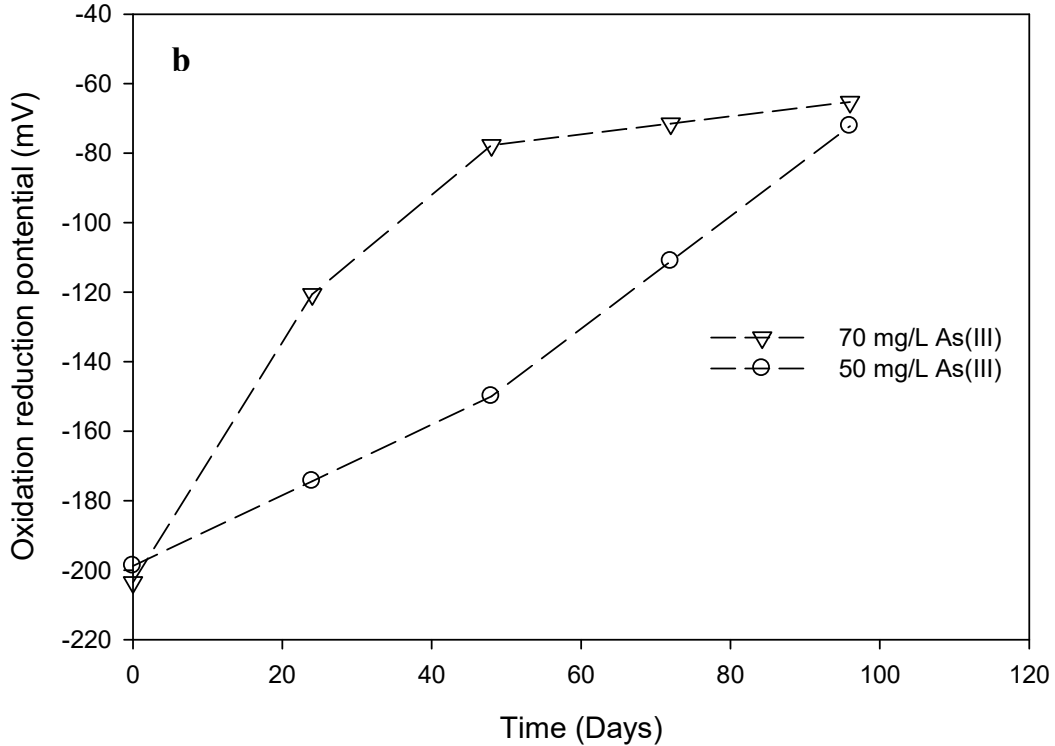
Figure 4.8: (a) pH of As(III) oxidation (b) Oxidation-reduction potential (ORP) at 50 and 70 mg/L

4.2 Threshold limit analysis

The threshold limit of As(III) and Cr(VI) concentrations were checked to have a better understanding of the metal interaction with the anaerobic consortium isolated. In a 100 ml bottle, As(III) concentration of 120 mg/L under varying Cr(VI) concentrations ranging from 20-200 mg/L was investigated. Results show that the consortium achieved near complete Cr(VI) reduction at Cr(VI) and As(III) concentrations up to $\leq$ 70 mg/L and 120 mg/L (Figure 4.9). When the Cr(VI) and As(III) concentration increases up to 100 mg/L and 120 mg/L, incomplete Cr(VI) reduction was observed. The corresponding As(III) oxidation (Figure 4.10 a) shows that As(III) at 120 mg/L was used in the redox process for possible Cr(VI) reduction. Metabolic or electron transport activities deteriorated or inhibited at higher concentration could be because of the dual toxic effect of both metalloid on the microbial cells or the concentration of As(III) in the solution required to achieve complete Cr(VI) oxidation had been used up (i.e. mole ratio of As(III) to Cr(VI)).

Stoichiometrically, three moles of As(III) are required for every two moles of Cr(VI). This will be explored in detail in this report.

It was seen that the isolate achieved Cr(VI) removal of efficiency above ($\geq$ 95%) at lower concentration ranging from 20-70 mg/L, whereas at high Cr(VI) concentration above $\geq$ 100 mg/L, lower Cr(VI) efficiency ($\leq$ 55%) was seen (Figure 4.10). A similar trend was observed with the corresponding 120 mg/L As(III) concentration in the solution (Figure 4.11). At lower Cr(VI) concentration ranging from 20-70 mg/L, the isolate achieved As(III) oxidation efficiency above ($\geq$ 71%), and complete As(III) oxidation with efficiency of 100%. Increasing Cr(VI) concentration above $\geq$ 100 mg/L, As(III) oxidation efficiency dropped from 100% to $\leq$ 29%. The resistance level of these cells towards Cr(VI) in the presence of As(III) is high when compared to other previous studies (Molokwane et al, 2000). It could be conclusive that these cells can actively perform at Cr(VI) and As(III) concentration and the threshold limit optimally lies between Cr(VI) and As(III) concentration of 70 mg/L and $\geq$ 120 mg/L without being inhibited. However, this was used as a guide for further studies.

4.3 Batch experiment

4.3.1 Cr(VI) reduction with concurrent As(III) oxidation

As(III) oxidation with concurrent Cr(VI) reduction experiments were performed in MSM amended with HCO_3^- at initial As(III) concentration ranging from 60-500 mg/L and a fixed initial Cr(VI) Cr(VI) of 70 mg/L. As(III) oxidation and removal from solution and associated Cr(VI) reduction was optimal within the concentrations below the toxicity threshold of either pollutant. The removal process for both pollutants was severely inhibited as As(III) concentration 500 mg/L and above (Figure 4.11 a-b). Biological processes were not severely inhibited at As(III) concentration $\leq$ 500 mg/L. Cr(VI) removal increased with increasing As(III) concentration until an optimum value of approximately 500 mg/L As(III), around which it is suggested the As(III) inhibition threshold lies. At the optimum As(III) loading, the mole ratio between As(III) oxidized and Cr(VI) reduced was 3:2. In order words, all the free available Cr(VI) in the solution has been reduced. At this stage As(III)-oxidizing bacteria could facilitate the redox conversion of As(III) (Dastidar & Wang 2009). Figure 4.12 shows that the mole of As(III) oxidized is proportional to more of As(V) formed. However, it was seen that As(III) oxidation began after a slight lag period of about 5 h, after which removal accelerated to completion at 50 h in batches with initial loading $\leq$ 80 mg/L (Figure 4.11b).
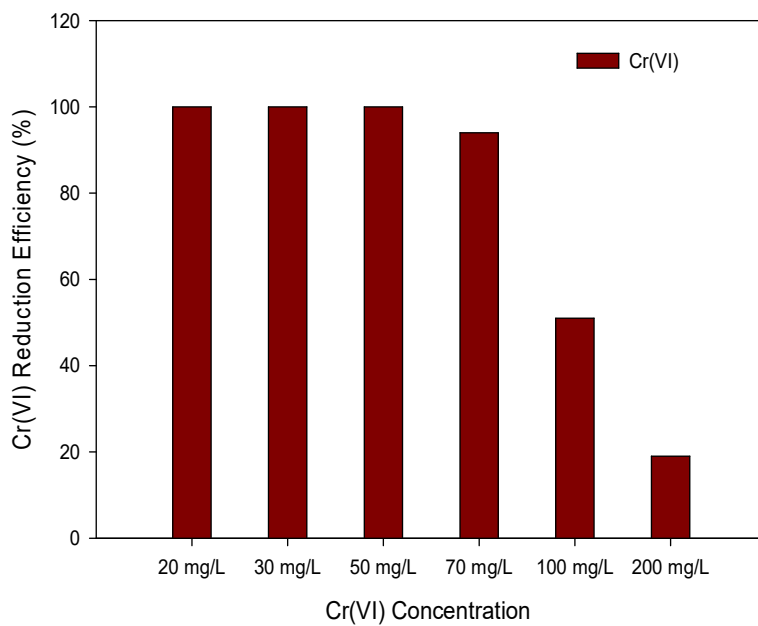
Figure 4.9: Cr(VI) reduction efficiency at different concentration ranging from (20-200) mg/L at 120 mg/L As(III) concentrations
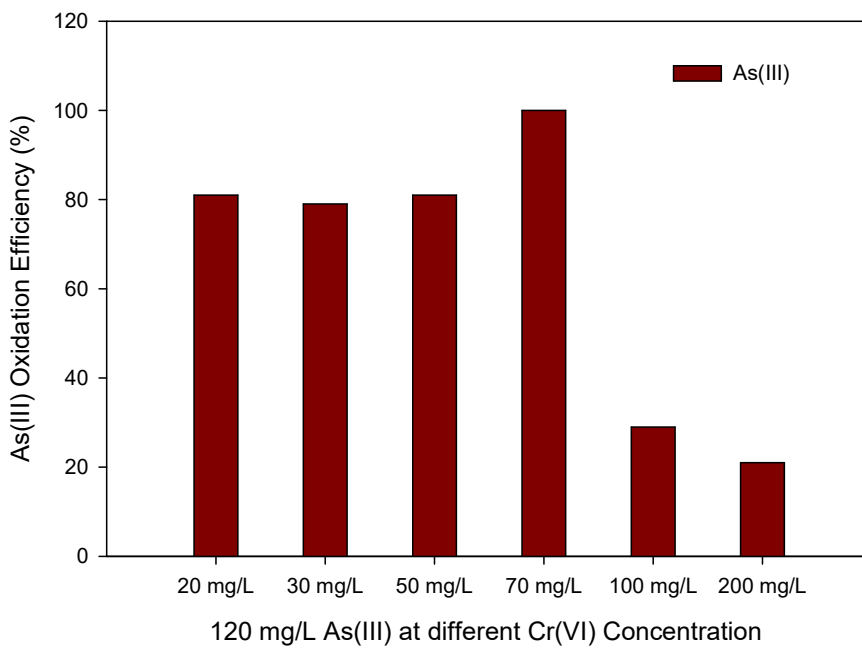
Figure 4.10: As(III) oxidation efficiency at different concentration ranging from 20-200 mg/L.

At higher initial loadings, it required longer incubation periods to reach 95% removal, i.e., 80 h 210 h at 120 and 300 loadings, respectively (Figure 4.11b).

A further increase of initial As(III) concentration above 300 mg/L resulted in the decrease in As(III) removal efficiency from 93% to 37% at 500 mg/L As(III) (Figure 4.14 a-b). The optimum redox response was discovered when the mole ratio of As(III) oxidized to Cr(VI) reduced approaches the stoichiometric value from the rough reaction Equation 3 (Figure 4.14 a-b). This implies that the initial redox rate was affected by the amount or mole ratio of As(III) and Cr(VI) concentrations. Second, the redox process is most likely mediated by metabolic processes by living cells (Thacker et al., 2006). This was elucidated by abiotic control shows both for Cr(VI) reduction and for As(III) oxidation, as shown earlier in Figure 4.12 a-b. The decrease in As(III) and Cr(VI) concentration in the abiotic was ascribed to the redox with components of the medium, which was satisfied with a short time of exposure.

The probability of redox conversion of Cr(VI) and As(III) occurring could possibly be based on three factors: (1) availability of Cr(VI)-oxidizing bacteria, which provides an electron through an enzymatic process to reduce Cr(VI) to reactive Cr(V), (2) availability of As(III) required to completely reduce Cr(VI) based on the stoichiometric relationship, (3) the availability of As(III)-oxidizing bacteria, which could oxidized As(III) concentration at lower mole ratio of 3:2. Couple redox conversion of Cr(VI) and As(III) follows Equation 3, as previously described by Igboamalu and Chirwa (2014). The possibility of factor 1 is based on mixed culture of Cr(VI) and As(III) with reductase and oxidase, and thermodynamic feasibility resulting in electron and energy generation. Factor 2 is based on stoichiometric mole ratio of As(III) oxidized to Cr(VI) reduced and finally, the presence of membrane-bound arsenite oxidase enzyme encoded by arsenite oxidase gene aioa (Heinrich-Salmeron et al., 2011).

Studies have reviewed co-metabolic remediation of metalloids, simultaneous reduction of Cr(VI) and degradation of phenol mediated by coculture of Escherichia coli ATCC 33456 and Pseudomonas putida DMP-1 (Shen & Wang, 1995) and by bacterial consortium (Nkhalambayausi-Chirwa & Wang, 2001). Simultaneous redox conversion of Cr(VI) and As(III) by chemical method has also been reported (Kim & Choi, 2011). Bacterial strains having both abilities, to reduce Cr(VI) and oxidize As(III), have not been reported so far. This is the first time that Cr(VI) reduction coupled to As(III) oxidation, with As(III) serving as the principal electron donor, has been reported.

$$As^{3+} + Cr^{5+} \rightarrow As^{5+} + Cr^{3+} \quad (\Delta G = \text{-256--468 kJ/mol}) \tag{3}$$
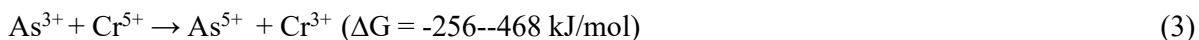
4.3.2 Evaluation of theoretical perspectives

The fate of Cr(VI) reduction and As(III) oxidation was further analysed by way of accomplishing mass balance of both metalloids to decide the stoichiometric relationship. Bearing in mind that As(III) oxidation is thermodynamically possible in the presence of a reactive form of Cr [Cr(V)], redox conversion of As(III) can be limited by means of reaction kinetics under physiological conditions (Chirwa & Wang, 2000). Furthermore, the kinetics of As(III) oxidation may be more advantageous by coupling As(III) oxidation to other energy-yielding reactions that include Cr(VI) reduction, etc. (Ishibashi et al., 1990; Shen & Wang, 1995). A great relationship was observed between As(III) oxidation and Cr(VI) reduction, as shown in Figures 4.11 a-b, which was further evaluated with regard to Correlation Coefficients, R^2 = 0.91-0.98 (Figure 4.13). The near perfect balance indicates that all the initial As(III) and Cr(VI) concentrations were converted (Chirwa & Wang, 2000). However, this indicates that the amount of As(III) oxidized per unit mole of Cr(VI) reduced increased with increasing initial As(III) concentration (Figure 4.13). Optimum conversion ratio was seen at As(III) and Cr(VI) concentrations of 100 mg/L and 70 mg/L, when the experimental mole ratio of 2.25:2 approaches the theoretical stoichiometric mole ratio of 3:2.

The lower conversion ratio at lower As(III) concentration was due to insufficient electrons available for Cr(VI) reduction. Alternatively, at higher As(III) concentration above 120 mg/L, the conversion ratio was also lowered due to insufficient electrons available for conversion of As(III) to As(V). This was attributed to a completed conversion of Cr(VI) to Cr(III) from the supply of excess electrons. Excess or unconverted As(III) was further oxidized by the electrons supplied by the arsenic-oxidizing bacteria through the electron transfer pathway (Mukhopadhyay et al., 2002). This suggests why the experimental conversion ratio exceeded the theoretical values, as represented in Figure 4.13. However, this conversion ratio improved until As(III) became toxic to the cells. The stoichiometric relation for redox conversion of As(III) and Cr(VI) is defined in Equation 4 with a calculated energy yield ranging from ΔG = -256 to -468 kJ/mol.

$$2CrO_4^{2-} + 3As^{3+} + 16H^+ \xrightarrow{\textit{microbes}} 2Cr^{3+} + 3As^{3+} + 8H_2O + (\Delta G = \text{-256--468 kJ/mol}) \tag{4}$$
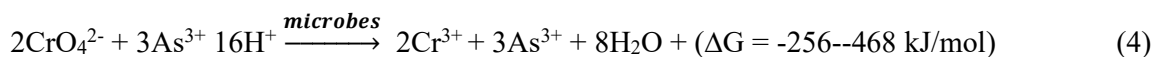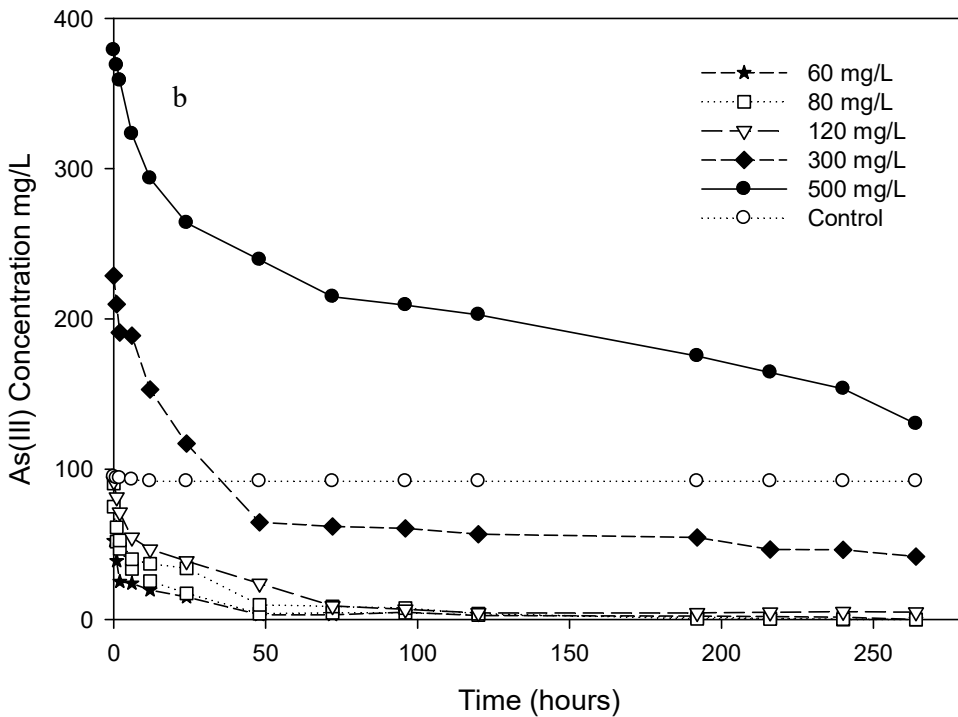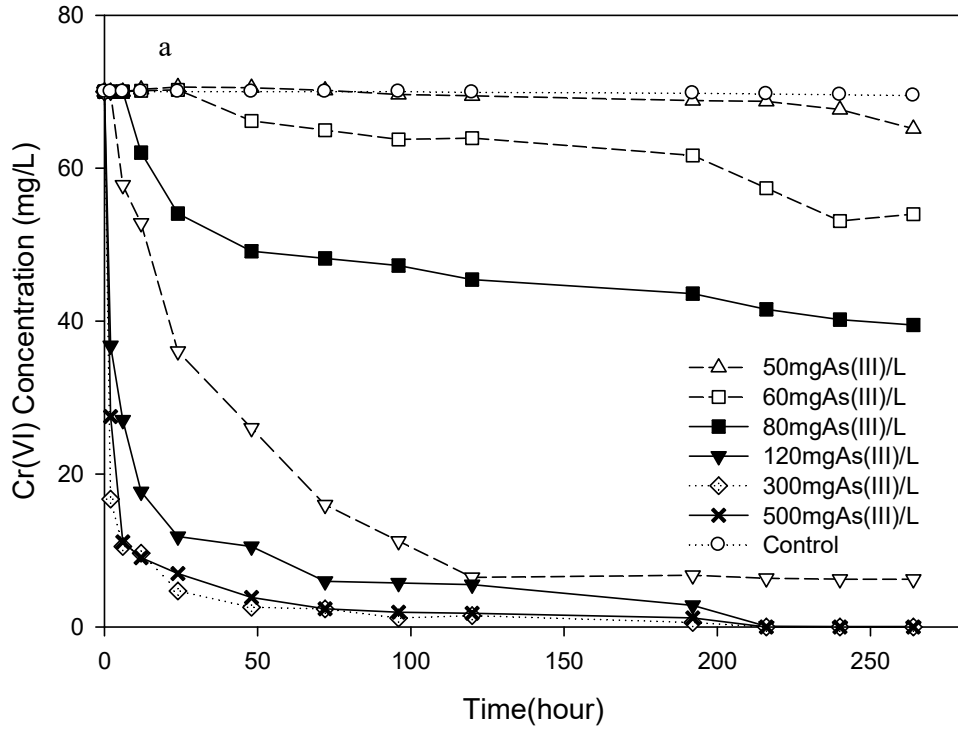
Figure 4.11: Effect of concentration on concurrent (a) As(III) oxidation, (b) Cr(VI) reduction, (c) removal efficiencies
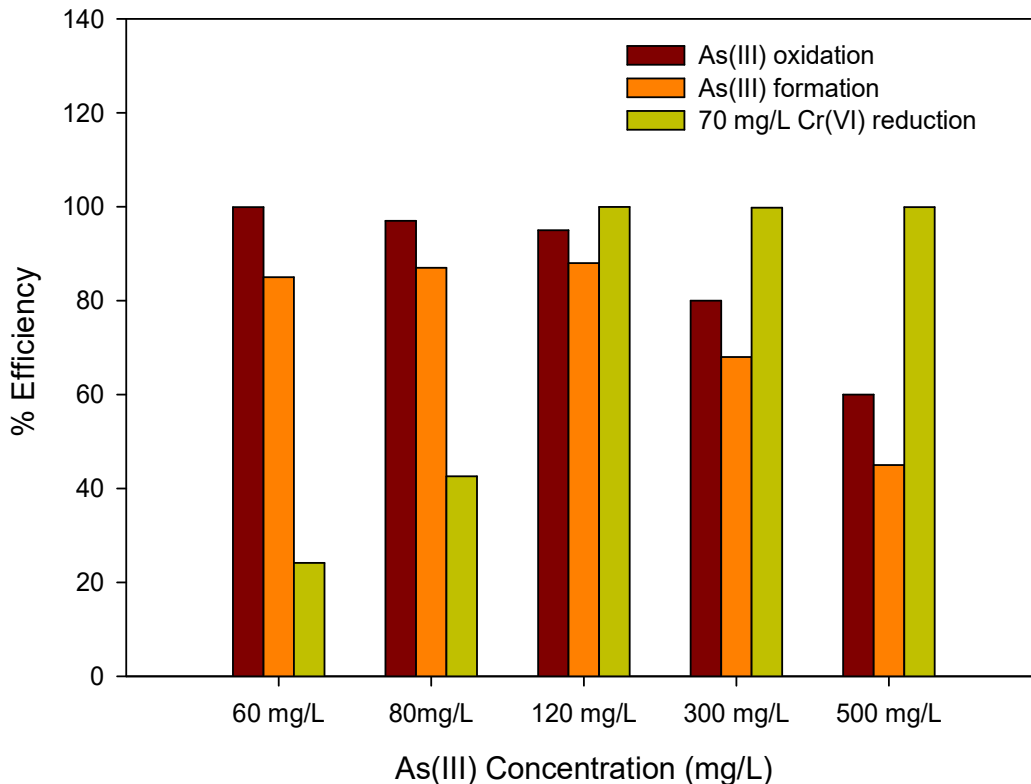
Figure 4.12: Removal efficiencies on concurrent Cr(VI) reduction and As(III) oxidation 60-500 mg/L

4.3.3 Impact of environmental factors

Previously it was reported that Cr(VI) reduction is favoured at pH range from 6-9 (Park et al., 2005), while As(III) oxidation, on the other hand, is favoured at neutral pH (Wagman et al., 1968). Bachate et al. (2012, 2013) reported pH of 6 and 7.2 for optimum As(III) reduction and Cr(VI) reduction. The impact of pH was tested within the anaerobic consortium containing Cr(VI) and As(III) concentration of 70 mg/L and 120 mg/L at different pH solutions of 1, 4, 7 and 10. At pH of 1, 95% Cr(VI) removal and 50% As(III) oxidation efficiency was observed (Figure 4.15). $HCrO_4^-$ and $HAsO_2$ were the dominant Cr and As species at this pH, and thus As(III) redox conversion was disfavoured. At pH of 4, 89% Cr(VI) removal and 30% As(III) oxidation efficiency was observed. At pH of 7, 97% Cr(VI) removal and 99% As(III) oxidation efficiency was observed, where $HCrO_4^-$ and $HAsO_2$ were the dominant Cr and As; thus redox conversion of Cr(VI) and As(III) was favoured at this pH.
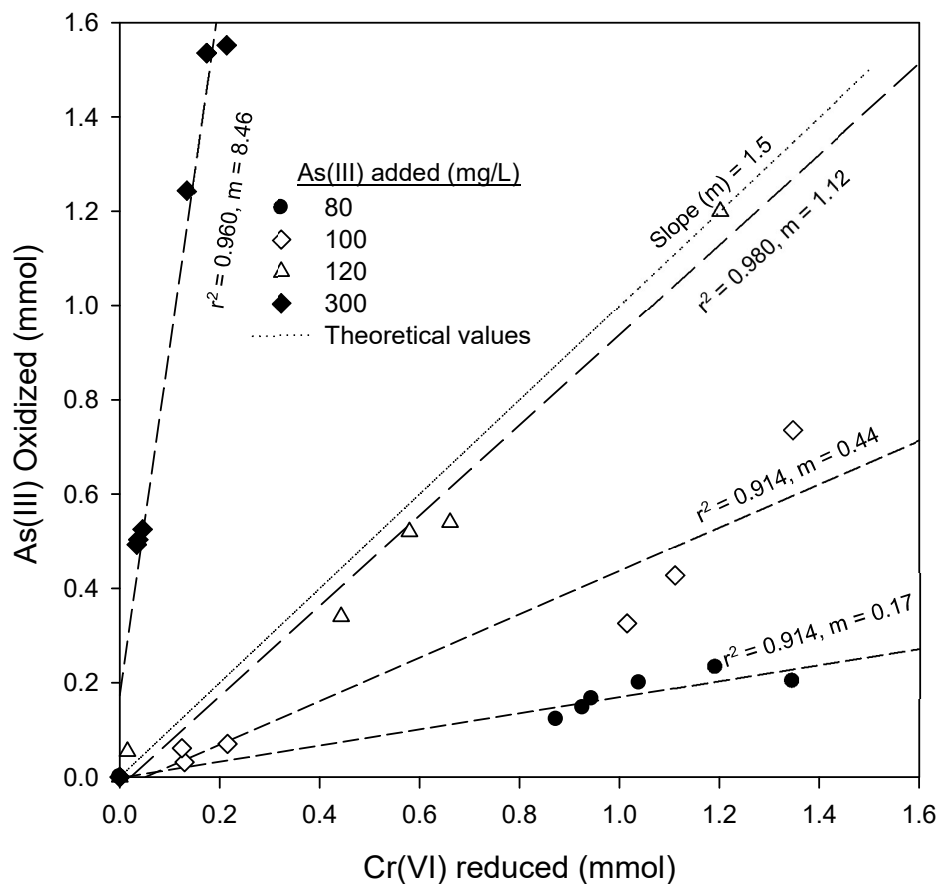
Figure 4.13: Relationship between As(III) oxidized and Cr(VI) reduced in the anaerobic consortium

The aim of the experiment was to investigate whether CO_2 was limiting during the reduction and oxidation of Cr(VI) and As (III) by the consortium. Batch studies were conducted with glucose, with and without sodium bicarbonate ($NaHCO_3$ – external source of CO_2). Cr(VI) reduction rate of 0.85, 1.3, and 1.8 mg/L·h and removal efficiency of $\geq 96\%$ were observed in the test with glucose, sodium bicarbonate and no carbon supply (control), respectively (Figure 4.14). Alternatively, As(III) oxidation rate of 2.1,1.91, and 1.90 mg/ L hour and removal efficiency of $\geq 80\%$ were also observed. It was observed that HCO_3^- or CO_2 was not a limiting aspect in the redox conversion Cr(VI) and As(III). Redox reaction observed in the control experiment (without CO_2 supply) suggest that redox reaction can take place naturally in the environment by utilizing environmental dissolved CO_2 through cell fixation process. Our experiment was carried out under anaerobic condition. However, during anaerobic glycolysis, NADH oxidized to NAD^+ so it can be re-used in glycolysis, and CO_2 is one of the end or by product anaerobic process. In this context, because of

the presence of dissolved CO_2, the redox reaction of Cr(VI) and As(III) is feasible because of system self-generated CO_2 is utilize as carbon source.

Further testing was done to validate electron mass switch during redox conversion of Cr(VI) and As(III). The electron mass switch is based on the oxidation and reduction strength of the tested solution, and it is measured as oxidation-reduction potential (ORP) in millivolts (mV) (Figure 4.16a-b). In the same test condition at 0-1 hr of incubation, initial oxidation-reduction analysis was recorded at average of -165 mV with pH of 7.24 at 70 mg/L Cr(VI) and -145 mV with pH of 7.15 at 50 mg/L Cr(VI) (Figure 4.16a). Oxidation-reduction potential was recorded as -90 mV, pH 7.25 at 70 mg/L and -98 mV, pH 7.20 after 98 hr incubation (Figure 4.16b). The ORP in both tests increased from low to high values, with a corresponding increase in pH values. However, this is governed by way of the appearance of As(V) and Cr(III), indicating an electron transfer during redox conversion of Cr(VI) and As(III).
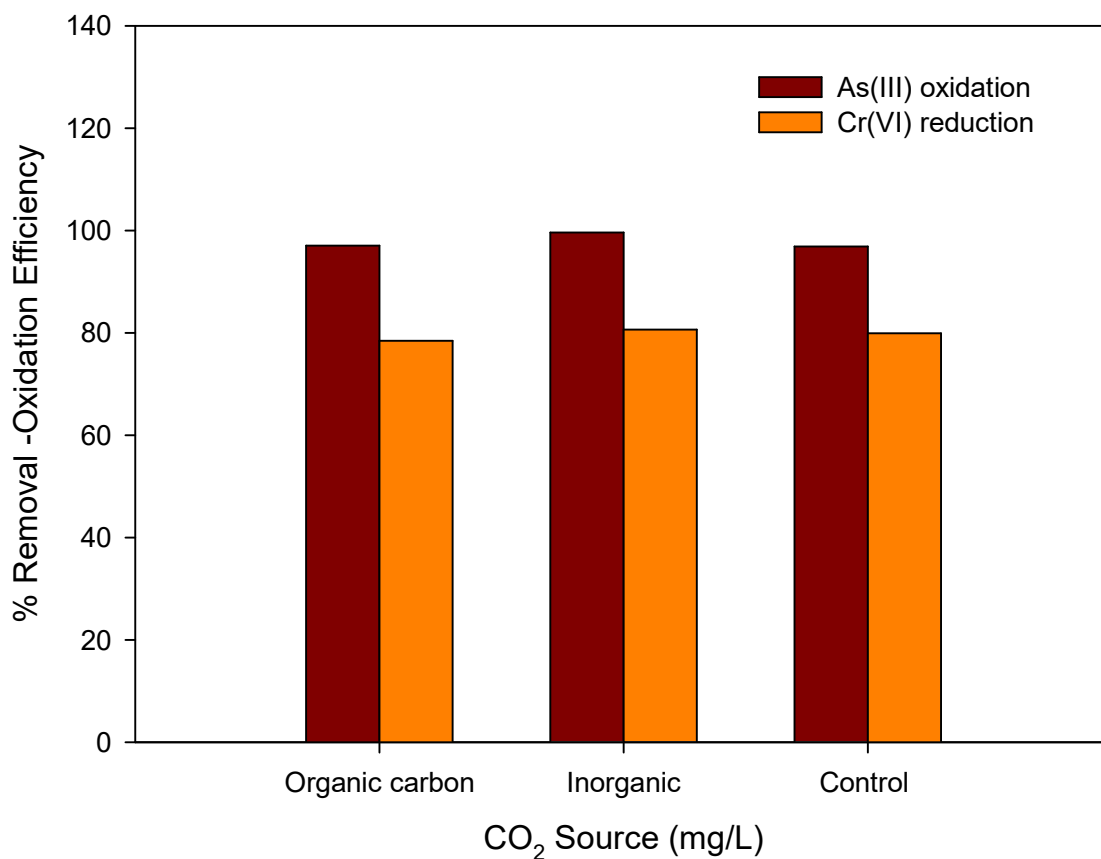
Figure 4.14: Effect of physical parameters (a) carbon sources
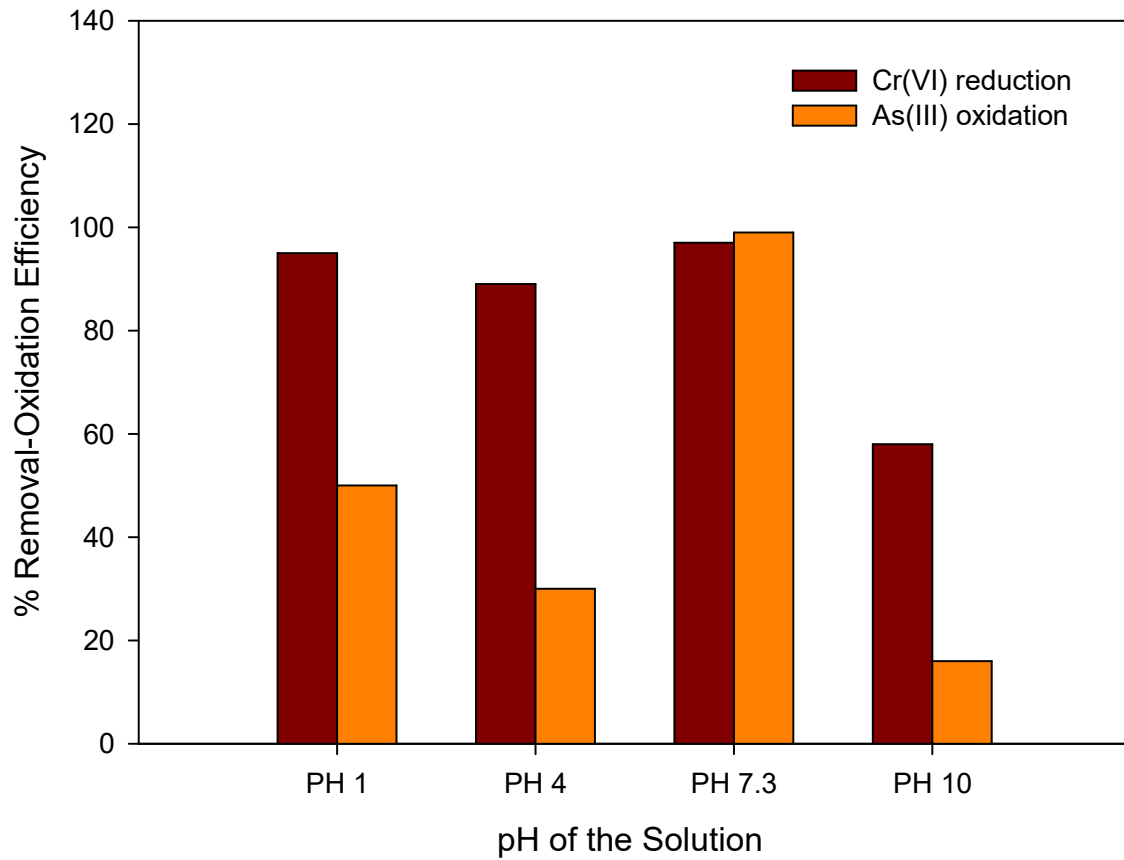
Figure 4.15: Effect of physical parameters pH, on concurrent As(III) oxidation and Cr(VI) reduction
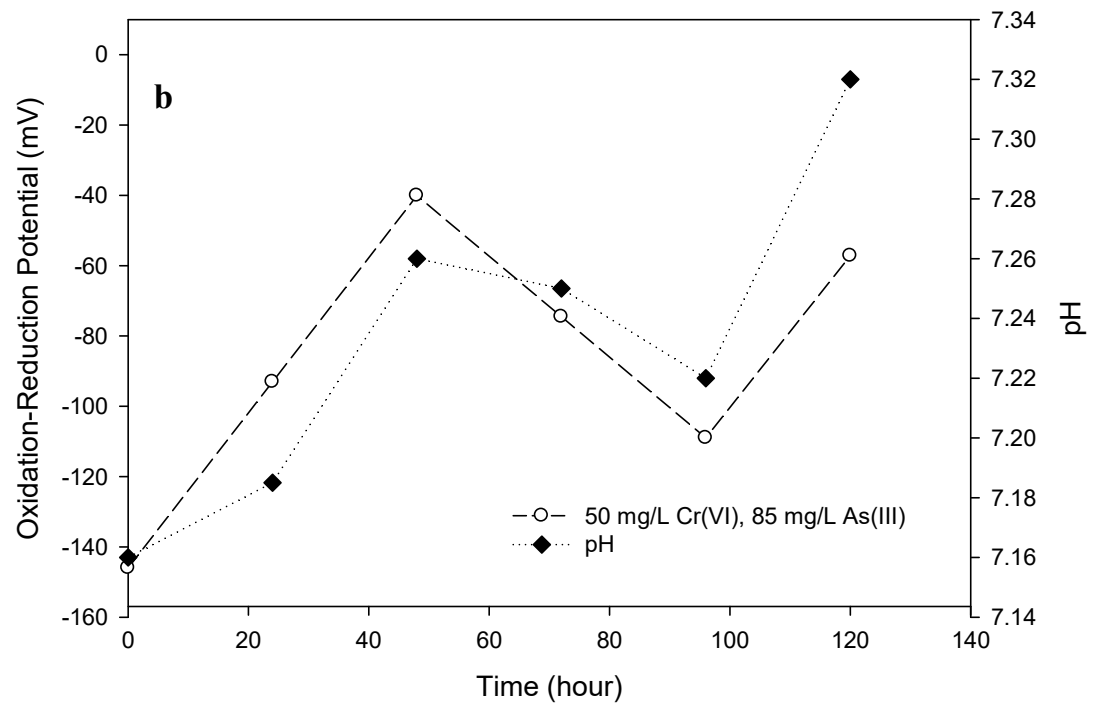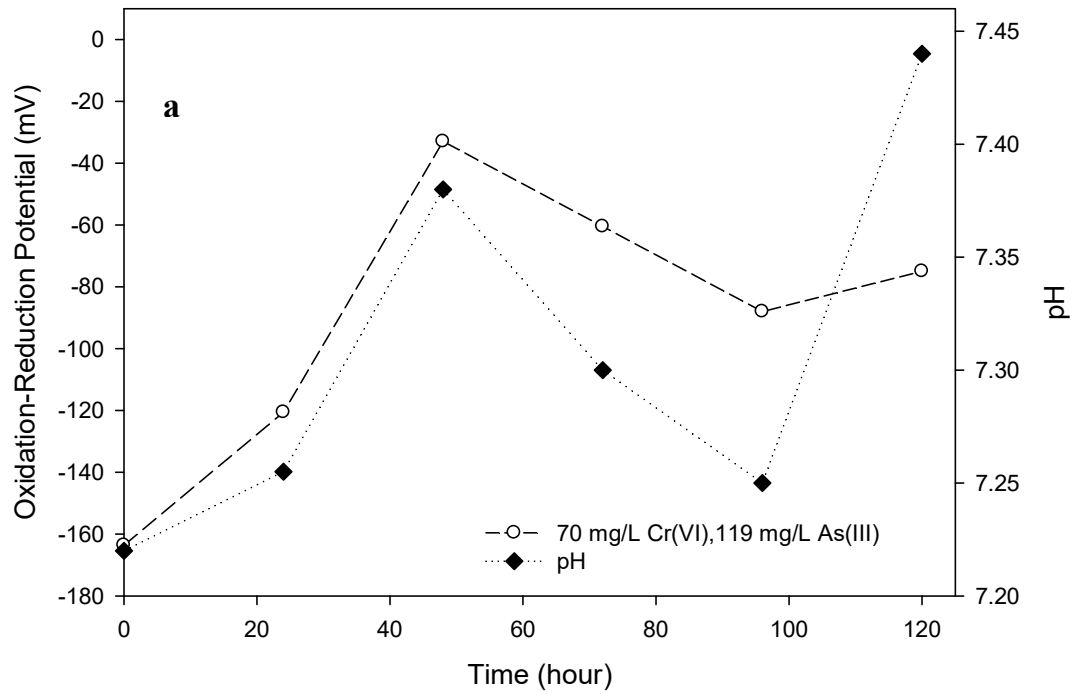
Figure 4.16: Effect of physical parameters (a) Oxidation Reduction Potential at 70 mg/L Cr(VI) (b) oxidation reduction potential at 50 mg/L Cr(VI) on concurrent As(III) oxidation and Cr(VI) reduction

CHAPTER 5

Performance of the Continuous Flow Biofilm Reactor

5.1 Biomass characteristics

Biofilm growth on the glass beads in the continuous-flow reactor was examined under an electron scan microscope. The purpose of this investigation was to establish the existence of biofilm on the glass beads. The glass beads used in this study were ground to create a rough surface area for microbial attachment. Samples of glass beads were collected from four different locations. Morphological observation showed a dense population of microbial growth or biofilm growth on the glass beads (Figure 5.1). However, the observed evidence of biofilm growth on the glass beads suggests that Cr(VI) feed content in the presence of As(III) was indeed reduced by biofilm attached to the glass beads.

5.2 Reactor start-up

The continuous-flow reactor experiment was started by inoculating the reactors with 100 mL of overnight-grown cells harvested from mixed culture containing 20 mg/L Cr(VI) and 40 mg/L As(III) in nutrient broth and operated for 24 h at pH 7 and 30°C in up flow feed mode for more than 14 days. The continuous-flow reactors were then continuously fed with the mineral medium containing 1.5 g/L of bicarbonate, a mineral medium and a stepwise increase in Cr(VI) and As(III) concentration ranging from 30 - 200 mg/L and 60 - 400 mg/L under a variable HRT of 5 h and 17h for PFR and 3h for CSTR for 24 days' continuous operation per phase from phases I-VIII. After the initial start-up period, the performance of the reactors under various influent Cr(VI) and As(III) concentrations, HRTs and other environmental factors were continuously monitored over 150 days of continuous operation. The operation conditions and performance for the entire experiment are summarized in tables 5.1–5.4.

Location: 1 and 2

Location: 3 and 4
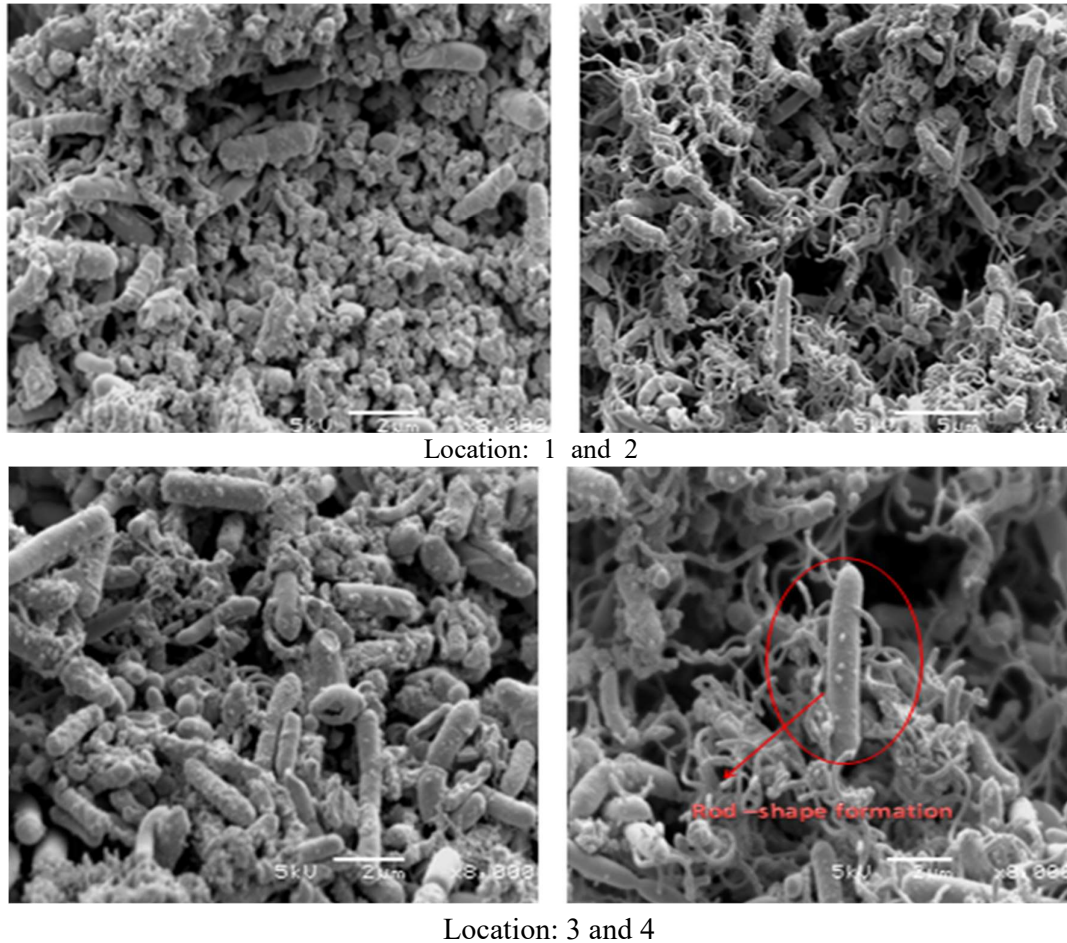
Figure 5.1: SEM photographs of a crevice at different magnifications showing biofilm attachment on the beads collected at four different locations

5.3 Glass bead packed-bed PFR with anaerobic CSTR retrofit

5.3.1 Performance evaluation

The bioreactor systems ('Reactor 1' and 'Reactor 3') were operated continuously for a period of 150 days over a range of influent Cr(VI) concentrations (30-200 mg/L) and As(III) concentrations in the ratio of 3.4:2 (51-340 mg/L) at optimal liquid detention times of 12 h. Figure 5.2 shows influent and effluent Cr(VI) concentrations throughout the operation of both reactors. The pattern of As(III) utilization is expected to corresponded to Cr(VI) reduction in the reactor, since As(III) was fundamentally used for Cr(VI) reduction, as previously described in the batch experiment. It is believed that As(III) concentration in the reactors was oxidized, which correlated with optimum Cr(VI) reduction. However, it is assumed that all the As(III) in the solution was used up for Cr(VI)
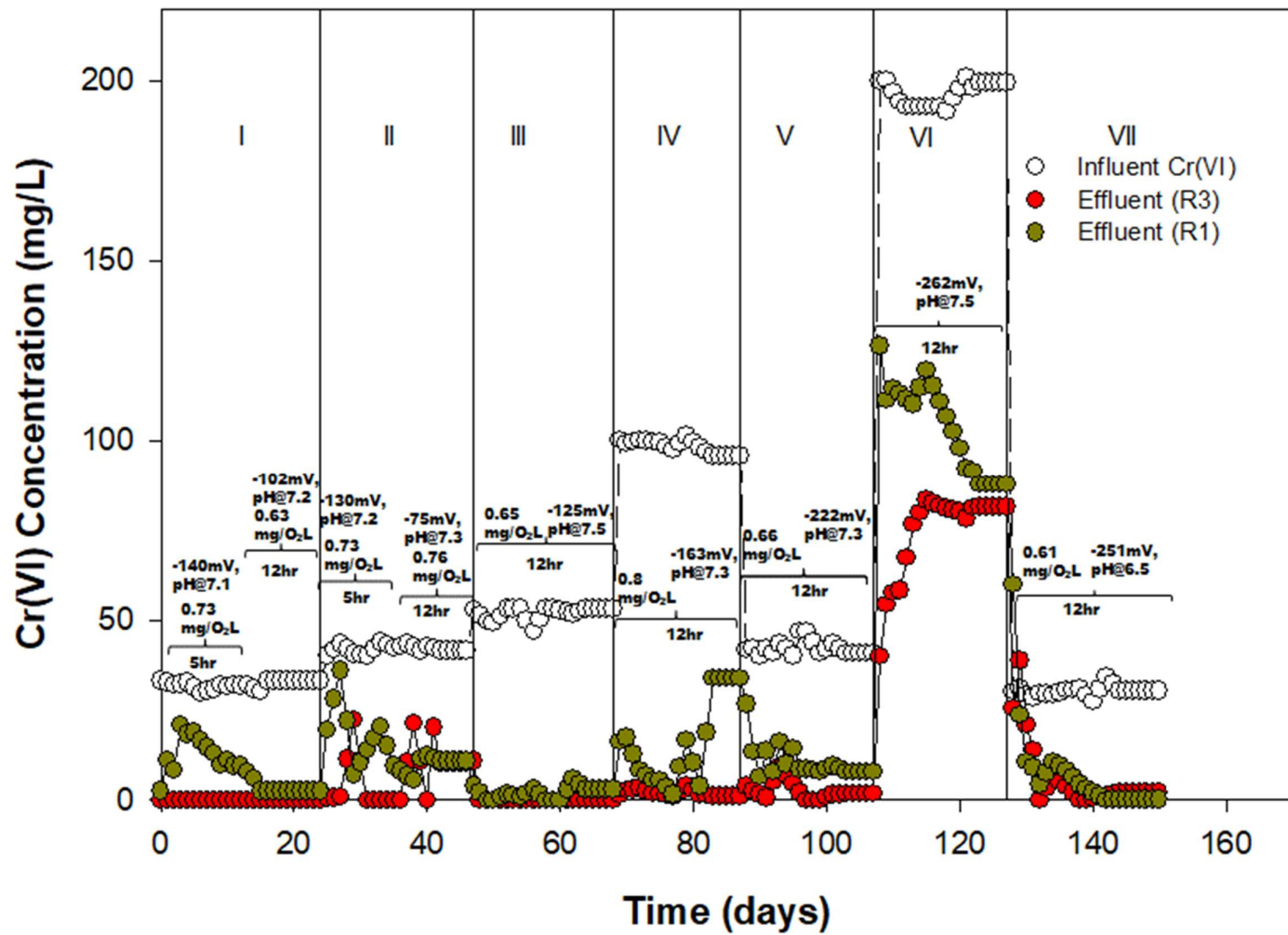
Figure 5.2: Cr(VI) Reduction in a glass bead packed PFR (Reactor 1), and anaerobic CSTR retrofit (Reactor 2) operation for 150 days.

reduction, while the precipitate was recovered as solid form after passing through sedimentation, filtration and drying (Figure 4.17).

In addition, results showed that the Cr(VI) reducing rate increases in the reactors with the increase in the Cr(VI) loading rate. However, there was an increase in Cr(VI) removal efficiency in all phases except phase VI, which had lower efficiency compared to the other phases. Cr(VI) removal efficiency reached a maximum of 78% under the high load conditions (Figure 5.2). Cr(VI) removal efficiency dropped significantly during a Cr(VI) overloading in phase VI. CSTR achieved a maximum of 97% under the high load condition. The operation conditions and performance for the glass bead media reactor with the CSTR experiment are summarized in table 5.1– 5.2.

However, the conditions of the operational phases are described in detail as follows:

PHASE I: The operation of the reactors (PFR – R1) and (CSTR – R2) started in the initial phase from day 1 up till day 24 after cell attachment was seen on the glass beads and reactor column walls. The continuous-flow glass bead packed bed reactor (PFR – R1) was operated in up flow mode under an influent Cr(VI) and As(III) concentrations of 30 and 60 mg/L on airtight condition, and an optimum HRT of 5 and 16 ± 0.8 h at pH of 7.2 ± 0.3, DO of 0.88 mg/L, ORP of -141 ± 0.31 mV and temperature of $31 \pm 0.9^{\circ}$C at the operation phase I (Table 5.1).

The CSTR – R2 reactor retrofit during this phase, receives final effluent flow from the PFR for further treatment with suspended biomass, it also serves as a growth medium for microbial cell recovery and recirculation. CSTR – R2 was also operated under airtight conditions, and an optimum HRT of 3 ± 0.8 h at pH of 7 ± 0.2, DO of 0.92 mg/L, ORP of -101 ± 0.2 mV and temperature of $31 \pm 0.7^{\circ}$C (Table 5.2). The average or cumulative effluent Cr (VI) concentration measured at 8 mg/L, and 6 mg/L in PFR and CSTR, respectively (Table 5.1). Under the operating conditions in phase (I), PFR with glass media was efficient in reducing Cr(VI) with a removal average or cumulative efficiency of $75 \pm 0.6\%$, whereas a much better effluent performance was seen with near complete reduction of Cr(VI) in the CSTR retrofit with a removal average or cumulative efficiency of $79 \pm 0.1\%$. A steady-state condition was not really achieved at this phase due to variable flow discrepancies. This was corrected at the end of this phase for optimum operation of the next phase.

PHASE II: The feed concentration at Phase II was increased from 30 mg/L to 40 mg/L Cr(VI) concentration and 80 mg/L As(III) as electron source and operated from day 25 to day 46. The

reactor was operated at initial 5 h HRT to investigate the effect of the HRT on the effluent quality. The result indicated that 12 h HRT gives better effluent performance than 5h HRT (Figure 5.2). The measured average steady-state effluent Cr(VI) concentration (9 ± 0.8 mg/L) in this phase did not differ significantly from the effluent Cr(VI) concentration of 8 mg/L obtained in phase I (Table 5.1). An average pH of 7 ± 0.3, DO of 0.61 mg/L, ORP of -123 ± 0.82 mV and temperature of 30 ± 0.5 was recorded during the steady-state condition (Table 5.1). Cr(VI) removal efficiency of $76 \pm ,0.54\%$ was achieved in this phase which is slightly higher than efficiency achieved in the previous phase.

The CSTR – R2 retrofit during this phase was also operated under airtight conditions similar to the previous phase, and at optimum HRT of 3 ± 0.8 h , pH of 7 ± 0.6, DO of 0.66 mg/L, temperature of 30 ± 0.5°C, and ORP of -121 ± 0.1 mV (Table 5.2). The average or cumulative effluent Cr (VI) concentration measured at 4 ± 0.2 mg/L is much lower than effluent concentration achieved by the PFR (tables 5.1 and 5.2). Under the operating conditions in phase II, PFR with glass media was efficient in reducing Cr(VI) with a removal average or cumulative efficiency of $76 \pm 0.84\%$, whereas a much better effluent performance was seen with near complete reduction of Cr(VI) in the CSTR retrofit with a removal average or cumulative efficiency of $90 \pm 0.56\%$.

Steady-state conditions were achieved, but the PFR performance was slightly affected by unstable operating conditions due to a significant biological growth in the feed bottle and variable flow discrepancies. These were minimized by cleaning the feed bottle with ethanol, prepared fresh medium and replacing the contaminated tubing with ethanol-cleaned tubing.

PHASE III: The feed concentration at Phase III was increased from 40 mg/L to 50 mg/L Cr(VI) concentration and 85 mg/L As(III) as electron source and operated from day 47 to day 68 optimum HRT of 12 h. The performance of the reactors is expected to improve at this phase as a result of sufficient microbial growth and system stability. The measured PFR average steady-state effluent Cr(VI) concentration (2 ± 0.7 mg/L) in this phase differs significantly from the effluent Cr(VI) concentration of 9 mg/L obtained in phase I and II (Table 5.1), with an average pH of 7 ± 0.9, DO of 0.90 mg/L, ORP of -103 ± 0.65 mV and temperature of 31 ± 0.7.

Table 5.1: Optimum steady-state performance of the continuous-flow glass bead packed bed reactor (Reactor 1)

Experimental Run	Duration day	HRT hours	Influent Cr(VI) mg/L	Influent As(III) mg/L	Effluent Cr(VI) mg/L	Cr(VI) Loadn. rate® mgL^{-1}d-^{1}	Cr(VI)Redn. rate® mgL^{-1}d-^{1}	Cr(VI) removal (%)	Temperature. (°C)	pH	DO mg/L	ORP mV
I[pahse1]	1-24	11±0.7	32±0.05	64±0.10	8±0.0[c]	0.12	0.08	75±0.00	31±0.9	7±0.3	0.88	-141±0.31
II[phase 2]	25-46	11±0.5	41±0.92	83±0.84	9±0.8[c]	0.16	0.12	76±0.62	30±0.5	7±0.3	0.61	-123±0.82
III[phase 3]	47-68	11±0.6	52±0.61	105±0.22	2±0.7	0.195	0.18	95±0.87	31±0.7	7±0.9	0.90	-103±0.65
IV[pase 4]	69-87[s]	11±0.5[s]	97±0.35[s]	194±0.69[s]	20±0.7[cs]	0.36[s]	0.28[s]	78±0.73[s]	30±0.7[s]	7±0.4[s]	1±0.5[s]	-122±0.93[s]
V[phase5]	88-107[r]	11±0.8[r]	42±0.37[r]	84±0.73[r]	8±0.23[cr]	0.16[r]	0.13[r]	80±0.58[r]	32±0.5[r]	6±0.9[r]	0.29[r]	-156±0.68[r]
VI[phase 6]	108-127[¥]	11±0.7[¥]	197±0.75[¥]	395±0.50[¥]	94±0.40[c¥]	0.75[¥]	0.38[¥]	52±0.26[¥]	31±0.6[¥]	7±0.4[¥]	1±00[¥]	-225±0.18[¥]
VII[phase 7]	128-150[r]	11±0.8[r]	30±0.43[r]	60±0.86[r]	0.8±0.09[r]	0.11[r]	0.16[r]	97±0.75[r]	30±0.6[r]	6±0.4[r]	0.97[r]	-291±0.92[r]

c = cumulative effluent after each phase at 17h HRT, s = shock load effect, r = recovery effect, ¥ = double shock load effect

Table 5.2: Optimum steady-state performance of the continuous stirred tank flow reactor (Reactor 3)

Experimental Run	Duration day	HRT hours	Influent Cr(VI) mg/L	Effluent Cr(VI) mg/L	Cr(VI) Loadn. rate® mgL^{-1}d^{-1}	Cr(VI)Redn. rate® mgL^{-1}d^{-1}	Cr(VI) removal (%)	Cr(VI) removal (%) (overall)	Temperature. (oC)	pH	DO mg/L	ORP mV
II[phase 2]	25-46	3±0.8	9±0.8[c]	4±0.2[c]	0.009	0.005	57±0.14	90±0.56	30±0.5	7±0.6	0.66	-121±0.10
III[phase 3]	47-68	3±0.7	2±0.7	0.7±0.20	0.003	0.002	74±0.1	98±0.33	30±0.8	7±0.15	0.50	-120±0.8
IV[pase 4]	69-87[s]	3±0.9[s]	20±0.7[cs]	2±0.5[cs]	0.020[s]	0.017[s]	87±0.92[s]	97±0.94[s]	31±0.4[s]	7±0.14[s]	0.35[s]	-192±0.6[s]
V[phase5]	88-107[r]	3±0.6[r]	8±0.23[cr]	2±0.81[cr]	0.008[r]	0.006[r]	74±0.72[r]	93±0.36[r]	31±0.1[r]	6±0.9[r]	0.29[r]	-162±0.8[r]
VI[phase 6]	108-127[¥]	3±0.7[¥]	94±0.40[c¥]	70±0.82[c¥]	0.091[¥]	0.022[¥]	24±0.69[¥]	63±0.67[¥]	32±0.6[¥]	7±0.3[¥]	1±0.2[¥]	-202±0.6[¥]
VII[phase 7]	128-150[r]	3±0.8[r]	0.8±0.09[r]	0.01±0.32[r]	0.001[r]	0.001[r]	98±0.87[r]	95±0.49[r]	30±0.8[r]	6±0.8[r]	0.29[r]	-341±0.2[r]

c = cumulative effluent after each phase at 17h HRT, s = shock load effect, r = recovery effect, ¥ = double shock load effect

In addition to this, the CSTR retrofit during this phase shows a better improvement by further reducing Cr(VI) effluent concentration from (2 ± 0.7 mg/L) to (0.7 ± 0.2 mg/L) (Table 5.2). The reactor was also operated under airtight conditions similar to the two previous phases, and at optimum HRT of 3 ± 0.8 h , pH of 7 ± 0.15, DO of 0.50 mg/L and temperature of 30 ± 0.8°C, and ORP of -120 ± 0.8 mV (Table 5.2).

Under steady-state operating conditions, PFR with glass media was efficient in reducing Cr(VI) with a removal average or cumulative efficiency of 95 ± 0.87%, whereas a much better effluent performance was seen with near complete reduction of Cr(VI) in the CSTR retrofit with a removal average or cumulative efficiency of 98 ± 0.61%. Cr(VI) breakthrough was observed in this phase (Phase III) when the influent Cr(VI) concentration was increased by 50 mg/L in the presence of As(III) concentration of 85 mg/L after 68 days of continuous operation in both reactors under favourable conditions.

PHASE IV: After system breakthrough, the feed concentration was increased from 50 mg/L to 100 mg/L Cr(VI) concentration and 170 mg/L As(III) as electron source, to evaluate the performance of both reactors at a higher Cr(VI) loading, the HRT was kept 17 (Table 5.1). The PFR was operated from day 69 to day 87 (Phase IV), and it responded to higher volumetric loading, which resulted in an increase in the effluent Cr(VI) concentration to 20 ± 0.7 mg/L (Figure 5.2). As of this, a 20% decrease in Cr(VI) removal efficiency was observed, given a removal efficiency of 78 ± 0.7%. An average pH of 7 ± 0.4, DO of 1.05 mg/L, ORP of -122 ± 0.93 mV and temperature of 30 ± 0.7 were recorded during the steady-state condition (Table 5.1).

The CSTR – R2 retrofit during this phase shows a better improvement by further reducing Cr(VI) effluent concentration from 20 mg/L to 2 mg/L (Table 5.2). The reactor was also operated under airtight conditions similar to the two previous phases, and at optimum HRT of 3 ± 0.8 h , pH of 7 ± 0.14, DO of 0.35 mg/L and temperature of 31 ± 0.4°C, and ORP of -192 ± 0.6 mV (Table 5.2). Under steady-state operating conditions, PFR with glass media was efficient in reducing Cr(VI) with a removal average or cumulative efficiency of 78 ± 0.7%, whereas a much better effluent performance was seen with near complete reduction of Cr(VI) in the CSTR retrofit, with a removal average or cumulative efficiency of 97 ± 0.94%.

PHASE V: After a high volumetric load rate was introduced, both reactors were checked for resilience (Phase V), and this was done by decreasing the feed of Cr(VI) concentration from 100

mg/L to 40 mg/L, and 68 mg/L As(III) as electron source. The PFR system was operated at the HRT of 12 h from 88 to 107 days, while maintaining other environmental conditions previously described. The PFR system showed a near recovery with effluent Cr(VI) concentration decreasing from 20 ± 0.7 mg/L to 8 ± 0.23 mg/L and a Cr(VI) removal efficiency of $80 \pm 0.57\%$ (Table 5.1). There was a much-improved effluent compared to the effluent concentration when the volumetric loading rate was previously increased. There are tendencies that a significant mass of biomass attached to the glass beads may have been washed off in this phase as there was no continuous cell recirculation from the previous three phases. However, this could be attributed to lower Cr(VI) removal efficiency observed at this phase. The ORP of -156 ± 0.68 mV, DO concentration of 0.29 mg/L, however, was observed (Table 5.1), while the temperature of the reactor was maintained at $32 \pm 0.5^{\circ}$C during this phase of operation.

The CSTR – R2 retrofit during this phase shows a better improvement by further reducing Cr(VI) effluent concentration from 8 ± 0.23 mg/L to 2 ± 0.81 mg/L (Table 5.2). The reactor was also operated under airtight conditions similar to the previous phases, and at optimum HRT of 3 ± 0.8 h , pH of 6 ± 0.9, DO of 0.29 mg/L and temperature of $31 \pm 0.1^{\circ}$C, and ORP of -162 ± 0.8 mV (Table 5.2). Under steady-state operating conditions, PFR with glass media was efficient in reducing Cr(VI) with a removal average or cumulative efficiency of $80 \pm 0.5\%$, whereas a much better effluent performance was seen in CSTR retrofit with near complete reduction of Cr(VI) and complete system recovery, with a removal average or cumulative efficiency of $93 \pm 0.36\%$. However, both reactors show system resilience to As(III) and Cr(VI) concentrations.

PHASE VI: After system recovery was observed in the previous phase, the reactor was operated under an influent Cr(VI) concentration of 200 mg/L and 340 mg/L As(III) as an electron source (Phase VI) after 2 h biomass circulation. The PFR system during this phase was operated at an HRT of 17h from 108 to 127 days. This was done to test if the microbial activity in the reactor could be inhibited at much higher concentration. The effluent Cr(VI) concentration of the PFR system increased from 8 ± 0.23 mg/L to 94 ± 0.4 mg/L (Figure 5.5) under this loading, before reaching a steady-state effluent concentration (Table 5.1). The result suggests that Cr(VI) reduction could be inhibited by the current load, as a result of dual toxic effect of As(III) and Cr(VI) microbial cells, or it could be as a result of lower HRT. However, much higher contact time and optimum biomass recirculation could be required for optimum reduction of Cr(VI) using electrons from As(III). DO concentration in the reactor increased slightly from 0.90 mg/L to 1 mg/L. (Table 5.1). The pH, ORP and temperature were recorded at 7 ± 0.4, -225 ± 0.18 mV and constant temperature of 31 ± 0.6,

with the Cr(VI) removal efficiency of $52 \pm 0.26\%$. In addition, Cr(VI) removal efficiency of the PFR system dropped significantly by 28%, which is closely related to the same percentage drop (20%) observed when the influent Cr(VI) and As(III) concentrations were increased to 100 mg/L and 170 mg/L, respectively. This suggests possible Cr(VI) and As(III) inhibition with regard to the biological activities under a high loading rate.

The CSTR – R2 retrofit system during this phase showed a slight improvement by further reducing the PFR system Cr(VI) effluent concentration from 94 ± 0.4 mg/L to 70 ± 0.82 mg/L (Table 5.2). However, only 24 mg/L of Cr(VI) concentration was further reduced after an additional 4 h HRT in a complete mixed reactor, suggesting an inhibition effect on the microbial activities. The reactor was also operated under airtight conditions similar to the previous phases, pH of 7 ± 0.3, with an increase in DO of 1.2 mg/L, temperature of 32 ± 0.6°C, and ORP of -202 ± 0.6 mV (Table 5.2). Under steady-state operating conditions, PFR with glass media Cr(VI) with a removal average or cumulative efficiency dropped from of $80 \pm 0.5\%$ to $52 \pm 0.26\%$, whereas a slight effluent performance was seen in the CSTR retrofit system with a Cr(VI) removal average or cumulative efficiency of $63 \pm 0.67\%$. The efficiency at this phase was much lower when compared to efficiency at previous phases.

PHASE VII: Both reactors were used for system resilience and recovery at lower volumetric load and this was done by decreasing the feed of Cr(VI) and As(III) concentration from 200 mg/L to 30 mg/L, and from 340 mg/L to 51 mg/L As(III), respectively. The PFR system was operated at the same HRT of 12 h from 128 to 150 days, while maintaining other environmental conditions previously described. The PFR system showed complete system recovery with an effluent Cr(VI) concentration decreasing from 94 ± 0.4 mg/L to 0.8 ± 0.09 mg/L (Figure 5.2) and a Cr(VI) removal efficiency of $97 \pm 0.46\%$ (Table 5.1). There was a much-improved effluent compared to the effluent concentration when the volumetric loading was previously increased. The ORP of -296 ± 0.92 mV was recorded and DO concentration of the system dropped from 1 mg/L to 0.97 mg/L, indicating more positive anaerobic environment, while the temperature and pH of the reactor was maintained at 30 ± 0.6°C and 6 ± 0.4 during this phase of operation (Table 5.1). In the same phase, the performance of the CSTR retrofit was also observed. Reactor recovery and system robust were also seen, suggesting microbial resilience. The CSTR retrofit system achieves Cr(VI) effluent concentration of 1.3 ± 0.32 mg/L at optimum physical conditions, as shown in Table 5.2.

5.3.2 System response to shock load

System response to shock load (i.e. increased influent Cr(VI) and As(III) concentrations) effect was observed in PFR– R1 and CSTR – R2 at Cr(VI) and As(III) concentrations of to 100 mg/L and 170 mg/L, As(III) and 200 mg/L Cr(VI) and 340 mg/L As(III) (Figure 5). It was seen that the Cr(VI) effluent concentration increases soon after Cr(VI) and As(III) influent concentration was increased. This trend was observed whenever the influent Cr(VI) and As(III) concentration were increased to a higher value in all phases. As(III) utilization preceded Cr(VI) reduction as the system adjusted to the new loading conditions. This trend suggests that higher metabolic activity in the bioreactor may result in a higher rate of Cr(VI) reduction.

The reactor load was increased up to 100 mg/L and 170 mg/L As(III) and further to 200 mg/L Cr(VI) and 340 mg/L As(III) as double shock load effect. The system was characterized by an increase in effluent Cr(VI) concentration at lower Cr(VI) removal efficiency of $78 \pm 0.7\%$ and $52 \pm 0.26\%$ at 100 mg/L and 200 mg/L in R1, and $63 \pm 0.67\%$ was seen R2 at 200 mg/L. The elevated Cr(VI) concentration in the effluent indicated that biological activity could be inhibited by dual toxic effect of Cr(VI) and As(III). Second, it could be that the redox reaction was incomplete as a result of insufficient HRT.

However, Cr(VI) reduction in both reactor R1 and R2 was recovered completely when the influent Cr(VI) concentration was reduced from 100 to 40 mg/L or 200 to 30 mg/L at As(III) concentration from 170 to 68 mg/L or 340 to 51 mg/L in phases V and VII, with Cr(VI) removal efficiency increasing from 78% to 80% at 100 mg/L and 52% to 97% at 200 mg/L in reactor 1, while in reactor 2 Cr(VI) removal efficiency increased from 63% to 95% at 200 mg/L. The biological activity recovery is evident in the rapid decrease in Cr(VI) concentration in phases V and VII.

The Cr(VI) reduction in the presence of As(III) in the bioreactor was indeed affected by the hydraulic detention time at 4 h, 5 h and 12 h. Theoretically, the redox process between Cr(VI) and As(III) could be categorized into two steps. The first step involves a microbial-induced process, which involves catalytic reduction of Cr(VI) to Cr(V). The second steps involve a chemical reaction between Cr(V) and As(III), which require high contact time for the reaction to complete. The effluent from R2 have better reduction efficiency because of additional retention time of 4 ± 0.6 h. However, the overall performance of the system was extremely good and the Cr(VI) removal efficiencies at 5 h was < 50%, while > 90% was achieved at 17h.

5.3.3 Analysis of the operating factors

Environmental factors such as ORP, pH, dissolved oxygen (DO) concentration and temperature were all the parameters of the phase evaluated for 150 days of continuous operation. The reactors' optimum operational condition is shown in Figure 5.3 a-b and 5.4 a-b. The reason for this was to estimate the optimum condition of the reactors for efficient reaction of Cr(VI) and As(III) in both mobilised and immobilised conditions.

The optimum DO, pH, and ORP level observed did not differ significantly between different operating conditions, varying from 0.032-1.3 mg/L, 6.36-7.38 and -385--5.7 mV for 'Reactor 1 (continuous-flow column (PFR) with glass bead packed bed) (Figure 5.2 a-b), and DO, pH, and ORP of 0.04 to 1.6 mg/L, 6.64-7.28 and -422-- 9.5 mV for 'Reactor 2' (continuous stirred tank reactor (CSTR)) (Figure 5.3 a-b). Typical values of DO, pH, and ORP were seen at an average of 0.83 mg/L, 7.1 and -164 mV for 'Reactor 1' and 0.62 mg/L, 7 and -218 mV for 'Reactor 2'.

Anaerobic conditions were observed in both immobilised (R1) and mobilised (R2) reactors (Figure 5.3 a and 5.4 b), except in phases IV and VI in (R1) and phase VI in (R2). These phases indicated a high DO level above 0.9 mg/L. This suggests variation in consortium composition under different Cr(VI) and As(III) loading. In addition, there was no significant change in the pH of the reactors, confirming the dominancy of Cr(VI) and As(III) (Figure 5.3 b and 5.4 b), except in phases V and VII, where the pH of both reactors dropped to 6. However, the overall pH condition of both reactors was recorded at 7.2; this corresponds to the observation made from the batch experiment, where optimum Cr(VI) reduction and As(III) oxidation occur at neutral pH conditions. This suggests that Cr(VI) removal and As(III) was optimum at neutral pH, facilitating the growth and metabolic activities of the microbes in the reactor.

Second, overall ORP was seen at the average of -164 mV in the range from -385 to -5.7 mV for 'Reactor 1' (Figure 5.3 b) and -218 mV from 422 to -87 mV for 'Reactor 2' (Figure 5.4 b). This however depicts oxidation-reduction potential or strength in both reactors throughout the operational phases (I-VII) with corresponding variation in the pH of the reactor. A fairly constant temperature was observed in both reactors throughout the operational phases (I-VII). The reactor optimum temperature was recorded at the average temperature of $32^{\circ}C$ at minimum and maximum values recorded at $25^{\circ}C$ and $35^{\circ}C$ (Figure 5.3 b and 5.4 b). This result suggests that microbial activities in the rector is optimum at pH ranging from $25^{\circ}C$- $35^{\circ}C$.
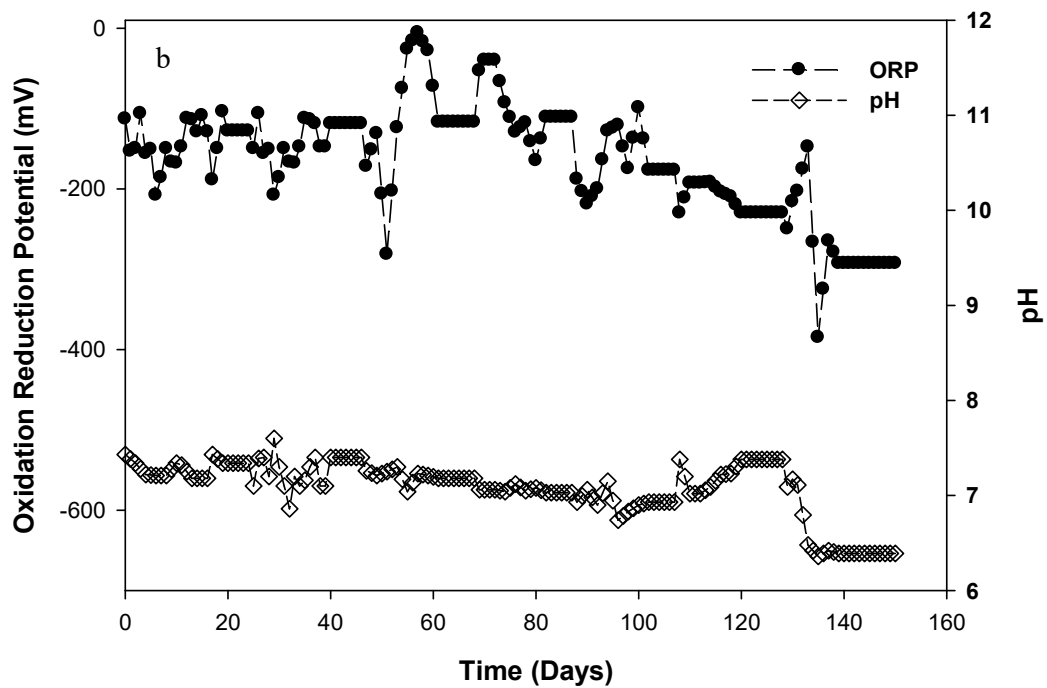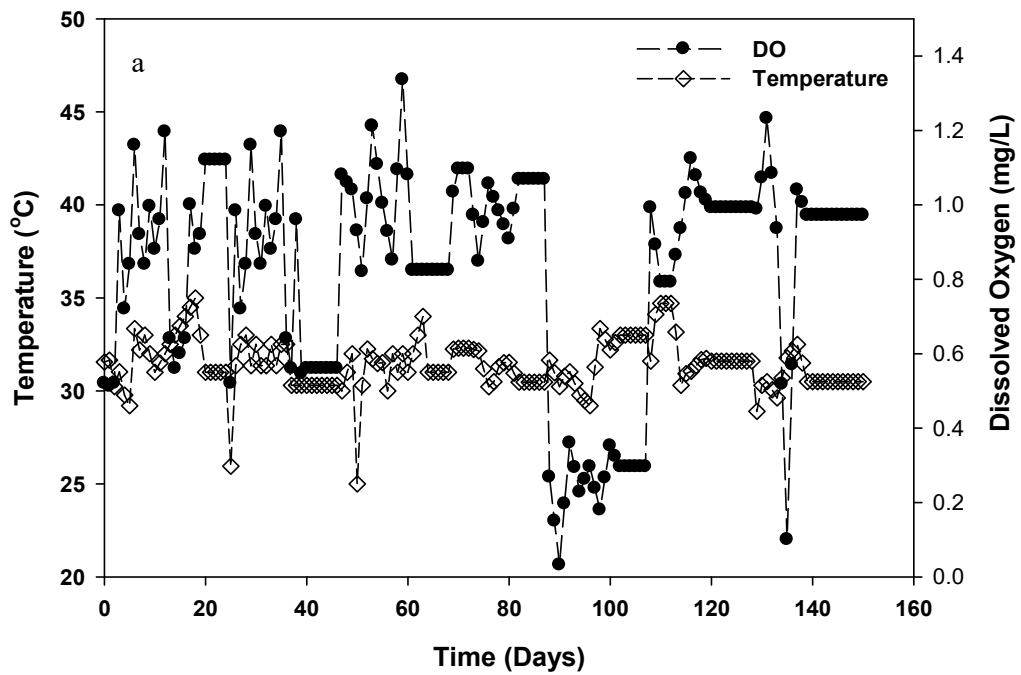
Figure 5.3: Glass bead packing PFR (Reactor 1) physical parameter (a) Temperature (^{o}C) and dissolved oxygen (mg/L); (b) ORP (mV) versus pH
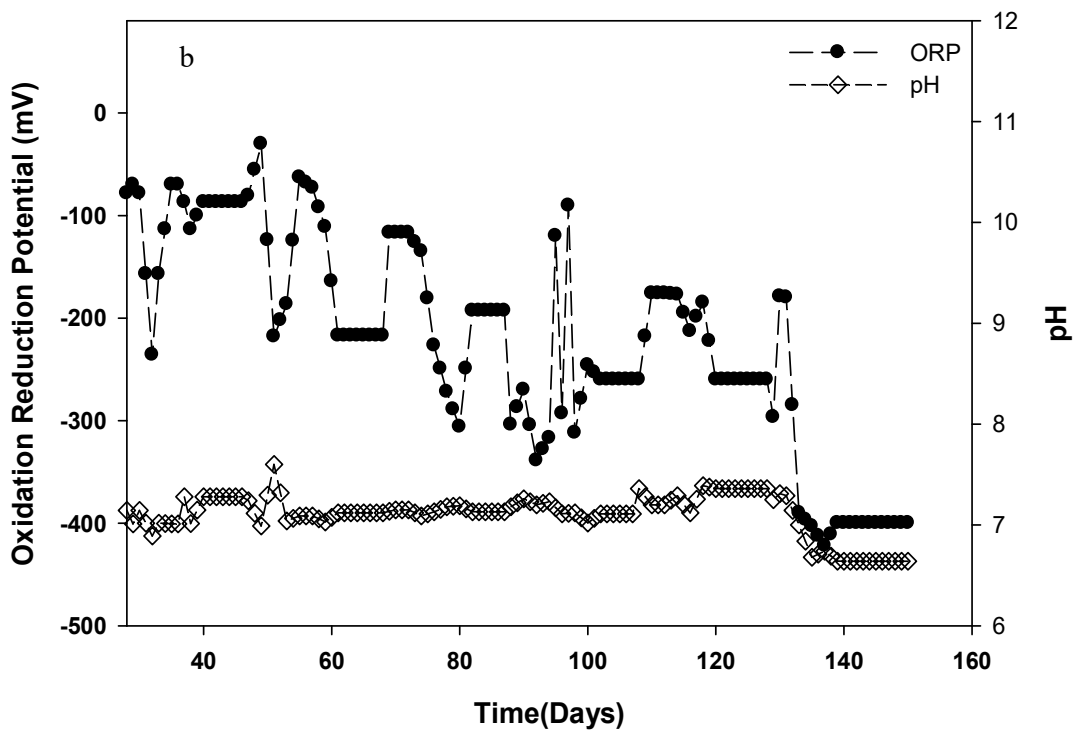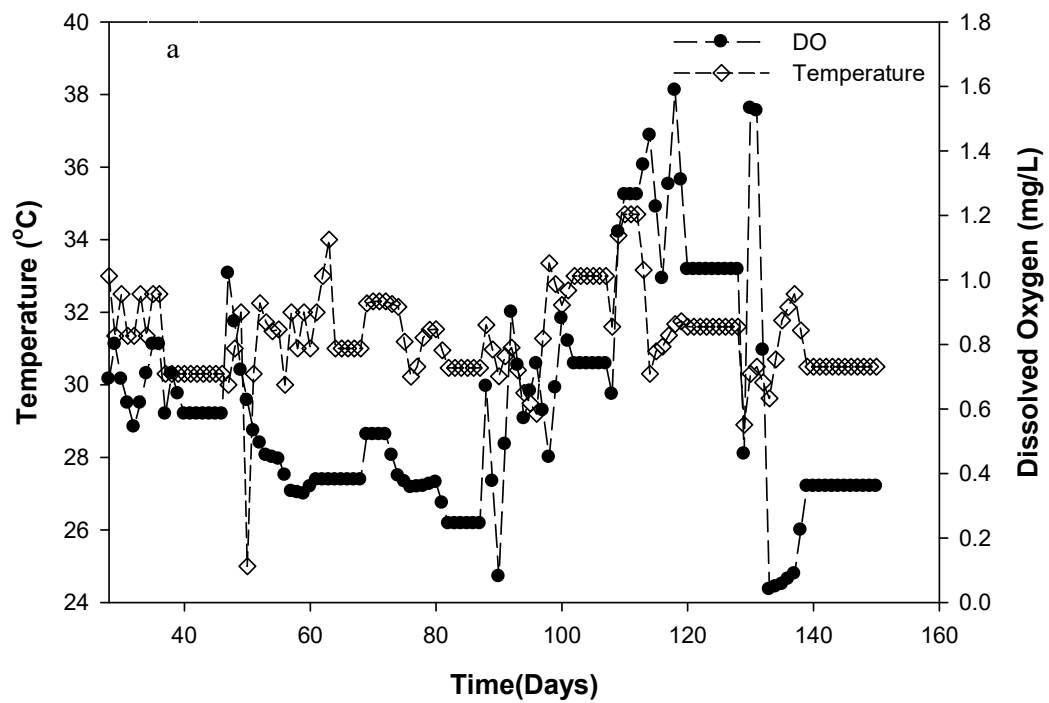
Figure 5.4: CSTR (Reactor 2) physical parameter (a) Temperature (°C) and dissolved oxygen (mg/L); (b) ORP (mV) versus pH

5.3.4 Mass transport along the longitudinal column

Cr(VI) reduction efficiency across the longitudinal reactor column was evaluated at different Cr(VI) concentrations of 30-200 mg/L, 40 mg/L (recovery) and As(III)concentration in the mole ratio of 3:2. Cr(VI) reduction profile across the reactor column, while utilizing As(III) as an electron source, was investigated. It is expected that Cr(VI) and As(III) mass concentration concurrently travels across the reactor column of 70 cm with drop in mass concentration as Cr(VI) reduction rate increases.

The result clearly indicated that the Cr(VI) reduction increases significantly over distance travelled across the column (Figure 5.5). Effluent at various sampling ports (H_1–H_4) indicated lower Cr(VI) concentration from equal space distance (x = 20-60 cm) at all phases of operation (I-VII), which correlates with a significant increase in Cr(VI)-reducing efficiency from (H_1–H_4). For instance, in Phase I, an operational run at 100 mg/L and 170 mg//L and a significant decrease in Cr(VI)-reducing efficiency were seen, compared to previous phases as a result of shock load effect, but Cr(VI)-reducing efficiency increases across the reactor column from (H_1–H_4) (Figure 5.6).

A similar trend was seen when the influent concentration was further increased up to 200 mg/L Cr(VI) concentration and 340 mg//L As(III) concentration, which resulted in a very significant decrease in Cr(VI) reduction efficiency across the longitudinal column, but Cr(VI) concentration increased from (H_1–H_4). For instance, at reactor distance (x = 20-60 cm), $\leq$ 29% - $\leq$ 44% Cr(VI) reduction efficiency was achieved (Figure 5.7). There was an increase in Cr(VI) removal efficiency along the column when the influent concertation was dropped from 100 mg/L Cr(VI) to 40 mg/L during system recovery, with an increase in Cr(VI) concentration from (H_1–H_4).

This suggests that Cr(VI) is reduced along the column, which is as a result of electron mass between Cr(VI) and As(III) across the column. However, the reduction of Cr(VI) across a vertical longitudinal reactor column is directly proportional to the height of the reactor, and the inhibitory effect observed was attributed to a loss of cell-reducing capacity, and dual toxic effect of Cr(VI) and As(III) or lower contact time effect.
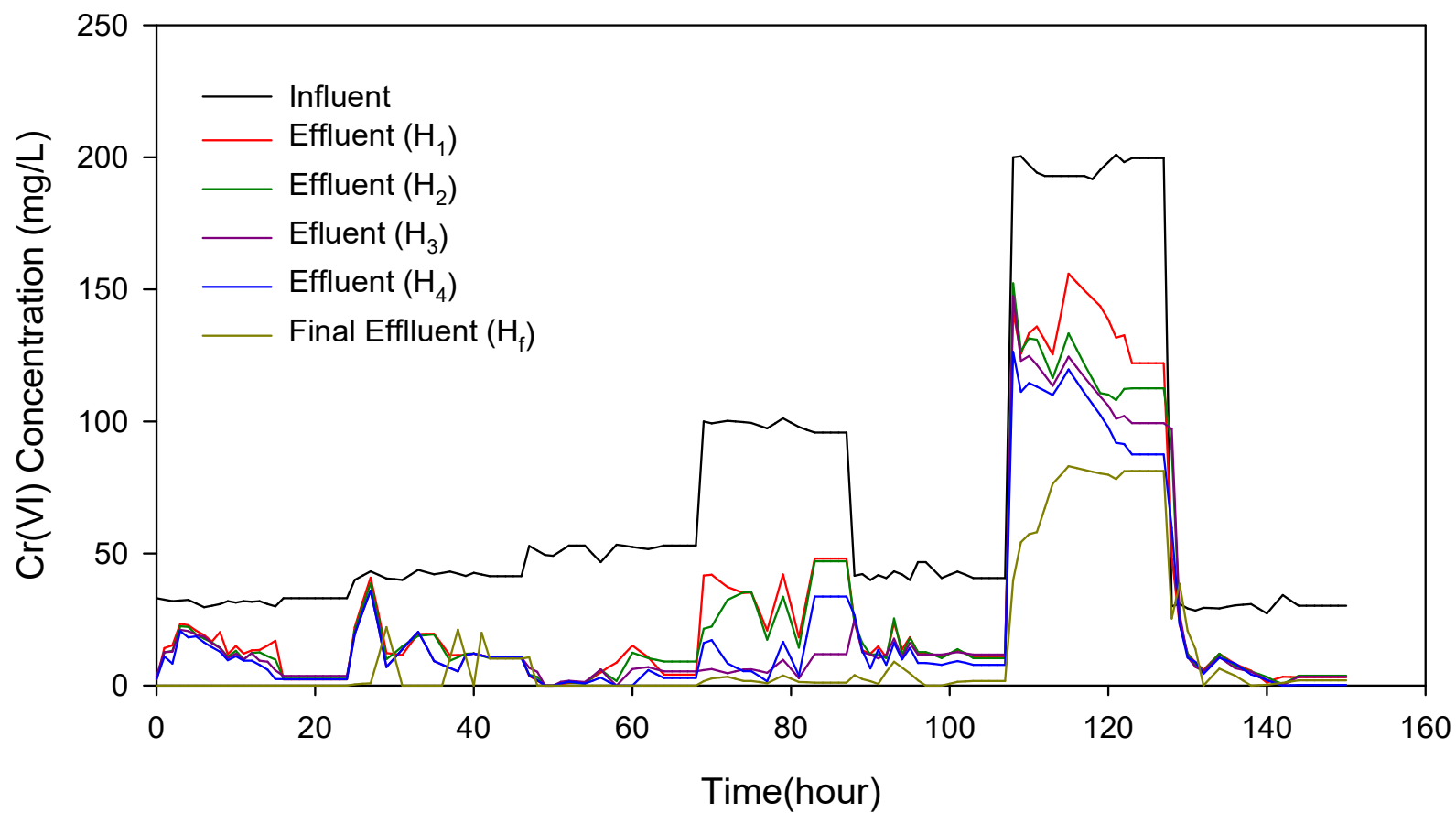
Figure 5.5: Cr(VI) removal along the glass bead packed PFR column (Reactor 3) (distance $\{x\}$ = 70 cm) at Cr(VI) concentration of 30 -200 mg/L of with proportional As(III) concentration of 51-340 mg
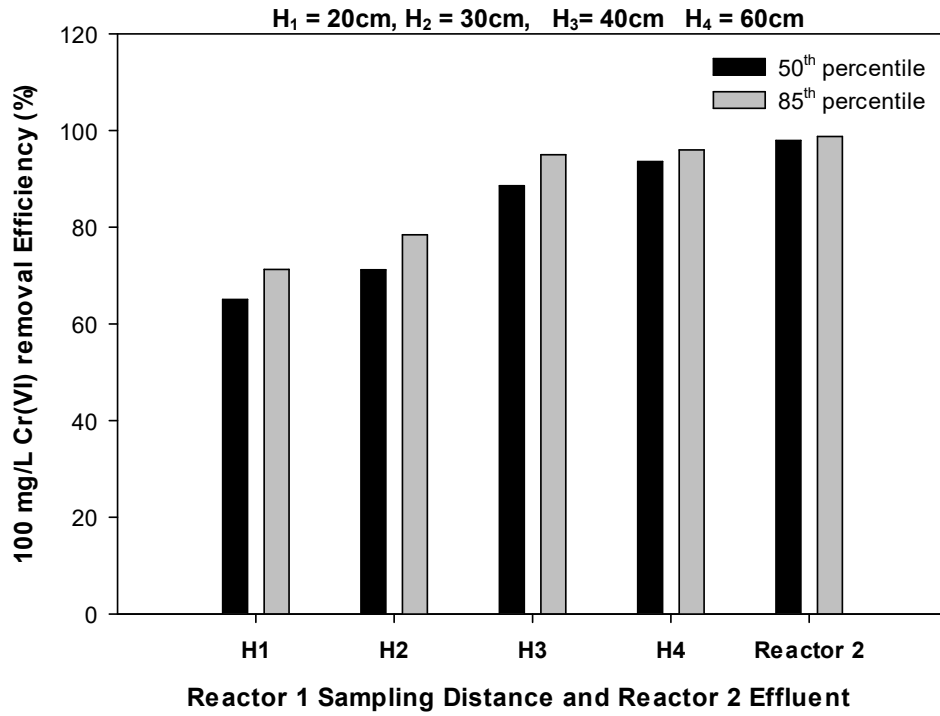
Figure 5.6: Cr(VI) removal along the longitudinal column (distance {x} = 70 cm) 100 mg/L Cr(VI) and 170 mg/L As(III)
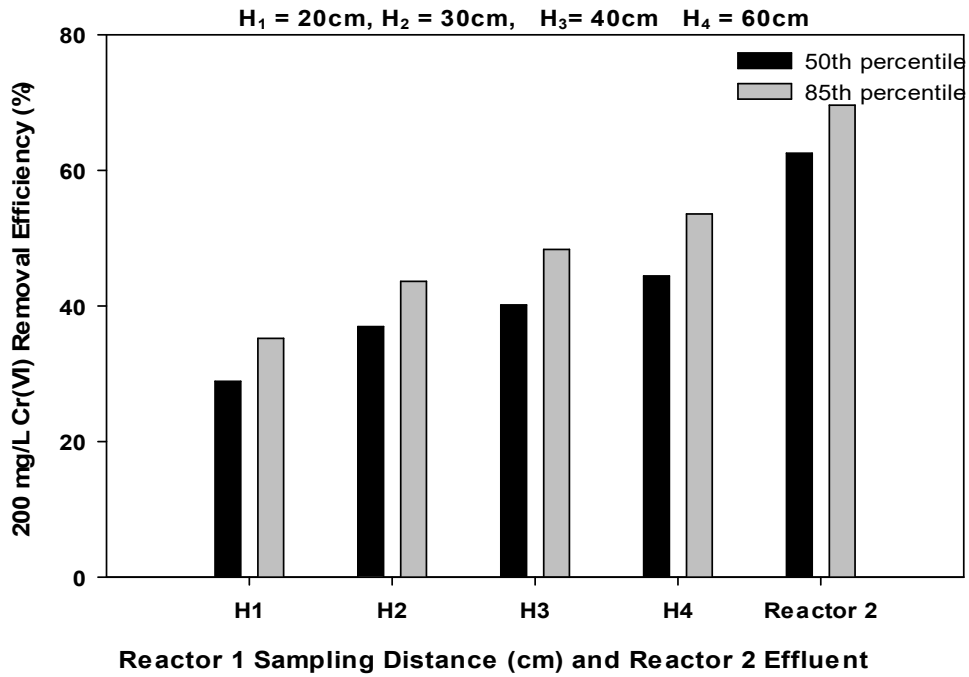
Figure 5.7: Cr(VI) removal along the longitudinal column (distance {x} = 70 cm) 200 mg/L of Cr(VI) and 340 mg/L As

5.4 Ceramic bead packed bed PFR with anaerobic CSTR retrofit

5.4.1 Performance evaluation

The performance of the immobilised and mobilised continuous-flow reactor with ceramic bead packed media (R3) and stirred tank reactor (CSTR) retrofit (R4) was observed for optimum reaction of Cr(VI) with available As(III) as an electron source. Both reactors were operated continuously for a duration of a 150 days over a range of influent Cr(VI) concentrations 30-200 mg/L similar to a glass bead media reactor. Reactor loading started after 14 days of incubation, when a significant number of microbes was seen attached to the bead and in suspension. Figure 5.8 indicates the influent and effluent Cr(VI) concentrations throughout the operational phases (I-VII) of R3 and R4.

The Cr(VI) breakthrough in the reactor was observed in Phase III when the influent Cr(VI) concentration was increased from 40 to 50 mg/L in the presence of 85 mg/L As(III) concentration. This was observed after 68 days of continuous operation, whereas system resilience at high Cr(VI) and As(III) load was investigated in phases IV and VI, with its corresponding system recovery in phases V and VII.

The conditions of the operational phases are described in detail as follows:

PHASE I: In Phase I, the duration of the operation of both reactors started in the initial phase from 1 to 24 days after cell attachment was seen on the ceramic beads and reactor column. The continuous-flow ceramic bead packed bed reactor (PFR) was operated in up-flow mode under influent Cr(VI) and As(III) concentrations of 30 and 60 mg/L in airtight conditions, and an optimum HRT of 17 ± 0.3 h (Table 5.3).

The assisted CSTR reactor retrofit during this phase receives final effluent flow from the PFR for further treatment with suspended biomass, and it also served as a growth medium for microbial cell recovery and recirculation. The CSTR was also operated under airtight conditions, and an optimum HRT of 5 ± 0.5 h (Table 5.4). The average or cumulative effluent Cr (VI) concentration measured at 7 mg/L, and 0 mg/L in PFR and CSTR, respectively (Table 5.1). Under the operating conditions in Phase I, PFR with ceramic media was efficient in reducing Cr(VI) with a removal average or cumulative efficiency of $75 \pm 0.4\%$, whereas a much better effluent performance was seen with near complete reduction of Cr(VI) in the CSTR retrofit, with a removal average or cumulative efficiency
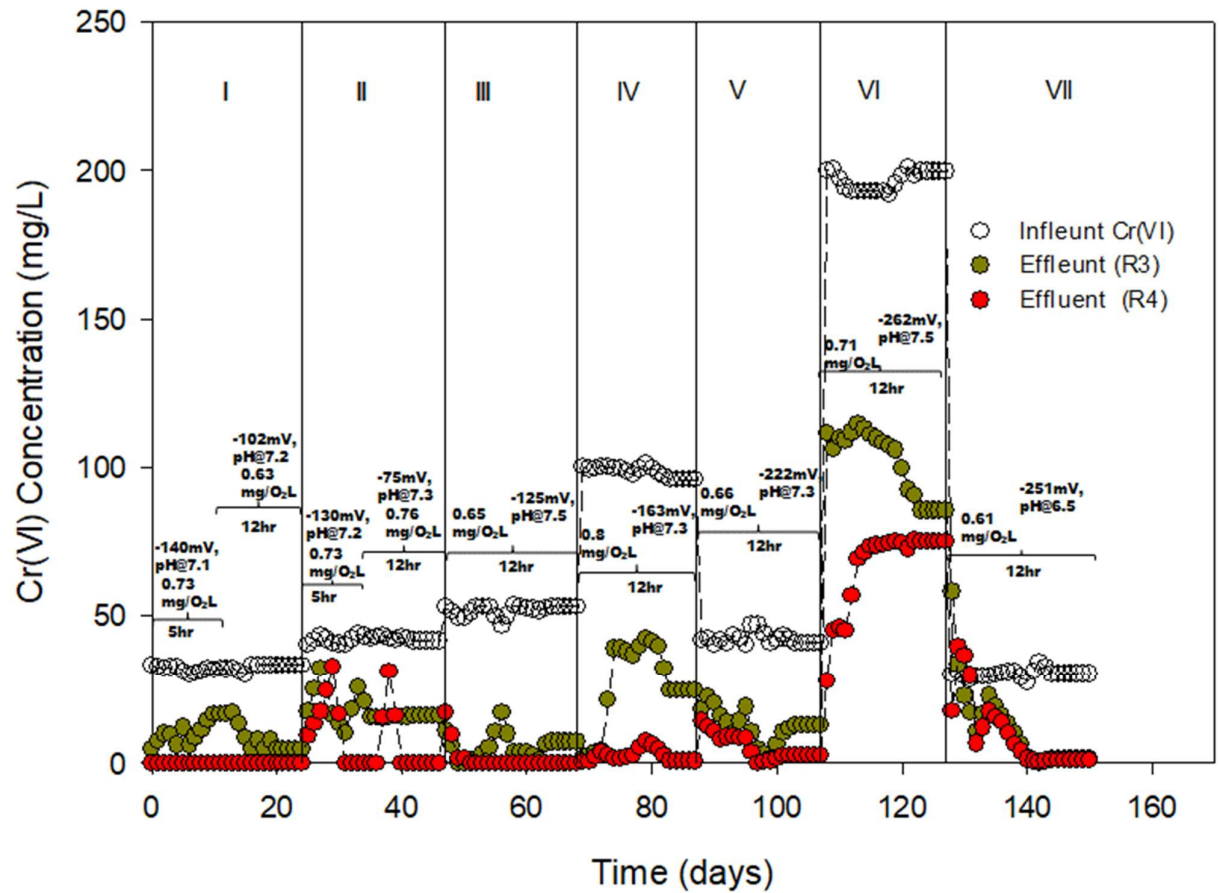
Figure 5.8: Cr(VI) reduction in a ceramic bead packed PFR (Reactor 3), and anaerobic CSTR retrofit (Reactor 4) operation for 150 days

of 100%. Flow from the CSTR was periodically recirculated to maintain the wash off attached cells on the glass bead.

PHASE II: The feed concentration in Phase II was increased from 30 mg/L to 40 mg/L Cr(VI) concentration and 68 mg/L As(III) as electron source and operated from day 25 to 46. The reactor was operated at initial 5 h HRT to investigate the effect of the HRT on the effluent quality. The result indicated that 12 h HRT gives better effluent performance than 5h HRT (Figure 5.9). The measured average steady-state effluent Cr(VI) concentration (15 ± 0.7 mg/L), at average pH of 7 ± 0.3, DO of 0.95 mg/L, ORP of -55 ± 0.33 mV and temperature of 30 ± 0.5, was seen during the steady-state condition (Table 5.3). Cr(VI) removal efficiency of $62 \pm 0.5\%$ was achieved in this phase, which is lower than the efficiency achieved in the previous phase.

The CSTR retrofit during this phase was also operated under airtight conditions similar to the previous phase, and at optimum HRT of 5 ± 0.5 h, pH of 7 ± 0.32, DO of 0.59 mg/L, temperature of 30 ± 0.7°C, and ORP of -96 ± 0.4 mV (Table 5.4). The average or cumulative effluent Cr (VI) concentration measured at 4 ± 0.8 mg/L is much lower than effluent concentration achieved by the PFR (Table 5.3 and 5.4). Under the operating conditions in phase II, PFR with glass media was efficient in reducing Cr(VI) with a removal average or cumulative efficiency of $62 \pm 0.5\%$, whereas a much better effluent performance was seen with near complete reduction of Cr(VI) in the CSTR retrofit with a removal average or cumulative efficiency of $88 \pm 0.59\%$. Steady-state condition was achieved, but the PFR performance was slightly affected by unstable operating conditions due to a significant biological growth in the feed bottle and variable flow discrepancies. These were minimized by cleaning the feed bottle with ethanol, prepared fresh medium and replacing the contaminated tubing with ethanol-cleaned tubing.

PHASE III: The feed concentration at Phase III was increased from 40 mg/L to 50 mg/L Cr(VI) concentration and 85 mg/L As(III) as electron source and operated from day 47 to 68, optimum HRT of 12 h. The performance of the reactors is expected to improve at this phase as a result of sufficient microbial growth and system stability. The measured PFR average steady-state effluent Cr(VI) concentration (5 ± 0.4 mg/L) in this phase differs significantly from the effluent Cr(VI) concentration obtained in phases I and II (Table 5.3). An average pH of 7 ± 0.2, DO of 0.83 mg/L, ORP of -124 ± 0.98 mV and temperature of 31 ± 0.5 was recorded during the steady-state condition (Table 5.3). Cr(VI) removal efficiency of $90 \pm 0.13\%$ was achieved in this phase, which was a much higher efficiency than what was achieved in the previous two phases.

Table 5.3: Optimum steady-state performance of the continuous-flow ceramic bead packed bed reactor (Reactor 2)

Experimental Run	Duration day	HRT hours	Influent Cr(VI) mg/L	Influent As(III) mg/L	Effluent Cr(VI) mg/L	Cr(VI) Loadn. rate® $mgL^{-1}d^{-1}$	Cr(VI)Redn. rate® $mgL^{-1}d^{-1}$	Cr(VI) removal (%)	Temperature. (oC)	pH	DO mg/L	ORP mV
I[pahse1]	1-24	12±0.3	32±0.05	64±0.10	7±0.3c	0.12	0.10	77±0.19	31±0.9	-	-	-
II[phase2]	25-46	12±0.2	41±0.92	83±0.84	15±0.7	0.16	0.10	62±0.55	30±0.5	7±0.3	0.95	-54±0.33
III[phase3]	47-68	12±0.1	52±0.61	105±0.22	5±0.42	0.20	0.18	90±0.00	31±0.5	7±0.2	0.83	-124±0.98
IV[phase4]	69-87[s]	12±0.2[s]	97±0.35[s]	194±0.69[s]	27±0.6[cs]	0.38[s]	0.30[s]	71±0.64[s]	30±0.8[s]	7±0.2[s]	1±0.0[s]	-144±0.0[s]
V[phase5]	88-107[r]	12±0.2[r]	42±0.37[r]	84±0.73[r]	11±0.21[cr]	0.16[r]	0.12[r]	73±0.54[r]	32±0.7[r]	7±0.2[r]	0.83[r]	-192±0.67[r]
VI[phase6]	108-127[¥]	12±0.2[¥]	197±0.75[¥]	395±0.50[¥]	89±0.06[c¥]	0.76[¥]	0.42[¥]	55±0.00[¥]	31±0.6[¥]	7±0.4[¥]	0.92[¥]	-238±0.7[¥]
VII[phase7]	128-150[r]	12±0.2[r]	30±0.45[r]	60±0.86[r]	1±0.38[r]	0.12[r]	0.11[r]	95±0.46[r]	30±0.5[r]	6±0.4[r]	0.99[r]	-264±0.00[r]

c = cumulative effluent after each phase at 17h HRT, s = shock load effect, r = recovery effect, ¥ = double shock load effect

Table 5.4: Optimum steady-state performance of the continuous stirred tank flow reactor (Reactor 4)

Experimental Run	Duration day	HRT hours	Influent Cr(VI) mg/L	Effluent Cr(VI) mg/L	Cr(VI) Loadn. rate® mgL-1d-1	Cr(VI)Redn. rate® mgL-1d-1	Cr(VI) removal (%)	Cr(VI) removal (%) (Overall)	Temperature. (ºC)	pH	DO mg/L	ORP mV
I[phase1]	1-24	3±0.5	7±0.3c	0.00c	0.01	0.01	100	100	30±0.5	-	-	-
II[phase2]	25-46	3±0.7	15±0.7	4±0.77[c]	0.02	0.01	69±0.62	88±0.59	30±0.7	7±0.32	0.59	-96±0.4
III[phase3]	47-68	3±0.8	5±0.42	0±0.00[c]	0.01	0.01	100±0.00	100±0.0	31±0.5	7±0.49	0.51	-140±0.8
IV[phase4]	69-87[s]	3±0.7[s]	27±0.6[cs]	2±0.9[cs]	0.01[s]	0.02[s]	89±0.49[s]	96±0.98[s]	30±0.8[s]	7±0.35[s]	0.61[s]	-191±0.6[s]
V[phase5]	88-107[r]	3±0.8[r]	11±0.21[cr]	1±0.76[cr]	0.01[r]	0.01[r]	84±0.30[r]	95±0.72[r]	32±0.7[r]	7±0.5[r]	0.48[r]	-245±0.9[r]
VI[phase6]	108-127[¥]	3±0.6[¥]	89±0.06[c¥]	74±0.55[c¥]	0.09[¥]	0.01[¥]	16±0.85[¥]	62±0.61[¥]	31±0.6[¥]	7±0.7[¥]	0.50[¥]	-394±0.1[¥]
VII[phase7]	128-150[r]	3±0.8[r]	1±0.38[r]	0.236[r]	0.001[r]	0.001[r]	88±0.41[r]	97±0.26[r]	30±0.5[r]	6±0.6[r]	0.24[r]	-394±0.1[r]

c = cumulative effluent after each phase at 17h HRT, s = shock load effect, r = recovery effect, ¥ = double shock load effect

The CSTR retrofit during this phase shows a better improvement by further reducing Cr(VI) effluent concentration from (5 ± 0.4 mg/L) to (0 mg/L) (Table 5.4). The reactor was also operated under airtight conditions similar to the previous phases, and at optimum HRT of 5 ± 0.5 h, pH of 7 ± 0.49, DO of 0.51 mg/L, temperature of 31 ± 0.5°C, and ORP of -140 ± 0.8 mV (Table 5.4). Under steady-state operating conditions, PFR with glass media was efficient in reducing Cr(VI) with a removal average or cumulative efficiency of 90 ± 0.13%, whereas a much better effluent performance was seen with near complete reduction of Cr(VI) in the CSTR retrofit with a removal average or cumulative efficiency of 100%. Cr(VI) breakthrough was observed in this phase (Phase III) when the influent Cr(VI) concentration was increased 50 mg/L in the presence of As(III) concentration of 85 mg/L after 68 days of continuous operation in both reactors under favourable conditions.

PHASE IV: After system breakthrough, the feed concentration was increased from 50 mg/L to 100 mg/L Cr(VI) concentration and 170 mg/L As(III) as electron source, to evaluate the performance of both reactors at a higher Cr(VI) loading, and the HRT was kept 12 h (Table 5.3). The PFR was operated from day 69 to 87 (Phase IV), and it responded to higher volumetric loading, which resulted in an increase in the effluent Cr(VI) concentration from 5 mg/L to 27 ± 0.6 mg/L (Figure 5.9). Because of this, 19% decrease in Cr(VI) removal efficiency was observed, given a removal efficiency of 71 ± 0.3%. An average pH of 7 ± 0.2, DO of 1 mg/L, ORP of -144 mV and temperature of 30 ± 0.8 was recorded during the steady-state condition (Table 5.3).

The CSTR retrofit during this phase shows a better improvement by further reducing Cr(VI) effluent concentration from 27 mg/L to 2.1 mg/L (Table 5.4). The reactor was also operated under airtight conditions similar to the previous phases, and at optimum HRT of 5 ± 0.4 h, pH of 7 ± 0.35, DO of 0.61 mg/L, temperature of 32 ± 0.7°C, and ORP of -191 ± 0.6 mV (Table 5.4). Under steady-state operating conditions, PFR with glass media was efficient in reducing Cr(VI) with a removal average or cumulative efficiency of 71 ± 0.3%, whereas a much better effluent performance was seen with near complete reduction of Cr(VI) in the CSTR retrofit, with a removal average or cumulative efficiency of 96 ± 0.98%.

PHASE V: After a high volumetric load rate was introduced, both reactors were checked for resilience (Phase V), and this was done by decreasing the feed Cr(VI) concentration from 100 mg/L to 40 mg/L, and 68 mg/L As(III) as electron source. The PFR system was operated at the HRT of 12 h from day 88 to 107, while maintaining other environmental conditions previously described. The PFR system showed a near recovery with effluent Cr(VI) concentration decreasing from 27 ± 0.6 mg/L to 11 ± 0.21 mg/L, with Cr(VI) removal efficiency of 72 ± 0.91% (Table 5.3). There was

slight improved effluent compared to the effluent concentration when the volumetric loading rate was previously increased. Slightly improved effluent after recovery could be attributed to a significant loss of biomass attached to the ceramic since there was no continuous cell recirculation prior to system recovery. The ORP of -192 ± 0.67 mV, DO concentration of 0.83 mg/L, however, was observed (Table 5.3), while the temperature of the reactor was maintained at 32 ± 0.7°C during this phase of operation.

Similarly, CSTR retrofit during this phase shows a better improvement by further reducing Cr(VI) effluent concentration from 2 ± 0.9 mg/L to 1 ± 0.76 mg/L (Table 5.4). The reactor was also operated under airtight conditions similar to the previous phases, and at optimum HRT of 5 ± 0.5 h, pH of 7 ± 0.5, DO of 0.48 mg/L and temperature of 31 ± 0.6°C, and ORP of -245 ± 0.1 mV (Table 5.4). Under steady-state operating conditions, PFR with ceramic media was efficient in reducing Cr(VI) with a removal average or cumulative efficiency of 72 ± 0.9%, whereas a much better effluent performance was seen in CSTR retrofit with near complete reduction of Cr(VI) and complete system recovery with a removal average or cumulative efficiency of 95 ± 0.72%. However, both reactors show system resilience to As(III) and Cr(VI) concentrations.

PHASE VI: After system recovery was observed in the previous phase, the reactor was operated under an influent Cr(VI) concentration of 200 mg/L and 340 mg/L As(III) as an electron source (Phase VI) after 2 h biomass circulation. The PFR system at this phase was operated at a HRT of 17h from day 108 to 127. This was done to test if the microbial activity in the reactor could be inhibited at much higher concentration. The effluent Cr(VI) concentration of the PFR system increased from 11 ± 0.21 mg/L to 89 ± 0.06 mg/L under this loading (Figure 5.9), before reaching a steady-state effluent concentration (Table 5.3). The result suggests that Cr(VI) reduction could be inhibited by the current load, as a result of dual toxic effect of As(III) and Cr(VI) microbial cell7, or it could be as a result of lower HRT. However, much higher contact time and optimum biomass recirculation could be required for optimum reduction of Cr(VI) using electrons from As(III). DO concentration in the reactor slightly increased from 0.82 mg/L to 0.92 mg/L, although still within the anaerobic condition range. The pH, ORP and temperature were recorded at 7 ± 0.4, -238 ± 0.7 mV and constant temperature of 31 ± 0.6, with the Cr(VI) removal efficiency of 55 ± 0.34% (Table 5.3). In addition, the Cr(VI) removal efficiency of the PFR system dropped significantly by 17%, which is closely related to the same percentage drop (19%) observed when the influent Cr(VI) and As(III) concentrations were increased to 100 mg/L and 170 mg/L, respectively. This suggests possible Cr(VI) and As(III) inhibition on the biological activities under high loading rates.

Similarly, the CSTR retrofit system during this phase shows a slight improvement by further reducing the PFR system Cr(VI) effluent concentration from 89 ± 0.06 mg/L to 74 ± 0.55 mg/L (Table 5.3). However, only 15 mg/L of Cr(VI) concentration was further reduced after an additional 5 h HRT in a complete mixed reactor, thus suggesting an inhibition effect on the microbial activities. The CSTR system was also operated under airtight conditions similar to the previous phases, pH of 7 ± 0.7, DO of 0.5 mg/L, constant temperature of 30 ± 0.5°C, and ORP of -394 ± 0.1 mV (Table 5.4). Under steady-state operating conditions, the removal efficiency of PFR with ceramic bead media dropped from of $72 \pm 0.9\%$ to $55 \pm 0.34\%$, whereas a slight effluent performance was seen in the CSTR retrofit system with a Cr(VI) removal average or cumulative efficiency of $62 \pm 0.61\%$. However, the efficiency at this phase is much lower when compared to efficiency in previous phases. The observed low Cr(VI) removal efficiency at higher feed concentrations is attributed to dual toxic effects of both compounds, limiting the viability of the process at high loading rates.

PHASE VII: After high volumetric load rate was re-introduced, both reactors were also checked again for the resilience and system recovery (Phase VII), and this was done by decreasing the feed Cr(VI) and concentration from 200 mg/L to 30 mg/L, and 51 mg/L As(III) as electron source. The PFR system was operated at the same HRT of 12 h from day 128 to 150, while maintaining other environmental conditions previously described. The PFR system showed complete system recovery with an effluent Cr(VI) concentration decreasing from 89 ± 0.06 mg/L to 1 ± 0.38 mg/L (Figure 5.9), with Cr(VI) removal efficiency of $96 \pm 0.31\%$ (Table 5.3). There was a much-improved effluent compared to the effluent concentration when the volumetric loading was previously increased. The ORP of -264 ± 0.7 mV was recorded and DO of 0.99 mg/L indicated more positive anaerobic environment, while temperature and pH of the reactor were maintained at 30 ± 0.5°C and 6 ± 0.4 during this phase of operation (Table 5.4).

In addition, there was not much difference in the performance of the CSTR retrofit to the PFR system during this phase. This was because the attached growth shows a system robust when the influent Cr(VI) concentration was increased to 30 mg/L with 51 mg/L As(III) as an electron source, suggesting that microbial growth activity was enhanced at this phase of operation or biomass increases as Cr(VI) concentration increases. The CSTR retrofit system achieved Cr(VI) effluent concentration of 0.24 mg/L at 5 ± 05 h, pH of 6 ± 0.6, DO of 0.24 mg/L and temperature of 30 ± 0.5°C, and much lower ORP of -394 ± 0.1 mV when compares to other phases (Table 5.4)

5.4.2 System response at shock load

The effect of system shock load was observed in the ceramic bead immobilised and stir tank mobilised reactors (R3 and R4). Figure 5.8 illustrates the system shock load at 100 mg/L and 170 mg/L As(III), and 200 mg/L Cr(VI) and 340 mg/L As(III), respectively. The data obtained depict the pattern of system response to the increased influent Cr(VI) and As(III) concentrations. Effluent Cr(VI) concentration began to increase soon after Cr(VI) and As(III) influent concentration was increased.

This trend was observed whenever the influent Cr(VI) and As(III) concentration was increased to a higher value in all phases. As(III) utilization preceded Cr(VI) reduction as the system adjusted to the new loading conditions. This trend suggests that higher metabolic activity in the bioreactor may result in higher rate of Cr(VI) reduction. This was characterized by an increase in effluent Cr(VI) concentration at lower removal efficiency of $71 \pm 0.3\%$ and $55 \pm 0.4\%$ at 100 mg/L and 200 mg/L in R3, and $62 \pm 0.61\%$ was seen at 200 mg/L in R4. The elevated Cr(VI) concentration in the effluent indicated that biological activity could be inhibited by dual toxic effect of Cr(VI) and As(III) or there is not sufficient HRT for the reaction to complete.

However, Cr(VI) reduction in both reactors was recovered completely when the influent Cr(VI) concentration was reduced from 100 to 40 mg/L or 200 to 30 mg/L at As(III) concentration from 170 to 68 mg/L or 340 to 51 mg/L in phases V and VII, with Cr(VI) removal efficiency increasing from 71% to 72% at 100 mg/L and 55% to 96% at 200 mg/L in reactor 3, while in reactor 4 Cr(VI) removal efficiency increased from 65% to 96% at 200 mg/L. However, biological activity recovered is evident due to a rapid decrease in Cr(VI) concentration in this phase.

Cr(VI) reduction in the presence of As(III) was also affected by the hydraulic detention time at 4 h, 5 h and 12 h. Theoretically, the redox process between Cr(VI) and As(III) could be categorized into two steps. The first step involves a microbial-induced process, which involves catalytic reduction of Cr(VI) to Cr(V). The second steps involve a chemical reaction between Cr(V) and As(III), which requires high contact time for the reaction to complete, suggesting the need for anaerobic tank retrofit (R4). The effluent from R4 has better reduction efficiency because of an additional retention time of 4 ± 0.6 h. The overall performance of the system was extremely good with the addition of the anaerobic tank retrofit. It was seen that at steady-state condition, Cr(VI) removal efficiencies at 5 h were < 50%, while > 90% was achieved at 12 h.

5.4.3 Impact of environmental factors

The impact of environmental factors such as ORP, pH, dissolved oxygen (DO) concentration and temperature was also observed during both reactors' (R3 and R4) operational run (Figure 5.9a-b and 5.10 a-b). This was important to evaluate the required optimum condition for feasible redox conversion of Cr(VI) and As(III) in the reactors. Second, it will determine the optimum condition for the microbial population growth.

Varying values of DO, pH, and ORP obtained did not differ significantly between different operating conditions, and it is varying from 0.532-1.3 mg/L, 6.32-7.4 and -390--6.2 mV for R3 (Figure 5.9 a-b), and 0.06-0.8 mg/L, 6.53 to 7.5 and -350--10 mV for R4 (Figure 5.11) a-b. Typical optimum values of DO, pH, and ORP were seen at 0.82 mg/L, 7.1 and -156 mV for 'R 3'and 0.46 mg/L, 7.3 and -195 mV for 'R4'.

Anaerobic conditions were observed in both reactors (R3 and R4) (Figure 5.9 a and 5.10b), except in Phase IV in reactor 1, where the DO level was slightly above 1.03 mg/L. The discrepancy observed might occur because of experimental errors at the point of sampling, or as a result of changes in consortium composition under different Cr(VI) and As(III) loading.

There was no significant change in the pH of the reactors (Figure 5.9 b and 5.10 b), except in Phase VII where the pH of both reactors dropped to 6.4. However, the overall pH condition of both reactors was recorded at 7.2, and this corresponds with the observation made from the batch experiment, where optimum Cr(VI) reduction and As(III) oxidation occur at neutral pH conditions. This suggests that Cr(VI) removal and As(III) was optimum at neutral pH.

Second, overall ORP was seen at the average of -156 mV for 'Reactor 1' (Figure 5.9 b) and -195 mV for 'Reactor 2' (Figure 5.10 b). This however depicts oxidation-reduction potential or strength in both reactors throughout the operational phases (I-VII) with corresponding variation in the pH of the reactor. A constant temperature was observed in both reactors throughout the operational phases (I-VII). The reactor optimum temperature was recorded at the average temperature of 32.8°C at minimum and maximum values recorded at 25°C and 34.5°C (Figure 5.9 b and 5.10 b). This
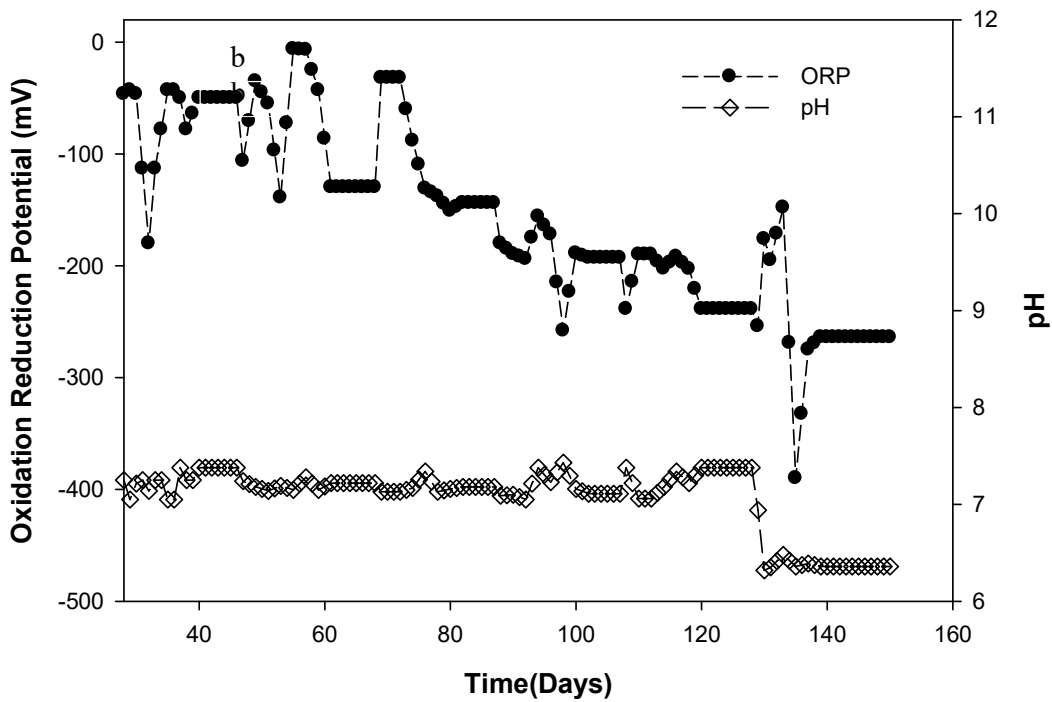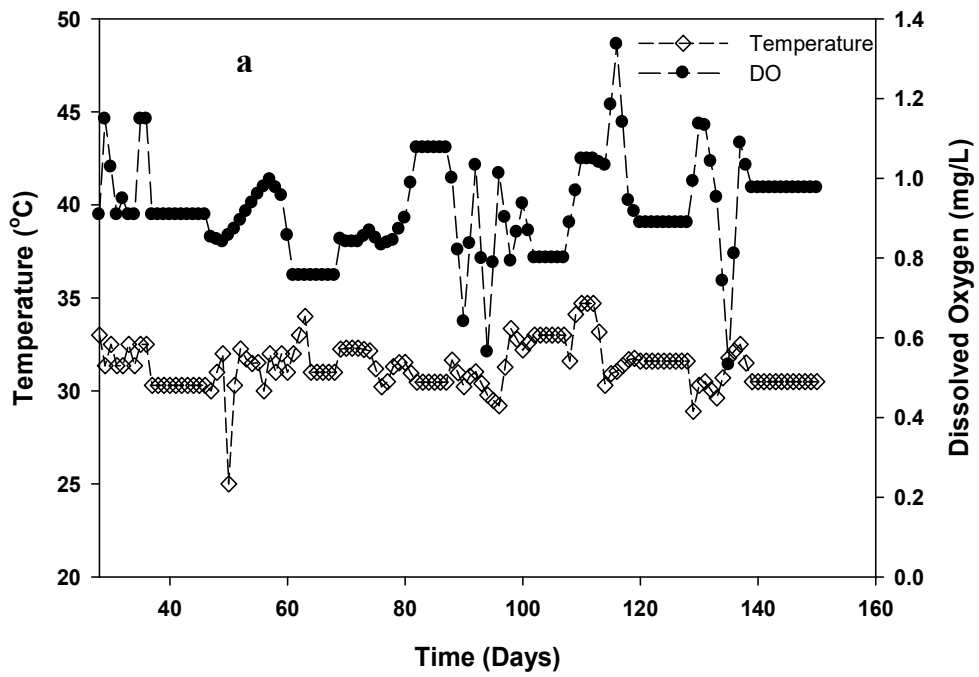
Figure 5.9: Ceramic bead packing PFR (Reactor 3) physical parameter (a) Temperature (°C) and dissolved oxygen (mg/L); (b) ORP (mV) versus pH
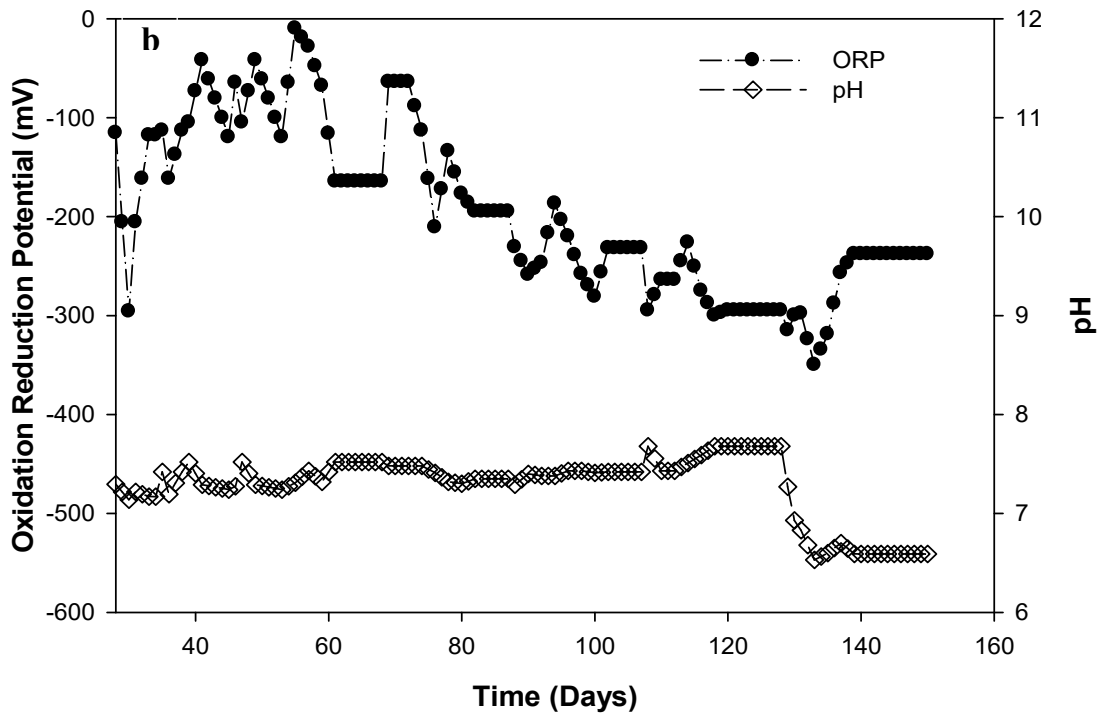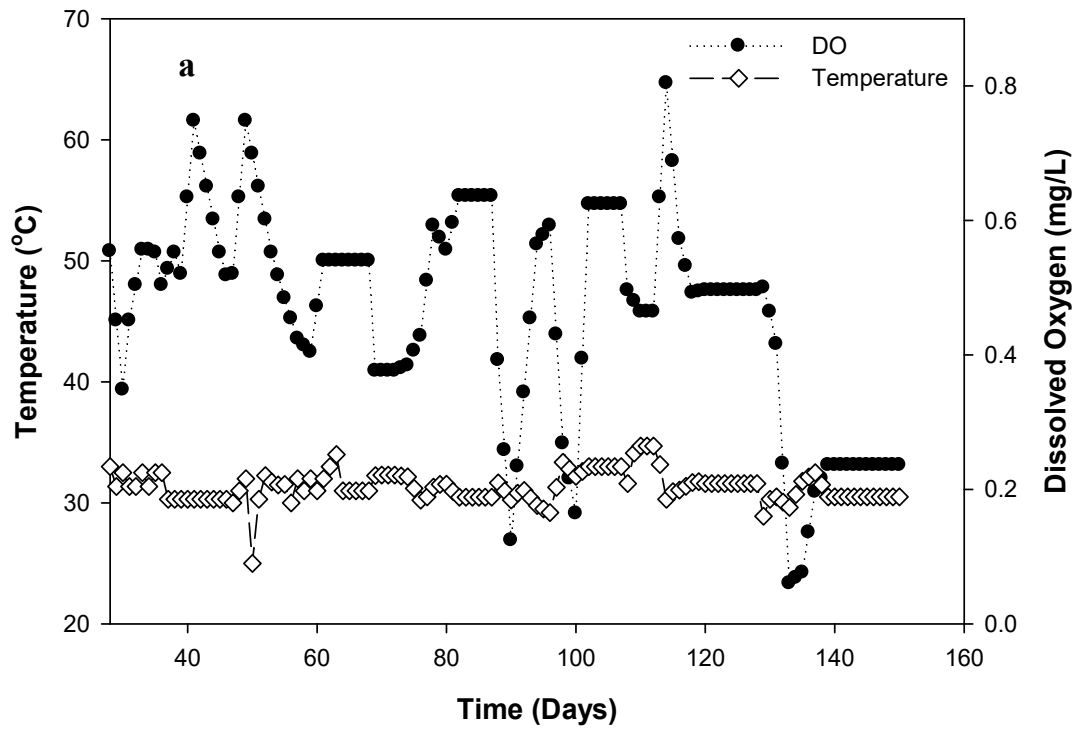
Figure 5.10: CSTR (Reactor 4) physical parameter (a) Temperature (^{o}C) and dissolved oxygen (mg/L); (b) ORP (mV) versus pH

indicates the required optimum temperature for microbial growth and metabolism, as reported previously.

5.4.4 Mass transport along the longitudinal column

Cr(VI) reduction efficiency across the longitudinal reactor column was evaluated at different Cr(VI) concentrations of 30-200 mg/L, 40 mg/L (recovery) and As(III) concentration in the mole ratio of 1.7:1. It is expected that Cr(VI) and As(III) mass concentration concurrently travels across the reactor column of 70 cm; there could be a possible drop in the concentration as the Cr(VI) reduction rate increases along the column. The results clearly indicated that Cr(VI) reduction increases significantly over distance travelled across the column. Effluent at various sampling ports (H$_1$–H$_4$) at equal space distance ($x = 20$-60 cm) indicated lower Cr(VI) concentration at all phases of operation (I-VII), which correlates with a significant increase in Cr(VI)-reducing efficiency (Figure 5.11).

For instance, in Phase I at influent Cr(VI) and As(III) concentration of 40 mg/L and 68 mg/L, Cr(VI) reducing efficiency increases across the column from 20-60 cm (Figure 5.12). A similar trend was observed when the influent Cr(VI) and As(III) concentration was increased. A further increase in Cr(VI)ˉreducing efficiency was seen when influent Cr(VI) and As(III) concentration was increased to 50 mg//L and 85 mg//L, where Cr(VI) removal efficiency increased from 84-90%, along the reactor column at distance x from 20-60 cm.

The effect of shock load along the reactor column was investigated and this was evaluated by increasing the influent Cr(VI) and As(III) concentration from 50 mg//L and 85 mg/L to 100 mg/L and 170 mg//L or 200 mg/L and 340 mg//L (Figure 5.13). When the reactor load was increased to 200 mg/L Cr(VI) concentration and 340 mg//L As(III) concentration, this resulted in a very significant decrease in Cr(VI) reduction efficiency across the longitudinal column, but increases from (H$_1$–H$_4$). For instance, at reactor distance ($x = 20$-60 cm), Cr(VI)-reducing efficiency increased from 32-46% (Figure 5.13).

These suggest that Cr(VI) concentration reduces along the column, which is as a result of electron mass between Cr(VI) and As(III) across the column. However, the reduction of Cr(VI) across a
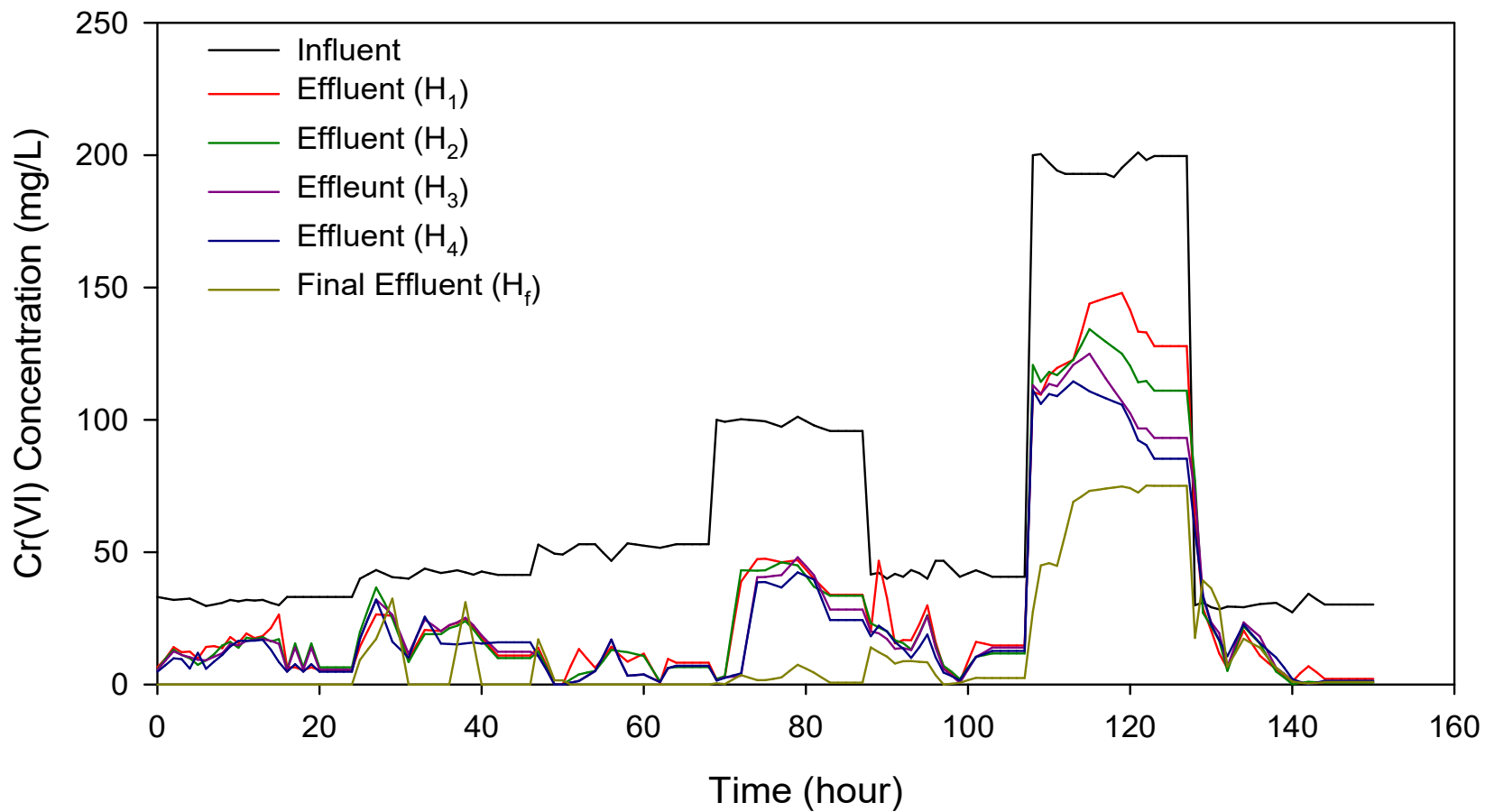
Figure 5.11: Cr(VI) removal along the ceramic packed PFR column (Reactor 3) (distance $\{x\}$ = 70 cm) at Cr(VI) concentration of 30 -200 mg/L of with proportional As(III) concentration of 51-340 mg/L
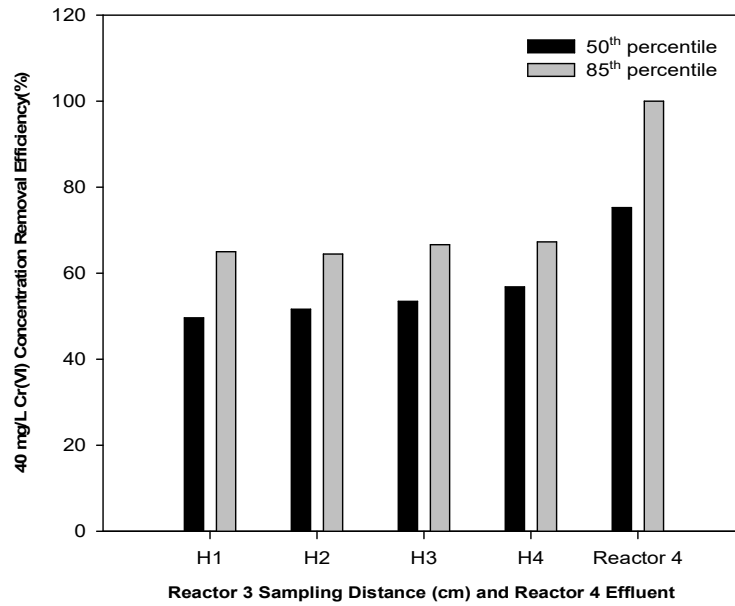
Figure 5.12: Cr(VI) removal along the longitudinal column (distance $\{x\} = 70$ cm); 40 mg/L

of

Cr(VI) and 68 mg As(III)/L concentration
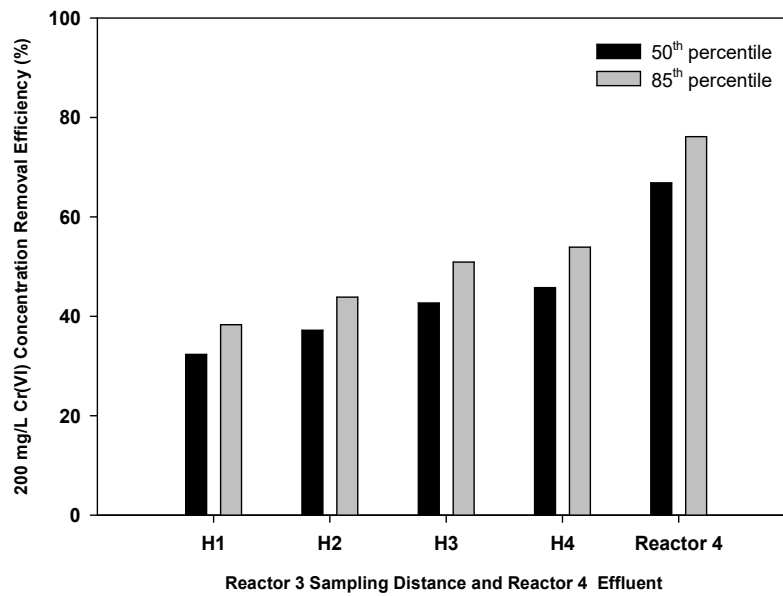
Figure 5.13: Cr(VI) removal along the longitudinal column (distance $\{x\} = 70$ cm) 200 mg/L
Cr(VI) and 340 mg/L As(III) concentration

vertical longitudinal reactor column is directly proportional to height of the reactor, and inhibitory effect observed at high Cr(VI) and As(III) load was attributed to loss of cell-reducing capacity.

5.5 Glass bead versus ceramic bead packed bed reactor

The comparative performance of a glass bead packed bed reactor and a ceramic bead packed bed reactor was evaluated based on the cumulative Cr(VI) removal efficiency (Figure 5.14). The result indicated that both reactors (glass bead or ceramic packed bed) achieved significant removal of Cr(VI), however, the effectiveness of removal decreased with an increase in porosity. The glass bead packed bed reactor has a smaller total surface area than the ceramic bead packed bed reactor, and as a result achieved higher Cr(VI) removal efficiency up to 79% even though it has a smaller surface area when compared to the ceramic bead packed bed reactor, with removal efficiency of 75%.

It was initially anticipated that the reactor with a larger surface area would have better performance, but the result stated otherwise, although there is insignificant difference between the efficiency of both reactors. The breakthrough characteristic of a column is typically packed bed reactor with moderate dispersion depicting an exponential rise to a maximum followed by reduction in effluent as the Cr(VI) cultures become established (Molokwane & Chirwa, 2009). It was seen that both reactors (glass or ceramic bead packed bed) did not reach system failure; rather it shows self-sustaining behaviour, indicating a steady increase in Cr(VI) removal.

The precipitate generated from the reactors were recovered after each experimental run, and the recovery process follows sedimentation, flocculation ($FeCL_2$) in a mixing tank and filtration (Figure 3.4 and 3.5). The percentage precipitate recovered increased as influent Cr(VI) and As(III) concentration increased with a clear effluent (Figure 5.15). Precipitate was recovered in the system for possible reuse, and this ensured that the precipitate was economically viable. However, the treatment involves biological reduction of toxic Cr(VI) to less toxic Cr(III), which precipitates in the form of hydroxides, oxides, and sulphates (Nickens et al., 2010; Chirwa & Molokwane 2011), and could be used for agricultural purposes.
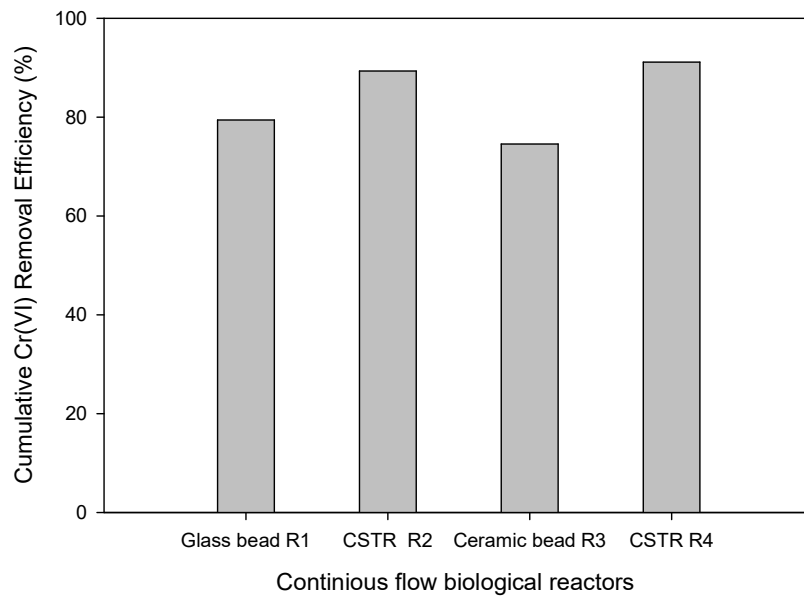
Figure 5.14: Cumulative Cr(VI) removal efficiency of R1, R2, R3, and R4
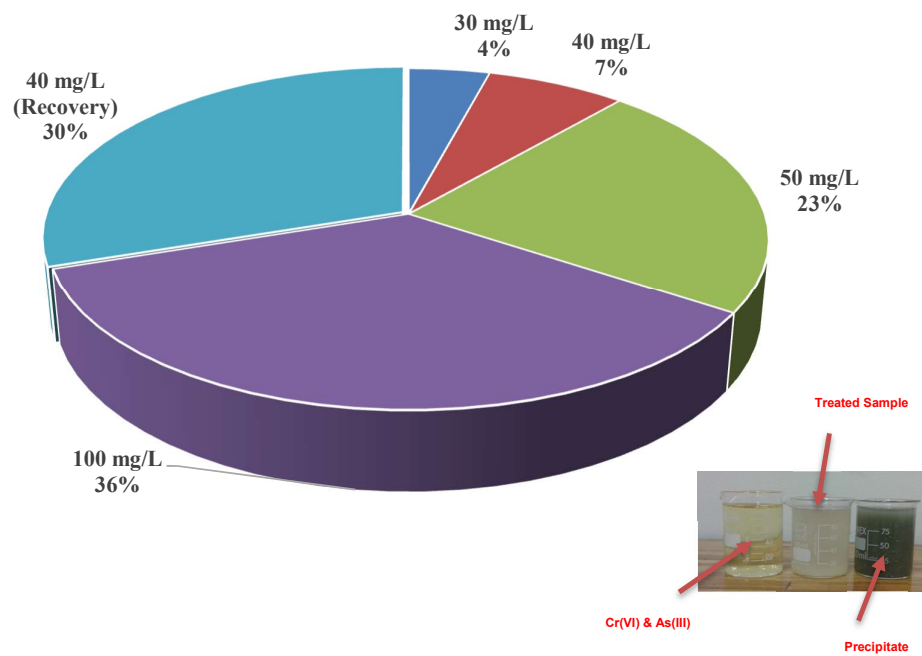
Figure 5.15: Percentage sludge recovery at different Cr(VI) load concentration

Biofilm Kinetic Model

6.1   Derivation from Basic Principles

6.1.1 Model description

Biokinetic data achieved in this experiment were estimated using an enzyme-based model. The model was initially developed by integrating enzyme kinetics and Cr(VI) reduction capacity to validate toxic effect of Cr(VI). The reduction capacity designates the maximum amount of Cr(VI) that a batch culture can reduce, and the loss of Cr(VI) reduction capacity in the bacterial cultures may be associated with toxic effects of Cr(VI). This model was formerly used to describe Cr(VI) reduction in *E. coli ATCC* 333456, *Bacillus sp.*, and consortium culture from Brits WWTP (Mtimuye, 2011; Molokwane et al., 2008; Chirwa & Wang, 2004; Wang & Sheng, 1997). In the contemporary study, optimum values of biokinetic parameters were estimated using a computer programme for simulation of the Aquatic System "*AQUASIM 2.0*" using a Levenberg–Marquardt Algorithm [Damped Least-Squares (DLS)] method in Sigma Plot v. 11 (Systat Software, Inc., San Jose, CA).

6.1.2 Model development

Cr(VI) reduction and As(III) oxidation are facilitated by enzymes in the microbial cell membrane, and these enzymes reduce Cr(VI) or oxidized As(III) while achieving other physiological functions (Viamajala 2003, Anderson et al., 2001; Heinrich-Salmeron et al., 2011). Model equation was predicted based on a Monod equation similar to the Michaelis-Menten equation, where enzyme activity is the driving force for the redox process (Shen & Wang, 1997). Michaelis-Menten was previously used to describe As(III) oxidation in a batch

culture of *Thiomonas arsenivorans* strains b6 (Dastida & Wang, 2010), and *Alcaligenes Faecal* strains 01201 (Suttigarn & Wang, 2005).

However, the activities of theses enzymes having a net effect can be represented by a complex enzyme E_T (Shen & Wang, 1994b). The Cr(VI) reduction rate kinetics were previously derived by Shen and Wang (1994) and were further improved by Molokwane (2008) based on the following assumptions:

- That Cr(VI) reduction is catalysed by a single or dual-site enzyme.
- That the enzyme is either regulated or induced, i.e. is produced when the cell is exposed to Cr(VI).
- That the Cr(VI) reduction sites on the enzyme are non-renewable, such that new enzymes are required to be produced to reduce new load or continue reducing Cr(VI).
- In the mixed culture, it is assumed that several Cr(VI)-reducing species of bacteria exist. However, the Cr(VI)-reducing activity of the whole culture may be represented by a common effect – the sum of or the highest of all the activities in all the Cr(VI)-reducing species.
- The sum of or the highest of the activities, $\sum E_i$ may be represented by one representative enzyme, E.

By first principles, a Cr(VI) enzymatic mathematical expression is described as follows:

$$Cr(VI) + En \underset{k_b}{\overset{k_a}{\rightleftharpoons}} E*Cr(III) \tag{6.1}$$

$$E*Cr(III) \xrightarrow{k_c} E + Cr(III) \tag{6.2}$$

Similarly, an As(VI) enzymatic mathematical expression can be represented as:

$$As(III) + E \underset{k_e}{\overset{k_d}{\rightleftharpoons}} E*As(V) \tag{6.3}$$

$$E^*As(V) \quad \overrightarrow{k_f} \quad E + As(V) \tag{6.4}$$

Let C represent Cr(VI) concentration and As(VI) concentration

Where: E_n = Enzyme, E_n^* Cr(VI) = Enzyme Cr(VI) complex, k_a = rate constant for forward reaction, k_b = rate constant for the reverse reaction, k_c = rate constant for the third reaction.

Therefore, the enzyme rate equation from reaction 6.1 and 6.2 is expressed as follows:

$$\frac{dE_n}{dt} = k_a C E_{nT} \tag{6.5}$$

$$\frac{dE_n^*}{dt} = k_a C E_n^* \tag{6.6}$$

Therefore,

$$\frac{dE_n^*}{dt} = \frac{dC}{dt} = k_c E_n^* \tag{6.7}$$

Combining Equation 6.5, 5.4 and 6.7, gives the rate of E^* formation represented as:

$$\frac{dE_n^*}{dt} = k_a C(E_{nT}) - k_b\left(E_n^*\right) - k_c\left(E_n^*\right) \tag{6.8}$$

$$E_T = E - E^* \tag{6.9}$$

Where:

E_n^* = total complex and uncomplex enzyme

Combining Equation 6.8 and 6.9 to have:

$$\frac{dE_n^*}{dt} = k_a C\left(E_n - E_n^*\right) - k_b\left(E_n^*\right) - k_c\left(E_n^*\right) \tag{6.10}$$

123

At steady-state condition, enzyme rate formation $\left(\dfrac{dE_n^*}{dt}=0\right)$ approaches zero, Equation 6.10 become;

$$k_a C(E_n - E_n^*) - k_b(E_n^*) - k_c(E_n^*) = 0 \qquad (6.11)$$

Solving for E_n^*:

$$k_a C(E_n - E_n^*) = k_b(E_n^*) + k_c(E_n^*)$$

$$k_a CE_n - k_a CE_n^* = k_b(E_n^*) + k_c(E_n^*)$$

$$k_a CE_n = k_a CE_n^* + k_b(E_n^*) + k_c(E_n^*)$$

$$k_a CE = (k_a C + k_b + k_c)E_n^*$$

$\therefore$ '$E*$' can be simplified as; $E_n^* = \left(\dfrac{k_a CE_n}{k_a C + k_b + Ck_c}\right)$

$$E^* = \left(\dfrac{CE_n}{C + \left(\dfrac{k_b + k_c}{k_a}\right)}\right) \qquad (6.12)$$

From Equation 6.12, the rate of Cr(VI) reduction was predicted, and represented as

$$-\frac{dC}{dt} = \left(\dfrac{CE_n}{C + \left(\dfrac{k_b + k_c}{k_a}\right)}\right) \qquad (6.13)$$

Comparing Equation 6.13 and 6.14:

$$-\frac{dC}{dt} = \left(\frac{k_{mc}C}{C+K}\right)X \qquad \text{(Monod equation)} \qquad (6.14)$$

Where: k_d is equivalent to k_{mc} = maximum specific Cr(VI) reduction rate (mg/L/h); E is equivalent to X = biomass concentration (mg/L): $\left(\frac{k_b + k_e}{k_a}\right)$ is equivalent to K (mg/L).

From Equation 6.14 it could be seen that the rate and the extent of Cr(VI) reduction in a bacterial system is proportional to the number of cells X in the system and the capacity of reduction.

$\therefore$, Total Biomass Concentration X can be represented as:

$$X = X_o - \left(\frac{C_o - C}{K_{\_c}}\right) \qquad (6.15)$$

Where: C_o = initial Cr(VI) concentration (mg. /L); X_o = initial biomass concentration (mg/L); C = Cr(VI) concentration at a time 't' (mg/L); and $K_{\_c}$ = maximum Cr(VI) reducing capacity (mg /mg).

Combining Equation 6.13 and 6.15, generate the non-inhibition model equation for Cr(VI) reduction:

$$-\frac{dC}{dt} = \frac{k_{\_mc}C}{C+K}\left(X_o - \left(\frac{C_o - C}{K_{\_c}}\right)\right) \qquad (6.16)$$

Where: k_{mc} = maximum specific Cr(VI) reduction rate (mg/L/hr); C_{ro} = initial Cr(VI) concentration (mg/L); X_o = initial biomass concentration (mg/L); C_r = Cr(VI) concentration at a time 't' (mg/L); $K_{\_c}$ = maximum Cr(VI) reducing capacity (mg/mg); and K = half velocity concentration (mg/L).

The final derived equation for enzymatic Cr(VI) reduction in the absence of reaction inhibition and cell deactivation terms by modification of Equation 6.16 is:

$$r = \frac{-d(C)}{dt} = \frac{k_m \cdot C \cdot X}{C + K_c} \tag{6.17}$$

where C = Cr(VI) concentration at time t (mg/L/h), k_{mc} = maximum specific Cr(VI) reduction rate coefficient (mg/L/h), K_c = half velocity constant (mg/L), and X = concentration of viable cells (mg/L) at any time t (h).

Similar expressions were derived previously by other researchers for Cr(VI) reduction in batch systems (Shen & Wang, 1994; Mazierski, 1995; Schmieman et al., 1998; Guha et al., 2001; Li et al., 2006). If the active enzyme expires after use in the Cr(VI) reduction process, then the deactivation of cell cellular activity is directly proportional to Cr(VI) reduced, which results in the modification of Equation 6.17 as follows:

$$-\frac{dC}{dt} = \frac{k_{mc}C}{(K_c + C)}\left(X_o - \frac{C_o - C}{R_c}\right) \tag{6.18}$$

where, k_{mc} = maximum specific Cr(VI) reduction rate (mg/L/h); C_o = initial Cr(VI) concentration (mg/L); X_o = initial biomass concentration (mg/L); C = Cr(VI) concentration (mg/L) at a time 't'; Rc = maximum Cr(VI) reducing capacity (mg/mg); Kc = half velocity concentration (mg/L).

Similar reasoning was applied to the As(III) oxidation process, such that the assumption is made that the As(III) oxidation will be similar in principle to Cr(VI) reduction kinetics. The only difference being that As(III) oxidation is more closely tied to the biomass growth rate than Cr(VI) reduction, as shown earlier in Figure 4.12b. In addition, if the active enzyme expires after use in the As(III) oxidation process, then the deactivation of cell activity is directly proportional to As(III) oxidised, which results in the modification of Equation 6.17 as follows:

$$-\frac{dS}{dt} = \frac{k_{mS}S}{(K_s + S)}\left(X_o - \frac{S_o - S}{R_s}\right) \tag{6.19}$$

where, k_{ms} = maximum specific As(III) oxidation rate (mg/L/h); S_o = initial As(III) concentration (mg/L); S_o = initial biomass concentration (mg/L); S = As(III) concentration

(mg/L) at a time '*t*'; Rs = maximum As(III) reducing capacity (mg/mg); Ks = half velocity concentration (mg/L)

Simulation will be performed for best fit of the equation versus time curves to estimate the biokinetic parameter values k_{mc}, k_{ms}, K_c, K_s, R_c and R_s and previous values of these obtained in concurrent batch studies of Cr(VI) reduction and phenol degradation, and As (III) oxidation by strain b6 is described in Table 6.1. In addition, kinetic parameters of these values were first estimated with initial guessed values, followed by simulation and optimization. Upper and lower constraints were set for each parameter to the exclusion of invalid parameter values. Whenever optimization converged or was very close to the constraint, the constraint was relaxed until it did not force the model. The procedure was repeated until unique values lying away from the constraint but between set limits were found for each parameter (Chirwa & Wang, 2004).

Table 6.1 Initial parameters (modified by Chirwa and Wang, 2005)

Parameter	Definition	Initial values	Units	Reference
K_{mc}	Maximum specific Cr(VI) reduction rate coefficient	0.0042	L/h	Shen & Wang (1995a)
K_c	Half-velocity Cr (VI) concentration	12	mg/L	Shen & Wang (1995a)
R_c	Cr (VI) reduction capacity	0.05	mg/mg	Shen & Wang (1995a)
K_{mp}	Maximum specific phenol reduction rate coefficient	0.035	L/h	Shen & Wang (1995a)
K_p	Half-velocity phenol concentration	940	mg/L	Shen & Wang (1995a)
K_{mc}	Maximum specific Cr(VI) reduction rate coefficient	0.6411	L/h	Igboamalu & Chirwa, (2014)
K_c	Half-velocity Cr (VI) concentration	732.3	mg/L	Igboamalu & Chirwa, (2014)
R_c	Cr (VI) reduction capacity	0.986	mg/mg	Igboamalu & Chirwa, (2014)
K_{ms}	Maximum specific As(III) reduction rate coefficient	0.85	L/h	Dastida & Wang 2010
K_s	Half-velocity As(III) concentration	33.2	mg/L	Dastida & Wang 2010

6.1.3 Simulation analysis

Data simulation with Aquasim uses the DASSL algorithm, which is based on the implicit (backward differencing) variable-step, variable-order Gear integration technique (Petzold, 1983; Gear, 1971; Reichart, 1998). This technique makes use of a numerically integrating system of ordinary and partial deferential equations in time and simultaneously solves the algebraic equations. Spatial discretization of partial deferential equations is done using conservative finite deference schemes (Le Veque, 1990, Reichart, 1998). From differential conservation law, the equation below was derived and developed in Aquasim. Also, the implementation of the DASSL algorithm allows the use of full or branded Jacobian matrix Equation 6.22, in solving the nonlinear system of algebraic equation (Reichart, 1998).

$$\frac{\partial \rho}{dt} = \frac{\partial j}{\partial z} + r \tag{6.20}$$

Equation 6.20 is discretised as 6.21

$$\frac{d}{dt} \rho(x_i, t) = \frac{j_{num}(x_{i+0.5}, t) - j_{num}(x_{i-0.5}, t)}{x_{i+0.5} - x_{i-0.5}} + r(x_i, t) \tag{6.21}$$

$$\underline{\underline{J}} = \frac{\partial F}{\partial y} \tag{6.22}$$

$$\underline{\underline{J}} = \begin{bmatrix} \frac{\partial f_1}{\partial x_1} \cdots \frac{\partial f_1}{dy} \\ \frac{\partial f_2}{\partial x_2} \cdots \frac{df_2}{dy} \end{bmatrix} \tag{6.23}$$

6.1.4   Parameter estimation

Aquasim estimate model parameters are represented by constant variables by minimizing equation 6.24 with the constraints $(\lambda_{min,i} \leq \lambda_i \leq \lambda_{max,i})$ (Reichart, 1998). This equation is described as the sum of the squares of the weighted deviations between measurements and calculated model results (Reichart, 1998). The minimization of equation 6.22 uses simplex algorithm or secant algorithm (Nelder & Mead, 1965; Ralston & Jennrich, 1978; Reichart, 1998).

$$x^2(\lambda) = \sum_{i=1}^{n} \left[\frac{U_{meas,i} - U_i(\lambda)}{\alpha_{meas,i}} \right]^2 \tag{6.24}$$

where: $U_{meas,i}$ = i-th measurement, $\alpha_{meas,i}$ = standard deviation, $U_i(\lambda)$ = calculated value of the model variable corresponding to the i-th measurement and evaluated at the time and location of this measurement, $\lambda = (\lambda_i,..,\lambda_m)$ = model parameters, $\lambda_{miin,i}, \lambda_{max,i}$ = minimum and maximum constant variable representing λ_i, n = number of points and x^2 = the sum of the deviation for all the fit targets.

6.1.5 Sensitivity analysis of the estimated parameters

Sensitivity analysis in Aquasim is solved by combined identifiability analysis and uncertainty analysis (Reichart, 1998). The aim of identifiability analysis with AQUASIM is to determine if the model parameters can be uniquely determined with the aid of available data and to estimate the uncertainty of the parameter estimates. This is done by estimating the standard error and correlation coefficient of the parameters during parameter estimation (Reichart, 1998). Equations 6.25 – 6.28 are distinguished by AQUASIM. Uncertainty analysis, on the other hand, is propagated to the uncertainty of model results (Reichart, 1998). Aquasim implemented the simplest error propagation method and the linearized propagation of standard deviations of neglecting the parameter correlation is given in Equation 6.40 (Reichart, 1998).

$$\delta_{y,\lambda}^{a,a} = \frac{\partial y}{\partial \lambda} \tag{6.25}$$

$$\delta^{r,a}_{y,\lambda} = \frac{1}{y}\frac{\partial y}{\partial \lambda} \tag{6.26}$$

$$\delta^{a,r}_{y,\lambda} = p\frac{\partial y}{\partial \lambda} \tag{6.27}$$

$$\delta^{r,r}_{y,\lambda} = \frac{p}{y}\frac{\partial y}{\partial \lambda} \tag{6.28}$$

Where:

y = arbitrary variable calculated by Aquasim, and λ= model parameter by a constant.

$$\delta_{y} = \sqrt{\sum_{i=1}^{m}\left(\frac{\partial y}{\partial \lambda_{i}}\right)^{2}\delta^{2}_{\lambda_{i}}} \tag{6.30}$$

where: λ_i= uncertainty model parameter, δ_i= standard deviations, $y(\lambda_i,...,\lambda_m)$= solution of the model equations for a given variable at a given location and time, δ_y = approximate standard deviation of the model result. The error contribution of each parameter is given as;

$$\delta^{err}_{y\lambda} = \frac{\partial y}{\partial \lambda}\delta_{\lambda} \tag{6.31}$$

Aquasim calculate equation 6.25 – 6.28, 6.30 and 6.31 by using the derivatives as follows:

$$\frac{\partial y}{\partial \lambda_{i}} \approx \frac{y(\lambda_{i} + \Delta\lambda_{i}) - y(\lambda_{i})}{\Delta\lambda_{i}}$$

Where: $\Delta\lambda_i$= 1% of the standard deviation δ_{λ_i}, of the parameter λ_i.

6.2   Model application to experimental results

6.2.1 Cr(VI) and As(III) redox simulation

During the current experimental observations, the batch data obtained was evaluated against Equation 6.18 and 6.19. After data fitting to the model using a Levenberg–Marquardt Algorithm [Damped Least-Squares (DLS)] method in SigmaPlot v. 11 (Systat Software, Inc., San Jose, CA), parameters were re-estimated with successfully convergence criteria met after 26 iteration and 51 simulation steps, the following preliminary kinetic results were obtained: $K_{mc} = 0.0009$ mg/L/h , $K_{ms} = 0.0006$ mg/L/h, $K_c = 986$ mg/mg, $K_s = 979$ mg/mg, $R_c = 0.013$ mg/Cr(VI) mg , $R_s = 0.0002$ mg/As(III) mg and $Xo = 120$ mg/L for the 80 mg/L and 70 mg/L initial As(III) and Cr(VI) concentration (Figure 6.1a).

Lower X^2; sum of the squares of the weighted deviations between measurements and calculated model results of 321 for Cr(VI) and 293 for As(III) with total of 613 was attained. The technique of estimation involved varying the trial (or initial estimates) of the parameters along with preliminary biomass concentration independently to attain the best fit simulation for the observed data (Dastida & Wang, 2010). However, further recalculation of the parameter does not improve this result. Good fits between model simulation and experimental data were noted for all data sets with initial As(III) and Cr(VI) concentration of 80-300 mg/L and 70 mg/L, respectively (Figure 6.1b and 6.2 a-b). The best fit parameters were used to simulate As(III) and Cr(VI) concentration of 100-300 mg/L and 70 mg/L.

Reduction or oxidation capacity R_c or R_s is inversely proportional to Cr(VI) and As(III) concentration per time and initial biomass concentration, as described in Equation 6.18 and 6.19. It is expected that as concentration of Cr(VI) and As(III) increases, reduction capacity will decrease. It was indeed evident that the reduction capacity is directly proportional to initial Cr(VI) and As(III) concentration. This implies that as R_c or R_s increases with an increase in Cr(VI) and As(III) concentration (Molokwane et al., 2008). A similar trend was observed in our model with simultaneous Cr(VI) reduction and As(III) oxidation. In this model, R_c or R_s increases as concentration significantly increases from 80-300 mg/L. The best fit preliminary parameter ($R_c = 0.0134$ mg/mg) obtained in the study was lower than ($R_c = 0.13$ mg/mg), reported by Shen and Wang (1995a), with an *E-coli* strain for concurrent Cr(VI) reduction and phenol degradation, although this value is with the constraint range reported in the same study

(Table 6.1). In a previous study by Igboamalu and Chirwa (2014) a high (R_c = 0.99 mg/mg) was reported, and this may be due to different types of microorganisms isolated for Cr(VI) and As(III) oxidation.

Maximum specific reduction rate K_{mc} and K_{ms} is directly proportional to Cr(VI) and As(III) concentration per time and initial biomass concentration, as described in Equation 6.18 and 6.19. The preliminary best fit of (K_{mc} = 0.0009 mg/L/h and K_{ms}= 0.0006) in the study was lower than K_{mc} (0.0042 mg/L/h) reported by Shen and Wang (1995a) with *E-coli* strain for concurrent Cr(VI) reduction and phenol degradation. A previous study by Igboamalu and Chirwa (2014) reported a high (K_{mc} = 0.6411 mg/L/h), and this may be due to different types of microorganisms isolated for Cr(VI) and As(III) oxidation. However, K_{ms} (0.85 mg/L/h) was reported with pure culture of *Thiomonas Arsenivorans* strains B6 (Dastida & Wang, 2010). The mechanism of As(III) oxidation in the B6 strains is different in the current study as Cr(VI) was used as an electron sink for As(III) oxidation in this comparison.

Half velocity concentration K_c or K_s is also inversely proportional to Cr(VI) and As(III) concentration per time and initial biomass concentration, as described in Equation 6.18 and 6.19. The best fit of (K_c = 986 mg/L/h and K_s= 979 mg/L/h) obtained in this study was higher K_{mc} (12 mg/L/h), reported by Shen and Wang (1995a), with *E-coli* strain for concurrent Cr(VI) reduction and phenol degradation. A previous study by Igboamalu and Chirwa (2014) reported a high (K_{mc} = 732.3 mg/L/h), and this may be due to different types of microorganisms isolated for Cr(VI) and As(III) oxidation or variation in cell growth. Previous studies of As(III) oxidation by heterotrophic or autotrophic strains have reported K_s ranging from (0.225-732 mg/L) (Philips & Taylor 1976; Turner & Legge 1954; Salmassi et al., 2002; Dastidar & Wang, 2010; Igboamalu & Chirwa, 2014).

However, previous studies on concurrent Cr(VI) reduction and As(III) oxidation have not been widely reported. The model predicted well with the experimental data at a wide range of Cr(VI) and As(III) concentration. Cr(VI) reduction kinetics obtained in this study, however, were indeed slightly different from those found in previous studies utilizing the same model (Molokwane et al., 2008). However, a difference in the model results may be attributed to the presence of As(III) in the experimental studies, correlated to biomass concentration of ±120 mg/L or variation in growth condition. Table 6.2 indicates some of the lower corresponding kinetic rates that were previously reported.
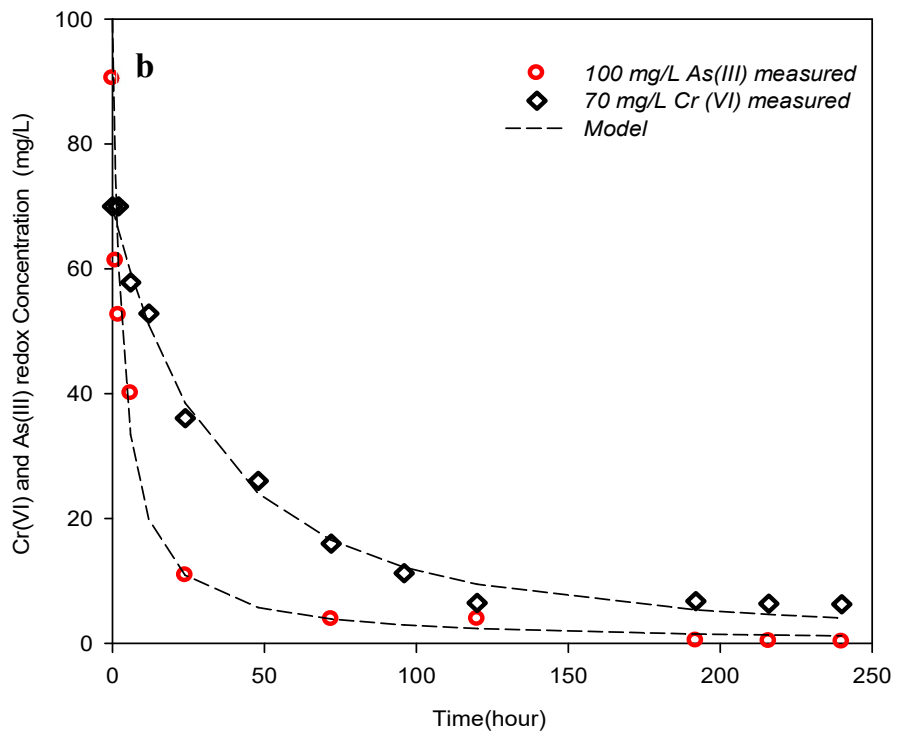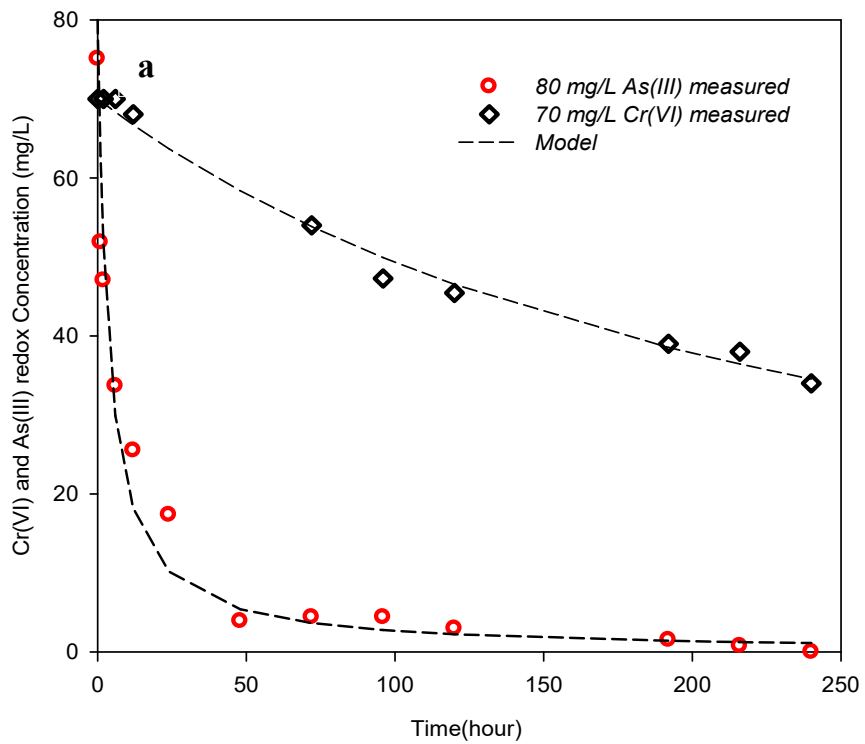
Figure 6.1: Kinetic modelling of the anaerobic consortium at (a) 80 mg/L As(III) and 70 mg/L Cr(VI), (b)100 mg/L As(III) and70 mg/L Cr(VI)

133
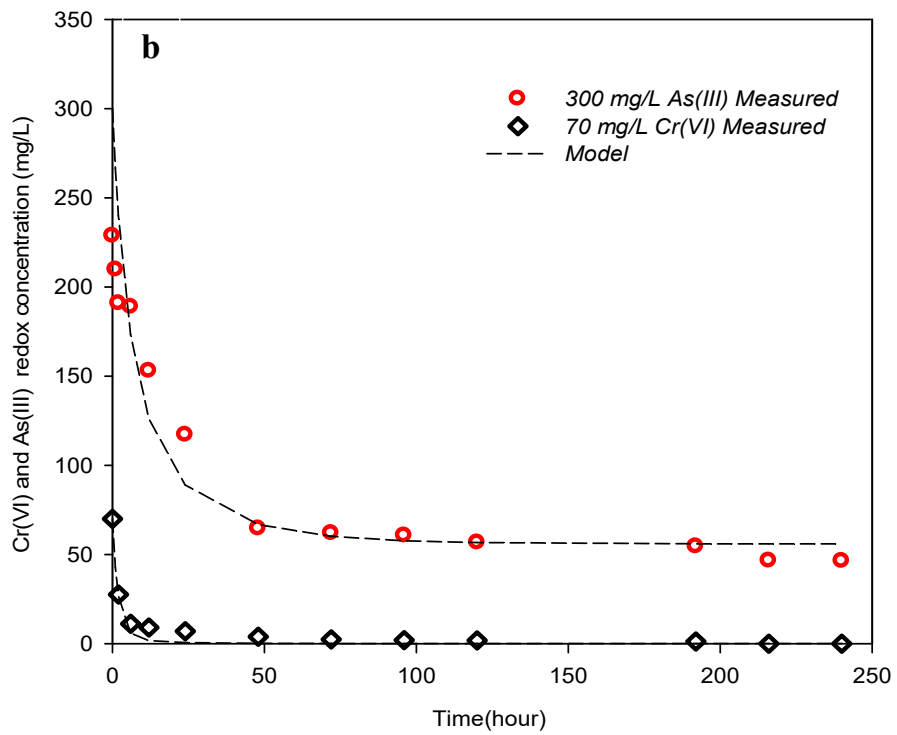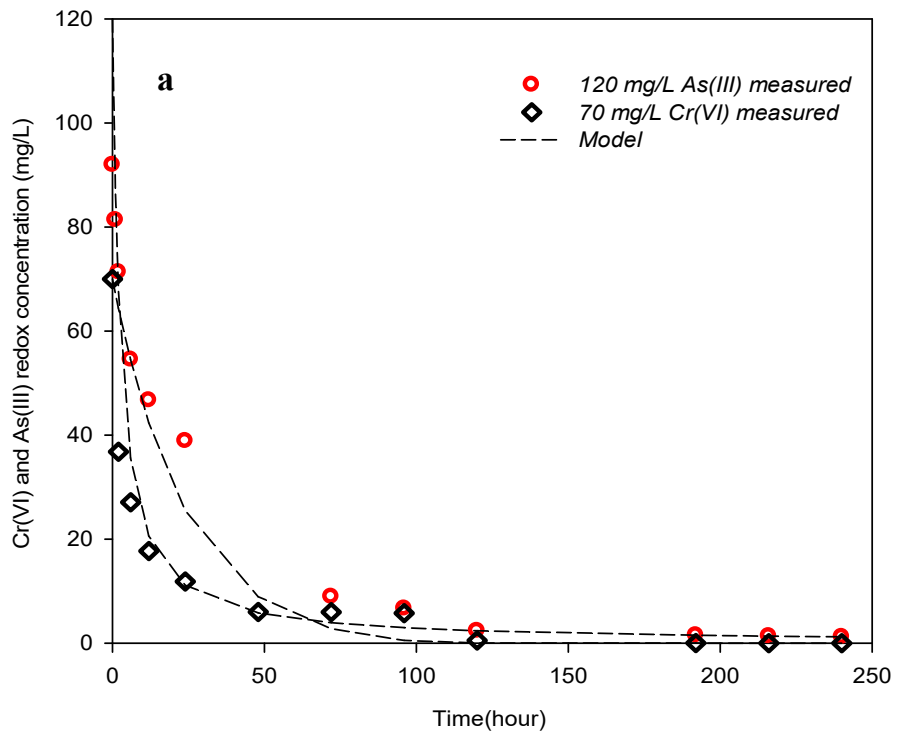
Figure 6.2: Kinetic modelling of the anaerobic consortium at (a) 120 mg/L As(III) and 70 mg/L Cr(VI), (b)300 mg/L As(III) and70 mg/L Cr(VI)

Table 6.2: Biokinetic parameter for Cr(VI) reduction and concurrent As(III) oxidation

Cr(VI) (mg/L)	As(III) (mg/L)	R_c (mg/mg)	R_s (mg/mg)	K_c (mg/L)	K_s (mg/L)	K_{mc} (mg/Lhr^{-1})	K_{ms} (mg/Lhr^{-1})	X^2 As	X^2 Cr
70	80	0.013	0.0002	986	979	0.009	0.0006	293	321
70	100	0.50	0.11	630	992	0.009	0.0006	1258	66.2
70	120	0.40	0.02	500	990	0.009	0.0006	1879	164
70	300	0.02	0.01	356	944	0.009	0.0006	1267	152

6.2.2 Sensitivity analysis

A sensitivity (identifiability and uncertainty) analysis was combined to check if the model Equation 6.18 and 6.19 parameters can be uniquely determined with the aid of available data and to estimate the uncertainty of the parameter estimates. The sensitivity coefficients of the best fit parameters were evaluated at 100 mg/L and 70 mg/L As(III) and Cr(VI), respectively. The function of the calculated concentration was then plotted with respect to six model parameters K_{mc}, K_{ms}, K_c, K_s, R_c, and R_s, against the independent variable t to measure the sensitivity and correlation between obtained kinetic parameters.

The data in Figure 6.3 and 6.4 evidently demonstrate a good separation between all the three sensitivity coefficients in both models. It is evident that the parameters are identifiable from the measured concentrations because of a small value of time. The sensitivity functions of the parameters K_{mc}, K_{ms}, K_c, and K_s are similar in shape, thus indicated that the calculated concentration increases with increasing K_c, and K_s, but decreases with increasing values of K_{mc}, and K_{ms}. This leads to a correlation between the estimates of these parameters (i.e. changes in calculated concentrations caused by a change in K_c and K_s is compensated by change in K_{mc}, and K_{ms}). Furthermore, the much smaller sensitivity of the calculated concentration to the parameter K_c and K_s in comparison to K_{mc}, and K_{ms} leads to larger uncertainty of the estimated K_c and K_s to K_{mc}, and K_{ms} (Reichart, 1998).

The observation made shows that these parameters were highly sensitive in the early hours of incubation, suggesting that cell Cr(VI) reduction and As(III) oxidation metabolism was high during this period of incubation. However, the dependence of Cr(VI) and As(III) concentration

'C' on these parameters is different. The sensitivity of Cr(VI) concentration 'C' with respect to K_{mc}, K_{ms}, K_c, K_s, and R_c increases from zero, reaches a maximum and then decreases again to zero (this is the behaviour of the absolute value of the sensitivity function, the negative sign indicates that Cr(VI) and As(III) concentration 'C' decrease with increasing values of K_{mc}, and K_{ms}, whereas the positive sign, on the other hand, indicates that Cr(VI) concentration 'C' increases with increased K_c, K_s, and R_c with exclusion of R_s that halts constant. This is consistent with previous studies, where half velocity concentration K is highly sensitive to model outcome at high substrate concentrations (Hung & Pavlostathis, 1999).

The parameters R_c, and R_s exhibit the least effect on the model predictions for the entire time range, as is indicated by the low values of their coefficients obtained from model simulation.
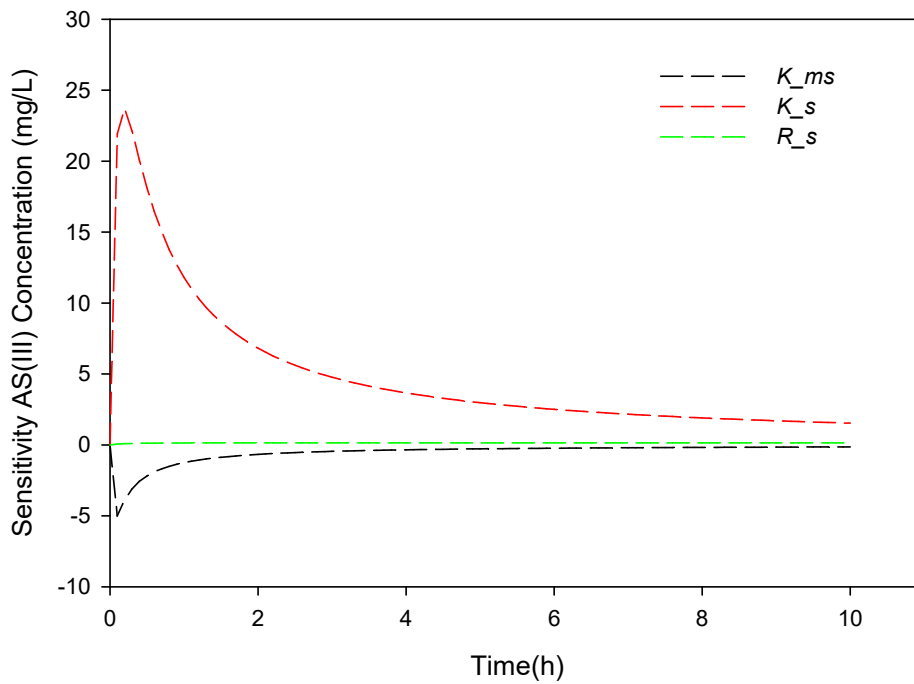
Figure 6.3: Sensitivity analysis with respect to Kmc, K_c, R_c,
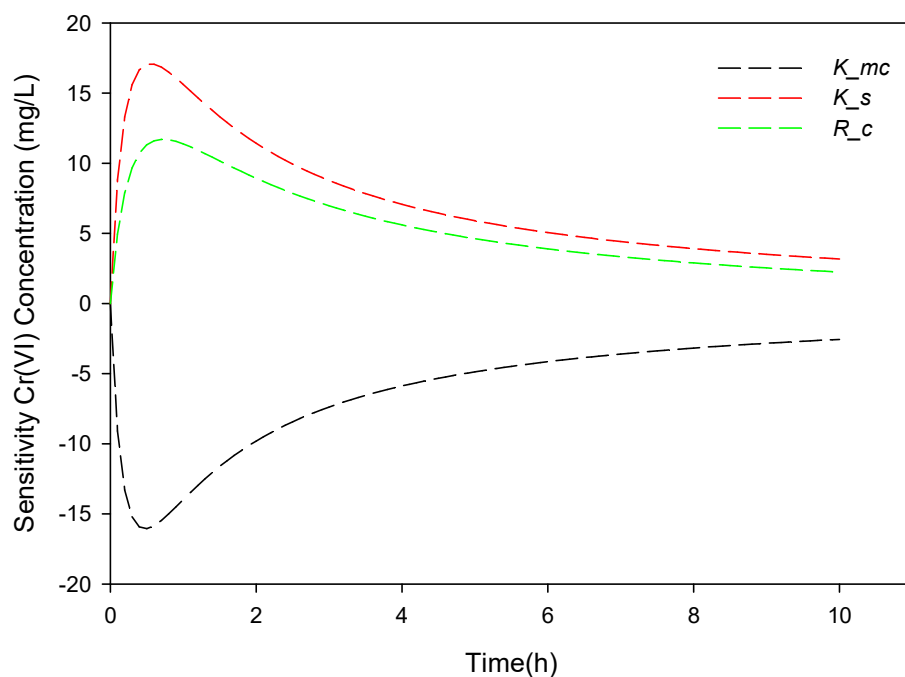
Figure 6.4: Sensitivity analysis with respect to Kms, K_s, R_s

6.3 Summary

Chapter 5 of this thesis evaluates a modified non-competitive inhibition model based on the Michaelis-Menten model to estimate parameters affecting the concurrent Cr(VI) reduction and As(III) oxidation in a mixed culture of chemoautotrophic anaerobic bacteria. This model was chosen because it described the complexity of enzymatic kinetics for metal reduction. It was seen that biological activities are the main mechanism for Cr(VI) reduction and As(III) oxidation, which are facilitated by enzymes. Such enzymatic Cr(VI) reduction and As(III) oxidation was best described by the developed model. The enzymatic model successfully represents concurrent Cr(VI) reduction and As(III) oxidation from the preliminary studies. It predicted and fitted well with the experimental data at a wide range of As(III) and Cr(VI) concentration of 80-300 mg/L and 70 mg/L, respectively. The model parameters obtained in this study, however, were indeed slightly different from those found in previous studies utilizing the same model. Secondly, the sensitivity analysis of the model parameters obtained was slightly similar to the parameters that were previously observed (Mtimuye, 2011). These values were seen to be very sensitive to the model.

CHAPTER 7

Continuous-flow modelling

7.1 Biokinetic model

7.1.1 Model description

The kinetic simulation of Cr(VI) reduction and As(III) oxidation has been studied in the batch of the current study prior to continuous-flow biofilm studies to assess the basics of each biological process at various time intervals (Igboamalu & Chirwa, 2016). The continuous plug flow (PFR) packed bed system was chosen to take advantage of the spatial and physiological heterogeneities and to enhance the performance of the anaerobic consortium in removing Cr(VI) and As(III) (Chirwa & Wang, 2005). However, reaction-microbial reduction in this study also significantly influences the fate and transport of Cr(VI) in a saturated porous media (Mtimuye & Chirwa, 2011).

The fundamental of this mode is based on advective-diffusive plug flow reactor compartment. This model is described by a one-dimensional advective transport of substance in a flow through reactor and substance transformation. However, this was solved using the computer program Identification and Simulation of Aquatic Systems (Aquasim 2.0) (Reichart, 1998). Aquasim 2.0 uses the fourth-order Runger-Kutta routine for solution of simultaneous ordinary and partial differential equations. Three types of components of a conservation law are distinguished in the advective-diffusion reactor compartment. The first component describes the conservation of water volume, the second compartment describes substances transported, dissolved or suspended within the water flow, and last, substances settled or sorbed to the surface or attached organisms within the compartment are described.

A similar model was formerly used to describe the modelling of Cr(VI) reduction and phenol degradation in a coculture biofilm reactor under inhibition kinetics conditions (Chirwa & Wang, 2005). There was no difference in the later model equation since both processes are

catalysed by enzymes. The previous model utilizes a diffusive biofilm theory with respect to particulate matter to accommodate cell density within the biofilm (Wanner & Gujer, 1986; Beaudoin et al., 1998; Wanner et al., 1995; Reichart, 1998). Second, the model was built on the underlying physical/chemical and biochemical laws to arrive at an approximation model (Chirwa and Wang, 2005). Initial values of kinetic parameters that were previously reported are described in Table 7.1.

Table 7.1: Initial continuous studies parameter

Parameters	Definition	Optimum values	Units	Reference
K_{mc}	Maximum specific Cr(VI) reduction rate coefficient	0.0096	L/h	Chirwa and Wang (2005)
K_c	Half-velocity Cr (VI) concentration	9.1	mg/L	Chirwa and Wang (2005)
R_c	Cr (VI) reduction capacity	0.13	mg/mg	Chirwa and Wang (2005)
K_{mp}	Maximum specific phenol reduction rate coefficient	1.23	L/h	Chirwa and Wang (2005)
K_p	Half-velocity phenol concentration	833	mg/L	Chirwa and Wang (2005))
R_s	Maximum specific As(III) reduction rate coefficient	0.86	mg/mg	Suttigarn and Wang (2007)
K_s	Half-velocity As(III) concentration	70	mg/L	Suttigarn and Wang (2007))

7.1.2 Advection process

Advection is defined as the transport of dissolved species along with bulk fluid flow. It is mathematically represented as:

$$-\frac{d\left(\overset{\backslash}{C}_b V_b\right)}{dt} = -r_{adv} = Q\left(\overset{\backslash}{C}_o - \overset{\backslash}{C}_b\right) \tag{7.1}$$

Where: r_{adv} = dissolved species transport rate (mg/L.h), $\overset{\backslash}{C}_b = \{C_r, A_s\}$, vector for the dissolved species concentration (mg/L); C = Cr(VI) concentration (mg/L), A_s = As(III) concentration (mg/L), $\overset{\backslash}{C}_o$ = influent dissolved species concentration (mg/L); V_b = bulk volume of the reactor (L), Q = volumetric discharge through the compartment (L/s) ($Q = AV$); A = cross sectional area (m^2); V = velocity of the flow (m/s).

7.1.3 Flux

One-dimensional flux of quantity $j_{\dot{C}}$ with one-dimensional densities is mathematically represented in Equation 7.2. It is a function of the species dispersion or diffusion coefficient and concentration.

$$- j_{\dot{C}} = \left(\frac{D_{wi} \dot{C}_b}{L_w} \right) A_f \tag{7.2}$$

Where: D_{wi} = Coefficient of dispersion of species in solution (cm^2/s); $\dot{C}_b = \{ C_r, A_s \}$, vector for the dissolved species concentration (mg/L); C_r = Cr(VI) concentration (mg/L), A_s = As(III) concentration (mg/L); L_f = biofilm thickness (m); A_f = biofilm surface area (m^2).

7.1.4 Dispersion or diffusion process

Diffusivity of Cr(V) and As(III) was determined using the equation described by Chirwa and Wang (2005). The Nernst-Haskell equation was used to estimate Cr(V) dispersion or diffusion in a solution equation 7.3. On the other hand, the diffusivity of As(III) for temperature effect correction was estimated using an equation by Wilke and Chang (1995). Equation 7.4:

$$D_{wc_r} = \left(\frac{RT}{F^2} \right) \frac{\lambda}{\varpi_i} \tag{7.3}$$

$$D_{wc_r} = \frac{(D_i)(\phi M_w)^{1/2} T}{\mu \eta_a^{3/5}} \tag{7.4}$$

Where: D_{wi} = dispersion coefficient of species in solution (cm^2/s); $\dot{C}_b = \{ C_r, A_s \}$, vector for the dissolved species concentration (mg/L); C_r = Cr(VI) concentration (mg/L), A_s = As(III) concentration (mg/L); L_f = biofilm thickness (m); A_f = biofilm surface area (m^2).

7.1.5 Kinetic equation

The rate of Cr(VI) reduction and As(III) oxidation was described with an equation developed from batch studies.

Equation 5.16:

$$-\frac{d\vec{C}}{dt} = \frac{k_{mi}\vec{C}_b}{\left(K_i + \vec{C}_b\right)}\left(X_o - \frac{\vec{C}_{bo} - \vec{C}_b}{R_i}\right)$$

(7.5)

Where: $\vec{C}_b = \{C_r, A_s\}$, vector for the dissolved species concentration (mg/L); C_r = Cr(VI) concentration (mg/L); A_s = As(III) concentration (mg/L); k_{mi} = maximum specific Cr(VI) reduction rate or As(III) oxidation rate (mg/L/h); C_{bo} = initial Cr(VI) or As(III) concentration (mg/L); X_o = initial biomass concentration (mg/L); R_i = maximum Cr(VI) reducing or As(III) oxidizing capacity (mg/mg); K_i = half velocity concentration (mg/L).

7.1.6 Reactor material balance

Dissolved species concentration vectors in the bulk liquid are a function of time and distance, and it is represented as $\vec{C}_b(t, x)$. The reactor material balance mathematical model can be written over the entire advective-diffusive compartment (plug flow) linked to CSTR volume for modelling of the fate and transport of Cr(VI) and As(III) species as:

$$V\frac{d\vec{C}_b}{dt} = -\vec{r}_{adv} - \vec{r}_{Cb}V - \vec{j}_{Cb}$$

(7.6)

Combing equation 7.1 to equation 7.6:

$$V\frac{d\vec{C}_b}{dt} = Q(\vec{C}_o - \vec{C}_b) - r_{\vec{C}_b}V - j_{\vec{C}_b}$$

(7.7)

Where: D_{wi} = dispersion coefficient of species in solution (cm²/s); $\overset{\rightharpoonup}{C}_b = \{C_r, A_s\}$, vector for the dissolved species concentration (mg/L); C = Cr(VI) concentration (mg/L), A_s = As(III) concentration (mg/L); L_f = biofilm thickness (m); A_f = biofilm surface area (m²).

Combining equation 7.7 and 7.5:

$$V\frac{d\overset{\rightharpoonup}{C}_b}{dt} = Q(\overset{\rightharpoonup}{C}_o - \overset{\rightharpoonup}{C}_b) - \frac{k_{mi}\overset{\rightharpoonup}{C}_b}{K_i + \overset{\rightharpoonup}{C}_b}\left(X_o - \frac{\overset{\rightharpoonup}{C}_o - \overset{\rightharpoonup}{C}}{R_i}\right)V - \frac{D_{wi}\overset{\rightharpoonup}{C}_b}{L_{wi}}A_f \tag{7.8}$$

Where: D_{wi} = dispersion coefficient of species in solution (cm²/s); $\overset{\rightharpoonup}{C}_b = \{C_r, A_s\}$, vector for the dissolved species concentration (mg/L); C = Cr(VI) concentration (mg/L), A_s = As(III) concentration (mg/L); L_f = biofilm thickness (m); A_f = biofilm surface area (m²); k_{mc} = maximum specific Cr(VI) reduction rate (mg/L/h); C_o = initial Cr(VI) concentration (mg/L); X_o = initial biomass concentration (mg/L); C_r = Cr(VI) concentration (mg/L) at a time 't'; R_c = maximum Cr(VI) reducing capacity (mg/mg); K_c = half velocity concentration (mg/L).

During steady-state operations, $V\frac{d\overset{\rightharpoonup}{C}_b}{dt} = 0$, and Equation 7.8 is simplified to:

$$Q(\overset{\rightharpoonup}{C}_o - \overset{\rightharpoonup}{C}_b) - \frac{k_{mc}C}{K_c + C}\left(X_o - \frac{C_o - C}{R_c}\right)V - \frac{D_{wi}C_b}{L_w}A_f = 0 \tag{7.9}$$

$$Q(\overset{\rightharpoonup}{C}_o - \overset{\rightharpoonup}{C}_b) = \frac{k_{mc}C}{K_c + C}\left(X_o - \frac{C_o - C}{R_c}\right)V - \frac{D_{wi}C_b}{L_w}A_f \tag{7.10}$$

In an advective-diffusive compartment (plug flow reactor) the rate of Cr(VI) reduction or As(III) oxidation can be described as:

$$\frac{dC}{dt} = -\frac{Q}{V}(\overset{\rightharpoonup}{C}_o - \overset{\rightharpoonup}{C}_b) = -\frac{k_{mc}C}{K_c + C}\left(X_o - \frac{C_o - C}{R_c}\right) - \frac{D_{wi}C_b}{L_w}\frac{A_f}{V} \tag{7.11}$$

Similarly, the rate of Cr(VI) reduction or As(III) oxidation in a CSTR is described as:

$$V \frac{d\acute{C}_b}{dt} = Q(\acute{C}_o - \acute{C}_b) - \frac{k_{mc}C}{K_c + C}\left(X_o - \frac{C_o - C}{R_c}\right)V \qquad (7.12)$$

Where: $\acute{C}_b = \{C_r, A_s\}$, vector for the dissolved species concentration (mg/L); C = Cr(VI) concentration (mg/L), k_{mc} = maximum specific Cr(VI) reduction rate (mg/L/h); C_o = initial Cr(VI) concentration (mg/L); X_o = initial biomass concentration (mg/L); C_r = Cr(VI) concentration (mg/L) at a time 't'; Rc = maximum Cr(VI) reducing capacity (mg/mg); Kc = half velocity concentration (mg/L).

During steady-state operations, $V\frac{d\acute{C}_b}{dt} = 0$ Equation 7.12 is simplified to:

$$Q(\acute{C}_o - \acute{C}_b) - \frac{k_{mc}C}{K_c + C}\left(X_o - \frac{C_o - C}{R_c}\right)V = 0 \qquad (7.13)$$

$$Q(\acute{C}_o - \acute{C}_b) = \frac{k_{mc}C}{K_c + C}\left(X_o - \frac{C_o - C}{R_c}\right)V \qquad (7.14)$$

Simplifying equation 7.14, and the rate of Cr(VI) or As(III) oxidation in a CSTR can be described as:

$$\frac{dC}{dt} = -\frac{Q}{V}(\acute{C}_o - \acute{C}_b) = -\frac{k_{mi}C}{K_i + C}\left(X_o - \frac{C_o - C}{R_i}\right) \qquad (7.15)$$

Moreover, kinetic parameter values were estimated with data obtained at steady-state conditions, followed by simulation and optimization using Aquasim 2.0. Upper and lower constraints were set for each parameter to the exclusion of invalid parameter values. Whenever optimization converged or was very close to the constraint, the constraint was relaxed until it did not force the model. The procedure was repeated until unique values lying away from the constraint but between set limits were found for each parameter (Chirwa & Wang, 2004). Model equation 7.15 was proposed in this study, and is based on the following assumption:

- As(III) does not act as an inhibitor on microbial growth at 20 mg/L.
- The flow in the column is one-dimensional.

- The porous media is homogenous.

- Temperature and pH are constant at steady-state operation.

- The reactor approaches steady-state operation.

- All substances dissolved in water flow.

- There was no sorption of substance within the reactor.

7.2 Glass bead bead-packed reactor operated in CSTR mode

7.2.1 Kinetics and parameter optimisation

Cr(VI) removal biokinetic parameters in a continuous feed glass bead packed bed reactor link to continuous-flow stirred-tank reactor (CSTR) under steady-state conditions were collected in phases (II–VII) Cr(VI), under influent Cr(VI) and As(III) concentrations ranging from 40-200 mg/L and 80-400 mg/L, respectively. This was followed by simulation of effluent at HRT of 5 and 12 h. Data from previous studies showed no significant chromium accumulation within the reactor, and neither adsorption nor hydroxides were assumed (Chirwa & Wang 2001).

The initial guess parameters affecting mass transport rate across the entire reactor are listed in Table 7.1. Numerical simulation was initialized by initial guessed values of the viable attached or suspended cell concentration X_o =120 mg/L and based on previous studies (Chirwa & Wang 2001, Igboamalu & Chirwa, 2014). To ascertain that the parameters estimated by the mathematical model (Equation 7.15) were reliable, upper and lower constraints were set for each parameter (Chirwa & Wang, 2001). The model equation under steady-state conditions (Equation 7.15) was simulated and iterated through the processes till predefined convergence norms were met for each reliant on variable. This process was repeated until sole values lying away from the constraints were initiated.

Using Equation 7.15, optimum kinetic parameters are summarized in Table 7.2, and it was overserved as follows: K_{mc} = 9.87 mg/L/h, K_c = 419 mg/L, and R_c = 0.97 mg/mg for Cr(VI) reduction in reactor1 (PFR), and K_{mc} = 0.054 mg/L/h, K_c = 675 mg/L in reactor 2 (CSTR). Figure 7.1 and 7.2 show the results of influent and effluent simulation within the optimization phases in reactor 1 and reactor 2. The kinetic parameters obtained from reactor K_{mc}, K_c and R_c in reactor 1 and 2 were much higher than data observed previously in a batch of the same cultures (Chapter 6). The corresponding values for the lower kinetic rates are as given in Table

7.1: K_{mc} =0.0042 L/h, and K_c=12.0 mg/L for Cr(VI) reduction (Shen & Wang 1995a). Chirwa and Wang (2005) also reported values of K_{mc} = 0.0095 mg/L/h, K_c = 9.1 mg/L, and R_c = 0.13 mg/mg, which is higher than the value obtained in the present study, suggesting that the mixed culture has a higher affinity towards Cr (VI) than pure culture. The variability in the estimated kinetic parameters obtained in batch and the CSTR cultures of *T.arsenivorans* strain b6 (this study) can be due to the method of estimation or the history of the specific culture prior to the start of the experiment, as discussed before by Grady et al. (1996), although batch operation is easier and economical compared to CSTR operation.

The biokinetic parameters obtained at steady-state conditions in the CSTR are more accurate and reliable than that obtained in batch study (Gallifuoco et al. 2002). This is because continuous cultures at steady states are in better-controlled and optimized environments than the transient growth conditions in batch study (Wang & Suttigarn 2007). Another advantage of CSTR over batch reactors is the dilution of the feed As(III) concentration to the reactor. This explains the reason for no significant inhibition observed for the range of influent As(III) concentrations (41-400 mg/L) fed to the CSTR in this study. However, significant inhibition was observed on As(III) oxidation for As(III) concentrations greater than 500 mg/L using anaerobic mixed cultures, as previously described (Figure 4.6 a).

Also, kinetic parameter K_{mc}, K_c and R_c obtained in reactor 1 differed significantly to reactor 2, suggesting that higher bioconversion rates were expected in the attached growth system due to the shielding effect of mass transport resistance against toxic effects on cells inside the biofilm (Semprini & McCarty, 1981). It was also reported that longer contact times enhance the continuous-flow reactor in respect of low biokinetic parameters (Semprini & McCarty, 1981). However, the reactor was operated at HRT of 12 h, more than reactor 2 of 3 h. The variability in the estimated values of the same parameter could be due to culture history prior to the start of the experiment or the mathematical routine employed to obtain the parameters, as discussed by Grady et al. (1996).

Second, the optimum dispersion coefficient D_{wc} = 6.1×10⁻⁷ m²/d obtained when the reactor was fed with Cr(VI) and As(III) concentration is much lower than the one observed previously D_{wc} = 9.1×10⁻⁵ m²/d in a Cr(VI) and phenol study *(*Chirwa & Wang, 2005). This suggests that the rate at which the contaminant disperses into the cell layer attached to the glass beads is

influenced by the concentration of As(III) correlating to Cr(VI) reduction as a result of electron mass transfer.

Cr(VI) in the presence of As(III) breakthrough under the high hydraulic loadings Phases X and XII was predominantly influenced by the attached cell washed off in PFR or cell loss in CSTR. An increase in hydraulic drag on biofilm surfaces was expected since the recycle flow rate was increased proportionally to influent feed rate to maintain a constant feed/recycle ratio (Chirwa & Wang 2001).

The model simulated the recovery of the reactor from overloaded conditions just as observed in the experiment in phases IV and VI. The model was sensitive to any slight changes in the maximum rate coefficient of Cr(VI) K_{mc} through the entire period of operation. Sensitivity to a specific parameter was determined by observing the deviation of the model from the best fit due to slight changes introduced to the optimum value data not shown.

Table 7.2: Optimum kinetic parameters of glass bead media in steady-state conditions

Parameters	Definition	Units	PFR Final Reactor 1	CSTR Reactor
K_{mc}	Maximum specific Cr(VI) reduction rate coefficient	mg/L/h	9.87	0.055
K_c	Half-velocity Cr (VI) concentration	mg/L	419	675
R_c	Cr (VI) reduction capacity	mg/mg	0.97	0.012
D_{wp}	Diffusivity	m^2/d	6.1×10^{-7}	0
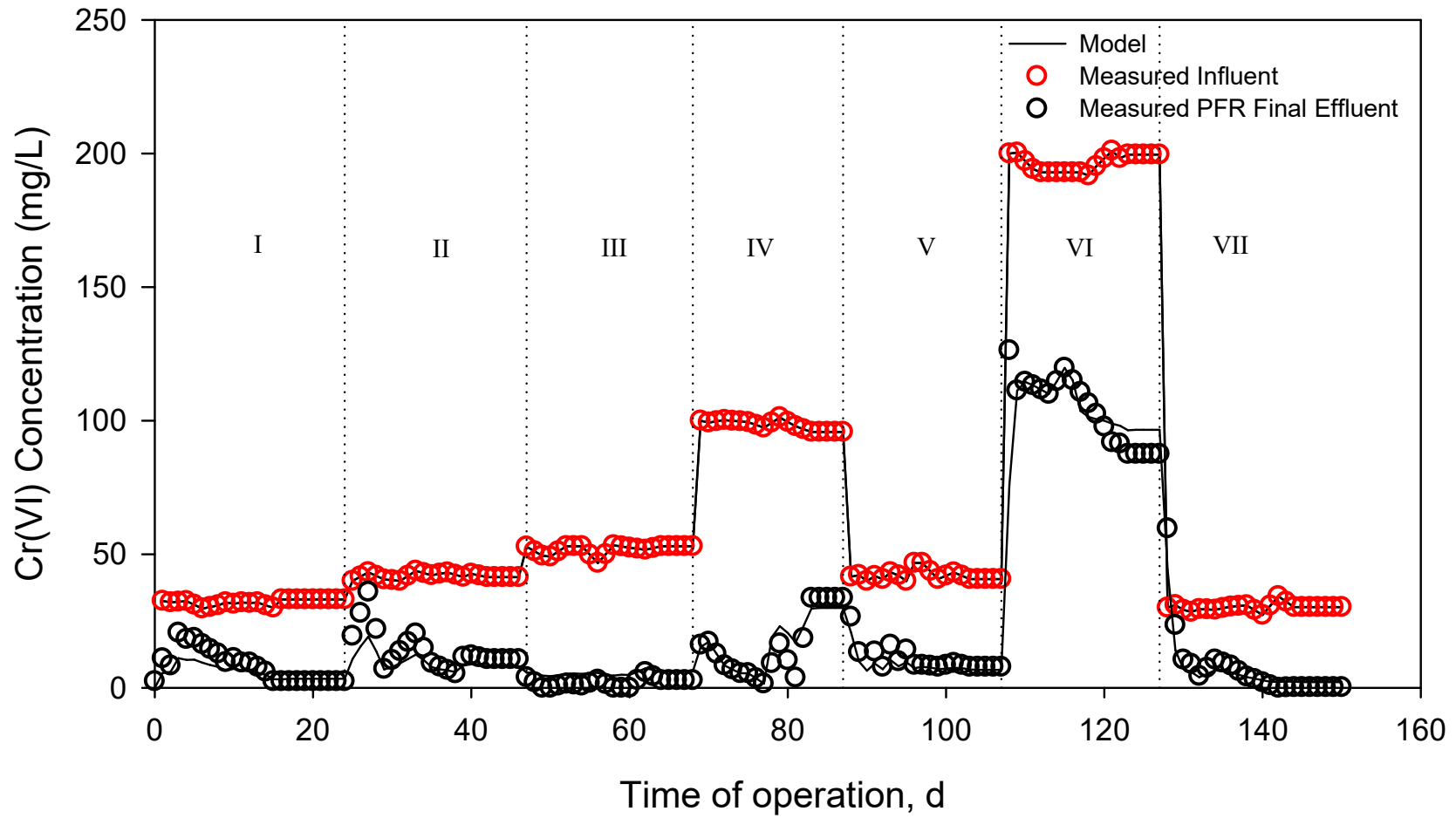
Figure 7.1: Simulation and optimization of influent and effluent Cr(VI) in a continuous-flow glass bead packed bed Reactor 1
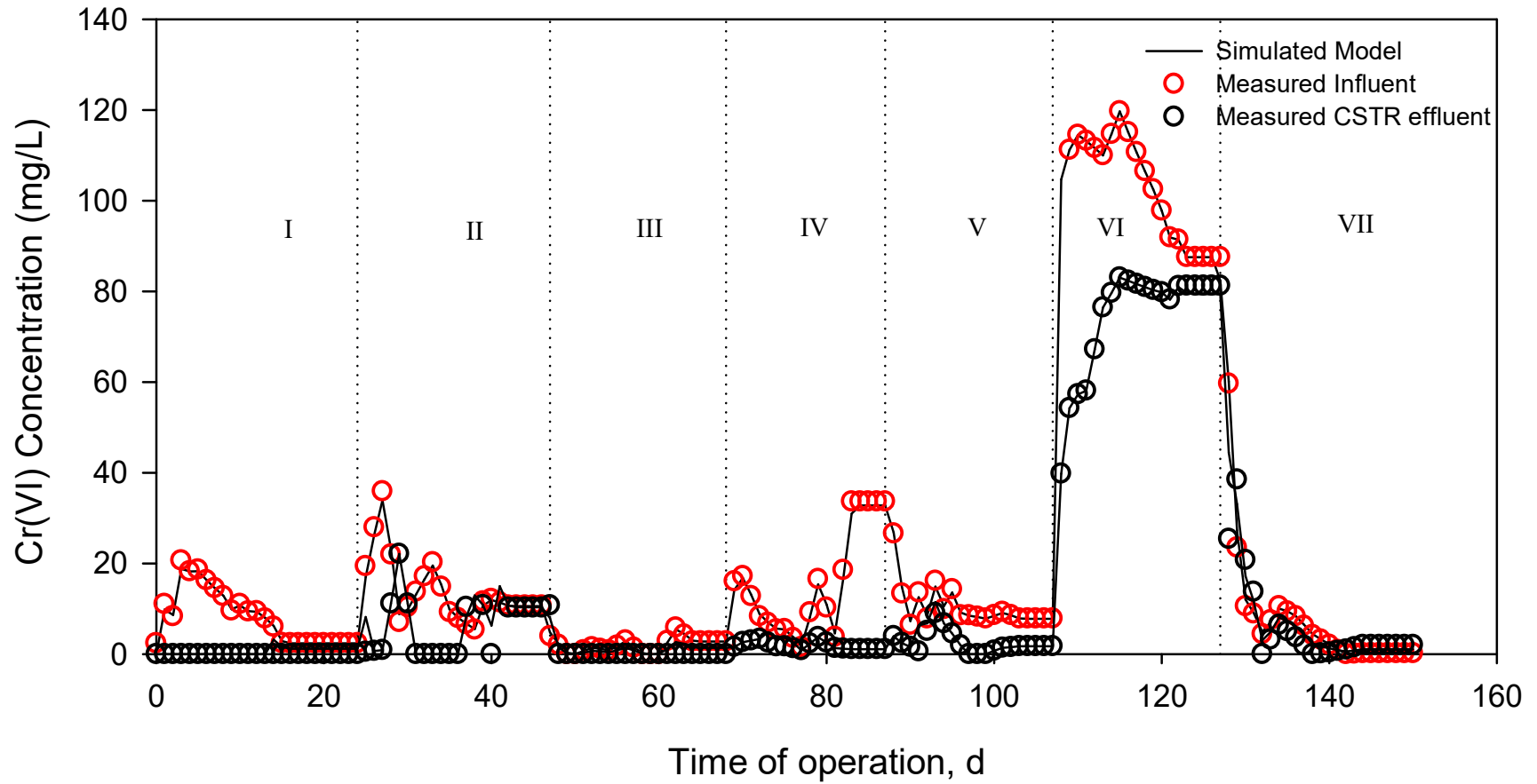
Figure 7.2: Simulation and optimization of influent and effluent Cr(VI) in a continuous-flow stirred tank Reactor

7.3 Ceramic bead bead-packed reactor operated in CSTR mode

7.3.1 Kinetics and parameter optimisation

Like the glass bead packed bed reactor described in section 7.73, Cr(VI) reduction kinetics was also estimated in a continuous-flow packed bed reactor with ceramic beads, and this was also linked to the continuous-flow stirred-tank reactor (CSTR) in steady-state conditions using Equation 7.15. Cr(VI) data obtained were collected in phases II–VII, under influent Cr(VI) and As(III) concentrations ranging from 40-200 mg/L and 80-400 mg/L, respectively. This was followed by simulation of effluent at HRT of 5 and 12 h. It was assumed that there was no significant chromium accumulation within the reactor, neither adsorption nor hydroxides, and this was based on previous reports (Chirwa & Wang, 2001).

Initial guess parameters affecting mass transport rates across the entire reactor are listed in Table 7.1. Numerical simulation was also initialized by initial guessed values of the viable attached or suspended cell concentration X_o =120 mg/L, based on previous studies (Chirwa & Wang 2001, Igboamalu & Chirwa, 2014). To ascertain that the parameters estimated by the mathematical model (Equation 7.15) were reliable, upper and lower constraints were set for each parameter (Chirwa & Wang, 2001).

Model equation under steady-state conditions (Equation 7.15) was simulated and iterated through the processes till predefined convergence norms were met for each reliant on variable. This process was repeated until sole values lying away from the constraints were initiated. Using Equation 7.15, optimum kinetic parameters are summarized in Table 7.4, and it was overserved after simulation, parameter estimation run and successful convergence criterion as follows: K_{mc} = 9.1 mg/L/h, K_c = 577 mg/L, and R_c = 0.9 mg/mg in reactor 3 (PFR), and K_{mc} = 9.1 mg/L/h, K_c = 647 mg/L and R_c = 1.4 mg/mg in reactor 4 (CSTR). Figure 7.4 and 7.5 show the results of influent and effluent simulation within the optimization phases in reactor 3 and reactor 4.

The kinetic parameters K_{mc}, K_c and R_c obtained in both reactors were also much higher than data observed previously in batches of the same cultures (Chapter 6), indicating higher

biological activities that utilizes energy generated in the process of cell growth and embolism. The corresponding values for the lower kinetic rates are as given in Table 7.1: K_{mc} =0.0042 L/h, and K_c =12.0 mg/L for Cr(VI) reduction (Shen & Wang 1995a), K_{mc} = 0.0095 mg/L/h, K_c = 9.1 mg/L, and R_c = 0.13 mg/mg for Cr(VI) reduction (Chirwa & Wang, 2005), and R_c = 0.86 mg/L/h, K_c = 70 mg/L also reported for As(III) oxidation (Dastidr & Wang, 2007) values that are higher than the value obtained in the present study, suggesting that the mixed culture has a higher affinity towards Cr (VI) than pure culture.

The variability in the estimated kinetic parameters obtained in batch and the CSTR cultures of *T.arsenivorans* strain b6 (this study) can be due to the method of estimation or the history of the specific culture prior to the start of the experiment, as discussed before by Grady et al., (1996). Although batch operation is easier and economical compared to CSTR operation, the kinetic parameters obtained at steady-state conditions in the CSTR are more accurate and reliable than that obtained in batch study (Gallifuoco et al., 2002). This is because continuous cultures at steady states are in better-controlled and optimized environments than the transient growth conditions in batch study (Wang & Suttigarn 2007).

Another advantage of CSTR over a batch reactor is the dilution of the feed As(III) concentration to the reactor. This explains the reason for no significant inhibition observed for the range of influent As(III) concentrations (41-400 mg/L) fed to the CSTR in this study. However, significant inhibition was observed on As(III) oxidation for As(III) concentrations greater than 500 mg/L using anaerobic mixed cultures, as previously described in Figure 4.6a.

Also, kinetic parameters K_{mc}, K_c and R_c obtained in reactor 3 did not differ significantly to reactor 4. It is unclear why the parameters are slightly the same, but it could be attributed to high porous media. It was also reported that longer contact times enhance the continuous-flow reactor with respect to low biokinetic parameters (Semprini & McCarty, 1981). However, the reactor was operated at HRT of 12 h, more than reactor 2 of 3 h. The variability in the estimated values of the same parameter could be due to culture history prior to the start of the experiment or the mathematical routine employed to obtain the parameters, as discussed by Grady et al. (1996).

Second, the optimum dispersion coefficient D_{wc} = 6.9×10^{-7} m^2/d obtained when the reactor was fed with Cr(VI) and As(III) concentration is much lower than the one observed previously: D_{wc}

= 9.1×10^{-5} m^2/d in a Cr(VI) and phenol study (Chirwa & Wang, 2005). This suggests that the rate at which the contaminant disperses into the cell layer attached to the glass beads is influenced by the concentration of As(III) correlating to Cr(VI) reduction as a result of electron mass transfer. However, this could be attributed to the much higher toxic effect of Cr(VI) and As(III) on microbial activities. Therefore, higher rates of Cr(VI) reduction observed at lower concentration is attributed to higher dispersion rate in the column.

Cr(VI) in the presence of As(III) breakthrough under the high hydraulic loadings in phases X and XII was also predominantly influenced by the attached cell washed off in PFR or cell loss in CSTR. An increase in hydraulic drag was expected since the recycle flow rate was increased to maintain the microbial community in the system (Chirwa & Wang, 2001). The model simulated the recovery of the reactor from overloaded conditions, just as observed in the experiment in phases IV, and VI. The model was sensitive to any slight changes in the maximum rate coefficient of Cr(VI) K_{mc} through the entire period of operation. Sensitivity to a specific parameter was determined by observing the deviation of the model from the best fit due to slight changes introduced to the optimum value data.

Table 7.3: Optimum kinetic parameters of ceramic bead media in steady-state conditions

Parameters	Definition	Units	PFR Final Reactor 3	CSTR Reactor 4
K_{mc}	Maximum specific Cr(VI) reduction rate coefficient	mg/L/h	9.02	9.02
K_c	Half-velocity Cr (VI) concentration	mg/L	577	647
R_c	Cr (VI) reduction capacity	mg/mg	0.91	1.4
D_{wp}	Diffusivity	m^2/d	6.9×10^{-7}	0
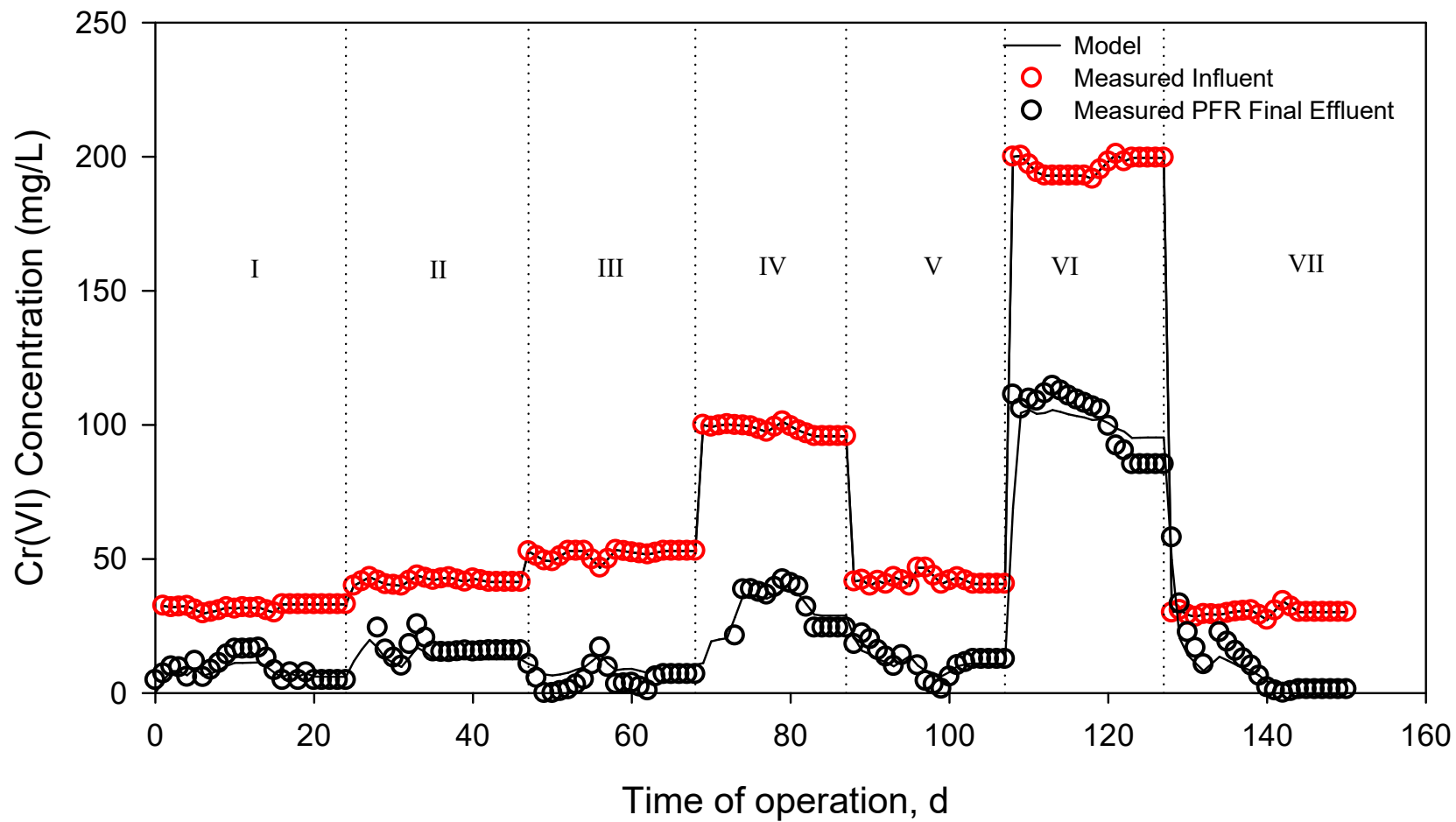
Figure 7.3: Simulation and optimization of influent and effluent Cr(VI) in a continuous-flow ceramic bead packed bed Reactor 3
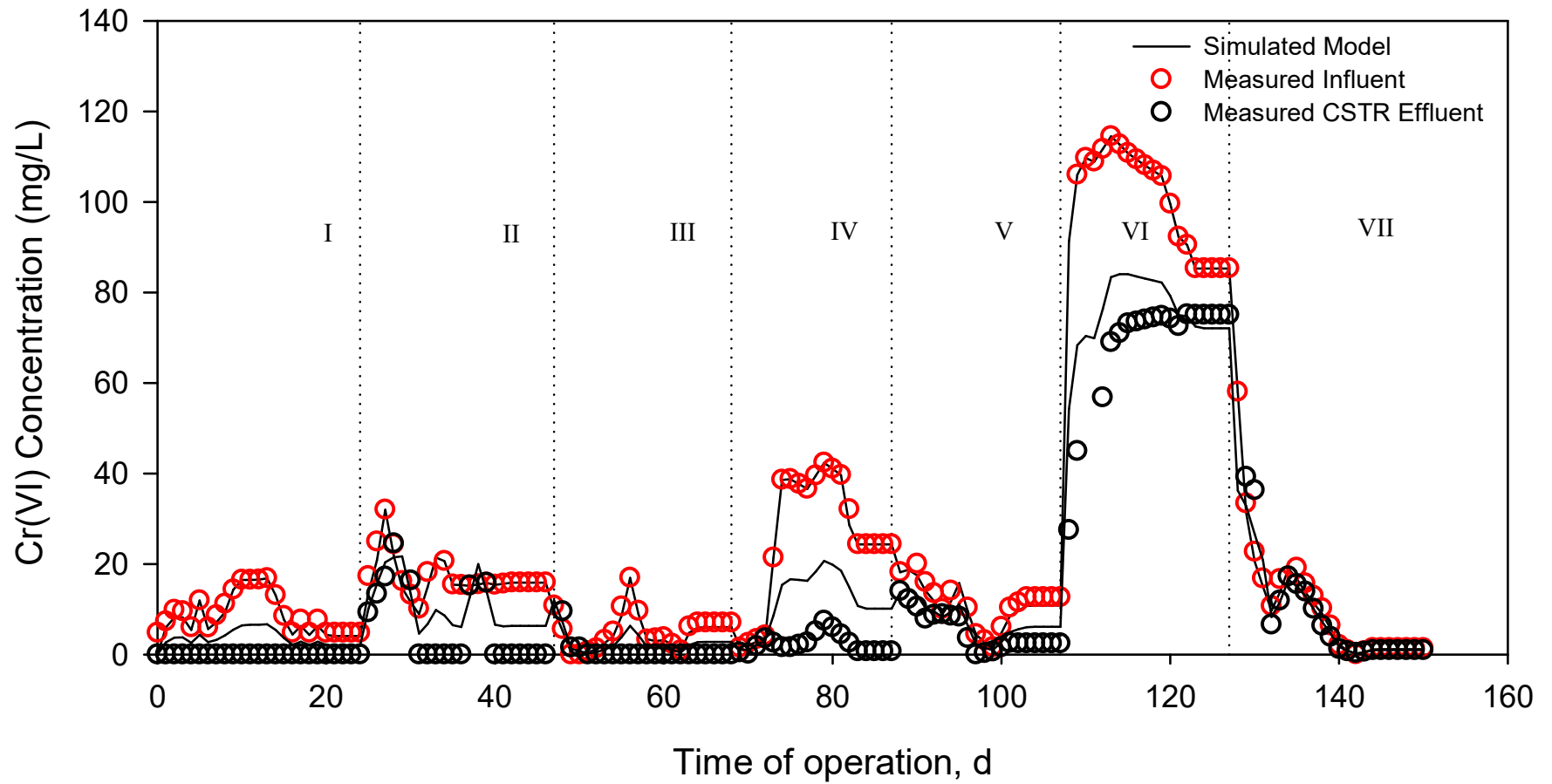
Figure 7.4: Simulation and optimization of influent and effluent Cr(VI) in a continuous-flow stirred tank Reactor 4

7.4 Summary

Chapter 7 of this thesis evaluated a modified non-competitive inhibition model in a continuous-flow packed bed reactor (with glass bead packing-bed link to CSTR for an example) or (with ceramic bead packing-bed link to CSTR for an example) for Cr(VI) reduction with As(III) as an electron source. This model was chosen because it described the enzymatic kinetics of the biological process, which is based on Michaelis-Menten or Monod fundamental derivation. The continuous-flow packed bed reactor was assumed as plug flow system, and it is based on an advective-diffusive plug flow reactor compartment described by a one-dimensional advective transport of substance. The model simulated the accumulation of metabolites under high Cr(VI) loadings with As(III) as an electron source. Parameters obtained in this study indicated higher removal kinetics than those obtained previously in batch systems and other studies. This was attributed to culture acclimation to Cr(VI) and As(III) and effects of mass transport resistance. The preliminary result K_{mc}, K_c and R_c developed from the modified model could be potentially suitable for simulation of concurrent Cr(VI) reduction and As(III) oxidation under high ranges of Cr(VI) and As(III) loadings 30-200 and 61-400 mg/d, respectively.

CHAPTER EIGHT

Conclusion and recommendations

8.1 Conclusion

A lot of mining activities take place in South Africa and the rest of Africa, ranging from ore, chrome, precious metal, gold mining, etc. These activities often generate a considerable amount of toxic waste, which may include: Cr(VI), As(III), Pb, CN, etc. as toxic wastes. In most waste that is generated there is the possibility that Cr(VI) will coexist with As(III) at a very high concentration, making the waste very difficult to dispose of. Because of this difficult and expensive treatment, most industries illegally dump the waste in the sewer system without treatment, which finally ends up in bodies of water, causing an environmental hazard. However, it has become crucial that we treat such waste or chromium-arsenic-containing wastes to an environmentally acceptable standard before disposal.

The current study proposed concurrent treatment of chromium-arsenic-containing wastes through a biological catalytic redox process. This was successfully achieved through an electron transfer pathway process (ETP), where Cr(VI) is reduced to less toxic Cr(III) by accepting two electrons from As(III), and oxidized to less toxic As(V) through a biologically catalysed process with anaerobic chemoautotrophic bacteria isolated from the local environment in South Africa. However, this is a novel biological treatment approach and it is cost effective as the microbial growth is facilitated by energy generated in the redox process.

The identified strains provided evidence of Cr(VI) reduction and As(III) oxidation capacity through successful concurrent reduction of Cr(VI) and As(III) concentrations in the batch system, and the ability to use energy generated from redox conversion of Cr(VI) and As(III) for growth and metabolism. These strains were successfully characterized using the 16S

rRNA/DNA phenotype fingerprinting method, and it predominantly consists of *Exiquobacterium sp, Bacillus sp,* and *Staphylococcus sp.*

In a batch system, concurrent Cr(VI) reduction and As(III) oxidation were successfully achieved at high concentrations up to 70 mg/L and 500 mg/L. An inhibition effect was not observed at this concentration; rather the redox process was enhanced, except in situations where there was insufficient energy for microbial growth and metabolism. It is conclusive that Cr(VI) reduction and As(III) oxidation were possible based on bioenergetic consideration and the electron transfer pathway. The evidence of Cr(VI) reduction and As(III) oxidation conclusively demonstrated that As(III) could serve as an inorganic electron donor for Cr(VI) reduction. The present study adds As(III) to the pool of known inorganic electron donors for reduction of Cr(VI) and beneficial oxidation of As(III) to As(V) in an anaerobic environment.

The feasibility of utilizing promising Cr(VI)-reducing and As(III)-oxidizing bacteria in a small-scale pilot study for bioremediation of chromium-arsenic contaminated wastewater was demonstrated by better performance of continuous packed bed reactors inoculated with indigenous anaerobic mixed culture from the local environment. A successful reduction of Cr(VI) at much higher Cr(VI) and As(III) concentration up to 200 mg/L and 400 mg/L was achieved. The reactor made a speedy recovery after double shock load effect at 100 and 200 mg/L of Cr(VI) and 200 and 400 mg/L As(III). Like a batch system, there were no inhibitory effects observed after 150 days of continuous operation, except in a situation where the microbial population was reduced because of a hydraulic wash-off. Second, Cr(VI) reduction efficiency across the longitudinal reactor column showed that Cr(VI) reduction or diffusion is proportional to the height of the column travelled.

Preliminary biokinetic parameter K_{mc}, K_{ms}, K_c, K_s, R_c, R_s and D_{wc} were successfully estimated from the experimental data obtained from the batch and continuous experiment, and this was simulated using a computer program for simulation of the aquatic system AQUASIM 2.0. Experimental data obtained in both batch and continuous experiments fitted well with the modified non-competitive model related to Cr(VI) reduction and As(III) oxidation under anaerobic conditions. Sensitivity analyses of these parameters show that K_{mc}, and K_c are the most sensitive to model predictions compared to R_c. However, the current model may be modified for application in engineered biological systems for treating wastewater with high concentrations of toxic metals that may co-exist in a contaminated environment.

8.2   Recommendations

A successful Cr(VI) reduction in the presence of As(III) was observed in a mixed culture of facultative anaerobes from Brits in North West Province, South Africa. However, this study did not quantify As(III) concentration in the continuous-flow system due to the limitation of As(III) measurement. Further studies are required to evaluate the simultaneous Cr(VI) reduction and As(III) oxidation in the continuous-flow system, as well as concurrent Cr(VI) and As(III) model analysis considering the biofilm system with single culture. However, the tendency of these facultative anaerobes to biocatalytically reduce Cr(VI) with concurrent oxidation of As(III), afford a promising steps towards bioremediation of Cr(VI) and As(III) in a chromium-arsenic-contaminated site.

Bibliography

1. Ahemad, M., 2014. Bacterial mechanisms for Cr (VI) resistance & reduction: an overview & recent advances. Folia microbiologica, 59(4), pp.321-332.

2. Ahmad, W.A., Zakaria, Z.A., Khasim, A.R., Alias, M.A. & Ismail, S.M.H.S., 2010. Pilot-scale removal of chromium from industrial wastewater using the ChromeBac™ system. Bioresource technology, 101(12), pp.4371-4378.

3. Ahmann, D., Roberts, A.L., Krumholz, L.R., & Morel, F.M., 1994. Microbe grows by reducing arsenic. Nature, 371(6500), pp.750-750.

4. Smith, A.H. & Steinmaus, C.M., 2009. Health effects of arsenic & chromium in drinking water: recent human findings. Annual review of public health, 30, pp.107-122.

5. &erson, G.L., Ellis, P.J., Kuhn, P. & Hille, R., 2001. Oxidation of arsenite by Alcaligenes faecalis. Environmental Chemistry of Arsenic (Frankenberger, WT, Jr., Ed.), pp.343-362.

6. &erson, G.L., Williams, J. & Hille, R., 1992. The purification & characterization of arsenite oxidase from Alcaligenes faecalis, a molybdenum-containing hydroxylase. Journal of Biological Chemistry, 267(33), pp.23674-23682.

7. Dastidar, A. & Wang, Y.T., 2010. Kinetics of arsenite oxidation by chemoautotrophic Thiomonas arsenivorans strain b6 in a continuous stirred tank reactor. Journal of Environmental Engineering, 136(10), pp.1119-1127.

8. American Public Health Association, American Water Works Association, Water Pollution Control Federation & Water Environment Federation, 1915. St&ard methods for the examination of water & wastewater (Vol. 2). American Public Health Association.

9. APHA/AWWA/WEF, 2012. St&ard Methods for the Examination of Water & Wastewater. St& Methods. In Eaton, A.D., Clesceri, L.S., Rice, E.W., Greenberg, A.E.,

Franson, M.A.H., Eds.; American Public Health Association, American Water Works Association, Water Environment Federation: Washington, D.C., USA, pp. 541.

10. Armitage, W.K., 2002. Chromium in South Africa's minerals industry 2001/200219th: South Africa Department of Minerals & Energy December 108-112.Bacterial Biofilms: a review of current research E. De Lancey Pulcini session III Néphrologie 22:439-441.

11. ATSDR, 2000. Chromium (TP-7) In: Toxicological Profile. US Department of Health & Human Services, Agency for Toxic Substances & Disease Registry, pp. 461.

12. ATSDR, 2008a. Chromium (TP-7) In: Toxicological Profile. US Department of Health & Human Services, Agency for Toxic Substances & Disease Registry, pp. 610.

13. Bachate, S.P., N&re, V.S., Ghatp&e, N.S. & Kodam, K.M., 2013. Simultaneous reduction of Cr (VI) & oxidation of As (III) by Bacillus firmus TE7 isolated from tannery effluent. Chemosphere, 90(8), pp.2273-2278.

14. Bachate, S.P., Khapare, R.M., & Kodam, K.M., 2012. Oxidation of arsenite by two β-proteobacteria isolated from soil. Applied microbiology & biotechnology, 93(5), pp.2135-2145

15. Bachmann, R.T., Wiemken, D., Tengkiat, A.B. & Wilichowski, M., 2010. Feasibility study on the recovery of hexavalent chromium from a simulated electroplating effluent using Alamine 336 & refined palm oil. Separation & Purification Technology, 75(3), pp.303-309.

16. Bailar, J.C., 1997, Chromium In: Parker, S.P. (Ed.), McGraw-Hill Encyclopaedia of Science & Technology, eighth ed. vol. 3. McGraw- Hill, New York.

17. Bansal, N., Coertee, J.J., Chirwa, E.M.N., 2017. In situ bioremediation of chromium (VI) in a simulated ferrochrome slag. Chemical Engineering Transactions, 61, pp. 55-60.

18. Barak, Y., Ackerley, D.F., Dodge, C.J., Banwari, L., Alex, C., Francis, A.J., & Matin, A., 2006. Analysis of novel soluble chromate & uranyl reductases & generation of an

improved enzyme by directed evolution. Applied & Environmental Microbiology, 72 (11), pp. 7074-7082

19.   Barceloux, D.G., 1999. Chromium, Clinical Toxicology 37(2), pp. 173-194.

20.   Barnhart, J., 1997. Occurrences, uses, & properties of chromium. Regulatory toxicology & pharmacology, 26(1), pp.S3-S7.

21.   Bates, M.N., Rey, O.A., Biggs, M.L., Hopenhayn, C., Moore, L.E., Kalman, D., Steinmaus, C., & Smith, A.H., 2004. Case-control study of bladder cancer & exposure to arsenic in Argentina. American Journal of Epidemiology, 159(4), pp.381-389.

22.   Beaudoin, D.L., Bryers, J.D., Cunningham, A.B. & Peretti, S.W., 1998. Mobilization of broad host range plasmid from Pseudomonas putida to established biofilm of Bacillus azotoformans. I. Experiments. Biotechnology & bioengineering, 57(3), pp.272-279.

23.   Becquer, T., Quantin, C., Sicot, M. & Boudot, J.P., 2003. Chromium availability in ultramafic soils from New Caledonia. Science of the Total Environment, 301(1-3), pp.251-261.

24.   Benramdane, L., Bressolle, F. & Vallon, J.J., 1999. Arsenic speciation in humans & food products: a review. Journal of chromatographic science, 37(9), pp.330-344..

25.   Berg, M., Tran, H.C., Nguyen, T.C., Pham, H.V., Schertenleib, R., & Giger, W., 2001. Arsenic contamination of groundwater & drinking water in Vietnam: a human health threat. Environmental science & technology, 35(13), pp.2621-2626.

26.   Beukes, J.P., Van Zyl, P.G. & Ras, M., 2012. Treatment of Cr (VI)-containing wastes in the South African ferrochrome industry-a review of currently applied methods. Journal of the Southern African Institute of Mining & Metallurgy, 112(5), pp.347-352.

27.   Beukes, J.P., Pienaar, J.J. & Lachmann, G., 2000. The reduction of hexavalent chromium by sulphite in wastewater-An explanation of the observed reactivity pattern. WATER SA-PRETORIA-, 26(3), pp.393-396.

28. Bhumbla, D.K., 1994. Aresnic mobilization & bioavailability in soils. Arsenic in the environment, Part I: Cycling & characterization, pp.51-82.

29. Boyle, R.W. & Jonasson, I.R., 1973. The geochemistry of arsenic & its use as an indicator element in geochemical prospecting. Journal of Geochemical Exploration, 2(3), pp.251-296.

30. Briggs, G.E. & Haldane, J.B.S., 1925. A note on the kinetics of enzyme action. Biochemical journal, 19(2), p.338.

31. Bryan, C.G., Marchal, M., Battaglia-Brunet, F., Kugler, V., Lemaitre-Guillier, C., Lièvremont, D., Bertin, P.N., & Arsène-Ploetze, F., 2009. Carbon & arsenic metabolism in Thiomonas strains: differences revealed diverse adaptation processes. BMC microbiology, 9(1), p.127.

32. Caldwell, D.E., 1995. Cultivation & study of biofilm communities, In H. M. Lappin Scott & J. W. Costerton (ed.), Microbial biofilms. University Press, Cambridge, U.K. p.64–79

33. Camargo, F.A.O., Bento, F.M., Okeke, B.C., & Frankenberger, W.T., 2003. Chromate reduction by chromium-resistant bacteria isolated from soils contaminated with dichromate. Journal of Environmental Quality, 32(4), pp.1228-1233.

34. Canadian Environmental Protection Act CEPA, 1994. Priority Substance List Assessment Report. Chromium & its compound.

35. Caravelli, A.H. & Zaritzky, N.E., 2009. About the performance of Sphaerotilus natans to reduce hexavalent chromium in batch & continuous reactors. Journal of hazardous materials, 168(2-3), pp.1346-1358.

36. Caravelli, A.H., Giannuzzi, L. & Zaritzky, N.E., 2008. Reduction of hexavalent chromium by Sphaerotilus natans a filamentous micro-organism present in activated sludges. Journal of Hazardous Materials, 156(1-3), pp.214-222.

37. Casiot, C., Pedron, V., Bruneel, O., Duran, R., Personné, J.C., Grapin, G., Drakidès, C., & Elbaz-Poulichet, F., 2006. A new bacterial strain mediating As oxidation in the Fe-rich biofilm naturally growing in a groundwater Fe treatment pilot unit. Chemosphere, 64(3), pp.492-496.

38. Cervantes, C., 1991. Bacterial interactions with chromate. Antonie van Leeuwenhoek, 59(4), pp.229-233.

39. Cervantes, C., Campos-García, J., Devars, S., Gutiérrez-Corona, F., Loza-Tavera, H., Torres-Guzmán, J.C. & Moreno-Sánchez, R., 2001. Interactions of chromium with microorganisms & plants. FEMS microbiology reviews, 25(3), pp.335-347.

40. Ch&ra, P., Sinha, S. & Rai, U.N., 1997. Bioremediation of chromium from water & soil by vascular aquatic plants. Phytoremediation of soil & water contaminants., pp.274-282.

41. Raja, C.E. & Omine, K., 2012. Arsenic, boron & salt resistant Bacillus safensis MS11 isolated from Mongolia desert soil. African Journal of Biotechnology, 11(9), pp.2267-2275..

42. Chen, J.M. & Hao, O.J., 1997. Biological removal of aqueous hexavalent chromium, Journal of Chemical Technology & Biotechnology, 69: pp.70-76.

43. Cheng, H., Hu, Y., Luo, J., Xu, B., & Zhao, J., 2009. Geochemical processes controlling fate & transport of arsenic in acid mine drainage (AMD) & natural systems. Journal of hazardous materials, 165(1-3), pp.13-26.

44. Cheung, K.H. & Gu, J.D., 2007. Mechanism of hexavalent chromium detoxification by microorganisms & bioremediation application potential: a review. International Biodeterioration & Biodegradation, 59(1), pp.8-15.

45. Cheunga, K.H. & Ji-Dong Gu, 2007. Mechanism of hexavalent chromium detoxification by microorganisms & bioremediation application potential: A review, Int. biodeterioration & biodegradation 59: pp.8–15

46. Chirwa, E.M. & Molokwane, P.E., 2011. Biological Cr(VI) reduction: Microbial diversity, kinetics & biotechnological solutions to pollution. In A. Sofo (Ed.), Biodiversity, InTech Online Publishers, United Kingdom. Chapter 5, pp.75-100.

47. Chirwa, E.M. & Wang, Y.T., 1997. Chromium (VI) reduction by Pseudomonas fluorescens LB300 in fixed-film bioreactor. Journal of Environmental Engineering, 123(8), pp.760-766.

48. Chirwa, E.M. & Wang, Y.T., 1997. Hexavalent chromium reduction by Bacillus sp. in a packed-bed bioreactor. Environmental science & technology, 31(5), pp.1446-1451.

49. Chirwa, E.M.N. & Wang, Y.T., 2000. Simultaneous Cr(VI) reduction & phenol degradation in an anaerobic consortium of bacteria. Water Research, 34(8), pp. 2376-2384.

50. Nkhalambayausi-Chirwa, E.M. & Wang, Y.T., 2001. Simultaneous chromium (VI) reduction & phenol degradation in a fixed-film coculture bioreactor: reactor performance. Water research, 35(8), pp.1921-1932.

51. Nkhalambayausi-Chirwa, E.M. & Wang, Y.T., 2004. Modeling hexavalent chromium removal in a Bacillus sp. fixed-film bioreactor. Biotechnology & bioengineering, 87(7), pp.874-883.

52. Clement, R.E. & Yang, P.W., 1997, Environmental analysis. Analytical Chemistry, 69 (12), 251R-287R.

53. Clifford, D.A., 1999. Ion exchange & Inorganic Adsorption. In R.D. Letterman, ed. Water Quality & Treatment: A H&book of Community Water Supplies, 5th ed., New York, NY: McGraw-Hill Inc.

54. Clifford, D.A., Ghurye, G.L. & Tripp, A.R., 2003. As removal using ion exchange with spent brine recycling. Journal-American Water Works Association, 95(6), pp.119-130.

55. Cortina, J.L., Litter, M.I., Gibert, O., Travesset, M., Ingallinella, A.M. & Fernández, R., 2016. Latin America experiences in arsenic removal from drinking water & mining effluents. J Total Environ, this issue.

56. Costa, M., 1997. Toxicity & carcinogenicity of Cr (VI) in animal models & humans. Critical reviews in toxicology, 27(5), pp.431-442.

57. Costerton, J.W. & Stewart, P.S., 2000. Persistent Bacterial Infections, Nataro JP, Blaser MJ, Cunningham-Rundles S, eds, ASM Press, Washington D.C. pg.; 423-39.

58. Crapart, S., Fardeau, M.L., Cayol, J.L., Thomas, P., Sery, C., Ollivier, B. & Combet-Blanc, Y., 2007. Exiguobacterium profundum sp. nov., a moderately thermophilic, lactic acid-producing bacterium isolated from a deep-sea hydrothermal vent. International Journal of Systematic & Evolutionary Microbiology, 57(2), pp.287-292.

59. Crapart, S., Fardeau, M.L., Cayol, J.L., Thomas, P., Sery, C., Ollivier, B. & Combet-Blanc, Y., 2007. Exiguobacterium profundum sp. nov., a moderately thermophilic, lactic acid-producing bacterium isolated from a deep-sea hydrothermal vent. International Journal of Systematic & Evolutionary Microbiology, 57(2), pp.287-292.

60. Cullen, W.R. & Reimer, K.J., 1989. Arsenic speciation in the environment. Chemical reviews, 89(4), pp.713-764.

61. Dastidar, A., 2010. Arsenite Oxidation by Pure Cultures of Thiomonas Arsenivorans Strain B6 in Bioreactor Systems.

62. Dastidar, A. & Wang, Y.T., 2009. Arsenite oxidation by batch cultures of Thiomonas arsenivorans strain b6. Journal of Environmental Engineering, 135(8), pp.708-715.

63. Davey, M.E. & O'toole, G.A., 2000. Microbial biofilms: from ecology to molecular genetics. Microbiology & molecular biology reviews, 64(4), pp.847-867.

64. Davies, J.A., Harrison, J.J., Marques, L.L., Foglia, G.R., Stremick, C.A., Storey, D.G., Turner, R.J., Olson, M.E., & Ceri, H., 2006. The GacS sensor kinase controls phenotypic

reversion of small colony variants isolated from biofilms of Pseudomonas aeruginosa PA14. FEMS microbiology ecology, 59(1), pp.32-46.

65. De Flora S., 2000. Threshold mechanisms & site specificity in chromium(VI) carcinogenesis. Carcinogenesis, 21(4), pp.533-541.

66. Dembitsky, V.M. & Levitsky, D.O., 2004. Arsenolipids. Progress in Lipd research., 43, pp.403-448.

67. Dhal, B., Thatoi, H.N., Das, N.N., & P&ey, B.D., 2013. Chemical & microbial remediation of hexavalent chromium from contaminated soil & mining/metallurgical solid waste: a review. Journal of hazardous materials, 250, pp.272-291.

68. Didier, L., Philippe, N.B., & Marie-Claire, L., 2009. Arsenic in contaminated waters: Biogeochemical cycle, microbial metabolism & biotreatment processes, Biochimie, 91, (10), pp.1229 – 1237.

69. Dong, X., Ma, L.Q., Gress, J., Harris, W. & Li, Y., 2014. Enhanced Cr (VI) reduction & As (III) oxidation in ice phase: important role of dissolved organic matter from biochar. Journal of hazardous materials, 267, pp.62-70.

70. Donlan, R.M. & Costerton, J.W., 2002. Biofilms: Survival Mechanisms of Clinically Relevant Microorganisms. Clinical Microbiology Reviews, 15(2), pp.167-193.

71. Elangovan, R. & Philip, L., 2009. Performance evaluation of various bioreactors for the removal of Cr(VI) & organic matter from industrial effluent, Biochemical Engineering Journal, 44, pp.174–186.

72. Ellis, P.J., Conrads, T., Hille, R., & Kuhn, P., 2001. Crystal structure of the 100 kDa arsenite oxidase from Alcaligenes faecalis in two crystal forms at 1.64 Å & 2.03 Å. Structure, 9(2), pp.125-132.

73. Emsley, J., 2011. Nature's building blocks: an AZ guide to the elements. Oxford University Press.

74. Encyclopedia, http://en.wikipedia.org/wiki/Chromium

75. Encyclopedia, https://en.wikipedia.org/wiki/Arsenic

76. Environmental Quebec, 1999. Politique de protection des sols et de Rehabilitations des Terrains Contamines. Government of Quebec Envirodoq EN980478.

77. EPA, 1995. Maximum Contaminant levels for inorganic contaminant. 40 CFR 141.62, US National Archives & Records Administration, Washington DC.

78. EVM Expert Group on Vitamins & Minerals Secretariat, 2002. Review of chromium. UK: EVM/99/26. REVISEDAUG2002, 25. 2002.

79. Federal Register, 2004. Occupational Safety & Health Administration. Occupational Exposure to Hexavalent Chromium. 69 Federal Register 59404.

80. Felsenstein, J., 1985. Confidence limits on phylogenies: an approach using the bootstrap. Evolution, 39 (4), , pp. 783-791.

81. Ferguson, J.F. & Gavis, J., 1972. A review of the arsenic cycle in natural waters. Water research, 6(11), pp.1259-1274.

82. Flemming, H.C., Neu, T.R. & Wozniak, D.J., 2007. The EPS matrix: the "house of biofilm cells". Journal of bacteriology, 189(22), pp.7945-7947.

83. Francesconi, K.A. & Edmonds, J.S., 1994. Determination of arsenic species in marine environmental samples, in: Arsenic in the Environment. Part I: Cycling & Characterization edited by Jerome O. Nriagu. John Wiley & Sons, Inc., New York.

84. Francis, C.A., Obraztsova, A.Y., & Tebo, B.M., 2000. Dissimilatory metal reduction by the facultative anaerobe Pantoea agglomerans SP1. Applied & environmental microbiology, 66(2), pp.543-548.

85. Garrido Hoyos, S.E., Avilés Flores, M., Ramírez Gonzalez, A., Grajeda Fajardo, C., Cardoso Zoloeta, S. & Velásquez Orozco, H., 2013. Comparing Two Operating

Configurations in a Full-Scale Arsenic Removal Plant. Case Study: Guatemala. Water, 5(2), pp.834-851.

86. Gear, C., 1971. The automatic integration of ordinary differential equations, Communication ACM, 14(3) , pp.176 – 179

87. Government of Canada, 1994c. Canadian Environmental Protection Act Priority Substances Assessment Report-Chromium & Its Compounds. Environment Canada & Health Canada, Ottawa.

88. Green, H.H., 1918. "Description of bacterium which oxidizes arsenite to arsenate, & one which reduces arsenate to arsenite, isolated from a cattle dipping-tank." South Africa.Journel of medical science, 14, pp.465-467

89. Gvozdyak, P.I., Mogilevich, N.F., Rylskii, A.F., & Grishchenko, N.I., 1986. Reduction of hexavalent chromium by collection strains of bacteria. Microbiology, 55(6), pp.770-773.

90. Han, F.X., Su, Y., Monts, D.L., Plodinec, M.J., Banin, A., & Triplett, G.E., 2003. Assessment of global industrial-age anthropogenic arsenic contamination. Naturwissenschaften, 90(9), pp.395-401.

91. Harper, D., 2001. Online etymology dictionary.

92. Harrison, J.J., Ceri, H., Roper, N.J., Badry, E.A., Sproule, K.M., & Turner, R.J., 2005. Persister cells mediate tolerance to metal oxyanions in Escherichia coli. Microbiology, 151(10), pp.3181-3195.

93. Hawley, E. L., Deeb, R. A., Kavanaugh, M. C., & Jacobs, J. A., 2004. Treatment technologies for chromium (VI). Chromium (VI) h&book, 275.

94. Heinrich-Salmeron, A., Cordi, A., Brochier-Armanet, C., Halter, D., Pagnout, C., Abbaszadeh-Fard, E., Montaut, D., Seby, F., Bertin, P.N., Bauda, P. & Arsène-Ploetze, F., 2011. Unsuspected diversity of arsenite-oxidizing bacteria revealed by a widespread

distribution of the aoxB gene in prokaryotes. Applied & environmental microbiology, pp.AEM-02884.

95. Helena, S.G., Bernine, K., Timothy, T., Jin-Kun, S., Jenna., J., Brajesh, D., Yong-Chul, J., & Yong, C., 2004. Arsenic & Chromium Speciation of Leachates from CCA-Treated Wood Report.

96. Hering, J.G., Katsoyiannis, I.A., Theoduloz, G.A., Berg, M., & Hug, S.J., 2017. Arsenic removal from drinking water: Experiences with technologies & constraints in practice (Doctoral dissertation, American Society of Civil Engineers).

97. Hering, J.G., Katsoyiannis, I.A., Theoduloz, G.A., Berg, M. & Hug, S.J., 2017. Arsenic removal from drinking water: Experiences with technologies & constraints in practice (Doctoral dissertation, American Society of Civil Engineers).

98. Horitsu H., Futo, S., Miyazawa Y., Ogai, S., & Kawai, K., 1987. Enzymatic reduction of hexavalent chromium by hexavalent chromium tolerant Pseudomonas ambigua G-1, Agricultural & Biological Chemistry, 51(9), pp.2417-2420.

99. IARC, 1990. Chromium, nickel & welding. IARC Monogr Eval Carcinog Risks Hum, 49: 1–648. PMID: 2232124.

100. ICDA (INTERNATIONAL CHROMIUM DEVELOPMENT ASSOCIATION), Statistical bulletin 2008 edition, 2008.

101. Igboamalu T.E, Chirwa E., 2016, Kinetic study of cr(vi) reduction in an indigenous mixed culture of bacteria in the presence of as(iii), Chemical Engineering Transactions, 49, pp. 439-444

102. Igboamalu T.E., Chirwa E.M.N., 2014, Cr6+ reduction in an indigenous mixed culture of bacteria in the presence of As3+, Chemical Engineering Transactions, 39, pp. 1237-1242

103. Igboamalu, T.E., Chirwa, E.M.N., 2014. Kinetic studies of Cr(VI) reduction in an indigenous mixed culture of bacteria in the presence of As(III). Proceedings of the Water Environment Federation, WEFTEC 2014, pp. 5308-5327.

104. Igboamalu, T.E., Chirwa, E.M.N., 2017. As(III) oxidation & Cr(VI) reduction insight in an indigenous mixed culture of anaerobic bacteria from a local environment. Chemical Engineering Transactions, 61, pp. 259–263.

105. Igboamalu, T.E. & Chirwa, E.M., 2018. As (III) Oxidation & Electron Mass Transfer Kinetic in an Enriched Mixed Culture of Bacillus sp., & Exiguobacterium sp., Isolated from Cow Dip in South Africa. Chemical Engineering Transactions, 64.

106. Ilialetdinov, A.N., Abdrashitova, S.A., 1981. Autotrophic oxidation of arsenic by a culture of Pseudomonas arsenitoxidans. Mikrobiologiya, 50, pp. 197-204.

107. International Agency for Research on Cancer, 1990. Chromium, nickel & welding," in IARC Monographs on the Evaluation of Carcinogenic Risks to Humans, vol. 49, The International Agency for Research on Cancer, Scientific Publications, Lyon, France.

108. Ishibashi, Y., Cervantes, C., & Silver, S., 1990. Chromium Reduction in Pseudomonas putida, Applied & Environmental Microbiology, 56(7), pp. 2268-2270.

109. Jain C., Ali I., 2000, Arsenic: occurrence, toxicity & speciation techniques. Water Research, 34, pp. 4304-4312

110. James BR (2002) Chemical transformations of chromium in soils: Relevance to mobility, bio-availability & remediation. In: The chromium file, no. 8, The International Chromium Development Association.http://www.chromium-asoc.com/publications/crfile8feb02.htm. Accessed: July 2001.

111. Jiang J.Q., Lloyd B., 2002, Progress in the development & use of ferrate(VI) salt as an oxidant & coagulant for water & wastewater treatment, Water research, 36, pp. 1397-1408.

112. Johnson, D.B., 2003. Chemical & microbiological characteristics of mineral spoils & drainage waters at ab&oned coal & metal mines. Water, Air & Soil Pollution: Focus, 3(1), pp.47-66.

113. Jukes, T.H., Cantor, C.R., 1969. Evolution of protein molecules, In Munro, H.N., (Ed.), Mammalian Protein Metabolism. Academic Press, New York, NY, pp. 21-123.

114. Kaimbi, L.A., Chirwa, E.M.N., 2013. Remobilization of trivalent chromium & the regeneration of in situ permeable reactive barriers during operation. Chemical Engineering Transactions, 35, pp. 835-840.

115. Kakonge, M., Microbial Cr(VI) reduction in indigenous cultures of bacterial, characterization & modelling Master's Thesis; University of Pretoria, Pretoria, South Africa; 2009. http://upetd.up.ac.za/thesis/available/etd-09222011-104550/ (accessed on 30/10/2010).

116. Katsoyiannis, I.A., Mitrakas, M. & Zouboulis, A.I., 2015. Arsenic occurrence in Europe: emphasis in Greece & description of the applied full-scale treatment plants. Desalination & Water Treatment, 54(8), pp.2100-2107.

117. Katz, S. & Salem, H., 1994. The Biological & Environmental Chemistry of Chromium. VCH Publishers, New York.

118. Kim, R.Y., Sung, J.K., Lee, J.Y., Kim, S.C., Jang, B.C., Kim, W.I., & Ok, Y.S., 2010. Chromium distribution in Korean soils: A review. Korean Journal of Soil Science & Fertilizer, 43(3), pp.296-303.

119. Kimbrough, D.E., Cohen, Y., Winer, A.M., Creelman, L., & Mabuni, C., 1999. A critical assessment of chromium in the environment, Critical Reviews, Environmental Science & Technology, 29(1), pp. 1–46.

120. Knowles, F.C. & Benson, A.A., 1983. The biochemistry of arsenic. Trends Biochemical Science., 8, pp. 178-180.

121. Köhler, M., Hofmann, K., Völsgen, F., Thurow, K., * Koch, A., 2001. Bacterial release of arsenic ions & organoarsenic compounds from soil contaminated by chemical warfare agents. Chemosphere, 42(4), pp.425-429.

122. Komori, K., Wang, P.C., Toda, K., & Ohtake, H., 1989. Factors affecting chromate reduction in Enterobacter cloacae strain HO1. Applied microbiology & biotechnology, 31(5-6), pp.567-570.

123. Kotaś, J. & Stasicka, Z., 2000. Chromium occurrence in the environment & methods of its speciation. Environmental Pollution 107 (3), pp. 263–283.

124. Kruger, M.C., Bertin, P.N., Heipieper, H.J., & Arsène-Ploetze, F., 2013. Bacterial metabolism of environmental arsenic—mechanisms & biotechnological applications. Applied microbiology & biotechnology, 97(9), pp.3827-3841.

125. Kruger, M.C., Bertin, P.N., Heipieper, H.J., & Arsène-Ploetze, F., 2013. Bacterial metabolism of environmental arsenic—mechanisms & biotechnological applications. Applied microbiology & biotechnology, 97(9), pp.3827-3841.

126. Kumar, A., Balouch, A., Pathan, A.A., Mahar, A.M., Abdullah, Jagirani, M.S., Mustafai, F.A., Zubair, M., Laghari, B., & Panah, P., 2017. Remediation techniques applied for aqueous system contaminated by toxic Chromium & Nickel ion. Geology, Ecology, & L&scapes, 1 (2), pp. 143-153.

127. Kumar, A.R. & Riyazuddin, P., 2010. Preservation of inorganic arsenic species in environmental water samples for reliable speciation analysis. TrAC Trends in Analytical Chemistry, 29(10), pp.1212-1223.

128. Kvasnikov, E.I., Stepanyuk, V.V., Klyushnikova, T.M., Serpokrylov, N.S., Simonova, G.A., Kasatkina, T.P., & Panchenko, L.P., 1985. A new chromium reducing, gram variable bacterium with mixed type of flagellation. Microbiology, 54(1), pp.69-75.

129. Lebedeva, E.V. & Lyalikova, N.N., 1979. REDUCTION OF CROCOITE BY PSEUDOMONAS-CHROMATOPHILA SP-NOV. Microbiology, 48(3), pp.405-410.

130. Leonard, A.L., 1991. Arsenic Metals & their compounds in the environment, VCH, Weinheim, pp. 751–772

131. Levenspiel, O., 1999. Chemical Reaction Engineering, 2nd Ed. Wiley Eastern Ltd, pp. 41-92.

132. LeVeque, R.J., 1990. Conservative methods for nonlinear problems. In Numerical Methods for Conservation Laws, pp. 122-135.

133. Li, Z., Jones, H.K., Zhang, P. & Bowman, R.S., 2007. Chromate transport through columns packed with surfactant-modified zeolite/zero valent iron pellets. Chemosphere, 68(10), pp.1861-1866.

134. Lièvremont, D., Bertin, P.N., & Lett, M.C., 2009. Arsenic in contaminated waters: biogeochemical cycle, microbial metabolism & biotreatment processes. Biochimie, 91(10), pp.1229-1237.

135. Lim, K.T., Shukor, M.Y., & Wasoh, H., 2014. Physical, chemical, & biological methods for the removal of arsenic compounds. BioMed research international, 2014.

136. Llovera, S., Bonet, R., Simon-Pujol, M.D., & Congregado, F., 1993. Chromate reduction by resting cells of Agrobacterium radiobacter EPS-916. Applied & Environmental Microbiology, 59(10), pp.3516-3518.

137. Llovera, S., Bonet, R., Simon-Pujol, M.D., & Congregado, F., 1993. Effects of culture medium ions on chromate reduction by resting cells of Agrobacterium radiobacter. Appl Microbiol Biotechnol, 39, pp. 424–426.

138. Lloyd, J.R., 2003. Microbial reduction of metals & radionuclides. FEMS Microbiology Reviews., 27, pp.411-425.

139. Lovley, D.R. & Phillips, E.J., 1994. Reduction of chromate by Desulfovibrio vulgaris & its c3 cytochrome. Applied & Environmental Microbiology, 60(2), pp.726-728.

140. Lovley, D.R. & Coates, J.D., 1997. Bioremediation of metal contamination. Current Opinion in Biotechnology. 8, pp.285-289

141. Lu, A. Zhong, S., Chen, J., Shi, J., Tang, J., & Lu, X., 2006. Removal of Cr(VI) & Cr(III) from aqueous solutions & industrial wastewaters by natural clino-pyrrhotite. Environmental Science & Technology, 40 (9), pp.3064-3069.

142. Mabrouk, M.E.M., Arayes, M.A., & Sabry, S.A., 2014. Hexavalent chromium reduction by chromate-resistant haloalkaliphilic Halomonas sp. M-Cr newly isolated from tannery effluent. Biotechnology & Biotechnological Equipment, 28 (4), 659-667.

143. MacLeod, F.A., Guiot, S.R. & Costerton, J.W., 1990. Layered structure of bacterial aggregates produced in an upflow anaerobic sludge bed & filter reactor. Applied & Environmental Microbiology, 56(6), pp.1598-1607.

144. Macy, J.M., Nunan, K., Hagen, K.D., Dixon, D.R., Harbour, P.J., Cahill, M., & Sly, L.I., 1996. Chrysiogenes arsenatis gen. nov., sp. nov., a new arsenate-respiring bacterium isolated from gold mine wastewater. International Journal of Systematic & Evolutionary Microbiology, 46(4), pp.1153-1157.

145. Marcovecchio, J.E., Botte, S.E., & Freije, R.H., 2007. Heavy metals, major metals, trace elements. In: Nollet, L.M.L. (Ed.), H&book of Water Analysis, second ed. CRC Press, London, pp. 275–311.

146. McEwan, A.G., Ridge, J.P., McDevitt, C.A., & Hugenholtz, P., 2002. The DMSO reductase family of microbial molybdenum enzymes; molecular properties & role in the dissimilatory reduction of toxic elements. Geomicrobiology Journal, 19(1), pp.3-21.

147. Megharaj, M., Avudainayagam, S., & Naidu, R., 2003. Toxicity of hexavalent chromium & its reduction by bacteria isolated from soil contaminated with tannery waste. Current microbiology, 47(1), pp.0051-0054.

148. Meli, C.K., 2009. Microbial Cr(VI) Reduction in Indigenous Cultures of Bacteria: Characterization & Modelling. Master of Science Dissertation, University of Pretoria. http://repository.up.ac.za/bitstream/h&le/2263/29842/dissertation.pdf;sequence=1.

149. Merian, E., 1984. Introduction on environmental chemistry & global cycles of Arsenic, Beryllium, Cadmium, Chromium, Cobalt, Nickel, Selenium, & their derivatives. Toxicological & Environmental Chemistry, pp.8:9-38.

150. Michel, C., Brugna, M., Aubert, C., Bernadac, A. & Bruschi, M., 2001. Enzymatic reduction of chromate: comparative studies using sulfate-reducing bacteria. Applied Microbiology & Biotechnology, 55(1), pp.95-100.

151. Mintek 2004, Mining & Metallurgy in South Africa; A Pictorial History. Mintek, in association with Phase 4:50

152. Mohan, D. & Pittman Jr, C.U., 2007. Arsenic removal from water/wastewater using adsorbents—a critical review. Journal of hazardous materials, 142(1-2), pp.1-53.

153. Mohan, D. & Pittman Jr, C.U., 2007. Arsenic removal from water/wastewater using adsorbents—a critical review. Journal of hazardous materials, 142(1-2), pp.1-53.

154. Molchanov, S., Gendel, Y., Ioslvich, I., & Lahav, O., 2007. Improved Experimental & Computational Methodology for Determining the Kinetic Equation & the Extant Kinetic Constants of Fe (II) Oxidation by Acidithiobacillus ferrooxidans. Applied Environmental. Microbiology, 73, pp.1742-1752.

155. Molokwane, P. E., Meli, K. C., & Nkhalambayausi-Chirwa, E. M. 2008. Chromium (VI) reduction in activated sludge bacteria exposed to high chromium loading: Brits culture (South Africa). Water research, 42(17), pp.4538-4548.

156. Molokwane, P.E. & Nkhalambayausi-Chirwa, E.M., 2009. Microbial culture dynamics & chromium (VI) removal in packed-column microcosm reactors. Water Science & Technology, 60(2), pp.381-388.

157. Molokwane, P.E. & Chirwa, E.M.N., 2009. Microbial culture dynamics & chromium (VI) removal in packed-column microcosm reactors. Water Science & Technology, 60(2), pp.381-388.

158. Molokwane, P.E. & Chirwa, E.M.N., 2013. Modelling biological Cr(VI) reduction in aquifer microcosm column systems. Water Science & Technology, 67 (12), pp.2733-2738

159. Mordenti, A., Piva, A., & Piva, G.I.A.N.F.R.A.N.C.O., 1997. The European perspective on organic chromium in animal nutrition. In Biotechnology in The Feed Industry. Proc. Alltech's 13th Annual Symposium. Nottingham University Press, Nottingham.

160. Mtimunye, P.J. & Chirwa, E.M.N., 2014. Characterization of the biochemical-pathway of uranium (VI) reduction in facultative anaerobic bacteria. Chemosphere, 113, pp.22-29.

161. Mtimunye, P.J. Steady-state model for hexavalent chromium reduction in simulated biological reactive barrier: microcosm analysis: Master's Thesis; University of Pretoria, Pretoria, South Africa; 2011. http://upetd.up.ac.za/thesis/available/etd-09222011-104550/ (accessed on 30/10/2012).

162. Mukhopadhyay R., Rosen B.P., Phung L.T., & Silver, S., 2002, Microbial arsenic: from geocycles to genes & enzymes. FEMS microbiology reviews, 26, pp.311-325.

163. Muller D., Lievremont D., Simeonova D.D., Hubert J.C., & Lett M.C., 2003, Arsenite oxidase aox genes from a metal-resistant β-proteobacterium, Journal of bacteriology, 185, pp.135-141.

164. Namasivayam, C. & Senthilkumar, S., 1998. Removal of arsenic (V) from aqueous solution using industrial solid waste: adsorption rates & equilibrium studies. Industrial & engineering chemistry research, 37(12), pp.4816-4822.

165. Nelder, J. & Mead, R., 1965. A simplex method for function minimization. Computer Journal, 7, pp.308 – 313

166. Nickens, K.P., Patierno, S.R., & Ceryak, S., 2010. Chromium genotoxicity: a double-edged sword. Chemico-biological interactions, 188(2), pp.276-288.

167. Nicolella, C., Van Loosdrecht, M.C.M., & Heijnen J.J., 2000. Particle-based Biofilm Reactor Technology. Tibtech, 18, pp.312-320.

168. Nies, D.H. & Silver, S., 1995. Ion efflux systems involved in bacterial metal resistances. Journal of industrial microbiology, 14(2), pp.186-199.

169. Nordstrom, D.K., 2002. Worldwide Occurrences of Arsenic in Ground Water, Science. 296, pp.2143-2145.

170. Ohtake, H., Fujii E., & Toda, K., 1990. Reduction of toxic chromate in an industrial effluent by use of a chromate-reducing strain of Enterobacter cloacae, Environmental Technology, 11, pp.663-668.

171. Oliveira, H., 2012. Chromium as an Environmental Pollutant: Insights on Induced Plant Toxicity, Journal of Botany, 2012, pp.1-8.

172. Oreml&, R.S. & Stolz, J.F., 2003. The Ecology of Arsenic. Science., 300 (5621) , pp. 939 - 944.

173. Oreml&, R.S., Hoeft, S.E., Santini, J.M., Bano, N., Hollibaugh, R.A., & Hollibaugh, J.T., 2002. Anaerobic oxidation of arsenite in Mono Lake water & by a facultative, arsenite-oxidizing chemoautotroph, strain MLHE-1. Applied & Environmental Microbiology, 68(10), pp.4795-4802.

174. Oreml&, R.S., Saltikov, C.W., Wolfe-Simon, F., & Stolz, J.F., 2009. Arsenic in the evolution of earth & extraterrestrial ecosystems. Geomicrobiology Journal, 26(7), pp.522-536.

175. OSHA Federal Register, 2006. Occupational Exposure to Hexavalent Chromium; Final Rule, Occupational Safety & Health Administration, 71 (39), 29 CFR Parts 1910-1926.

176. O'Toole, G. A. & Mah, T.F.C., 2001. Mechanisms of biofilm resistance to antimicrobial agents. Trends in microbiology, 9(1) , pp.34-39.

177. Páez-Espino, D., Tamames, J., de Lorenzo, V., & Cánovas, D., 2009. Microbial responses to environmental arsenic. Biometals, 22(1), pp.117-130.

178. Palmer, C.D. & Wittbrodt, P.R., 1991. Processes affecting the remediation of chromium-contaminated sites. Environmental health perspectives, 92, p.25.

179. Papp, J. F., 1999. U.S. Geological Survey. Minerals Yearbook, 17: 1-17.8

180. Park, D., Yun, Y. S., Hye Jo, J., & Park, J. M., 2005. Mechanism of hexavalent chromium removal by dead fungal biomass of Aspergillus niger. Water Research, 39(4) , pp.533-540.

181. Pechova, A. & Pavlata, L., 2007. Chromium as an essential nutrient: a review. Veterinarni Medicina, 52 (1), pp. 1-18.

182. Perry, B.D., 2016. The control of East Coast fever of cattle by live parasite vaccination: A science-to-impact narrative. One Health, 2, pp. 103-114.

183. Petrilli, F. L. & De Flora, S., 1977. Toxicity & mutagenicity of hexavalent chromium on Salmonella typhimurium, Applied & Environmental Microbiology, 33(4), pp.805–809.

184. Petzold, L., 1983. Adescription of DASSL: A differential/algebraic system solver. In Stepleman, R. E., editor, Scientific Computing, IMACS/North-Holl&, pp. 65-68.

185. Ralston, M. & Jennrich, R. 1978. DUD – a derivative-free algorithm for non-linear least squares. Technometrics, 20(1), pp. 7- 14.

186. Ramudzuli, M.R. & Horn, A.C. 2014. Arsenic residues in soil at cattle dip tanks in the Vhembe district, Limpopo Province, South Africa. South African Journal of Science, 110 (7-8) , pp. 1-7.

187. Reichart, P., 1998. Swiss Federal Institute for Environmental Science & Technology (EAWAG) CH Dubendorf, Switzerl&, ISBN: 3906484-16-5.

188. Rhine, E.D., Onesios, K.M., Serfes, M.E., Reinfelder, J.R. & Young, L.Y., 2008. Arsenic transformation & mobilization from minerals by the arsenite oxidizing strain WAO. Environmental science & technology, 42(5), pp.1423-1429.

189. Rhine, E.D., Phelps, C.D., & Young, L.Y. 2006. Anaerobic arsenite oxidation by novel denitrifying isolates. Environmental Microbiology. 8(5), pp.899-908.

190. Rittmann, B.E. & McCarty, P.L., 2001. Environmental Biotechnology: Principles & Application. McGraw-Hill, New York.

191. Rizvi, F.Z., Kanwal, W. & Faisal, M., 2016. Chromate-Reducing Profile of Bacterial Strains Isolated from Industrial Effluents. Polish Journal of Environmental Studies, 25(5).

192. Rodriguez E., Azevedo, R., Fern&es, P., & Santos, C., 2011 Cr(VI) induces DNA damage, cell cycle arrest & polyploidization: a flow cytometric & comet assay study in Pisum sativum, Chemical Research in Toxicology, 24(7), pp.1040-1047.

193. Romanenko V.I. & Koren'kov V.N., 1977. A pure culture of bacteria utilizing chromate & dichromate as hydrogen acceptors in growth under anaerobic conditions." Mikrobiologiya, 46, pp. 414– 417.

194. Romanenko, V.I. & Koren'kov, V.N., 1977. Pure culture of bacteria using chromates & bichromates as hydrogen acceptors during development under anaerobic conditions. Mikrobiologiia, 46(3), pp.414-417.

195. Rosen B.P., 2002. Biochemistry of arsenic detoxification. FEBS letters,529,86-92

196. Roslev, P., Madsen, P.L., Thyme, J.B., & Henriksen, K., 1998. Degradation of phthalate & di-(2-ethylhexyl) phthalate by indigenous & inoculated microorganisms in sludge-amended soil. Applied & Environmental Microbiology, 64 (12) , pp. 4711-4719.

197. Sami, K. & Druzynski, A.L., 2003. Predicted Spatial Distribution of Naturally Occurring Arsenic, Selenium & Uranium in Groundwater in South Africa-Reconnaissance Survey-Water Research Commission, WRC Report.

198. Sancha, A.M., 2006. Review of coagulation technology for removal of arsenic: case of Chile. Journal of health, population, & nutrition, 24(3), pp.267.

199. Santini J.M., Sly L.I., Schnagl R.D., Macy J.M., 2000, A new chemolithoautotrophic arsenite-oxidizing bacterium isolated from a gold mine: phylogenetic, physiological, & preliminary biochemical studies, Applied & environmental microbiology,66, pp.92-97.

200. Schwartz, R.A., 1997. Arsenic & the skin. International journal of dermatology, 36(4), pp.241-250.

201. Singh, S., Lee, W., DaSilva, N.A., Mulch&ani, A. & Chen, W., 2008. Enhanced arsenic accumulation by engineered yeast cells expressing Arabidopsis thaliana phytochelatin synthase. Biotechnology & bioengineering, 99(2), pp.333-340.

202. Shanker, A.K., Cervantes, C., Loza-Tavera, H., & Avudainayagam, S., 2005. Chromium toxicity in plants, Environment International, 31: 739–753.

203. Sharma, D.C., Chatterjee, C., & Sharma, C.P., 1995. Chromium accumulation & its effects on wheat (Triticum aestivum L. cv. HD 2204) metabolism. Plant Science 111, pp.145–151.

204. Sharma, K., 2002. Microbial Cr(VI) reduction: role of electron donors, acceptors, & mechanisms, with special emphasis on clostridium spp, A dissertation presented by graduate school of University of Florida in partial fulfilment of the requirement for the degree of doctor philosophy. University of Florida.

205. Shen, H. & Wang, Y.T., 1994. Biological reduction of chromium by E. coli. Journal of Environmental engineering, 120(3), pp.560-572.

206. Shen, H. & Wang, Y., 1993. Characterization of enzymatic reduction of hexavalent chromium by Escherichia coli ATCC 33456. Applied & Environmental Microbiology, 59(11), pp.3771-3777.

207. Shen, H. & Wang, Y.T., 1995. Modeling simultaneous hexavalent chromium reduction & phenol degradation by a defined coculture of bacteria. Biotechnology & bioengineering, 48(6), pp.606-613.

208. Shupack, S.I., 1991. The chemistry of chromium & some resulting analytical problems. Environmental Health Perspectives, 92, pp.7-11.

209. Silver, S. & Phung, L.T., 2005. A bacterial view of the periodic table: genes & proteins for toxic inorganic ions. Journal of Industrial Microbiology & Biotechnology, 32(11-12), pp.587-605.

210. Singh, S., Lee, W., DaSilva, N.A., Mulch&ani, A., & Chen, W., 2008. Enhanced arsenic accumulation by engineered yeast cells expressing Arabidopsis thaliana phytochelatin synthase. Biotechnol. Bioeng., 99 (2), pp.333 - 340.

211. Smedley, P.L. & Kinniburgh, D.G., 2002. A review of the source, behavior & distribution of arsenic in natural waters. Applied Geochemistry. 17, pp.517-568.

212. Smedley, P.L., Edmunds, W.M., & Pelig-Ba, K.B., in: J.D. Appleton, R. Fuge, G.J.H. McCall (Eds.), Environmental Geochemistry & Health, vol. 113, Geological Society Special Publication, London, 1996, , pp.153.

213. Smith, A.H., Hopenhayn-Rich, C., Bates, M.N., Goeden, H.M., Hertz-Picciotto, I., Duggan, H.M., Wood, R., Kosnett, M.J. & Smith, M.T., 1992. Cancer risks from arsenic in drinking water. Environmental health perspectives, 97, pp.259-267.

214. Stolz, J.F. & Oreml&, R.S., 1999. Bacterial respiration of arsenic & selenium. FEMS microbiology reviews, 23(5), pp.615-627.

215. Stolz, J.F., Basu, P., Santini, J.M. & Oreml&, R.S., 2006. Arsenic & selenium in microbial metabolism. Annu. Rev. Microbiol., 60, pp.107-130.

216. Stoodley P., Boyle J.D., De Beer, D., & Lappin-Schott H.M., 1999. Evolving perspectives of biofilm structure, Biofoling, 14(1) , pp.75-90.

217. Sullivan, C., Tyrer, M., Cheeseman, C.R. & Graham, N.J., 2010. Disposal of water treatment wastes containing arsenic—a review. Science of the Total Environment, 408(8), pp.1770-1778.

218. Sun, W., Sierra-Alvarez, R., Hsu, I., Rowlette, P. & Field, J.A., 2010. Anoxic oxidation of arsenite linked to chemolithotrophic denitrification in continuous bioreactors. Biotechnology & bioengineering, 105(5), pp.909-917.

219. Sun, W., Sierra- Alvaryz, R., Milner, L., & Field, J., 2008. Anoxic oxidation of Arsenite linked to denitrification in sludge & sediment, Water Research; 42, pp. 4569 – 4577.

220. Sun, W., Sierra-Alvarez, R., Milner, L. & Field, J.A., 2010. Anaerobic oxidation of arsenite linked to chlorate reduction. Applied & environmental microbiology, 76(20), pp.6804-6811.

221. Suttigarn A. & Wang Y.T., 2005, Arsenite oxidation by, Alcaligenes faecalis strain O1201, Journal of Environmental Engineering, 31, pp.1293-1301

222. Suzuki, T.O.H.R.U., Miyata, N., Horitsu, H., Kawai, K., Takamizawa, K., Tai, Y. & Okazaki, M., 1992. NAD (P) H-dependent chromium (VI) reductase of Pseudomonas ambigua G-1: a Cr (V) intermediate is formed during the reduction of Cr (VI) to Cr (III). Journal of bacteriology, 174(16), pp.5340-5345.

223. Tamura, K., Stecher, G., Peterson, D., Filipski, A., & Kumar, S., 2013. MEGA6: Molecular Evolutionary Genetics Analysis version 6.0. Molecular Biology & Evolution, 30 (12) , pp 2725-2729.

224. Tapase, S.R. & Kodam, K.M., 2018. Assessment of arsenic oxidation potential of Microvirga indica S-MI1b sp. nov. in heavy metal polluted environment. Chemosphere, 195, pp.1-10.

225. Tchounwou, P.B., Centeno, J.A., & Patlolla, A.K., 2004, Arsenic toxicity, mutagenesis, & carcinogenesis–a health risk assessment & management approach, Molecular & cellular biochemistry, 255, pp 47-55

226. Thacker, U., Parikh, R., Shouche, Y., & Madamwar, D., 2006. Hexavalent chromium reduction by Providencia sp. Process Biochemistry, 41(6), pp.1332-1337.

227. Thomas Jefferson, 2018. Arsenic Element. National Accelerator Facility - Office of Science Education, https://education.jlab.org/itselemental/ele033.html

228. Thomas Jefferson, 2018. Arsenic Element. National Accelerator Facility - Office of Science Education, https://education.jlab.org/itselemental/ele033.html

229. Tsuji, J.S., Perez, V., Garry, M.R., & Alex&er, D.D., 2014. Association of low-level arsenic exposure in drinking water with cardiovascular disease: A systematic review & risk assessment. Toxicology, 323, pp. 78-94.

230. Turner, A., 1999. the story so far: An overview of developments in UK food regulation & associated advisory committees. British food journal, 101(4), pp.274-284.

231. Turpeinen, R., Kairesalo, T., & Häggblom, M. M., 2004. Microbial community structure & activity in arsenic-, chromium-& copper-contaminated soils. FEMS Microbiology Ecology, 47(1), pp. 39-50.

232. U.S. (NAS), 1974.Geochemistry & the environment. Washington DC. U.S. Government Printing Office.

233. U.S. EPA National Primary Drinking Water Regulations, Federal Register 65(2000): 63027.

234. Vahidnia, A., Van der Voet, G.B., & De Wolff, F.A., 2007. Arsenic neurotoxicity—a review. Human & experimental toxicology, 26(10), pp.823-832.

235. Viamajala, S., Peyton, B.M. & Petersen, J.N., 2003. Modeling chromate reduction in Shewanella oneidensis MR-1: Development of a novel dual-enzyme kinetic model. Biotechnology & bioengineering, 83(7), pp.790-797.

236. Vidali, M., 2001. Bioremediation. an overview. Pure & Applied Chemistry, 73(7), pp.1163-1172.

237. Volesky, B. & May-Phillips, H.A., 1995. Biosorption of heavy metals by Saccharomyces cerevisiae. Applied Microbiology & Biotechnology, 42(5), pp.797-806.

238. Wackett, L.P., Dodge, A.G. & Ellis, L.B., 2004. Microbial genomics & the periodic table. Applied & Environmental Microbiology, 70(2), pp.647-655.

239. Wagman, D.D., Evan, W.H., Parker, V.B., Halow, I., Bailey, S.M., & Schumn, R.H., 1968. Selected Values of Chemical Thermodynamic Properties, Technical Note. 270-3, NBS, Washington, 95-98.

240. Wang, Y. & Shen, H., 1997. Modelling Cr(VI) reduction by pure bacterial cultures. Water Research, 31, pp. 727-732.

241. Wang, Y.T. & Shen, H., 1995. Bacterial reduction of hexavalent chromium. Journal of Industrial Microbiology, 14(2), pp.159-163.

242. Wang, Y.T., Chirwa, E.M. & Shen, H., 2000. Cr (VI) reduction in continuous-flow coculture bioreactor. Journal of Environmental Engineering, 126(4), pp.300-306.

243. Wang, Z., Bush, R.T., Sullivan, L.A. & Liu, J., 2013. Simultaneous redox conversion of chromium (VI) & arsenic (III) under acidic conditions. Environmental science & technology, 47(12), pp.6486-6492.

244. Wanner, O., Cunningham A., & Lundman, R., 1995. Modeling biofilm accumulation & mass transport in a porous medium under high substrate loading. Biotechnology & Bioengineering, 47, pp. 703 – 712.

245. Wanner, O. & Gujer, W., 1984. Competition in biofilm. Water Science Technoogy, 17:27 – 44

246. Watnick, P.I. & Kolter, R., 1999. Steps in the development of a Vibrio cholera biofilm. Mol. Microbiol., 34, pp. 586-595.

247. Wessels, C.E., 2017. Reduction of selenium by Pseudomonas Stutzeri NT-l; Growth reduction & kinetics. MEng Dissertation, University of Pretoria. Available online at: https://repository.up.ac.za/h&le/2263/62802.

248. WHO Arsenic Compounds, Environmental Health Criteria 224, 2nd ed., World Health Organisation, Geneva, 2001.

249. Williams, M., 2001. Arsenic in mine waters: an international study. Environmental Geology, 40(3), pp.267-278.

250. Woutersen, R.A., Appelman, L.M., Van Garderen-Hoetmer, A., & Feron, V.J., 1986. Inhalation toxicity of acetaldehyde in rats. III. Carcinogenicity study. Toxicology, 41(2), pp. 213-231.

251. Yamauchi, H. & Fowler, B.A., 1994. Toxicity & metabolism of inorganic & methylated arsenicals. In: Arsenic in the Environment. Part II: Human Health & Ecosystem Effects editedby Jerome O. Nriagu. John Wiley & Sons, Inc., New York.

252. Zahoor, A. & Rehman, A., 2009. Isolation of Cr (VI) reducing bacteria from industrial effluents & their potential use in bioremediation of chromium containing wastewater. Journal of Environmental Sciences, 21(6), pp.814-820.

253. Zakaria, Z.A., Zakaria, Z., Surif, S., & Ahmad, W.A., 2007. Biological detoxification of Cr(VI) using wood-husk immobilized Acinetobacter haemolyticus. Journal of Hazardous Materials, 148 (1–2), pp.164-171.

254. Zayed, A.M. & Terry, N., 2003. Chromium in the environment: Factors affecting biological remediation. Plant soil, 249, pp.139-156.

APPENDIX A
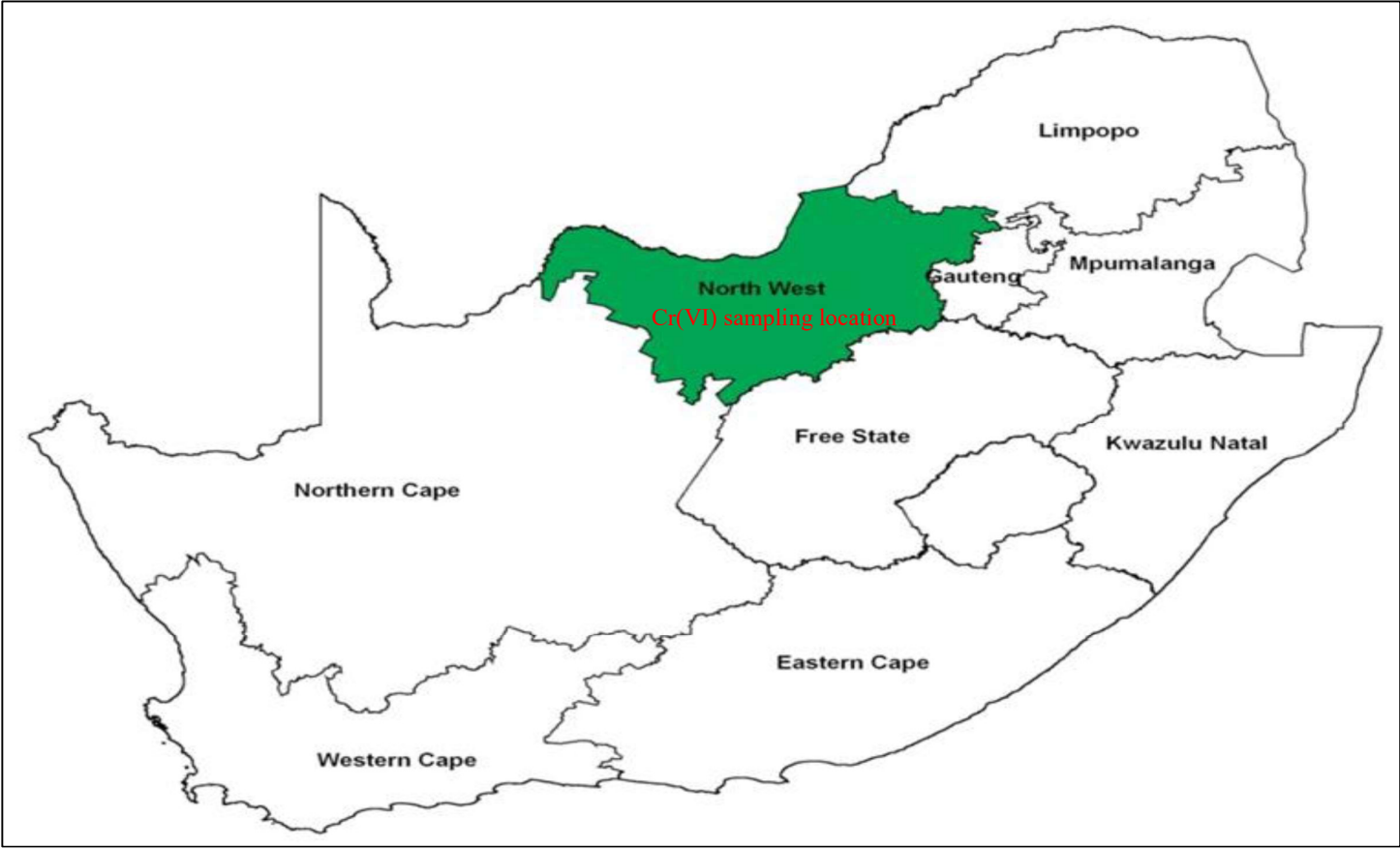
Brit WWTW Sampling locations

APPENDIX B

The location off the soil and water samples from a cow dip farm in Tzaneen, Limpopo Province, South Africa

APPENDIX C

```
***************************************************************
*********
AQUASIM Version 2.0 (win/mfc) - Listing of System Definition

***************************************************************
*********
Date and time of listing:  04/23/2018 19:38:44
***************************************************************
*********
Variables
***************************************************************
*********
As_meas:        Description:        As(III) measured
                Type:               Real List Variable
                Unit:               mg/L
                Argument:           T
                Standard Deviations: global
                Rel. Stand. Deviat.: 0
                Abs. Stand. Deviat.: 1
                Minimum:            0
                Maximum:            1e+009
                Interpolation Method: linear interpolation
                Sensitivity Analysis: inactive
                Real Data Pairs (13 pairs):
                    0           75.074
                    1           51.838
                    2           47.01
                    6           33.668
                    12          25.5045
                    24          17.341
                    48          3.899
                    72          4.4
                    96          4.4
                    120         2.9575
                    192         1.515
                    216         0.7575
                    240         0
----------------------------------------------------------------
---------
C:              Description:        Concentration
                Type:               Dyn. Volume State Var.
                Unit:               mg/L
                Relative Accuracy:  1e-006
                Absolute Accuracy:  1e-006
----------------------------------------------------------------
---------
Co:             Description:        Inital concentration
                Type:               Formula Variable
```

```
              Unit:               mg/L
              Expression:         70
--------------------------------------------------------------
---------
Cr:           Description:        Cr(VI) toxicity threshold
concentra
                                  tion
              Type:               Formula Variable
              Unit:               mg/L
              Expression:         50
--------------------------------------------------------------
---------
C_meas:       Description:        Cr(VI) measured
              Type:               Real List Variable
              Unit:               mg/L
              Argument:           T
              Standard Deviations: global
              Rel. Stand. Deviat.: 0
              Abs. Stand. Deviat.: 1
              Minimum:            0
              Maximum:            1e+009
              Interpolation Method: linear interpolation
              Sensitivity Analysis: inactive
              Real Data Pairs (12 pairs):
                 0              70
                 2              70
                 6              70
                 12             62.035928
                 24             54.071856
                 48             49.135063
                 72             48.203593
                 96             47.272122
                 120            45.432468
                 192            43.592814
                 216            41.54358
                 240            40.192947
--------------------------------------------------------------
---------
k:            Description:        limiting constant
              Type:               Formula Variable
              Unit:               mg/L
              Expression:         4.31716
--------------------------------------------------------------
---------
K_c:          Description:        half velocity
concentration
              Type:               Constant Variable
              Unit:               mg/L
              Value:              986.31219
              Standard Deviation: 1
```

```
                  Minimum:              0
                  Maximum:              1000
                  Sensitivity Analysis: active
                  Parameter Estimation: active
-----------------------------------------------------------------
---------
K_i:              Description:          inhibition coefficient
                  Type:                 Formula Variable
                  Unit:                 mg/L
                  Expression:           1000
-----------------------------------------------------------------
---------
K_mc:             Description:          maximum specific Cr(VI)
reduction r
                                        ate
                  Type:                 Constant Variable
                  Unit:                 mg/L/hr
                  Value:                0.00085749048
                  Standard Deviation:   1
                  Minimum:              0
                  Maximum:              10
                  Sensitivity Analysis: active
                  Parameter Estimation: active
-----------------------------------------------------------------
---------
K_ms:             Description:          maximum specific As(III)
utilizatio
                                        n rate
                  Type:                 Constant Variable
                  Unit:                 mg /mg cell
                  Value:                0.000559024
                  Standard Deviation:   1
                  Minimum:              0
                  Maximum:              10
                  Sensitivity Analysis: active
                  Parameter Estimation: active
-----------------------------------------------------------------
---------
K_s:              Description:          half velocity
concentration
                  Type:                 Constant Variable
                  Unit:                 mg/L
                  Value:                979.63113
                  Standard Deviation:   1
                  Minimum:              0
                  Maximum:              1000
                  Sensitivity Analysis: active
                  Parameter Estimation: active
-----------------------------------------------------------------
---------
```

190

```
R_c:              Description:      maximum Cr(VI) reducing
capacity
                  Type:             Constant Variable
                  Unit:             mg Cr(VI)/mg cell
                  Value:            0.013406862
                  Standard Deviation: 0.1596222
                  Minimum:          0
                  Maximum:          1000
                  Sensitivity Analysis: active
                  Parameter Estimation: active
--------------------------------------------------------------
---------
R_s:              Description:      Saturation constant
                  Type:             Constant Variable
                  Unit:             mg/L
                  Value:            0.00015777962
                  Standard Deviation: 1
                  Minimum:          0
                  Maximum:          10
                  Sensitivity Analysis: active
                  Parameter Estimation: active
--------------------------------------------------------------
---------
S:                Description:      As(III)_Concentration
                  Type:             Dyn. Volume State Var.
                  Unit:             mg/L
                  Relative Accuracy: 1e-006
                  Absolute Accuracy: 1e-006
--------------------------------------------------------------
---------
So:               Description:      Inital concentration
                  Type:             Formula Variable
                  Unit:             mg/L
                  Expression:       80
--------------------------------------------------------------
---------
T:                Description:      time
                  Type:             Program Variable
                  Unit:             hour
                  Reference to:     Time
--------------------------------------------------------------
---------
Xo:               Description:      initial biomass
concentration
                  Type:             Formula Variable
                  Unit:             mg/L
                  Expression:       100
**************************************************************
*********
Processes
```

```
**************************************************************
*********
A_s:            Description:        As oxidation
                Type:               Dynamic Process
                Rate:               K_ms*S*(Xo-((So-
S/R_s)))/(S+K_s)
                Stoichiometry:
                  Variable: Stoichiometric Coefficient
                  S: -1
------------------------------------------------------------
---------
Cr:             Description:        Cr_reduction
                Type:               Dynamic Process
                Rate:               K_mc*C*(Xo-((Co-
C/R_c)))/(C+K_c)
                Stoichiometry:
                  Variable: Stoichiometric Coefficient
                  C: -1
**************************************************************
*********
Compartments
**************************************************************
********
Reactor2:       Description:        batch
                Type:               Mixed Reactor Compartment
                Compartment Index:  0
                Active Variables:   C, Co, K_c, R_c, T, K_mc,
Xo, R_s,
                                    S, So, K_ms
                Active Processes:   Cr, A_s
                Initial Conditions:
                  Variable(Zone): Initial Condition
                  C (Bulk Volume) : Co
                  S(Bulk Volume) : So
                Inflow:             0
                Loadings:
                Volume:             1
                Accuracies:
                  Rel. Acc. Q:      0.001
                  Abs. Acc. Q:      0.001
                  Rel. Acc. V:      0.001
                  Abs. Acc. V:      0.001
**************************************************************
*********
Definitions of Calculations
**************************************************************
********
A_s:            Description:        As(III) oxidation
                Calculation Number: 1
                Initial Time:       0
```

```
                    Initial State:         given, made consistent
                    Step Size:             0.1
                    Num. Steps:            100
                    Status:                active for simulation
                                           active for sensitivity
analysis
--------------------------------------------------------------
---------
C_r:                Description:           Cr(VI) reduction
                    Calculation Number:    0
                    Initial Time:          0
                    Initial State:         given, made consistent
                    Step Size:             0.1
                    Num. Steps:            100
                    Status:                active for simulation
                                           active for sensitivity
analysis

*************************************************************
*********
Definitions of Parameter Estimation Calculations
*************************************************************
*********
fit1:               Description:
                    Calculation Number:    0
                    Initial Time:          0
                    Initial State:         given, made consistent
                    Status:                active
                    Fit Targets:
                      Data: Variable (Compartment,Zone,Time/Space)
                      C_meas : C (Reactor2,Bulk Volume,0)
                      As_meas : S (Reactor2,Bulk Volume,0)
*************************************************************
********
Plot Definitions
*************************************************************
*********
plot1:              Description:           Cr(VI)reduction
                    Abscissa:              Time
                    Title:                 Cr(VI)reduction
                    Abscissa Label:         Time (hour)
                    Ordinate Label:        Cr(VI) concentration
(mg/L)
                    Curves:
                      Type: Variable [CalcNum, Comp.,
Zone,Time/Space]
                        Value: C [0, Reactor2, Bulk Volume,0]
                        Value: C_meas [0, Reactor2, Bulk Volume,0]
--------------------------------------------------------------
---------


                             193
```

```
plot2:          Description:          As(III) oxidation
                Abscissa:             Time
                Title:                As(III) oxidation
                Abscissa Label:       Time (hour)
                Ordinate Label:       As(III) oxidation (mg/L)
                Curves:
                   Type: Variable [CalcNum, Comp.,
Zone,Time/Space]
                   Value: S [0, Reactor2, Bulk Volume,0]
                   Value: As_meas [0, Reactor2, Bulk Volume,0]
****************************************************************
*********
Calculation Parameters
****************************************************************
*********
Numerical Parameters:    Maximum Int. Step Size:  1
                         Maximum Integrat. Order: 5
                         Number of Codiagonals:   1000
                         Maximum Number of Steps: 1000
----------------------------------------------------------------
---------
                         Fit Method:              simplex
                         Max. Number of Iterat.:  1000
****************************************************************
*********
Calculated States
****************************************************************
*********
Calc. Num.  Num. States Comments
0           13          Range of Times: 0 - 240




****************************************************************
*********
AQUASIM Version 2.0 (win/mfc) - Sensitivity Analysis File

****************************************************************
**********

Date and time of listing:  04/23/2018 21:24:08


Ranking of mean absolute sensitivities and error
contributions:
```

Calculation Number: 1
  Compartment: Reactor2
    Zone: Bulk Volume
      Variable: C

	Parameter:	Sens AR: [mg/L]	Parameter:	Error Contr.: [mg/L]
1	K_c	7.298	R_c	54.46
2	K_mc	6.282	K_mc	15.7
3	R_c	5.458	Co	0.06297
4	Co	4.408	K_c	0.008181
5	K_s	8.825e-006	R_s	0.0001403
6	So	8.667e-006	K_ms	2.255e-005
7	K_ms	2.255e-007	So	8.667e-008
8	R_s	2.244e-008	K_s	9.014e-009

      Variable: S

	Parameter:	Sens AR: [mg/L]	Parameter:	Error Contr.: [mg/L]
1	K_s	4.901	R_s	80.5
2	So	2.273	K_ms	54.66
3	K_ms	0.5466	So	0.02273
4	R_s	0.1409	K_s	0.005006
5	K_mc	2.328e-006	R_c	1.401e-005
6	K_c	2.04e-006	K_mc	5.821e-006
7	Co	1.977e-006	Co	2.825e-008
8	R_c	1.404e-006	K_c	2.287e-009

Calculation Number: 0
  Compartment: Reactor2
    Zone: Bulk Volume

Variable: C
                Parameter: Sens AR: Parameter:
Error Contr.:
                                [mg/L]
[mg/L]
        1   K_c   7.298   R_c
54.46
        2   K_mc   6.282   K_mc
15.7
        3   R_c   5.458   Co
0.06297
        4   Co   4.408   K_c
0.008181
        5   K_s   8.825e-006   R_s
0.0001403
        6   So   8.667e-006   K_ms
2.255e-005
        7   K_ms   2.255e-007   So
8.667e-008
        8   R_s   2.244e-008   K_s
9.014e-009
        Variable: S
                Parameter: Sens AR: Parameter:
Error Contr.:

CONTINUOUS FLOW REACTOR SYSTEM

****
****
AQUASIM Version 2.0 (win/mfc) - Listing of System Definition

****
****
Date and time of listing: 04/25/2018 16:32:15

****
****
Variables
****
****
A_f: Description: biofilm surface area
            Type: Formula Variable
            Unit: m2
            Expression: 28.9*(0.002+z)


```
C:              Description:        Concentration
                Type:              Dyn. Volume State Var.
                Unit:              g/m^3
                Relative Accuracy: 1e-006
                Absolute Accuracy: 1e-006
-----------------------------------------------------------------
---------
C1:             Description:        Concentration
                Type:              Dyn. Volume State Var.
                Unit:              g/m^3
                Relative Accuracy: 1e-006
                Absolute Accuracy: 1e-006
-----------------------------------------------------------------
---------
Cin:            Description:        Inital concentration
                Type:              Real List Variable
                Unit:              g/m^3
                Argument:          t
                Standard Deviations: global
                Rel. Stand. Deviat.: 0
                Abs. Stand. Deviat.: 1
                Minimum:           0
                Maximum:           1e+009
                Interpolation Method: linear interpolation
                Sensitivity Analysis: inactive
                Real Data Pairs (151 pairs):
                    0            2.4
                    1            11.02
                    2            8.33
                    3            20.62
                    4            18.24
                        .            .
                        .            .
                    146          0.18
                    147          0.18
                    148          0.18
                    149          0.18
                    150          0.18
-----------------------------------------------------------------
---------
Cout_1:         Description:        Column outlet
                Type:              Real List Variable
                Unit:              mg/l
                Argument:          t
                Standard Deviations: global
                Rel. Stand. Deviat.: 0
                Abs. Stand. Deviat.: 1
                Minimum:           0
                Maximum:           1e+009
                Interpolation Method: linear interpolation
```

```
                Sensitivity Analysis: inactive
                Real Data Pairs (151 pairs):
                   0                  0
                   1                  0
                   2                  0
                   3                  0
                   4                  0
                      .                  .
                      .                  .
                   146              1.98
                   147              1.98
                   148              1.98
                   149              1.98
                   150              1.98
--------------------------------------------------------------
--------
c_de:          Description:        Coefficient for
detachment velocit
                Type:               Constant Variable
                Unit:
                Value:              1
                Standard Deviation: 1
                Minimum:            0
                Maximum:            10
                Sensitivity Analysis: inactive
                Parameter Estimation: inactive
--------------------------------------------------------------
---------
C_meas:        Description:        Cr(VI) measured
                Type:               Real List Variable
                Unit:               mg/L
                Argument:           t
                Standard Deviations: global
                Rel. Stand. Deviat.: 0
                Abs. Stand. Deviat.: 1
                Minimum:            0
                Maximum:            1e+009
                Interpolation Method: linear interpolation
                Sensitivity Analysis: inactive
                Real Data Pairs (12 pairs):
                   0                70
                   2                70
                   6                57.797738
                   12               52.814371
                   24               36.047904
                   48               26.011311
                   72               15.974717
                   96               11.224218
                   120              6.4737192
                   192              6.7531603
```

```
                    216              6.3572854
                    240              6.2408516
          ------------------------------------------------------------
          ---------
C_out_2:       Description:       Cr(VI) measured
               Type:              Real List Variable
               Unit:              mg/L
               Argument:          t
               Standard Deviations: global
               Rel. Stand. Deviat.: 0
               Abs. Stand. Deviat.: 1
               Minimum:           0
               Maximum:           1e+009
               Interpolation Method: linear interpolation
               Sensitivity Analysis: inactive
               Real Data Pairs (150 pairs):
                    1                0
                    2                0
                    3                0
                    4                0
                    5                0

                      .                .
                      .                .
                    146              1.9785276
                    147              1.9785276
                    148              1.9785276
                    149              1.9785276
                    150              1.9785276
          ------------------------------------------------------------
          ---------
D_wc:          Description:       Diffusion coefficient of
Cr(VI) in
                                  water
               Type:              Constant Variable
               Unit:              m^2/d
               Value:             6.9055485e-007
               Standard Deviation: 1
               Minimum:           0
               Maximum:           100
               Sensitivity Analysis: active
               Parameter Estimation: inactive
          ------------------------------------------------------------
          ---------
D_X:           Description:       Suspended inactivated
cells and par
                                  ticles diffusivity in
pure water
               Type:              Formula Variable
               Unit:              m^2/d
               Expression:        0.0001
```

```
------------------------------------------------------------
---------
epsX:          Description:        biomass volume fraction
               Type:               Formula Variable
               Unit:
               Expression:         Xo/(rho_X)
------------------------------------------------------------
---------
J_flux:        Description:        Dissolved species flux
rate
               Type:               Formula Variable
               Unit:
               Expression:         ((D_wc*C)/L_f)*A_f
------------------------------------------------------------
---------
K_c:           Description:        half velocity
concentration
               Type:               Constant Variable
               Unit:               mg/L/hr
               Value:              674.97508
               Standard Deviation: 1
               Minimum:            0
               Maximum:            1000
               Sensitivity Analysis: active
               Parameter Estimation: active
------------------------------------------------------------
---------
K_mc:          Description:        maximum specific Cr(VI)
reduction r
                                   ate
               Type:               Constant Variable
               Unit:               mg/L/hr
               Value:              0.054773796
               Standard Deviation: 1
               Minimum:            0
               Maximum:            10
               Sensitivity Analysis: active
               Parameter Estimation: active
------------------------------------------------------------
---------
L_f:           Description:        Biofilm thickness
               Type:               Program Variable
               Unit:               m
               Reference to:       Biofilm Thickness
------------------------------------------------------------
---------
L_fo:          Description:        Initial biofilm thickness
               Type:               Constant Variable
               Unit:               m
               Value:              1
```

```
              Standard Deviation:  1
              Minimum:             0
              Maximum:             10
              Sensitivity Analysis: inactive
              Parameter Estimation: inactive
--------------------------------------------------------------
---------
Q:            Description:         Discharge
              Type:                Program Variable
              Unit:                m^3/d
              Reference to:        Discharge
--------------------------------------------------------------
---------
Q_in:         Description:         Bulk fluid volumetric
influent rate
              Type:                Formula Variable
              Unit:                m^3/d
              Expression:          0.00778
--------------------------------------------------------------
---------
Q_out:        Description:          effluent rate
              Type:                Formula Variable
              Unit:                m^3/d
              Expression:          0.00778
--------------------------------------------------------------
---------
rho_X:        Description:         Biomass density (mass per
unit soli
                                   d phase volume)
              Type:                Constant Variable
              Unit:                gCr/m^3
              Value:               1
              Standard Deviation:  1
              Minimum:             0
              Maximum:             1000000
              Sensitivity Analysis: inactive
              Parameter Estimation: inactive
--------------------------------------------------------------
---------
R_c:          Description:         maximum Cr(VI) reducing
capacity
              Type:                Constant Variable
              Unit:                mg Cr(VI)/mg cell
              Value:               0.01223674
              Standard Deviation:  0.1596222
              Minimum:             0
              Maximum:             10
              Sensitivity Analysis: active
              Parameter Estimation: active
```

201

```
----------------------------------------------------------------
---------
S:              Description:        As(III)_Concentration
                Type:               Dyn. Volume State Var.
                Unit:               mg/L
                Relative Accuracy:  1e-006
                Absolute Accuracy:  1e-006
----------------------------------------------------------------
---------
t:              Description:        time
                Type:               Program Variable
                Unit:               d
                Reference to:       Time
----------------------------------------------------------------
---------
tau:            Description:        Hydraulic retention time
                Type:               Formula Variable
                Unit:               h
                Expression:         V_b/Q
----------------------------------------------------------------
---------
u_F:            Description:        Advective velocity of the
biofilm s
                                    olid matrix
                Type:               Program Variable
                Unit:               m/d
                Reference to:       Growth Velocity of
Biofilm
----------------------------------------------------------------
---------
V_b:            Description:        Reactor Volume
                Type:               Formula Variable
                Unit:               m3
                Expression:         0.0055
----------------------------------------------------------------
---------
Xo:             Description:        initial biomass
concentration
                Type:               Formula Variable
                Unit:               mg/L
                Expression:         100
----------------------------------------------------------------
---------
z:              Description:        distance from the
substratum
                Type:               Program Variable
                Unit:               m
                Reference to:       Space Coordinate Z
****************************************************************
********
```

```
Processes
*************************************************************
*********
Cr:             Description:          Cr_reduction
                Type:                 Dynamic Process
                Rate:                 K_mc*C*(Xo-((Cin-
C/R_c)))/(C+K_c)
                Stoichiometry:
                  Variable: Stoichiometric Coefficient
                  C : -1
*************************************************************
*********
Compartments
*************************************************************
*********
CSTR:           Description:          CSTR
                Type:                 Mixed Reactor Compartment
                Compartment Index:    0
                Active Variables:     C, Cin
                Active Processes:     Cr
                Initial Conditions:
                Inflow:               Q_in
                Loadings:
                  Variable : Loading
                  C : Q_in*Cin
                Volume:               0.001
                Accuracies:
                  Rel. Acc. Q:        0.001
                  Abs. Acc. Q:        0.001
                  Rel. Acc. V:        0.001
                  Abs. Acc. V:        0.001
-------------------------------------------------------------
---------
Sampler:        Description:
                Type:                 Mixed Reactor Compartment
                Compartment Index:    0
                Active Variables:     C, Cout_1
                Active Processes:     Cr
                Initial Conditions:
                Inflow:               Q_in
                Loadings:
                  Variable : Loading
                  C : Q_in*Cout_1
                Volume:               0.001
                Accuracies:
                  Rel. Acc. Q:        0.001
                  Abs. Acc. Q:        0.001
                  Rel. Acc. V:        0.001
                  Abs. Acc. V:        0.001
```

```
****************************************************************
*********
Links
****************************************************************
*********
link1:          Type:               Advective Link
                Link Index:         0
                Compartment In:     CSTR
                Connection In:      Outflow
                Compartment Out:    Sampler
                Connection Out:     Inflow
                Bifurcations:
****************************************************************
********
Definitions of Calculations
****************************************************************
*********
C_r:            Description:        Cr(VI) reduction
                Calculation Number: 0
                Initial Time:       0
                Initial State:      given, made consistent
                Step Size:          0.1
                Num. Steps:         300
                Status:             active for simulation
                                    active for sensitivity
analysis
****************************************************************
*********




****************************************************************
*********
Definitions of Parameter Estimation Calculations
****************************************************************
*********
fit1:           Description:
                Calculation Number:  0
                Initial Time:        0
                Initial State:       given, made consistent
                Status:              active
                Fit Targets:
                  Data : Variable (Compartment,Zone,Time/Space)
                  Cin : C (CSTR,Bulk Volume,0)
                  Cout_1 : C (Sampler,Bulk Volume,0)
****************************************************************
*********
Plot Definitions
```

```
****************************************************************
*********
CSTR:           Description:        CSTR
                Abscissa:           Time
                Title:              CSTR
                Abscissa Label:     Time(day)
                Ordinate Label:     Cr(VI) concentrationmg/L
                Curves:
                  Type : Variable
[CalcNum,Comp.,Zone,Time/Space]
                  Value : C [0,CSTR,Bulk Volume,0]
                  Value : Cin [0,CSTR,Bulk Volume,0]
----------------------------------------------------------------
---------
Sampler_out:    Description:        Sampler_out
                Abscissa:           Time
                Title:              Sampler_out
                Abscissa Label:     Time(day)
                Ordinate Label:     Cr(VI) Concentration
                Curves:
                  Type : Variable
[CalcNum,Comp.,Zone,Time/Space]
                  Value : C [0,Sampler,Bulk Volume,0]
                  Value : Cout_1 [0,Sampler,Bulk Volume,0]
****************************************************************
*********
Calculation Parameters
****************************************************************
*********
Numerical Parameters:    Maximum Int. Step Size:  1
                         Maximum Integrat. Order: 5
                         Number of Codiagonals:   1000
                         Maximum Number of Steps: 1000
----------------------------------------------------------------
---------
                         Fit Method:              simplex
                         Max. Number of Iterat.:  1000
****************************************************************
*********
Calculated States
****************************************************************
********
Calc. Num.  Num. States Comments
0           151         Range of Times: 0 - 150
****************************************************************
*********
```

205

```
*************************************************************
*********
AQUASIM Version 2.0 (win/mfc) - Listing of System Definition

*************************************************************
*********
Date and time of listing:  04/25/2018 16:40:51
*************************************************************
*********
Variables
*************************************************************
*********
A_f:            Description:        biofilm surface area
                Type:               Formula Variable
                Unit:               m2
                Expression:         28.9*(0.002+z)
        ---------------------------------------------------------------
---------
C:              Description:        Concentration
                Type:               Dyn. Volume State Var.
                Unit:               g/m^3
                Relative Accuracy:  1e-006
                Absolute Accuracy:  1e-006
        ---------------------------------------------------------------
---------
C1:             Description:        Concentration
                Type:               Dyn. Volume State Var.
                Unit:               g/m^3
                Relative Accuracy:  1e-006
                Absolute Accuracy:  1e-006
        ---------------------------------------------------------------
---------
Cin:            Description:        Inital concentration
                Type:               Real List Variable
                Unit:               g/m^3
                Argument:           t
                Standard Deviations: global
                Rel. Stand. Deviat.: 0
                Abs. Stand. Deviat.: 1
                Minimum:            0
                Maximum:            1e+009
                Interpolation Method: linear interpolation
                Sensitivity Analysis: inactive
                Real Data Pairs (150 pairs):
                    1           32.495922
                    2           31.908646
                    3           32.177814
                    4           32.446982
                    5           31.052202
                        .                   .

                        206
```

```
                   .                    .
            146            30.185185
            147            30.185185
            148            30.185185
            149            30.185185
            150            30.185185
---------------------------------------------------------------
---------
Cout_1:        Description:        Column outlet
               Type:               Real List Variable
               Unit:               mg/l
               Argument:           t
               Standard Deviations: global
               Rel. Stand. Deviat.: 0
               Abs. Stand. Deviat.: 1
               Minimum:            0
               Maximum:            1e+009
               Interpolation Method: linear interpolation
               Sensitivity Analysis: inactive
               Real Data Pairs (151 pairs):
                  0              2.4
                  1              11.02
                  2              8.33
                  3              20.62
                  4              18.24
                     .                    .
                     .                    .
                146            0.18
                147            0.18
                148            0.18
                149            0.18
                150            0.18
---------------------------------------------------------------
---------
c_de:          Description:        Coefficient for
detachment velocit
               Type:               Constant Variable
               Unit:
               Value:              1
               Standard Deviation: 1
               Minimum:            0
               Maximum:            10
               Sensitivity Analysis: inactive
               Parameter Estimation: inactive
---------------------------------------------------------------
---------
C_meas:        Description:        Cr(VI) measured
               Type:               Real List Variable
               Unit:               mg/L
               Argument:           t
```

```
              Standard Deviations:  global
              Rel. Stand. Deviat.:  0
              Abs. Stand. Deviat.:  1
              Minimum:              0
              Maximum:              1e+009
              Interpolation Method: linear interpolation
              Sensitivity Analysis: inactive
              Real Data Pairs (12 pairs):
                0              70
                2              70
                6              57.797738
               12              52.814371
               24              36.047904
               48              26.011311
               72              15.974717
               96              11.224218
              120              6.4737192
              192              6.7531603
              216              6.3572854
              240              6.2408516
------------------------------------------------------------
---------
C_out_2:      Description:          Cr(VI) measured
              Type:                 Real List Variable
              Unit:                 mg/L
              Argument:             t
              Standard Deviations:  global
              Rel. Stand. Deviat.:  0
              Abs. Stand. Deviat.:  1
              Minimum:              0
              Maximum:              1e+009
              Interpolation Method: linear interpolation
              Sensitivity Analysis: inactive
              Real Data Pairs (150 pairs):
                1              0
                2              0
                3              0
                4              0
                5              0
                  .              .
                  .              .
              146              1.9785276
              147              1.9785276
              148              1.9785276
              149              1.9785276
              150              1.9785276
------------------------------------------------------------
---------
D_wc:         Description:          Diffusion coefficient of
Cr(VI) in
```

```
                                    water
            Type:                   Constant Variable
            Unit:                   m^2/d
            Value:                  6.1100901e-007
            Standard Deviation:     1
            Minimum:                0
            Maximum:                100
            Sensitivity Analysis: active
            Parameter Estimation: active
-------------------------------------------------------------
---------
D_X:        Description:            Suspended inactivated
cells and par
                                    ticles diffusivity in
pure water
            Type:                   Formula Variable
            Unit:                   m^2/d
            Expression:             0.0001
-------------------------------------------------------------
---------
epsX:       Description:            biomass volume fraction
            Type:                   Formula Variable
            Unit:
            Expression:             Xo/(rho_X)
-------------------------------------------------------------
---------
J_flux:     Description:            Dissolved species flux
rate
            Type:                   Formula Variable
            Unit:
            Expression:             ((D_wc*C)/L_f)*A_f
-------------------------------------------------------------
---------
K_c:        Description:            half velocity
concentration
            Type:                   Constant Variable
            Unit:                   mg/L/hr
            Value:                  419.00225
            Standard Deviation:     1
            Minimum:                0
            Maximum:                1000
            Sensitivity Analysis: active
            Parameter Estimation: active
-------------------------------------------------------------
--------
K_mc:       Description:            maximum specific Cr(VI)
reduction r
                                    ate
            Type:                   Constant Variable
            Unit:                   mg/L/hr
```

```
                 Value:                9.8724687
                 Standard Deviation:   1
                 Minimum:              0
                 Maximum:              10
                 Sensitivity Analysis: active
                 Parameter Estimation: active
----------------------------------------------------------------
---------
L_f:             Description:          Biofilm thickness
                 Type:                Program Variable
                 Unit:                m
                 Reference to:        Biofilm Thickness
----------------------------------------------------------------
---------
L_fo:            Description:          Initial biofilm thickness
                 Type:                Constant Variable
                 Unit:                m
                 Value:               1
                 Standard Deviation:  1
                 Minimum:             0
                 Maximum:             10
                 Sensitivity Analysis: inactive
                 Parameter Estimation: inactive
----------------------------------------------------------------
---------
Q:               Description:          Discharge
                 Type:                Program Variable
                 Unit:                m^3/d
                 Reference to:        Discharge
----------------------------------------------------------------
---------
Q_in:            Description:          Bulk fluid volumetric
influent rate
                 Type:                Formula Variable
                 Unit:                m^3/d
                 Expression:          0.00778
----------------------------------------------------------------
---------
Q_out:           Description:           effluent rate
                 Type:                Formula Variable
                 Unit:                m^3/d
                 Expression:          0.00778
----------------------------------------------------------------
---------
rho_X:           Description:          Biomass density (mass per
unit soli
                                       d phase volume)
                 Type:                Constant Variable
                 Unit:                gCr/m^3
                 Value:               1
```

```
                  Standard Deviation:   1
                  Minimum:              0
                  Maximum:              1000000
                  Sensitivity Analysis: inactive
                  Parameter Estimation: inactive
----------------------------------------------------------------
---------
R_c:              Description:          maximum Cr(VI) reducing
capacity
                  Type:                 Constant Variable
                  Unit:                 mg Cr(VI)/mg cell
                  Value:                0.96927734
                  Standard Deviation:   0.1596222
                  Minimum:              0
                  Maximum:              10
                  Sensitivity Analysis: active
                  Parameter Estimation: active
----------------------------------------------------------------
---------
S:                Description:          As(III)_Concentration
                  Type:                 Dyn. Volume State Var.
                  Unit:                 mg/L
                  Relative Accuracy:    1e-006
                  Absolute Accuracy:    1e-006
----------------------------------------------------------------
---------
t:                Description:          time
                  Type:                 Program Variable
                  Unit:                 d
                  Reference to:         Time
----------------------------------------------------------------
---------
tau:              Description:          Hydraulic retention time
                  Type:                 Formula Variable
                  Unit:                 h
                  Expression:           V_b/Q
----------------------------------------------------------------
---------
u_F:              Description:          Advective velocity of the
biofilm s
                                        olid matrix
                  Type:                 Program Variable
                  Unit:                 m/d
                  Reference to:         Growth Velocity of
Biofilm
----------------------------------------------------------------
---------
V_b:              Description:          Reactor Volume
                  Type:                 Formula Variable
                  Unit:                 m3
```

211

```
                Expression:         0.0055
----------------------------------------------------------------
---------
Xo:             Description:        initial biomass
concentration
                Type:               Formula Variable
                Unit:               mg/L
                Expression:         100
----------------------------------------------------------------
---------
z:              Description:        distance from the
substratum
                Type:               Program Variable
                Unit:               m
                Reference to:       Space Coordinate Z
*************************************************************
*********
Processes
*************************************************************
*********
Cr:             Description:        Cr_reduction
                Type:               Dynamic Process
                Rate:               K_mc*C*(Xo-((Cin-
C/R_c)))/(C+K_c)
                Stoichiometry:
                  Variable : Stoichiometric Coefficient
                  C : -1
*************************************************************
*********
Compartments
*************************************************************
*********
Column:         Description:        Advection-Diffussive
compartment
                Type:               Advective-Diffusive Comp.
                Compartment Index:  0
                Active Variables:   C, Cin
                Active Processes:    Cr
                Initial Conditions:
                Inflow:             Q_in
                Loadings:
                  Variable : Loading
                  C : Q_in*Cin
                Lateral Inflow:     0
                Start Coordinate:   0
                End Coordinate:     1
                Cross Section:      0.0079
                Glob. Diffusivity:  D_wc
                Num. of Grid Pts:   102 (low resolution)
                Accuracies:
```

```
                        Rel. Acc. Q:        0.001
                        Abs. Acc. Q:        1e-006
                        Rel. Acc. D:        1e-006
                        Abs. Acc. D:        1e-006
---------------------------------------------------------------
---------
Sampler:         Description:
                 Type:               Mixed Reactor Compartment
                 Compartment Index:  0
                 Active Variables:   C, Cout_1
                 Active Processes:   Cr
                 Initial Conditions:
                 Inflow:             Q_in
                 Loadings:
                   Variable : Loading
                   C : Q_in*Cout_1
                 Volume:             0.001
                 Accuracies:
                   Rel. Acc. Q:      0.001
                   Abs. Acc. Q:      0.001
                   Rel. Acc. V:      0.001
                   Abs. Acc. V:      0.001
***************************************************************
*********
Links
***************************************************************
*********
link1:           Type:               Advective Link
                 Link Index:         0
                 Compartment In:     Column
                 Connection In:      Outlet
                 Compartment Out:    Sampler
                 Connection Out:     Inflow
                 Bifurcations:
***************************************************************
*********
Definitions of Calculations
***************************************************************
*********
C_r:             Description:        Cr(VI) reduction
                 Calculation Number: 0
                 Initial Time:       0
                 Initial State:      given, made consistent
                 Step Size:          0.1
                 Num. Steps:         300
                 Status:             active for simulation
                                     active for sensitivity
analysis
***************************************************************
*********
```

```
Definitions of Parameter Estimation Calculations
***************************************************************
*********
fit1:          Description:
               Calculation Number:   0
               Initial Time:         0
               Initial State:        given, made consistent
               Status:               active
               Fit Targets:
                 Data : Variable (Compartment,Zone,Time/Space)
                 Cin : C (Column,Water Body,0)
                 Cout_1 : C (Sampler,Bulk Volume,0)
***************************************************************
*********
Plot Definitions
***************************************************************
*********
Columnin:      Description:          Column
               Abscissa:             Time
               Title:                Column
               Abscissa Label:       Time(day)
               Ordinate Label:       Cr(VI) concentrationmg/L
               Curves:
                 Type : Variable
[CalcNum,Comp.,Zone,Time/Space]
                 Value : C [0,Column,Water Body,0]
                 Value : Cin [0,Column,Water Body,0]
-----------------------------------------------------------------
---------
Columnout_1:   Description:          Columnout
               Abscissa:             Time
               Title:                Columnout
               Abscissa Label:       Time(day)
               Ordinate Label:       Cr(VI) Concentraation
               Curves:
                 Type : Variable
[CalcNum,Comp.,Zone,Time/Space]
                 Value : C [0,Sampler,Bulk Volume,0]
                 Value : Cout_1 [0,Sampler,Bulk Volume,0]
***************************************************************
*********
Calculation Parameters
***************************************************************
*********
Numerical Parameters:    Maximum Int. Step Size:  1
                         Maximum Integrat. Order: 5
                         Number of Codiagonals:   1000
                         Maximum Number of Steps: 1000
-----------------------------------------------------------------
---------
```

```
                        Fit Method:              simplex
                        Max. Number of Iterat.:  1000
****************************************************************
*********
Calculated States
****************************************************************
*********
Calc. Num.  Num. States  Comments
0           151          Range of Times: 0 - 150
****************************************************************
*********




****************************************************************
*********
Definitions of Parameter Estimation Calculations
****************************************************************
*********
fit1:          Description:
               Calculation Number:   0
               Initial Time:         0
               Initial State:        given, made consistent
               Status:               active
               Fit Targets:
                 Data : Variable (Compartment,Zone,Time/Space)
                 Cin : C (CSTR,Bulk Volume,0)
                 Cout_1 : C (Sampler,Bulk Volume,0)
****************************************************************
*********
Plot Definitions
****************************************************************
*********
CSTR:          Description:          CSTR
               Abscissa:             Time
               Title:                CSTR
               Abscissa Label:       Time(day)
               Ordinate Label:       Cr(VI) concentrationmg/L
               Curves:
                 Type : Variable
[CalcNum,Comp.,Zone,Time/Space]
                 Value : C [0,CSTR,Bulk Volume,0]
                 Value : Cin [0,CSTR,Bulk Volume,0]
----------------------------------------------------------------
----------
Sampler_out:   Description:          Sampler_out
               Abscissa:             Time
               Title:                Sampler_out
```

215

```
                 Abscissa Label:      Time(day)
                 Ordinate Label:      Cr(VI) Concentraation
                 Curves:
                   Type : Variable
[CalcNum,Comp.,Zone,Time/Space]
                   Value : C [0,Sampler,Bulk Volume,0]
                   Value : Cout_1 [0,Sampler,Bulk Volume,0]
*****************************************************************
*********
Calculation Parameters
*****************************************************************
*********
Numerical Parameters:    Maximum Int. Step Size:  1
                         Maximum Integrat. Order: 5
                         Number of Codiagonals:   1000
                         Maximum Number of Steps: 1000
-----------------------------------------------------------------
---------
                         Fit Method:              simplex
                         Max. Number of Iterat.:  1000
*****************************************************************
*********
Calculated States
*****************************************************************
*********
Calc. Num.  Num. States Comments
0           151         Range of Times: 0 - 150
*****************************************************************
*********



*****************************************************************
*********
AQUASIM Version 2.0 (win/mfc) - Parameter Estimation File

*****************************************************************
*********


*****************************************************************
*********
Date and time of listing:  04/25/2018  17:16:45
*****************************************************************
*********
Variables
*****************************************************************
*********
A_f:          Description:          biofilm surface area
              Type:                 Formula Variable
              Unit:                 m2
              Expression:           28.9*(0.002+z)
```

216

```
----------------------------------------------------------------
---------
C:              Description:          Concentration
                Type:                Dyn. Volume State Var.
                Unit:                g/m^3
                Relative Accuracy:   1e-006
                Absolute Accuracy:   1e-006
----------------------------------------------------------------
---------
C1:             Description:          Concentration
                Type:                Dyn. Volume State Var.
                Unit:                g/m^3
                Relative Accuracy:   1e-006
                Absolute Accuracy:   1e-006
----------------------------------------------------------------
---------
Cin:            Description:          Inital concentration
                Type:                Real List Variable
                Unit:                g/m^3
                Argument:            t
                Standard Deviations: global
                Rel. Stand. Deviat.: 0
                Abs. Stand. Deviat.: 1
                Minimum:             0
                Maximum:             1e+009
                Interpolation Method: linear interpolation
                Sensitivity Analysis: inactive
                Real Data Pairs (150 pairs):
                    1            32.495922
                    2            31.908646
                    3            32.177814
                    4            32.446982
                    5            31.052202
                        .            .
                        .            .
                    146          30.185185
                    147          30.185185
                    148          30.185185
                    149          30.185185
                    150          30.185185
----------------------------------------------------------------
---------
Cout_1:         Description:          Column outlet
                Type:                Real List Variable
                Unit:                mg/l
                Argument:            t
                Standard Deviations: global
                Rel. Stand. Deviat.: 0
                Abs. Stand. Deviat.: 1
                Minimum:             0
```

217

```
                    Maximum:               1e+009
                    Interpolation Method: linear interpolation
                    Sensitivity Analysis: inactive
                    Real Data Pairs (151 pairs):
                        0               4.79
                        1               7.27
                        2               9.85
                        3               9.54
                        4               5.97
                          .               .
                          .               .
                        146             1.38
                        147             1.38
                        148             1.38
                        149             1.38
                        150             1.38
         ----------------------------------------------------------------
         ---------
         c_de:          Description:           Coefficient for
         detachment velocit
                        Type:                  Constant Variable
                        Unit:
                        Value:                 1
                        Standard Deviation:    1
                        Minimum:               0
                        Maximum:               10
                        Sensitivity Analysis: inactive
                        Parameter Estimation: inactive
         ----------------------------------------------------------------
         ---------
         C_meas:        Description:           Cr(VI) measured
                        Type:                  Real List Variable
                        Unit:                  mg/L
                        Argument:              t
                        Standard Deviations:  global
                        Rel. Stand. Deviat.:   0
                        Abs. Stand. Deviat.:   1
                        Minimum:               0
                        Maximum:               1e+009
                        Interpolation Method: linear interpolation
                        Sensitivity Analysis: inactive
                        Real Data Pairs (12 pairs):
                            0               70
                            2               70
                            6               57.797738
                            12              52.814371
                            24              36.047904
                            48              26.011311
                            72              15.974717
                            96              11.224218
```

```
                         120               6.4737192
                         192               6.7531603
                         216               6.3572854
                         240               6.2408516
      ---------------------------------------------------------------
      ---------
      C_out_2:        Description:        Cr(VI) measured
                      Type:               Real List Variable
                      Unit:               mg/L
                      Argument:           t
                      Standard Deviations: global
                      Rel. Stand. Deviat.: 0
                      Abs. Stand. Deviat.: 1
                      Minimum:            0
                      Maximum:            1e+009
                      Interpolation Method: linear interpolation
                      Sensitivity Analysis: inactive
                      Real Data Pairs (150 pairs):
                         1                 0
                         2                 0
                         3                 0
                         4                 0
                         5                 0
                            .                 .
                            .                 .
                         146               1.9785276
                         147               1.9785276
                         148               1.9785276
                         149               1.9785276
                         150               1.9785276
      ---------------------------------------------------------------
      ---------
      D_wc:           Description:        Diffusion coefficient of
      Cr(VI) in
                                          water
                      Type:               Constant Variable
                      Unit:               m^2/d
                      Value:              6.9055485e-007
                      Standard Deviation: 1
                      Minimum:            0
                      Maximum:            100
                      Sensitivity Analysis: active
                      Parameter Estimation: active
      ---------------------------------------------------------------
      ---------
      D_X:            Description:        Suspended inactivated
      cells and par
                                          ticles diffusivity in
      pure water
                      Type:               Formula Variable
```

219

```
                        Unit:                  m^2/d
                        Expression:            0.0001
          -----------------------------------------------------------
----------
epsX:       Description:           biomass volume fraction
            Type:                  Formula Variable
            Unit:
            Expression:            Xo/(rho_X)
          -----------------------------------------------------------
----------
J_flux:     Description:           Dissolved species flux
rate
            Type:                  Formula Variable
            Unit:
            Expression:            ((D_wc*C)/L_f)*A_f
          -----------------------------------------------------------
----------
K_c:        Description:           half velocity
concentration
            Type:                  Constant Variable
            Unit:                  mg/L/hr
            Value:                 577.41278
            Standard Deviation:    1
            Minimum:               0
            Maximum:               1000
            Sensitivity Analysis: active
            Parameter Estimation: active
          -----------------------------------------------------------
----------
K_mc:       Description:           maximum specific Cr(VI)
reduction r
                                   ate
            Type:                  Constant Variable
            Unit:                  mg/L/hr
            Value:                 9.4451734
            Standard Deviation:    1
            Minimum:               0
            Maximum:               10
            Sensitivity Analysis: active
            Parameter Estimation: active
          -----------------------------------------------------------
----------
L_f:        Description:           Biofilm thickness
            Type:                  Program Variable
            Unit:                  m
            Reference to:          Biofilm Thickness
          -----------------------------------------------------------
----------
L_fo:       Description:           Initial biofilm thickness
            Type:                  Constant Variable
```

```
                     Unit:                 m
                     Value:                1
                     Standard Deviation:   1
                     Minimum:              0
                     Maximum:              10
                     Sensitivity Analysis: inactive
                     Parameter Estimation: inactive
-------------------------------------------------------------
---------
Q:                   Description:          Discharge
                     Type:                 Program Variable
                     Unit:                 m^3/d
                     Reference to:         Discharge
-------------------------------------------------------------
---------
Q_in:                Description:          Bulk fluid volumetric
influent rate
                     Type:                 Formula Variable
                     Unit:                 m^3/d
                     Expression:           0.00778
-------------------------------------------------------------
---------
Q_out:               Description:           effluent rate
                     Type:                 Formula Variable
                     Unit:                 m^3/d
                     Expression:           0.00778
-------------------------------------------------------------
---------
rho_X:               Description:          Biomass density (mass per
unit soli
                                           d phase volume)
                     Type:                 Constant Variable
                     Unit:                 gCr/m^3
                     Value:                1
                     Standard Deviation:   1
                     Minimum:              0
                     Maximum:              1000000
                     Sensitivity Analysis: inactive
                     Parameter Estimation: inactive
-------------------------------------------------------------
---------
R_c:                 Description:          maximum Cr(VI) reducing
capacity
                     Type:                 Constant Variable
                     Unit:                 mg Cr(VI)/mg cell
                     Value:                0.91137295
                     Standard Deviation:   0.1596222
                     Minimum:              0
                     Maximum:              10
                     Sensitivity Analysis: active
```

```
                   Parameter Estimation: active
------------------------------------------------------------
---------
S:              Description:        As(III)_Concentration
                Type:               Dyn. Volume State Var.
                Unit:               mg/L
                Relative Accuracy:  1e-006
                Absolute Accuracy:  1e-006
------------------------------------------------------------
---------
t:              Description:        time
                Type:               Program Variable
                Unit:               d
                Reference to:       Time
------------------------------------------------------------
---------
tau:            Description:        Hydraulic retention time
                Type:               Formula Variable
                Unit:               h
                Expression:         V_b/Q
------------------------------------------------------------
---------
u_F:            Description:        Advective velocity of the
biofilm s
                                    olid matrix
                Type:               Program Variable
                Unit:               m/d
                Reference to:       Growth Velocity of
Biofilm
------------------------------------------------------------
---------
V_b:            Description:        Reactor Volume
                Type:               Formula Variable
                Unit:               m3
                Expression:         0.0055
------------------------------------------------------------
---------
Xo:             Description:        initial biomass
concentration
                Type:               Formula Variable
                Unit:               mg/L
                Expression:         100
------------------------------------------------------------
---------
z:              Description:        distance from the
substratum
                Type:               Program Variable
                Unit:               m
                Reference to:       Space Coordinate Z
```
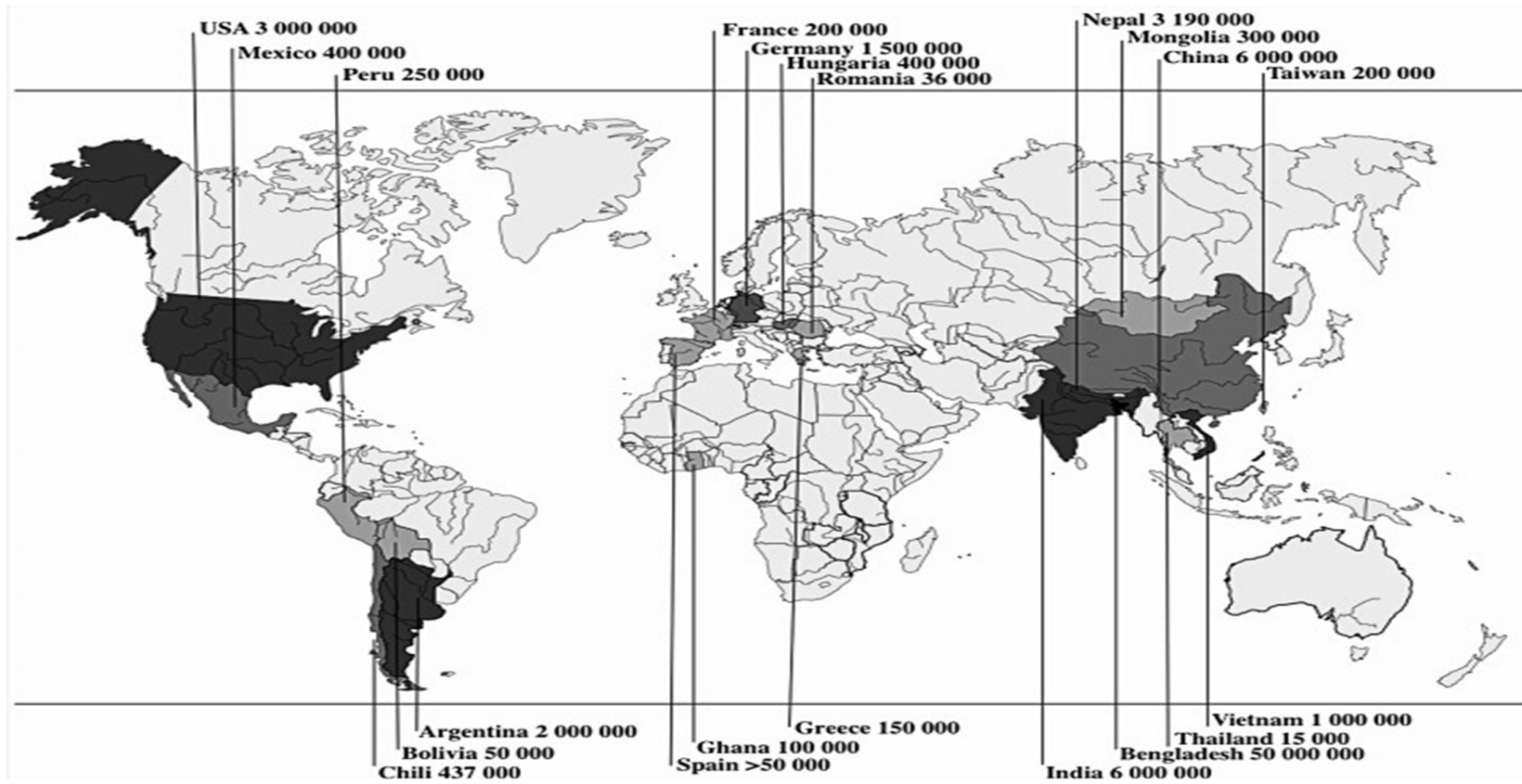
222

Figure 5.9: World map of populations at risk, based on the data currently available in the literature. The figures give the number of people whose daily water consumption includes arsenic levels (Didier et al., 2009).
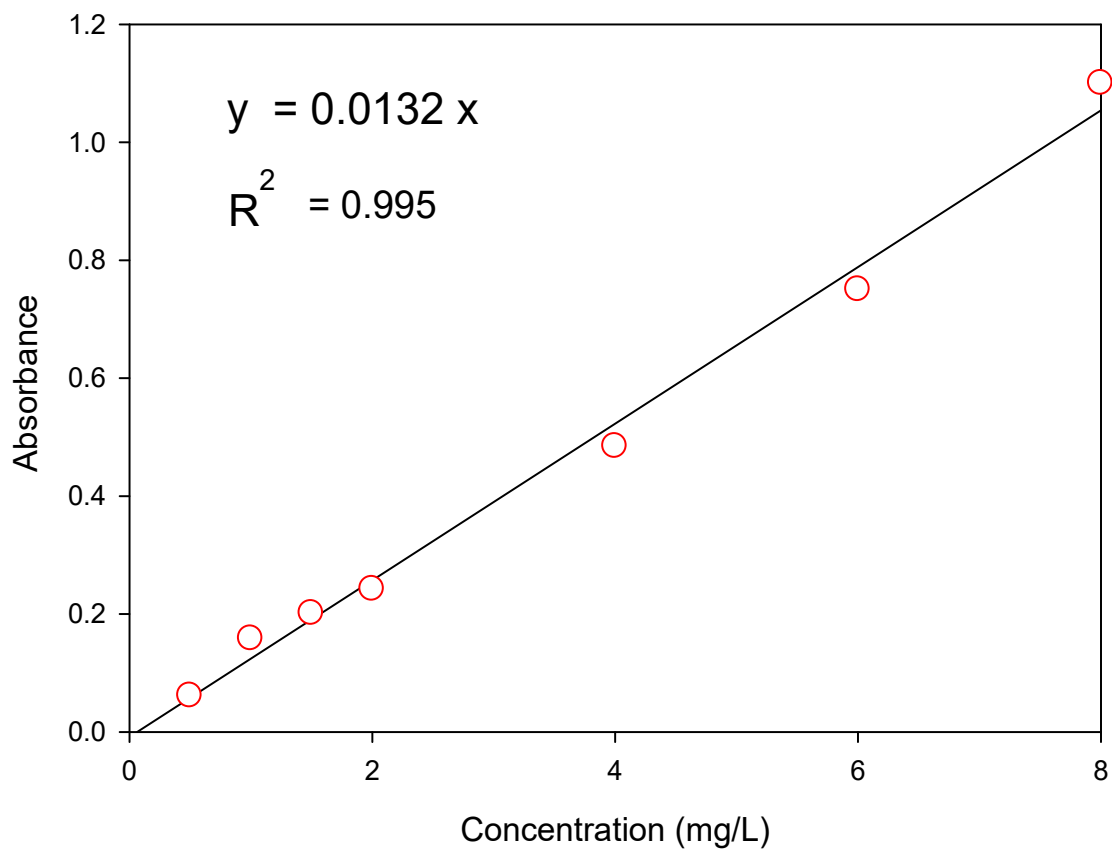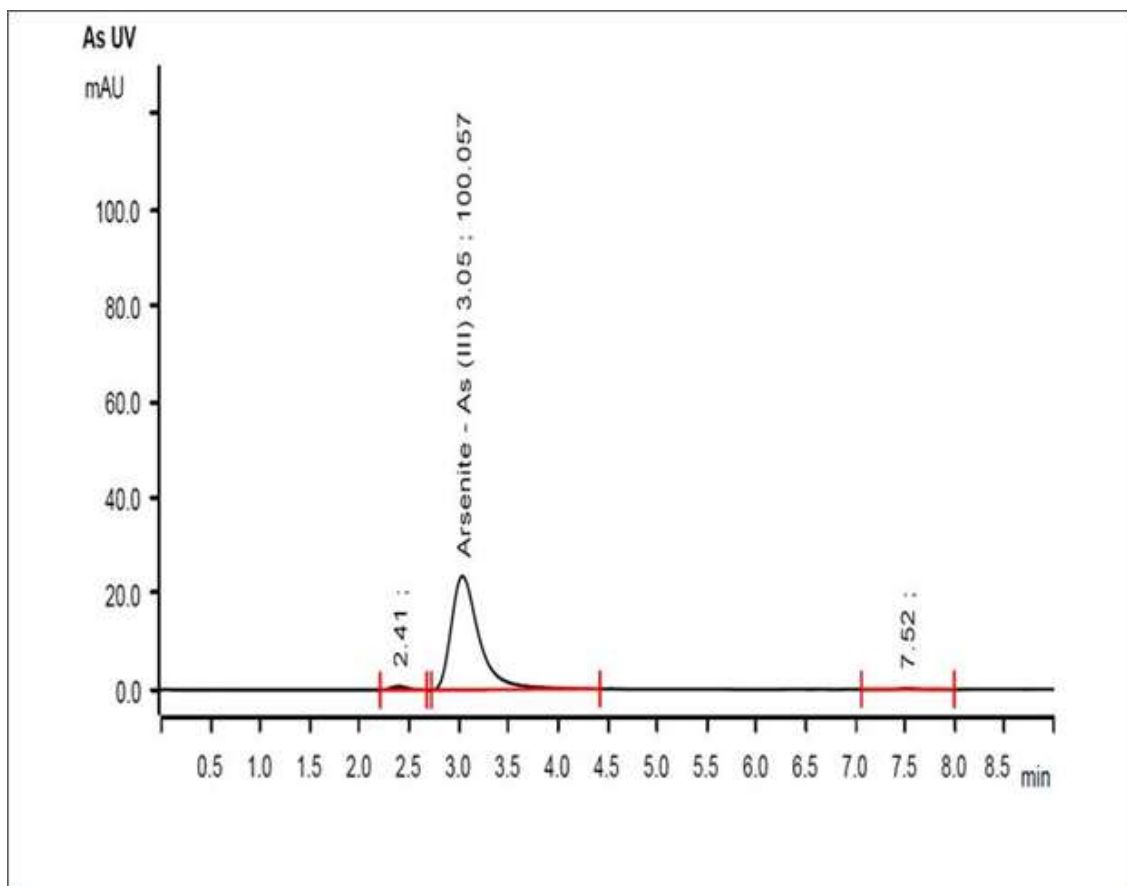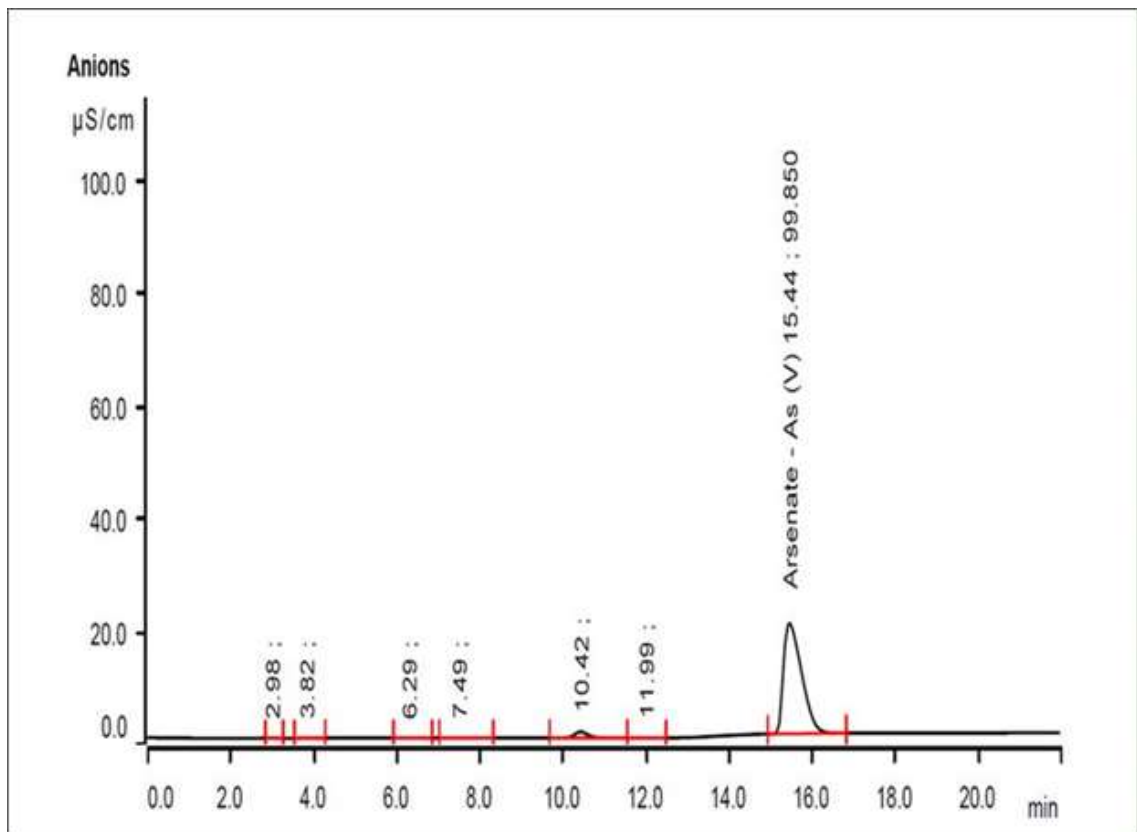
Figure 5.10 Concentration versus absorbance, a linear graph with regression of R^2 of 99.95%

APPENDIX F

IC chromatogram of As(V) standard solution calibration with conductivity detector 1 (850 Professional IC 1), Metrosep A Supp 5 100/4.0 column, at retention time of 15.4mins Figure 4.14: IC chromatogram of As(III) standard solution with Detector (944 Professional UV/VIS Detector Vario 1), Metrosep A Supp 5 100

IC chromatogram of As(V) standard solution calibration with conductivity detector 1 (850 Professional IC 1), Metrosep A Supp 5 100/4.0 column, at retention time of 15.4mins Figure 4.14: IC chromatogram of As(III) standard solution with Detector (944 Professional UV/VIS Detector Vario 1), Metrosep A Supp 5 100/4.0 column, at the retention time of 2.98 mins

APPENDIX H

Initial screening of Cr(VI)-reducing activity with 120 mg/L As(III) as electron donor with selected pure isolates A_4, Y_4, CR_4, and AS_4

Incubation time (hour)	Cr(VI) Concentration (mg/L)						
	Test 2				Control 1^{II}	Control 2^{III}	Control 3^{IV}
	Isolate A_4^{I}	Isolate Y_4^{I}	Isolate As_4^{I}	Isolate Cr_4^{I}			
0	70±0.2	70±0.7	70±01	70±0.8	70±0.3	70±0.1	70±0.3
24	70±0.3	69	45±0.7	43±0.6	70±0.4	69±0.5	65±0.4
30	67±0.7	68±0.7	40±0.4	38±0.8	70±0.0	68±0.6	63±0.7
48	66±0.6	63±0.8	29±0.8	29±0.2	70±0.6	67±0.7	63±0.1
72	64±0.7	62±0.7	24±0.4	27±0.9	71±0.4	67±0.1	63±0.2
120	62±0.7	62±0.6	21±0.3	21±0.4	70±0.9	66±0.8	63±0.1
144	61±0.9	59±0.3	12±0.2	7±0.6	68±0.4	66±0.5	63±0.0
(%) Removed	18±0.2	10±0.4	82±0.5	89±0.9	2±0.3	4±0.5	9±0.9